

GAUSSIAN-MOMENT RELAXATION CLOSURES FOR
VERIFIABLE NUMERICAL SIMULATION OF FAST
MAGNETIC RECONNECTION IN PLASMA

By
Evan Alexander Johnson

A DISSERTATION SUBMITTED IN PARTIAL FULFILLMENT OF THE
REQUIREMENTS FOR THE DEGREE OF

DOCTOR OF PHILOSOPHY
(MATHEMATICS)

at the
UNIVERSITY OF WISCONSIN – MADISON
2011

© Copyright by Evan Alexander Johnson 2011

Abstract

The motivating question for this dissertation was to identify the minimal requirements for fluid models of plasma to allow converged simulations that agree well with converged kinetic simulations of fast magnetic reconnection. We show that truncation closure for the deviatoric pressure or for the heat flux results in singularities. Due to the strong pressure anisotropies that arise in magnetic reconnection we propose Gaussian-moment two-fluid MHD with isotropization of the pressure tensor and a Gaussian-BGK closure for the heat flux tensor as the simplest model that is likely to agree reasonably well in the diffusion region with kinetic simulations of fast magnetic reconnection.

For two-dimensional problems invariant under 180-degree rotation about the origin, we show that if the entropy production, heat flux, diffusive entropy flux, or deviatoric pressure vanishes in a neighborhood of the origin then any steady state solution with nonzero reconnection rate must be singular. In particular, models which simulate any species using a Vlasov equation or an adiabatic five-moment or ten-moment model cannot support converged steady nonsingular magnetic reconnection. Therefore, for such problems, converged simulation of steady magnetic reconnection requires that a nonzero collision operator be explicitly specified.

To study dynamic nonlinear magnetic reconnection we simulate the GEM magnetic reconnection challenge problem with an adiabatic two-fluid-Maxwell model with pressure isotropization. Our deviatoric pressure tensor agrees well with published kinetic simulations at the time of peak reconnection, but sometime thereafter the numerical solution becomes unpredictable and develops near-singularities that crash the simulation unless positivity limiters are applied. To explain these difficulties we show that steady reconnection requires heat flux and argue that sustained reconnection approximates steadily driven reconnection.

This prompts the need for a 10-moment gyrotropic heat flux closure. Using a Chapman-Enskog expansion with a Gaussian-BGK collision operator yields a heat flux closure for a magnetized 10-moment charged gas which generalizes the closure of McDonald and Groth. We argue for this closure against an entropy-respecting closure.

Acknowledgements

I want to express appreciation for some of the people who have been important to me.

Professional acknowledgements

Firstly, my advisor, **James Rosmanith**. He has approximated the ideal in an advisor. I love working with him. He is patient, generous with his time, and treats students with respect. He has encouraged me and has underscored what I need to do without ever chastising or disparaging me for my ignorance or lack of progress.

I have greatly valued his openness. He knows his field and is transparent about the extent of his knowledge. He structures things cleanly. He is a model of clarity in how he presents something to an audience and a superb teacher. He is clear and transparent in his own thought process and is adept in engaging the thought process of another. Consequently, he has imparted to me not just what he knows but how he thinks.

I admire his dedication, reliability, and availability, in his work, in his involvement with students, and in his relationship with his family.

Secondly, I would also like to express appreciation to **Jerry Brackbill**. I was struck from the moment I met him by his enthusiasm and openness. Over the past year he has given me extensive help and counsel. I specifically want to thank Jerry and his wife, Isabel, for coming all the way from Portland so that he could serve on my committee.

In addition, I would like to thank a number of people in the plasma physics community who have been helpful to me, especially when I was getting started.

Nick Murphy was the person I went to for help when learning the basics of magnetic reconnection. He pointed me toward important recent developments, such as the role of secondary instabilities.

When I have become stuck on critical gritty details, **Ping Zhu** has been the person I can go to who will work through the details with me.

Ammar Hakim was the one who originally inspired me to work on the ten-moment model. His work (with Shumlak and Loverich) on two-fluid simulation of the GEM problem laid the foundation on which James and I built. Ammar has pointed me to interesting problems and has challenged me with critical questions about my numerical approach.

I would like to thank **Carl Sovinec**, both for serving on my committee and for his hospitality to me and James in including and involving us in seminars and arranging for us to meet with visiting speakers such as Uri Shumlak and Jim Drake. Carl embodies the culture of openness and thoughtful consideration that characterizes the plasma physics group at UW-Madison. I specifically wish to thank him for his careful reading of my dissertation and his thoughtful responses.

I would also like to thank **Daniel den Hartog** for personal counsel and professional advice. I admire the role that he serves both in the plasma community, which he has helped me to understand, and in the Christian community of which I am a part.

Thanks to David Levermore for pointing me to the role of entropy evolution and suggesting that I use the Gaussian-BGK collision operator.

Personal acknowledgements

I would like to express appreciation to the people whose presence has given meaning to my life and the work that I have devoted myself to, and it is to them that I would like to dedicate this work.

To my housemates who have been not just enduring friends but men who have cared about what I care about and with whom I have joined in developing our vision of the world and our role in it:

To *Angelo Scherer*: Your thoughtful questions have elicited many of my best thoughts and ideas. By walking into the light you have laid the foundation for building the community life that you envision. May the Lord continue to use you to bring disconnected people into spiritually transforming communities.

To *Jon Shea*: Your flood of passion and heart of compassion have drawn me out of myself and helped me to see into the heart and experience of others. When I lent you books and cultural resources you responded with such enthusiasm that it was really you who converted me and got me excited about the writings of Wendell Berry and Lao Tzu. May the Lord bless and guide you and Rebecca in all your ways.

To *Miles Kirby*: Your understanding spirit has lifted me. Your respectfulness, positivity, and genuine honesty has shown me by example better ways to handle interpersonal conflict. Thanks for plugging me into the creative, communitarian social networks that you are so active in. Your passion for population health is based not in abstraction but in ground-level personal relationships and shared experience. The woman you married complements beautifully your gift of sincere personal connection. I am thrilled that you and Katie can go to Kenya for two years, and I hope to meet you again in Africa!

To *Ryan Doucette*: Thanks for praying and gardening with me! The books you have introduced me to have expanded my vision of life. Your appreciation for children, old books, gardening, animals, and the north woods of Wisconsin is unique and of great value; may the Lord give you opportunity to serve your community with your love for particular places and particular things. Your prayerful and peaceable spirit has calmed me.

To *Michael Peterson*: I have appreciated living with someone who also looks for a pattern of community life that is attached to and stewards the land. You are an example of simplicity, cheerfulness, steadfastness, and gratitude. Your cooking skill and musicianship have spiced and enriched my life. May your life's work and dreams come to a full fruition.

To those who have profoundly influenced my life:

To *Paul Meyer*: You opened my world. You introduced me to the Great Books tradition, the Catholic magisterial intellectual tradition, and indirectly to the wisdom of Eastern Orthodox spirituality. Your respectfulness, forthrightness, and humility have built my trust and brought down my barriers.

To *John Vogel* and the faculty at *Trinity School River Ridge*: Among you I experienced an intellectual community patterned after the body of Christ, and it is from you that I carry my vision of what a community of learners is to be and to do. John, I am indebted to you for what you were to me as my mentor teacher. Your fatherly love for your students, your exuberant love for mathematics, and your genuine interest in the full range of pursuits of the other faculty embody my ideal of a teacher.

To *Mark Whitters* and the *Servants of the Word*: Through you I experienced a brotherhood that shares a common life of purposeful manhood. It seems evident that the gift of the Sword of the Spirit communities that you serve is the quality of their family life, and by forgoing having families of your own you have established a foundation of family life that promises to have a transforming effect on communities for generations to come. Your common life of prayer and service embodies the pattern of life that I desire to carry with me and share with others. Mark, you tell it like it is. You built my trust and I appreciated the respect you conveyed and your good humor. DOC, your involvement with Cornerstone (both in Detroit and Uganda) has been an inspiration to me. Thank you to Nico, Stan, Ed, and many others who helped me discern my life calling.

To *Wafik Lotfallah*: Thank you for praying with me, for sharing your wisdom, for helping me to understand the historical experience of Christian communities in the Islamic world, and for introducing me to Saint Mary and Saint Rewais Coptic Orthodox Church in Madison. You are

a model to me professionally as a professor and mathematician and personally by your respectful candor, perceptive understanding, and peaceful spirit which reaches across barriers of mistrust. We pray for the continued renewal of Egyptian society.

To those who profoundly deepened my life by sharing with me from their own experience what it means to set aside the Lord's day, particularly Peter Kim and Phil Johnson.

To those who helped me as a young man to grow into maturity:

To *Walter Schultz*: You love truth. Your dictum — “wisdom, when it encounters truth, bows to it” — expresses the pattern of your life. You are truly a professor of philosophy. You have been a model to me of a man who cares for his students in a way that is not superficial but deep and life-changing. Thank you for praying for me each month. I appreciate the personal interest that you and Mary have always expressed in my life.

To *Eric Thomsen*: You have been my model of cheer, personal regard, humility, and intellectual seriousness. With you I could push the boundaries and still belong and be respected. You live out the truth that “the fear of the Lord is the beginning of wisdom.” When I was seeking my life direction I remember you exclaiming, “You’re a researcher!”

To *Carl Fischer*: Thank you for your open home and for treating my friends as your friends. The love of Jesus shines in you.

To ***Geneva Campus Church***: Geneva has been the center of my life for the last eight years. In you I have found a group of Christians who care about the world, who are engaged with the life and calling of the university, and who are thoughtful and wise. You have provided a context in which I and other students have been nurtured in maturity; by humility and truth, you have modeled family relationship and community life.

To *Sylvia Boomsma*: You and Bob have been to me and to many other students like second parents. I was moved by your love and commitment to one another and by your faith, hope, and love that came out so clearly as Bob was dying. You have both been earthy, real, and thoughtful. Sylvia, I appreciate the prayer notices that you send out, in particular for those who suffer persecution. In the days before Bob died he urged me to do plasma physics “to the *n*th degree,” and it has been a great pleasure to attempt it.

To Marcia Bosscher: Thank you for being such a hospitable neighbor. Your open home has been a blessing to many.

To Mike and Beth Winnowski: You personally represent the culture of forthrightness, thoughtful response, and transparency that I have valued at Geneva.

To others with whom I have been engaged in prayer groups:

To Terry Morrison: I appreciate your steadfast interest in the course of my life.

To Gayle Reed: Your personal and physical trials have deepened and refined you. The books by Brother Yun and Andrew Murray that you gave me changed my life.

To friends I have made here in Madison:

To *Ron and Margaret Miller*: Ron, you are a man who cares about others and senses how they feel. Thanks to you and to your mom, Margaret, for the hospitality you have shown to me.

To friends I have made over the past year:

To Micah Behr and Li Ke: thanks for your encouragement and understanding.

To two visiting political science professors from China:

To *Bai Wengang*: I admire your commitment to truth regardless of the cost and your wisdom in tracing modern political patterns to their ancient precedents. Ancient Chinese political wisdom — that legitimate government is derived from the mandate of Heaven, that good government consists in the exaltation of the virtuous, that the foundation of government is a community of standards and the cultivation of virtue (Micius), and that an orderly society turns on the formation of a moral atmosphere and an understanding of duties (Confucius) — provides needed correctives to modern

American and Chinese public life.

To *Zheng Xiaohua*: I appreciate your concern for good local government and caring communities. You have provoked me to seek a deeper understanding of the American experiment with democracy.

To *my family*:

To my brother, Michael and my sister, Laura: I appreciate the questions you ask, the carefully considered judgments you offer, your hospitality, the love you have for your families, and the passions and convictions that compel you. Michael, you have been a force of stability and reason. Laura, you have been a discerning observer who understands my dreams. You were the one who told me I should study physics.

To my parents: You have invested immeasurably in me. You have imparted to me a love of truth, the value of kindness, and a way of reasoning through an issue. Thank you for shepherding my mathematical development. Mom, I appreciate your wisdom and sympathy. Dad, thank you for teaching me to ask questions about the world.

To two men who have died who were my closest friends, who were there for me at my lowest point and who I wish I had been there for:

To my grandfather, *Aldridge Johnson*: You were simple, sincere, and affectionate.

To *Matthew Beise*: You were my first adult friend and the person who most shared what I loved – physics, Greek, and Hebrew. I miss you.

And to the one who will ultimately judge this work, to Jesus Christ, the true and faithful martyr, the firstborn from the dead and the ruler of the kings of the earth.

List of Figures

| | | |
|----|---|-----|
| 1 | Cartoon of symmetric antiparallel 2D separator reconnection (wikipedia). | 3 |
| 2 | Hierarchy of models considered in this work. | 10 |
| 3 | Equations of the two-species Boltzmann-Maxwell model (standard of truth). | 10 |
| 4 | Equations of the 10-moment 2-fluid Maxwell model. | 11 |
| 5 | Equations of the 5-moment 2-fluid Maxwell model. | 12 |
| 6 | Equations of 10-moment 2-fluid MHD. | 13 |
| 7 | Equations of 5-moment 2-fluid MHD. | 14 |
| 8 | Ten-moment Gaussian-BGK closure. | 15 |
| 9 | Five-moment Gaussian-BGK closure. | 16 |
| 10 | Relaxation coefficients | 17 |
| 11 | Peak rate of reconnection versus isotropization period in the half-scale symmetric pair plasma GEM problem. | 80 |
| 12 | Time until 30% of flux is reconnected in the half-scale symmetric pair plasma GEM problem. | 81 |
| 13 | Reconnection for no isotropization (hyperbolic 10-moment model) in the half-scale symmetric pair plasma GEM problem. | 83 |
| 14 | Reconnected flux for moderate isotropization in the half-scale symmetric pair plasma GEM problem. | 84 |
| 15 | Reconnected flux for fast isotropization in the half-scale symmetric pair plasma GEM problem. | 85 |
| 16 | Reconnected flux for the five-moment model (instantaneous isotropization) in the half-scale symmetric pair plasma GEM problem. | 86 |
| 17 | Peak rate of reconnection versus isotropization period in the full-scale symmetric pair plasma GEM problem. | 87 |
| 18 | Time until 30% of flux is reconnected in the full-scale symmetric pair plasma GEM problem. | 88 |
| 19 | Reconnected flux for moderate isotropization in the full-scale symmetric pair plasma GEM problem. | 89 |
| 20 | Reconnection rate for moderate isotropization in the full-scale symmetric pair plasma GEM problem. | 90 |
| 21 | Profile of “Ohm’s law” terms at the peak reconnection time of 34 (angular) gyroperiods in the full-scale symmetric pair plasma GEM problem. | 91 |
| 22 | Anomalous resistivity along the y-axis at the peak reconnection time of 34 (angular) gyroperiods in the full-scale symmetric pair plasma GEM problem. | 92 |
| 23 | Magnetic field lines and current at the time of peak reconnection rate. | 93 |
| 24 | GEM simulations: reconnecting flux for 10- and 5-moment models. | 96 |
| 25 | Magnetic field at 16% reconnected | 97 |
| 26 | Off-diagonal components of electron pressure tensor | 99 |
| 27 | Diagonal components of electron pressure tensor | 100 |
| 28 | Electron gas at $t = 16$ (nascent singularity) | 102 |
| 29 | Electron gas at $t = 20$ (developing singularity) | 103 |
| 30 | Electron gas at $t = 26$ (splitting singularity) | 104 |

| | | |
|----|--|-----|
| 31 | Electron gas at $t = 28$ (split singularity, just before crashing) | 105 |
|----|--|-----|

List of Tables

- 1 Comparison of time required to reconnect one unit of flux for kinetic and two-fluid simulations of the GEM problem. 98
- 2 Eigenstructure for solutions to adiabatic ten-moment linearized stagnation point flow. 140

Contents

| | |
|--|-------------|
| Abstract | i |
| Acknowledgements | ii |
| List of Figures | vi |
| List of Tables | viii |
| Contents | ix |
| 1 Introduction | 1 |
| 1.1 Conventions | 1 |
| 1.2 Plasma | 1 |
| 1.3 Magnetic reconnection | 2 |
| 1.4 Fast magnetic reconnection | 4 |
| 1.4.1 Background | 4 |
| 1.4.2 Historical background for fast magnetic reconnection | 5 |
| 1.4.3 The GEM problem | 6 |
| 1.4.4 Entropy production and heat flux requirements for steady magnetic reconnection | 9 |
| 1.4.5 Gyrotropic ten-moment heat flux closure | 9 |
| 1.5 Model equations | 9 |
| 2 Models of Plasma | 18 |
| 2.1 Overview | 18 |
| 2.1.1 Kinetic models | 19 |
| 2.1.2 Fluid models | 19 |
| 2.2 Equations of kinetic models | 22 |
| 2.2.1 Particle models (PIC) | 22 |
| 2.2.2 Boltzmann/Vlasov equations | 23 |
| 2.3 Fluid balance equations of Galilean-invariant gas dynamics | 24 |
| 2.3.1 Notational conventions for fluid moments | 24 |
| 2.3.2 Conservation moments | 26 |
| 2.3.3 Pressure evolution | 27 |
| 2.3.4 Temperature evolution | 27 |
| 2.4 Entropy evolution | 28 |
| 2.4.1 Kinetic entropy evolution | 28 |
| 2.4.2 Maxwellian limit | 29 |
| 2.4.3 Gas-dynamic entropy evolution | 29 |
| 2.5 Entropy-respecting forms for closure | 31 |
| 2.5.1 Five-moment closure | 32 |
| 2.5.2 Ten-moment closure | 33 |
| 2.5.3 Equivalence of ten-moment and five-moment stress closure for near-isotropy | 36 |
| 2.6 Perturbative closure | 39 |
| 2.6.1 BGK and Gaussian-BGK collision operators | 39 |

| | | |
|----------|--|-----------|
| 2.6.2 | Chapman-Enskog expansion | 41 |
| 2.6.3 | Perturbative stress closure | 42 |
| 2.6.4 | Perturbative heat flux closure | 44 |
| 2.6.5 | Comparison of heat flux closures | 45 |
| 2.7 | Intraspecies closure coefficients | 46 |
| 2.7.1 | Viscosity and heat conductivity are functions of temperature independent of density. | 47 |
| 2.7.2 | Positivity-preserving heat conductivity closure | 47 |
| 2.7.3 | Braginskii closure coefficients | 48 |
| 2.8 | Interspecies collisional closures | 49 |
| 2.9 | MHD equations | 51 |
| 2.9.1 | Ohm's law | 51 |
| 2.9.2 | Mass density evolution | 53 |
| 2.9.3 | Momentum density evolution | 54 |
| 2.9.4 | Energy density evolution | 55 |
| 2.9.5 | Incompressible MHD | 55 |
| 2.9.6 | Entropy evolution for two-fluid MHD | 56 |
| 2.10 | Summary | 56 |
| 3 | Steady Magnetic Reconnection | 57 |
| 3.1 | Definition of rotationally symmetric 2D magnetic reconnection | 57 |
| 3.1.1 | Translational symmetry | 57 |
| 3.1.2 | Rotational symmetry | 57 |
| 3.1.3 | Consequences of symmetries for tensor components | 58 |
| 3.1.4 | Reflectional symmetry | 59 |
| 3.2 | 2D magnetic reconnection | 59 |
| 3.3 | Ohm's law (current evolution) at the origin | 61 |
| 3.3.1 | MHD | 61 |
| 3.3.2 | Two-fluid-Maxwell | 61 |
| 3.3.3 | Implications of Ohm's law at the origin | 62 |
| 3.4 | Steady rotationally symmetric 2D reconnection requires heat flux. | 63 |
| 3.4.1 | Outline of the physical argument | 64 |
| 3.4.2 | Consequences of the argument for models | 65 |
| 3.4.3 | Vlasov model | 66 |
| 3.4.4 | Quadratic moment models need heat flux | 66 |
| 3.4.5 | Steady reconnection requires heat flux. | 69 |
| 3.4.6 | The ten-moment hyperbolic model does not support steady reconnection (at least for reflectional symmetry) | 70 |
| 3.4.7 | Singular solutions | 71 |
| 4 | GEM challenge problem | 72 |
| 4.1 | GEM magnetic reconnection challenge problem | 72 |
| 4.1.1 | Specification of the GEM problem | 72 |
| 4.1.2 | Discussion of the initial perturbation | 75 |
| 4.2 | System of equations used to solve the GEM problem | 77 |

| | | |
|----------|--|------------|
| 5 | GEM pair plasma simulations | 79 |
| 5.1 | Rescaled pair-plasma GEM problem | 79 |
| 5.2 | Full-scaled pair plasma GEM problem | 87 |
| 5.3 | Conclusion | 94 |
| 6 | GEM hydrogen plasma simulations | 95 |
| 7 | Numerical method | 106 |
| 7.1 | Discontinuous Galerkin method | 106 |
| 7.2 | Source term | 107 |
| 7.3 | Flux term | 108 |
| 7.4 | Variation limiters | 108 |
| 7.4.1 | Limiting of a 1D scalar problem | 109 |
| 7.4.2 | Limiting of a 1D system | 109 |
| 7.4.3 | 2D limiting for a Cartesian mesh | 110 |
| 7.5 | Positivity limiting | 110 |
| 8 | Conclusions and future work | 111 |
| 8.1 | New results | 111 |
| 8.2 | Questions raised | 112 |
| A | Modeling | 115 |
| A.1 | Maxwellian and Gaussian distributions | 115 |
| A.1.1 | Maxwellian case | 116 |
| A.1.2 | Gaussian case | 118 |
| A.1.3 | Expressions for entropy | 120 |
| A.1.4 | Number density | 122 |
| A.1.5 | Consistent entropy for interacting species | 122 |
| A.2 | Collisionless Nondimensionalization | 123 |
| A.3 | Knudsen Number | 126 |
| A.4 | Prandtl Number | 126 |
| A.4.1 | Rate of momentum diffusion | 126 |
| A.4.2 | Rate of temperature diffusion | 127 |
| A.4.3 | Formula for the Prandtl number | 127 |
| A.5 | Explicit closures | 128 |
| A.5.1 | Splice tensor operators | 128 |
| A.5.2 | Gyrotropic tensors | 129 |
| A.5.3 | Gyrotropic linear operators on symmetric matrices | 129 |
| A.5.4 | Implicit closures in splice product form | 130 |
| A.5.5 | Heat flux | 130 |
| A.5.6 | Deviatoric pressure tensor | 131 |
| A.5.7 | Heat flux tensor | 133 |
| B | Reconnection | 137 |
| B.1 | Inflow ODE for the ten-moment equations. | 137 |
| B.1.1 | Component evolution | 137 |
| B.2 | Adiabatic ten-moment stagnation point flow. | 138 |
| B.2.1 | Abstract framework for linearization about the X-point | 138 |
| B.2.2 | Stagnation point flow for an adiabatic isotropizing ten-moment gas | 139 |

| | |
|--|------------|
| C Numerics | 143 |
| C.1 Source ODE | 143 |
| C.1.1 Basic Equations | 143 |
| C.1.2 The electro-momentum system | 144 |
| C.1.3 The pressure tensor system | 150 |
| C.1.4 Rotation of the pressure tensor | 150 |
| C.2 Eigenstructure of the flux Jacobian for a ten-moment gas | 152 |
| C.2.1 Ten-moment system in conservation form | 152 |
| C.2.2 Quasilinear system in primitive quantities | 153 |
| C.2.3 Quasilinear 1-D system in primitive variables | 153 |
| C.2.4 Eigenstructure for primitive variables | 154 |
| C.2.5 Eigenstructure for “conserved” variables | 156 |
| C.2.6 Eigenvectors for “conserved” variables | 158 |
| Bibliography | 162 |
| Vocabulary Glossary | 166 |
| Symbol Glossary | 167 |
| Index | 170 |

Chapter 1

Introduction

For convenience, most mathematical symbols are hyperlinked to the symbol glossary, which in turn references points in the text where each term is defined or discussed.

1.1 Conventions

For clarity and to avoid misunderstand we specify that

- The term “**collisions**” is used in the broadest possible sense to include all microscale interactions of particles with the electromagnetic field. The language of collisions is thus used in an axiomatic sense, rather than in the typically more restricted sense which refers specifically to a detailed description of particle-particle (Coulomb) interactions. In particular, it is assumed that the evolution equation of the density functions $f_i(t, \mathbf{x}, \mathbf{v})$ for the ions and $f_e(t, \mathbf{x}, \mathbf{v})$ for the electrons satisfy kinetic equations of the form

$$\begin{aligned}\partial_t f_i + \mathbf{v} \cdot \nabla_{\mathbf{x}} f_i + \mathbf{a}_i \cdot \nabla_{\mathbf{v}} f_i &= C^T_i = C_i + C_{ie}, \\ \partial_t f_e + \mathbf{v} \cdot \nabla_{\mathbf{x}} f_e + \mathbf{a}_e \cdot \nabla_{\mathbf{v}} f_e &= C^T_e = C_e + C_{ei},\end{aligned}$$

where we call C^T_s , C_s and C_{sp} [collision operators](#); C_i , C_e , and $C_{ie} + C_{ei}$ conserve mass, momentum, and energy, and the appropriate entropy inequalities are assumed to be satisfied.

- The terms [kinetic equation](#) and [Boltzmann equation](#) are used as synonyms.
- The terms [Gaussian-moment model](#) and [ten-moment model](#) are used as synonyms.
- The terms [Maxwellian-moment model](#) and [five-moment model](#) are used as synonyms.

1.2 Plasma

A gas is a fluid composed of freely moving particles. **Plasma** is a gas of charged particles, which interact with the electromagnetic field. Most of the universe consists of plasma threaded by magnetic field lines. The negatively charged particles are typically electrons but may also be negatively charged dust grains. The positively charged particles are ions, typically protons or positrons. In this document we are primarily concerned with **two-species** plasmas, which consist of a species of positively charged particles and a species of negatively charged particles. In the case of **pair plasmas**, the negatively charged particles are electrons and the positively charged particles are positrons. Positrons are the antiparticles of electrons; they have the same mass but opposite charge. In the case of **hydrogen plasmas**, the positively charged particles are protons and the negatively charged particles are electrons. The ratio of proton mass to electron mass is large (approximately 1836).

Plasma is a type of magnetohydrodynamic fluid¹. A **magnetohydrodynamic (MHD) fluid** is a fluid that conducts electricity and has a magnetic field. In the presence of a magnetic field electrical current results in a force on the fluid perpendicular to the direction of the magnetic field and the direction of the current. An MHD description of a fluid becomes necessary when the magnetic field is strong enough to modify fluid flow (enough to affect phenomena and quantities of interest).

Each species in a plasma can be regarded as a separate fluid. One can define bulk fluid variables by appropriately summing or averaging the fluid variables of each species. Since these fluids occupy the same space, they can interact directly through frictional drag force and thermal heat exchange. The motion of a species fluid relative to the velocity of the bulk fluid is called the **drift velocity** of the species. A **two-fluid** model is used for a two-species plasma and represents each species as a distinct fluid. **Two-fluid MHD** regards the (bulk) MHD fluid as composed of positively and negatively charged fluids whose charge densities are assumed to cancel.

Magnetic field evolution is determined by the electric field. The electric field is given by **Ohm's law**, which specifies the electric field in terms of electrical current, magnetic field, fluid velocity, and the pressures of the positive and negative particles.

Written in full, Ohm's law is the evolution equation for electrical current solved for the electric field. The full Ohm's law is complicated, and Ohm's law can only be used by assuming that fluid quantities have been specified by approximate closure relationships.

Simplified models of MHD assume a simplified Ohm's law. In the classical description of electromagnetism, magnetic field is independent of reference frame but electrical field is not. **Ideal MHD** assumes that the electric field is zero in the reference frame of the fluid. **Resistive MHD** assumes that in the reference frame of the fluid the electric field equals the resistivity times the electrical current.

For a two-species plasma consisting of equal densities of positive and negative charge, **resistive Hall MHD** is a more accurate model (in comparison to resistive MHD) which defines the electric field in the reference frame of total drift, which we define to be the fluid velocity plus the sum of the drift velocities of the positively and negatively charged gases; ideal Hall MHD assumes that the electric field is zero in this frame, i.e., that the resistivity is zero [27].

In general, ideal models of MHD imply the existence of a *flux-transporting velocity* such that the electric field is zero in the reference frame of this velocity. In ideal models of MHD the component of the electric field parallel to the magnetic field is always zero ([57], page 189).

1.3 Magnetic reconnection

A **magnetic field line** is a curve through space that is everywhere parallel to the local magnetic field. The **magnetic flux** through an infinitesimal surface element is the surface area times the component of the magnetic field perpendicular to the surface. The magnetic field is **divergence-free**; this means that the total flux of magnetic field out of a closed region equals the total flux into the region. As a consequence, by choosing representative magnetic field lines appropriately, it is possible to think of the strength of the magnetic field as proportional to the density of magnetic field lines. We can then say that the magnetic flux through a surface is proportional to the number of magnetic field lines passing through the surface.

¹Technically a magnetohydrodynamic fluid should be quasi-neutral and have non-relativistic flow speeds.

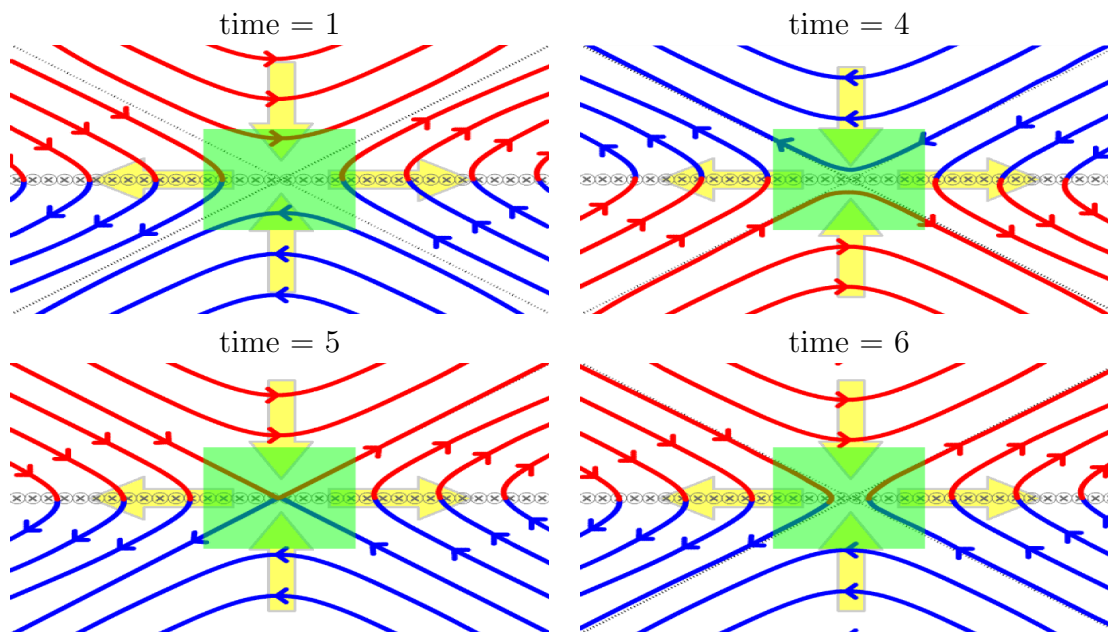


Figure 1: Cartoon of symmetric antiparallel 2D separator reconnection (wikipedia).

At the origin the magnetic field is zero. Symmetry forces physical velocities to be zero at the origin, including the bulk fluid velocity, the fluid velocity of each species, and any flux-transporting flow. The magnetic field lines which intersect the origin are called **separatrices** and partition the domain into four regions. In an ideal plasma model the separatrices would be frozen in the fluid and therefore it would be impossible to transfer flux across the separatrices. The reconnected flux is defined to be the amount of flux transferred from one region to another. The green rectangle at the center signifies the diffusion region. The ratio of its long side to its short side is called its aspect ratio.

The magnetic field evolution equation says that the rate of change of magnetic flux through a surface equals the *circulation integral* of the electric field around the boundary of the surface. In ideal MHD the electric field in the reference frame of the fluid is zero. Therefore, the magnetic flux through a surface element that is carried with the fluid cannot change (because any circulation integral of a uniformly zero electric field is zero). The result is that in ideal MHD magnetic field lines are carried with the fluid and cannot change their topology, i.e. how they are connected ([57], p186). This is known as the *frozen-in flux condition*. In regions where ideal MHD does not hold, magnetic field lines can slip through the fluid and break and **reconnect**, i.e. change their topology (how they are connected).

The amount of reconnection is difficult to define in a precise and general way. For the example of 2D separator reconnection as depicted in figure 1, a set of magnetic field lines called separatrices partitions the spatial domain into four regions such that in an ideal model flux could not be transferred from one domain to another. In this case we can define the amount of reconnection to be the amount of flux transferred from one of these regions to a neighboring region.

A definition of magnetic reconnection in general geometry requires a covariant (relativistic) description of the electromagnetic field [27]. Since this dissertation only studies 2D problems symmetric under 180-degree rotation in the plane about the origin, it defines magnetic reconnection only for this case; the rate of reconnection turns out simply to be the out-of-plane electric field component at the origin, as argued in section 3.2.

1.4 Fast magnetic reconnection

1.4.1 Background

Magnetic reconnection is ultimately controlled by Faraday's evolution equation for the magnetic field,

$$\partial_t \mathbf{B} + \nabla \times \mathbf{E} = 0;$$

so the evolution of magnetic field \mathbf{B} is determined by the electric field \mathbf{E} . Plasma physics studies the evolution of plasmas on time scales larger than the plasma period ω_p^{-1} (the time of oscillation in response to charge separation) and larger than the Debye length λ_D (the distance traveled by an electron in a plasma period moving at the thermal velocity v_{ts} , which is the distance over which charge shielding occurs) [22]. On these scales the assumption of **quasineutrality** holds and *Ohm's law* (4.4) for the electric field applies. For a plasma consisting of electrons and ions, Ohm's law is

$$\begin{aligned} \mathbf{E} = & \mathbf{B} \times \mathbf{u} && \text{(ideal term)} \\ & + \boldsymbol{\eta} \cdot \mathbf{J} && \text{(resistive term)} \\ & + \frac{m_i - m_e}{e\rho} \mathbf{J} \times \mathbf{B} && \text{(Hall term)} \\ & + \frac{1}{e\rho} \nabla \cdot (m_e \mathbb{P}_i - m_i \mathbb{P}_e) && \text{(pressure term)} \\ & + \frac{m_i m_e}{e^2 \rho} \left[\partial_t \mathbf{J} + \nabla \cdot \left(\mathbf{u} \mathbf{J} + \mathbf{J} \mathbf{u} - \frac{m_i - m_e}{e\rho} \mathbf{J} \mathbf{J} \right) \right] && \text{(inertial term),} \end{aligned} \tag{1.1}$$

where \mathbf{u} is fluid velocity, \mathbf{J} is electrical current density, ρ is mass density, and \mathbb{P}_i and \mathbb{P}_e are the ion and electron pressure tensors; the constants are the ion mass m_i , the electron mass m_e , and the magnitude of the charge on an electron, e . The resistivity $\boldsymbol{\eta}$ requires a closure, typically a function of (electron) temperature unless an anomalous resistivity is defined.

This work restricts consideration to problems symmetric under 180-degree rotation, because it allows a simple analysis of the X-point which identifies constraints and requirements for reconnection. As argued in section 3.2, at the X-point Ohm's law reduces to

$$\begin{aligned} \mathbf{E} = & \boldsymbol{\eta} \cdot \mathbf{J} && \text{(resistive term)} \\ & + \frac{1}{e\rho} \nabla \cdot (m_e \mathbb{P}_i - m_i \mathbb{P}_e) && \text{(pressure term)} \\ & + \frac{m_i m_e}{e^2 \rho} \left[\partial_t \mathbf{J} + \nabla \cdot \left(\mathbf{u} \mathbf{J} + \mathbf{J} \mathbf{u} - \frac{m_i - m_e}{e\rho} \mathbf{J} \mathbf{J} \right) \right] && \text{(inertial term)} \end{aligned} \tag{1.2}$$

where only the out-of-plane component survives. Since the rate of reconnection is the out-of-plane component of the electric field at the origin, this confirms that one of these three terms must be nonzero to support reconnection.

Magnetohydrodynamic (MHD) models of plasma explicitly assume a form of Ohm's law and evolve a system sufficient to determine the quantities it involves. Ideal MHD discards all terms in Ohm's law except the ideal term and is the simplest model of plasma. In ideal MHD magnetic reconnection is not possible. The next simplest model, resistive MHD, also retains the resistive term. Resistive MHD allows magnetic reconnection to occur, because magnetic field lines can diffuse through the plasma; as we will discuss, steady reconnection rates are slow for resistive MHD unless an anomalous resistivity is used. Resistive Hall MHD includes the Hall term as well, allowing much faster rates of steady reconnection. Models which include terms of Ohm's law beyond resistive MHD are collectively known as *extended MHD* models.

1.4.2 Historical background for fast magnetic reconnection

The notion of magnetic reconnection was introduced by Dungey ([14], 1953). In the subsequent decades people attempted to explain reconnection in terms of resistive MHD. Sweet ([58], 1958) and Parker ([49], 1957) developed a model of steady two-dimensional magnetic reconnection. The Sweet-Parker model assumes that magnetic reconnection occurs in a thin, rectangular *diffusion region* containing nearly antiparallel magnetic field lines. The **aspect ratio** of a rectangle denotes the ratio consisting of the length of the long side divided by the length of the short side. In the Sweet-Parker model of reconnection the aspect ratio of the diffusion region is assumed to be large, implying that the magnetic field lines have a “Y-type” configuration. Plasma is assumed to flow slowly into the broad sides of the rectangle and rapidly out of the narrow sides of the rectangle. In the diffusion region, gradients in the magnetic field result in diffusion of the magnetic field (and hence slipping of magnetic field lines through the plasma) and a sheet of electrical current. Using this model, Parker ([50], 1963) estimated a typical rate of magnetic reconnection in solar flares based on Spitzer’s formula for resistivity (which is based on Coulomb collisions and asserts that resistivity is a function of temperature, see [41]) and found that the predicted rate of reconnection was at least one hundred times too small to account for observed solar flare time scales.

The essential impediment to fast reconnection in the Sweet-Parker model is the tension between the need for a narrow diffusion region (so that magnetic field gradients can be sufficiently strong) and a wide diffusion region (so that plasma can flow out of the narrow sides of the rectangle rapidly enough). Subsequent models of steady reconnection obtained faster rates of reconnection by assuming anomalously high values of resistivity in the diffusion region and/or by assuming an “X-type” magnetic field configuration (in particular a diffusion region with a small aspect ratio) which allows strong magnetic field gradients at the X-point while opening up the outflow so that it is not throttled by being confined to a narrow rectangle [52]. The first such model was devised by Petschek ([51], 1964) and consisted of an X-type magnetic field geometry with a miniature Sweet-Parker region at the center. The Petschek model allowed much faster reconnection rates than the Sweet-Parker model, and thus Sweet-Parker reconnection became designated as *slow reconnection* while reconnection rates on the order given by the Petschek model were identified as *fast reconnection*.

When numerical simulation of magnetic reconnection became feasible, it was found that magnetic reconnection resulted in Y-type configurations and slow reconnection if a uniform resistivity was assumed, whereas X-type configurations and fast reconnection occurred if anomalously high values of resistivity were assumed near the X-point [7]. There are physical reasons to expect anomalously high values of resistivity near the X-point. First, resistive drag may depend nonlinearly on electric current. Electrical currents are strong in the reconnection region. Electrical currents represent relative drift of ions and electrons. If this relative drift becomes strong enough, a streaming instability develops, limiting interspecies drift and greatly increasing resistivity. Second, resistivity may be *spatially* dependent in a weakly collisional plasma where fluid closures cannot be rigorously justified. Spitzer’s formula for resistivity assumes collisional transport theory, which is applicable when the mean free path of a particle is small relative to the length scale of variations in the magnetic field and gas-dynamic quantities. Particle mean free paths are much larger than the width of current sheets or diffusion layers where reconnection occurs, and so collisional transport theory is not applicable even when, as in the solar corona, it is applicable to large-scale structures (see [52], page 45); thus, the reconnection region is governed by collisionless physics in essentially all space and laboratory plasmas where magnetic reconnection is important [8].

Thus, for resistive MHD the game of modeling reconnection naturally became to determine anomalous values of resistivity that account for fast reconnection. By assuming a *spatially* dependent anomalous resistivity one can essentially prescribe a desired rate of reconnection. Some space

modelers have taken the approach of prescribing spatially anomalous resistivities which give results that seem to agree with observational and statistical data. Such an approach can be effective in a specific problem domain such as space weather modeling, but in general we prefer the simplest models with the greatest explanatory and predictive success, which are based in physical principles, and which give physical insight.

One can obtain fast rates of reconnection using an anomalous resistivity that is dependent on current but spatially independent. The project to formulate a spatially independent anomalous resistivity that accurately models reconnection has fallen short, however, on two accounts. First, there are many formulas for anomalous resistivity, and a simple basis for these formulas has been elusive [54, 61, 8]. Second, in weakly collisional regimes steady reconnection is supported primarily by the divergence of the species pressure tensors rather than by resistive drag, and therefore attempting to attribute the reconnection electric field to a resistive term is artificial and does not promise to give physical insight; the end road of insisting on an anomalous resistivity framework is that an appropriate formula for the anomalous resistivity will probably be found to be in terms of the divergence of the electron pressure tensor!

Although a uniform resistivity results in a long, thin current sheet and slow reconnection, this configuration is often unstable. Furth, Killeen, and Rosenbluth ([15], 1963) found that a current sheet with an aspect ratio of about 2π or greater is unstable to spontaneous reconnection which forms magnetic islands. This process is called the *tearing mode instability*, and the magnetic islands are referred to as *plasmoids*. Bulanov *et al.* ([11], 1978) repeated the tearing mode calculation of [15] assuming linear outflow along the current sheet and found that the outflow had a stabilizing effect.

Jumping forward to the past decade, Loureiro, Schekochihin, and Cowley (2007, [39]) performed an asymptotic analysis in the inverse of the aspect ratio of the current sheet and showed that for a current sheet of sufficiently large length L (for which the Lundquist number $\text{Lu} := Lv_A/\eta$ is greater than a critical value of about 4×10^4 , corresponding to an aspect ratio of about 200; see [29]), a chain of plasmoids rapidly forms. Subsequent simulations have confirmed that the ejection of these plasmoids allows fast reconnection rates even in resistive MHD. The consequence is that although resistive MHD with uniform resistivity does not admit fast reconnection, for sufficiently large (e.g. astrophysical) domains statistically steady fast reconnection can be expected via the cascading formation and ejection of plasmoids [29]. Nevertheless, one can still make the categorical assertion that resistive MHD with uniform resistivity does not support steady-state fast reconnection.

In laboratory plasmas Lundquist numbers are typically on the order of 10^3 (page 44 in [52]), which is too small to give rise to plasmoid-mediated reconnection; instead one expects (slow) Sweet-Parker reconnection if the ion inertial length δ_s is larger than the Sweet-Parker layer thickness. For ion skin depth smaller than the Sweet-Parker layer thickness one expects fast, *Hall-mediated reconnection* instead, as discussed in the next section. (See p315 in [64] and Figure 1 in [30].)

1.4.3 The GEM problem

The inadequacy of resistive MHD to account for reconnection electric fields in the diffusion region lead to studies of reconnection using extended MHD. The historical development of these studies is traced in [56], and lead to the following observations regarding 2D separator reconnection. As shown for collisional tearing in [59], the Hall current effect becomes important for a current sheet whose width is comparable to the ion inertial length. Outside of the current sheet gradients are small, and the ideal term dominates in Ohm's law. Within the current sheet the Hall term becomes

significant and the ions decouple from the magnetic field lines, defining the *ion diffusion region*. In a smaller region the electron pressure term (or inertial term) becomes significant and the electrons decouple from the magnetic field as well, defining the *electron diffusion region*.

The culmination of these studies and observations was the formulation and simulation of the *Geospace Environmental Modeling magnetic reconnection challenge problem (GEM problem)* in 2001 [6]. The GEM problem was formulated to study the ability of plasma models to resolve fast magnetic reconnection [6]. The GEM problem identified two-fluid/Hall effects as critical to allow fast reconnection. Although ideal Hall MHD does not admit reconnection, resistive Hall MHD (even with small resistivity) was found to admit fast reconnection [56], as if the Hall term were a catalyst accelerating the much slower rate of reconnection that occurs in resistive MHD without the Hall term.

I remark that ideal Hall MHD (Ohm's law using only the ideal term and the Hall term) does not allow reconnection because a flux-transporting flow exists; magnetic field lines are essentially frozen to the electrons. The ideal Hall MHD simulations in [56] were able to get fast reconnection rates because of the presence of numerical resistivity; the results therefore cannot be converged. Finding 3 at the end of section 1 suggests that in their simulations reconnection is supported by numerical resistivity with an anomalously high value near the X-point. It appears that it is still an open question whether converged fast reconnection is possible in resistive Hall MHD with uniform resistivity. If the answer is no, then one may conclude that short of anomalous closures nonzero divergence of the pressure tensor is necessary for converged steady fast magnetic reconnection. This suggests a study of reconnection with a two-fluid model with resistivity but without viscosity, with and without the inertial term.

Pair plasma GEM simulations

Since the seminal GEM problem studies had identified the Hall effect as the essential physics to admit fast reconnection, it was natural to investigate reconnection rates in pair plasmas, for which $m_e = m_i$ and the Hall term of Ohm's law is absent. Particle simulations by Bessho and Bhattacharjee of antiparallel reconnection [3, 4, 5] have demonstrated that fast reconnection rates occur even in the case of pair plasmas; they find that the divergence of the pressure tensor is the term of equation (1.2) that primarily supports the reconnection electric field. For the guide-field case, in which the out-of-plane component of the magnetic field at the origin is nonzero, Chacón *et al.* [12] subsequently demonstrated that steady fast reconnection is possible in a viscous incompressible model of pair plasma if viscosity dominates but not if resistivity dominates.

In this work we simulate the pair plasma version of the GEM problem with a two-fluid adiabatic model without resistivity and show that rates of reconnection are still fast (although our rate of reconnection is only 60% of the rate in the PIC simulations reported e.g. in [4]).

Two-fluid GEM simulations

The fluid models used in the seminal GEM problem studies did not include the pressure and inertial terms of Ohm's law. It is therefore natural to ask whether the inclusion of these terms would allow significantly improved agreement of fluid simulation of magnetic reconnection with kinetic simulations.

In 2005 Hakim, Loverich, and Shumlak simulated fast magnetic reconnection with an adiabatic inviscid [five-moment two-fluid Maxwell model](#) model which implies an Ohm's law that includes the

Hall term, the inertial term, and a pressure term with scalar pressures [20]². Their figure 10 shows their reconnected flux values superimposed on the reconnection rates reported in the seminal GEM problem papers and arguably shows improved agreement with particle simulations in comparison to the Hall MHD simulations. In 2007 Hakim submitted simulations of the GEM problem with a two-fluid Maxwell model which uses a hyperbolic (adiabatic inviscid) five-moment model for the electrons and a hyperbolic model for the ions and again obtained reconnection rates that agree well with kinetic simulations [19].³

The models used by Loverich, Hakim, and Shumlak are hyperbolic. In particular, for the electrons they use hyperbolic five-moment gas dynamics, which uses truncation closures for the deviatoric pressure and heat flux. As a proxy for Ohm's law (1.1) one may consider the electron momentum equation (2.8) solved for the electric field:

$$\begin{aligned}
 \mathbf{E} &= \mathbf{B} \times \mathbf{u}_e && \text{(ideal term)} \\
 &+ \frac{-\mathbf{R}_e}{q_e n_e} && \text{(resistive term)} \\
 &+ \frac{\nabla \cdot \mathbb{P}_e}{q_e n_e} && \text{(pressure term)} \\
 &+ \frac{m_e}{q_e} d_t \mathbf{u}_e && \text{(inertial term)}.
 \end{aligned} \tag{1.3}$$

At the X-point symmetry the ideal term disappears, simplifying this to the equivalent of equation (1.2). In the simulations of Loverich, Hakim, and Shumlak the resistive term is zero and the pressure term vanishes at the X-point because the deviatoric pressure is zero. This would force the electron velocity at the X-point to ramp with reconnected flux. As our simulations indicate (see figure 16), this almost certainly is not realized in their simulations for later times, and therefore their solutions are presumably not converged for later times. Furthermore, based on kinetic simulations (see e.g. figure 14), we expect the pressure term to dominate at the X-point.

We were therefore motivated to consider two-fluid model with viscosity in both species fluids. An easy way to implement viscosity in a gas is to represent it using a [ten-moment model](#) (also known as a [Gaussian-moment model](#) with relaxation to isotropy. A ten-moment model with relaxation to isotropy agrees with a viscous five-moment model for fast isotropization rates and small pressure anisotropies. For slow isotropization rates, large pressure anisotropies can develop. In kinetic simulations, strong pressure anisotropy is in fact observed at the X-point (see figure 6 of [55]), adding to our motivation for use of a ten-moment isotropizing model for both electrons and ions rather than a five-moment viscous model.

Using the ten-moment two-fluid model to simulate the GEM problem, we obtain qualitatively good agreement with kinetic simulations for plots of the pressure tensor at the time of peak reconnection rate (roughly 16–18, where the unit of time is a typical ion angular gyroperiod as defined in the GEM problem); at this time the pressure is highly agyrotropic in the immediate vicinity of reconnection point. In the approximate time interval from 18 to 28 the rate of reconnection remains approximately constant while the electron temperature tensor becomes increasingly singular near the X-point. For a coarse mesh this temperature singularity does not interfere with the normal

² This paper used the finite volume wave propagation method described in [37]. Loverich, Hakim, and Shumlak also performed a complementary study using the Discontinuous Galerkin method at about the same time; this study was (finally!) accepted for publication in [40].

³ In particular, Hakim attains one nondimensionalized unit of reconnected flux at a nondimensionalized time of about 17.6, in comparison to the values of 15.7 obtained using a PIC simulation [53] and 17.7 using a Vlasov simulation [55]; see table 1.

progression and saturation of reconnection, probably due to numerical thermal diffusion, but when the mesh is refined the singularity becomes sharp and ultimately prevents normal progression of reconnection. The specific terminating behavior is erratic and hard to predict, but in general at the X-point the temperature parallel to the outflow axis will become very cold while the temperature parallel to the inflow axis will become very hot. Unless positivity limiters are applied the simulation crashes when a non-positive-definite temperature tensor develops. (Typically the anisotropically hot spot at the origin splits into two hot spots along the outflow axis before this crash occurs.) If positivity limiters are applied then a secondary island at the origin is likely to form. If symmetry is enforced then this stops reconnection, but if not then spontaneous symmetry-breaking can eject the island and allow reconnection to proceed.

1.4.4 Entropy production and heat flux requirements for steady magnetic reconnection

The characteristic behavior of dynamical systems turns critically on the character of their equilibria. To understand the difficulties encountered with the GEM problem when an adiabatic model is used, we consider the entropy production and heat flux requirements for steady magnetic reconnection. We show that for models which lack a mechanism for heat flux, in reconnection problems that are symmetric under 180-degree rotation about the origin (as holds for the GEM problem), solutions which exhibit steady reconnection must be singular.

1.4.5 Gyrotropic ten-moment heat flux closure

We therefore consider what an appropriate 10-moment heat flux closure would be. In the presence of a magnetic field appropriate diffusive closures need to be *gyrotropic* rather than isotropic. We therefore generalize the isotropic ten-moment heat flux closure recently formulated by McDonald and Groth to the gyrotropic case.

1.5 Model equations

For subsequent reference, in this section we list the systems of equations that define the models discussed in this work. All simulations have been performed using the 10-moment two-fluid Maxwell model or the 5-moment two-fluid Maxwell model.

The relationship among models is laid out in figure 2. As the standard of truth we take the Boltzmann-Maxwell model displayed in figure 3. The 10-moment two-fluid Maxwell equations that we solve are displayed in figure 4. The 5-moment two-fluid Maxwell equations that we solve are displayed in figure 5. Taking the light speed to infinity converts the two-fluid Maxwell models to MHD models. In solving the two-fluid Maxwell equations our goal is to approximate the MHD systems, which we attempt to do by using a sufficiently high light speed. We therefore display the equations of 10-moment 2-fluid MHD in figure 6 and display the equations of 5-moment 2-fluid MHD in figure 7. This work calculates intraspecies collisional closure coefficients using a Chapman-Enskog expansion with a Gaussian-BGK collision operator. The resulting formulas for closure coefficients are displayed for the ten-moment model in figure 8 and for the five-moment model in figure 9.

Model hierarchy

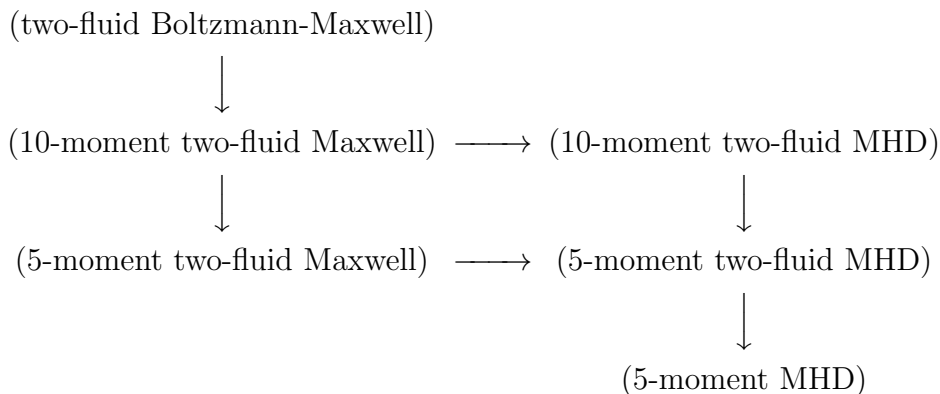


Figure 2: Hierarchy of models considered in this work.

Motion down and to the right indicates use of simplifying limits. Motion down reduces the number of moments evolved. Motion to the right takes light speed to infinity.

Boltzmann-Maxwell model

- **Kinetic/Boltzmann equations:**

$$\partial_t f_i + \mathbf{v} \cdot \nabla_{\mathbf{x}} f_i + \mathbf{a}_i \cdot \nabla_{\mathbf{v}} f_i = C_i + C_{ie}$$

$$\partial_t f_e + \mathbf{v} \cdot \nabla_{\mathbf{x}} f_e + \mathbf{a}_e \cdot \nabla_{\mathbf{v}} f_e = C_e + C_{ei}$$

- **Maxwell's equations:**

$$\partial_t \mathbf{B} + \nabla \times \mathbf{E} = 0, \quad \nabla \cdot \mathbf{B} = 0$$

$$\partial_t \mathbf{E} - c^2 \nabla \times \mathbf{B} = -\mathbf{J}/\epsilon_0, \quad \nabla \cdot \mathbf{E} = \sigma/\epsilon_0$$

- **Definitions:**

$$\sigma := \sum_s \frac{q_s}{m_s} \int f_s d\mathbf{v},$$

$$\mathbf{J} := \sum_s \frac{q_s}{m_s} \int \mathbf{v} f_s d\mathbf{v}$$

$$\mathbf{a}_i := \frac{e}{m_i} (\mathbf{E} + \mathbf{v} \times \mathbf{B}),$$

$$\mathbf{a}_e := \frac{-e}{m_e} (\mathbf{E} + \mathbf{v} \times \mathbf{B})$$

Figure 3: Equations of the two-species Boltzmann-Maxwell model (standard of truth). The interspecies collision operators C_{ie} and C_{ei} are generally ignored in this work, but the intraspecies collision operators C_i and C_e play a critical role.

Ten-moment two-fluid Maxwell model

Gas dynamics equations

$$\begin{aligned} \bar{\delta}_t^i \begin{bmatrix} \rho_i \\ \rho_i \mathbf{u}_i \\ \rho_i \mathbf{e}_i \end{bmatrix} + \begin{bmatrix} 0 \\ \nabla \cdot \mathbb{P}_i \\ \text{Sym2}(\nabla \cdot (\mathbb{P}_i \mathbf{u}_i)) + \nabla \cdot \mathbf{q}_i \end{bmatrix} &= \sigma_i \begin{bmatrix} 0 \\ \mathbf{E} + \mathbf{u}_i \times \mathbf{B} \\ \text{Sym2}(\mathbf{u}_i \mathbf{E} + \mathbf{e}_i \times \mathbf{B}) \end{bmatrix} + \begin{bmatrix} 0 \\ \mathbf{R}_i \\ \mathbb{R}_i + \mathbb{Q}_i \end{bmatrix} \\ \bar{\delta}_t^e \begin{bmatrix} \rho_e \\ \rho_e \mathbf{u}_e \\ \rho_e \mathbf{e}_e \end{bmatrix} + \begin{bmatrix} 0 \\ \nabla \cdot \mathbb{P}_e \\ \text{Sym2}(\nabla \cdot (\mathbb{P}_e \mathbf{u}_e)) + \nabla \cdot \mathbf{q}_e \end{bmatrix} &= \sigma_e \begin{bmatrix} 0 \\ \mathbf{E} + \mathbf{u}_e \times \mathbf{B} \\ \text{Sym2}(\mathbf{u}_e \mathbf{E} + \mathbf{e}_e \times \mathbf{B}) \end{bmatrix} + \begin{bmatrix} 0 \\ \mathbf{R}_e \\ \mathbb{R}_e + \mathbb{Q}_e \end{bmatrix} \end{aligned}$$

Maxwell's equations:

$$\begin{aligned} \partial_t \mathbf{B} + \nabla \times \mathbf{E} &= 0, & \nabla \cdot \mathbf{B} &= 0 \\ \partial_t \mathbf{E} - c^2 \nabla \times \mathbf{B} &= -\mathbf{J}/\epsilon_0, & \nabla \cdot \mathbf{E} &= \sigma/\epsilon_0 \end{aligned}$$

Definitions:

$$\begin{aligned} \sigma_i &= en_i, & \sigma_e &= -en_e, & \sigma &= \sigma_i + \sigma_e \\ \mathbf{J} &= \sigma_i \mathbf{u}_i + \sigma_e \mathbf{u}_e \\ \bar{\delta}_t^s \alpha &:= \partial_t \alpha + \nabla \cdot (\mathbf{u}_s \alpha) \end{aligned}$$

Closures:

$$\begin{aligned} \mathbb{R}_s &= -\tau_s^{-1} \mathbb{P}_s^\circ \\ \mathbf{q}_s &= -\frac{2}{5} \mathbf{K}_s \cdot \text{Sym3}(\boldsymbol{\pi}_s \cdot \nabla \mathbb{T}_s) \\ \mathbf{R}_i &= -\mathbf{R}_e = \sigma_i \sigma_e \boldsymbol{\eta} \cdot (\mathbf{u}_e - \mathbf{u}_i) \\ \mathbb{Q}_s &= ? \mathbb{Q}_s^f + \mathbb{Q}_s^t? \\ \mathbb{Q}_e^f &= \frac{m_i}{m_i + m_e} \text{Sym2}((\alpha_e^\parallel - \alpha_e^\perp) \mathbf{R}_i \mathbf{w}_e + \alpha_e^\perp \mathbf{R}_i \cdot \mathbf{w}_e \mathbb{1})? \\ \mathbb{Q}_e^t &= \frac{2}{3} K_{ei} n_e n_i (\mathbb{T}_i - \mathbb{T}_e)? \end{aligned}$$

Figure 4: Equations of the 10-moment 2-fluid Maxwell model.

The interspecies collisional terms \mathbf{R}_s and \mathbb{Q}_s are generally ignored in this work. The intraspecies collisional terms \mathbb{R}_s are used in the simulations and play a critical role; we study reconnection as the isotropization rates τ_s are dialed between 0 and ∞ . The simulations neglect \mathbf{q}_s , evidently causing late-time singularities.

Five-moment two-fluid Maxwell model

Gas dynamics equations

$$\begin{aligned} \bar{\delta}_t^i \begin{bmatrix} \rho_i \\ \rho_i \mathbf{u}_i \\ \rho_i e_i \end{bmatrix} + \begin{bmatrix} 0 \\ \nabla p_i + \nabla \cdot \mathbb{P}_i^\circ \\ \nabla \cdot (\mathbf{u}_i p_i) + \nabla \cdot (\mathbf{u}_i \cdot \mathbb{P}_i^\circ) + \nabla \cdot \mathbf{q}_i \end{bmatrix} &= \sigma_i \begin{bmatrix} 0 \\ \mathbf{E} + \mathbf{u}_i \times \mathbf{B} \\ \mathbf{u}_i \cdot \mathbf{E} \end{bmatrix} + \begin{bmatrix} 0 \\ \mathbf{R}_i \\ Q_i \end{bmatrix} \\ \bar{\delta}_t^e \begin{bmatrix} \rho_e \\ \rho_e \mathbf{u}_e \\ \rho_e e_e \end{bmatrix} + \begin{bmatrix} 0 \\ \nabla p_e + \nabla \cdot \mathbb{P}_e^\circ \\ \nabla \cdot (\mathbf{u}_e p_e) + \nabla \cdot (\mathbf{u}_e \cdot \mathbb{P}_e^\circ) + \nabla \cdot \mathbf{q}_e \end{bmatrix} &= \sigma_e \begin{bmatrix} 0 \\ \mathbf{E} + \mathbf{u}_e \times \mathbf{B} \\ \mathbf{u}_e \cdot \mathbf{E} \end{bmatrix} + \begin{bmatrix} 0 \\ \mathbf{R}_e \\ Q_e \end{bmatrix} \end{aligned}$$

Maxwell's equations:

$$\begin{aligned} \partial_t \mathbf{B} + \nabla \times \mathbf{E} &= 0, & \nabla \cdot \mathbf{B} &= 0 \\ \partial_t \mathbf{E} - c^2 \nabla \times \mathbf{B} &= -\mathbf{J}/\epsilon_0, & \nabla \cdot \mathbf{E} &= \sigma/\epsilon_0 \end{aligned}$$

Definitions:

$$\begin{aligned} \sigma_i &= en_i, & \sigma_e &= -en_e, & \sigma &= \sigma_i + \sigma_e \\ \mathbf{J} &= \sigma_i \mathbf{u}_i + \sigma_e \mathbf{u}_e \\ \bar{\delta}_t^s \alpha &:= \partial_t \alpha + \nabla \cdot (\mathbf{u}_s \alpha) \end{aligned}$$

Closures:

$$\begin{aligned} \mathbb{P}_s^\circ &= -\boldsymbol{\mu} : \text{Sym}2(\nabla \mathbf{u})^\circ \\ \mathbf{q}_s &= -\mathbf{k} \cdot \nabla T \\ \mathbf{R}_i &= -\mathbf{R}_e = \sigma_i \sigma_e \boldsymbol{\eta} \cdot (\mathbf{u}_e - \mathbf{u}_i) \\ Q_s &= ?Q_s^f + Q_s^t(?) \\ Q_i^f &= \mathbf{R}_i \cdot (\mathbf{u}_e - \mathbf{u}_i) \frac{m_e}{m_i + m_e} (?) \\ Q_i^t &= K_{ie} n_i n_e (T_e - T_i) (?) \end{aligned}$$

Figure 5: Equations of the 5-moment 2-fluid Maxwell model.

The interspecies collisional terms \mathbf{R}_s and Q_s are generally ignored in this work. The simulations also neglect \mathbb{P}_s° and \mathbf{q}_s , evidently causing late-time singularities.

Ten-moment two-fluid MHD

Pressure evolution:

$$n_i d_t \mathbb{T}_i + \text{Sym2}(\mathbb{P}_i \cdot \nabla \mathbf{u}_i) + \nabla \cdot \mathbf{q}_i = \frac{q_i}{m_i} \text{Sym2}(\mathbb{P}_i \times \mathbf{B}) + \mathbb{R}_i + \mathbb{Q}_i$$

$$n_e d_t \mathbb{T}_e + \text{Sym2}(\mathbb{P}_e \cdot \nabla \mathbf{u}_e) + \nabla \cdot \mathbf{q}_e = \frac{q_e}{m_e} \text{Sym2}(\mathbb{P}_e \times \mathbf{B}) + \mathbb{R}_e + \mathbb{Q}_e$$

mass and momentum:

$$\partial_t \rho + \nabla \cdot (\mathbf{u} \rho) = 0$$

$$\rho d_t \mathbf{u} + \nabla \cdot (\mathbb{P}_i + \mathbb{P}_e + \mathbb{P}^d) = \mathbf{J} \times \mathbf{B}$$

Electromagnetism

$$\partial_t \mathbf{B} + \nabla \times \mathbf{E} = 0, \quad \nabla \cdot \mathbf{B} = 0$$

$$\mathbf{J} = \mu_0^{-1} \nabla \times \mathbf{B}$$

Ohm's law

$$\mathbf{E} = \boldsymbol{\eta} \cdot \mathbf{J} + \mathbf{B} \times \mathbf{u} + \frac{m_i - m_e}{e\rho} \mathbf{J} \times \mathbf{B}$$

$$+ \frac{1}{e\rho} \nabla \cdot (m_e \mathbb{P}_i - m_i \mathbb{P}_e)$$

$$+ \frac{m_i m_e}{e^2 \rho} \left[\partial_t \mathbf{J} + \nabla \cdot \left(\mathbf{u} \mathbf{J} + \mathbf{J} \mathbf{u} - \frac{m_i - m_e}{e\rho} \mathbf{J} \mathbf{J} \right) \right]$$

Definitions:

$$d_t := \partial_t + \mathbf{u}_s \cdot \nabla$$

$$\mathbb{P}^d := \rho_i \mathbf{w}_i \mathbf{w}_i + \rho_e \mathbf{w}_e \mathbf{w}_e$$

$$\mathbf{w}_i = \frac{m_e \mathbf{J}}{e\rho}, \quad \mathbf{u}_i = \mathbf{u} + \mathbf{w}_i$$

$$\mathbf{w}_e = \frac{m_i \mathbf{J}}{-e\rho}, \quad \mathbf{u}_e = \mathbf{u} + \mathbf{w}_e$$

Closures:

$$\mathbb{R}_s = -\tau_s^{-1} \mathbb{P}_s^o$$

$$\mathbf{q}_s = -\frac{2}{5} \mathbf{K}_s \text{: Sym3}(\boldsymbol{\pi} \cdot \nabla \mathbb{T}_s)$$

$$-\mathbf{R}_i = \mathbf{R}_e = ne \boldsymbol{\eta} \cdot \mathbf{J}$$

$$\mathbb{Q}_s = \mathbb{Q}_s^f + \mathbb{Q}_s^t?$$

Figure 6: Equations of 10-moment 2-fluid MHD.

This system is derived but not simulated in this work. Simulations instead solve the two-fluid Maxwell equations with light speed intended to be sufficiently high to approximate this system.

Five-moment two-fluid MHD

Pressure evolution:

$$\begin{aligned}\frac{3}{2}nd_tT_i + p_i\nabla\cdot\mathbf{u}_i + \mathbb{P}_i^\circ:\nabla\mathbf{u}_i + \nabla\cdot\mathbf{q}_i &= Q_i \\ \frac{3}{2}nd_tT_e + p_e\nabla\cdot\mathbf{u}_e + \mathbb{P}_e^\circ:\nabla\mathbf{u}_e + \nabla\cdot\mathbf{q}_e &= Q_e\end{aligned}$$

mass and momentum:

$$\begin{aligned}\partial_t\rho + \nabla\cdot(\mathbf{u}\rho) &= 0 \\ \rho d_t\mathbf{u} + \nabla\cdot(\mathbb{P}_i + \mathbb{P}_e + \mathbb{P}^d) &= \mathbf{J}\times\mathbf{B}\end{aligned}$$

Electromagnetism

$$\begin{aligned}\partial_t\mathbf{B} + \nabla\times\mathbf{E} &= 0, \quad \nabla\cdot\mathbf{B} = 0 \\ \mathbf{J} &= \mu_0^{-1}\nabla\times\mathbf{B}\end{aligned}$$

Ohm's law

$$\begin{aligned}\mathbf{E} &= \boldsymbol{\eta}\cdot\mathbf{J} + \mathbf{B}\times\mathbf{u} + \frac{m_i-m_e}{e\rho}\mathbf{J}\times\mathbf{B} \\ &+ \frac{1}{e\rho}\nabla\cdot(m_e(p_i\mathbf{1} + \mathbb{P}_i^\circ) - m_i(p_e\mathbf{1} + \mathbb{P}_e^\circ)) \\ &+ \frac{m_im_e}{e^2\rho}\left[\partial_t\mathbf{J} + \nabla\cdot\left(\mathbf{u}\mathbf{J} + \mathbf{J}\mathbf{u} - \frac{m_i-m_e}{e\rho}\mathbf{J}\mathbf{J}\right)\right]\end{aligned}$$

Definitions:

$$\begin{aligned}d_t &:= \partial_t + \mathbf{u}_s\cdot\nabla \\ \mathbb{P}^d &:= \rho_i\mathbf{w}_i\mathbf{w}_i + \rho_e\mathbf{w}_e\mathbf{w}_e \\ \mathbf{w}_i &= \frac{m_e\mathbf{J}}{e\rho}, \quad \mathbf{u}_i = \mathbf{u} + \mathbf{w}_i \\ \mathbf{w}_e &= \frac{m_i\mathbf{J}}{-e\rho}, \quad \mathbf{u}_e = \mathbf{u} + \mathbf{w}_e\end{aligned}$$

Closures:

$$\begin{aligned}\mathbb{P}_s^\circ &= -\boldsymbol{\mu}:\text{Sym}2(\nabla\mathbf{u})^\circ \\ \mathbf{q}_s &= -\mathbf{k}\cdot\nabla T \\ -\mathbf{R}_i &= \mathbf{R}_e = ne\boldsymbol{\eta}\cdot\mathbf{J} \\ Q_s &= Q_s^f + Q_s^t?\end{aligned}$$

Figure 7: Equations of 5-moment 2-fluid MHD.

This system is derived but not simulated in this work. Simulations instead solve the two-fluid Maxwell equations with light speed intended to be sufficiently high to approximate this system.

Ten-moment relaxation closure

Implicit closure (A.20)

$$\mathbf{q} + \text{Sym3}(\tilde{\omega} \mathbf{b} \times \mathbf{q}) = -\frac{2}{5}k \text{Sym3}(\boldsymbol{\pi} \cdot \nabla \mathbb{T}),$$

Definitions:

$$\begin{aligned} \mathbf{b} &:= \mathbf{B}/|\mathbf{B}| \\ \omega_c &:= \frac{q_s}{m_s} |\mathbf{B}| \\ \tilde{\omega} &:= \tilde{\tau} \omega_c \\ \varpi &:= \tau \omega_c \\ \tilde{\tau} &:= \tau / \text{Pr} \end{aligned}$$

Explicit closure (A.35)

$$\begin{aligned} \mathbf{q} &= -\frac{2}{5}k \tilde{\mathbf{K}} : \text{Sym3}(\boldsymbol{\pi} \cdot \nabla \mathbb{T}) \\ &= -\frac{2}{5}k \text{Sym3}(\tilde{\mathbf{K}}' : \text{Sym3}(\boldsymbol{\pi} \cdot \nabla \mathbb{T})) \end{aligned}$$

where equation (A.37) gives

$$\begin{aligned} \tilde{\mathbf{K}} &= \left(\mathbb{1}_{\parallel}^3 + \frac{3}{2} \mathbb{1}_{\parallel} (\mathbb{1}_{\perp}^2 + \mathbb{1}_{\wedge}^2) \right) \\ &+ \frac{3}{1 + \tilde{\omega}^2} \left(\mathbb{1}_{\perp} \mathbb{1}_{\parallel}^2 - \tilde{\omega} \mathbb{1}_{\wedge} \mathbb{1}_{\parallel}^2 \right) \\ &+ \frac{3}{1 + 4\tilde{\omega}^2} \left(\frac{\mathbb{1}_{\perp}^2 - \mathbb{1}_{\wedge}^2}{2} \mathbb{1}_{\parallel} - 2\tilde{\omega} \mathbb{1}_{\wedge} \mathbb{1}_{\perp} \mathbb{1}_{\parallel} \right) \\ &+ (k_0 \mathbb{1}_{\perp}^3 + k_1 \mathbb{1}_{\wedge} \mathbb{1}_{\perp}^2 + k_2 \mathbb{1}_{\wedge}^2 \mathbb{1}_{\perp} + k_3 \mathbb{1}_{\wedge}^3), \end{aligned}$$

Definitions:

$$\begin{aligned} \mathbb{1}_{\parallel} &:= \mathbf{b} \mathbf{b} \\ \mathbb{1}_{\perp} &:= \mathbb{1} - \mathbb{1}_{\parallel} \\ \mathbb{1}_{\wedge} &= \mathbb{1} \times \mathbf{b} \end{aligned}$$

Relations:

$$\frac{2}{5}k = \frac{p\tau}{m \text{Pr}}$$

The remaining coefficients are (A.34)

$$\begin{aligned} k_3 &:= \frac{-6\tilde{\omega}^3}{1 + 10\tilde{\omega}^2 + 9\tilde{\omega}^4} = -\frac{2}{3}\tilde{\omega}^{-1} + \mathcal{O}(\tilde{\omega}^{-3}), \\ k_2 &:= \frac{6\tilde{\omega}^2 + 3\tilde{\omega}(1 + 3\tilde{\omega}^2)k_3}{1 + 7\tilde{\omega}^2} = \mathcal{O}(\tilde{\omega}^{-2}), \\ k_1 &:= \frac{-3\tilde{\omega} + 2\tilde{\omega}k_2}{1 + 3\tilde{\omega}^2} = -\tilde{\omega}^{-1} + \mathcal{O}(\tilde{\omega}^{-3}), \\ k_0 &:= 1 + \tilde{\omega}k_1 = \mathcal{O}(\tilde{\omega}^{-2}). \end{aligned}$$

Figure 8: Ten-moment Gaussian-BGK closure.

All tensor products in the formula for $\tilde{\mathbf{K}}$ are splice symmetric products. The formula for $\tilde{\mathbf{K}}'$ is exactly the same as for $\tilde{\mathbf{K}}$ except that the products may be taken simply to be splice products as in (A.38).

Five-moment relaxation closure

Implicit closure (A.18), (A.19)

$$\begin{aligned}\mathbf{q} + \tilde{\omega}\mathbf{b} \times \mathbf{q} &= -k\nabla T, \\ \mathbb{P}^\circ + \text{Sym}2(\tilde{\omega}\mathbf{b} \times \mathbb{P}^\circ) &= -\mu 2\mathbf{e}^\circ\end{aligned}$$

Definitions:

$$\begin{aligned}\mathbf{b} &:= \mathbf{B}/|\mathbf{B}| \\ \omega_{cs} &:= \frac{q_s}{m_s}|\mathbf{B}| \\ \tilde{\omega} &:= \tilde{\tau}_s \omega_{cs} \\ \varpi &:= \tau_s \omega_{cs} \\ \tilde{\tau} &:= \tau/\text{Pr}\end{aligned}$$

Explicit closure (A.26):

$$\begin{aligned}\mathbf{q} &= -k\tilde{\mathbf{k}} \cdot \nabla T, \\ \mathbb{P}^\circ &= -2\mu\tilde{\boldsymbol{\mu}}:\mathbf{e}^\circ \\ &= -2\mu\text{Sym}(\tilde{\boldsymbol{\mu}}':\mathbf{e}^\circ)\end{aligned}$$

where by (A.25) and (A.30),

$$\begin{aligned}\tilde{\mathbf{k}} &:= \mathbb{1}_\parallel + \frac{1}{1 + \tilde{\omega}^2} \left(\mathbb{1}_\perp - \tilde{\omega} \mathbb{1}_\wedge \right), \\ \tilde{\boldsymbol{\mu}} &:= \left(\mathbb{1}_\parallel \mathbb{1}_\parallel + \frac{\mathbb{1}_\perp \mathbb{1}_\perp + \mathbb{1}_\wedge \mathbb{1}_\wedge}{2} \right) \\ &\quad + \frac{2}{1 + \tilde{\omega}^2} (\mathbb{1}_\perp \mathbb{1}_\parallel - \tilde{\omega} \mathbb{1}_\wedge \mathbb{1}_\parallel) \\ &\quad + \frac{1}{1 + 4\tilde{\omega}^2} \left(\frac{\mathbb{1}_\perp \mathbb{1}_\perp - \mathbb{1}_\wedge \mathbb{1}_\wedge}{2} - 2\tilde{\omega} \mathbb{1}_\wedge \mathbb{1}_\perp \right).\end{aligned}$$

Definitions:

$$\begin{aligned}\mathbb{1}_\parallel &:= \mathbf{b}\mathbf{b} \\ \mathbb{1}_\perp &:= \mathbb{1} - \mathbb{1}_\parallel \\ \mathbb{1}_\wedge &= \mathbb{1} \times \mathbf{b}\end{aligned}$$

Relations:

$$\begin{aligned}\mu_s &= p_s \tau_s \\ \frac{2}{5}k_s &= \frac{\mu_s}{m_s \text{Pr}_s}\end{aligned}$$

Figure 9: Five-moment Gaussian-BGK closure.

The tensor products in the formula for $\tilde{\boldsymbol{\mu}}$ in (1.5) are splice symmetric products. The formula for $\tilde{\boldsymbol{\mu}}'$ is exactly the same as for $\tilde{\boldsymbol{\mu}}$ except that the products may be taken simply to be splice products.

Relaxation coefficients

Relaxation periods

$$\tau_0 := \frac{12\pi^{3/2}}{\ln \Lambda} \left(\frac{\epsilon_0}{e^2} \right)^2, \quad (2.77)$$

$$\begin{aligned} \tau'_{ii} &= \tau_0 \sqrt{m_i} \frac{T_i^{3/2}}{n_i} \quad \text{or} \\ &= \tau_0 \sqrt{m_i} \frac{\sqrt{\det(\mathbb{T}_i)}}{n_i}, \end{aligned}$$

$$\begin{aligned} \tau'_{ee} &= \tau_0 \sqrt{m_e} \frac{T_e^{3/2}}{n_e} \quad \text{or} \\ &= \tau_0 \sqrt{m_e} \frac{\sqrt{\det(\mathbb{T}_e)}}{n_e}, \end{aligned}$$

$$\begin{aligned} \tau_i &= .96\tau'_{ii}, \\ \tau_e &= .52\tau'_{ee}, \end{aligned}$$

Temperature-determined coefficients

$$\mu_i = \tau_i p_i,$$

$$\mu_e = \tau_e p_e,$$

$$\frac{2}{5}k_i = \frac{\mu_i}{m_i \text{Pr}_i},$$

$$\frac{2}{5}k_e = \frac{\mu_e}{m_e \text{Pr}_e},$$

$$\text{Pr}_i = .61 \approx \frac{2}{3},$$

$$\text{Pr}_e = .58 \approx \frac{2}{3},$$

$$\eta_0 := \frac{m_e \sqrt{2}}{e^2 n_e \tau'_{ee}},$$

$$\eta_{\parallel} := .51\eta_0,$$

$$\lim_{\omega \rightarrow \infty} \eta_{\perp} = \eta_0$$

These closures for a hydrogen plasma have been derived by Braginskii and others (see section 2.7.3) using a Coulomb collision operator and assuming a strongly collisional plasma. Fast magnetic reconnection is a collisionless phenomenon and therefore substantial deviation is expected from these closures. Therefore, we are content with rough and simple approximations of Braginskii's coefficients. In particular, there is likely no great loss in assuming a scalar resistivity with value η_0 or likewise assuming isotropic relaxation for other nondiffusive closure coefficients (in comparison to the Braginskii closure).

Figure 10: Relaxation coefficients

Chapter 2

Models of Plasma

The purpose of this chapter is primarily to develop the equations listed at the end of the previous chapter.

2.1 Overview

We consider plasma to consist of charged particles of two types of particles (called *species*) subject only to electromagnetic forces. We ignore gravitational effects, quantum effects, and nuclear forces.

Therefore, as our fundamental standard of truth we assume that the electromagnetic field is governed by Maxwell's equations of electromagnetism and that particle motion is governed by the Lorentz force law and the relativistic version of Newton's second law.

Our practical standard of truth will be the nonrelativistic Boltzmann equation. This involves two simplifications: (1) we represent particle distributions with a continuum distribution and (2) we neglect relativity. Each of these simplifications entails issues and problems.

Regarding the first simplification, the Boltzmann equation is incomplete as a standard of truth until a collision operator is specified. One of the main points of this dissertation is to study the dependence of reconnection on the choice of collision operator.

Regarding the second simplification, we expect fundamental physical laws to be invariant under change of reference frame. Physical laws are **Lorentz-invariant** if they remain unchanged under Lorentz transformations. A **Lorentz transformation** is a linear transformation of space-time that leaves light speed invariant and respects the direction of time and the scale and orientation of space-time. Physical laws are **Galilean-invariant** if they remain unchanged under Galilean transformations. A **Galilean transformation** is a linear transformation of space-time that leaves time and distance invariant and respects the direction of time and the scale and orientation of space. We say that physical laws *satisfy a relativity principle* if they are Galilean-invariant or Lorentz-invariant. We say that physical laws are *relativistic* (in the sense of Einstein's theory of special relativity) if they are Lorentz-invariant.

The non-relativistic Boltzmann-Maxwell system is an intermediate system which is neither fully Lorentz-invariant nor fully Galilean-invariant. Maxwell's equations (with prescribed Lorentz-invariantly-defined current and charge density) are Lorentz-invariant. The nonrelativistic Boltzmann equation (with prescribed Galilean-invariantly-defined electromagnetic field) are Galilean-invariant. One of these systems must be modified for the system to satisfy a relativity principle.

The simplifying assumptions of MHD provide a fully Galilean-invariant system, essentially by taking the light speed to infinity. MHD models that admit fast magnetic reconnection admit fast waves and require implicit numerical methods, which are not easy to implement.

The non-relativistic Boltzmann-Maxwell system that I have chosen to implement is something of a toy model. It leads to fluid models that are conceptually simple and can be implemented with

explicit numerical methods. Nonrelativistic two-fluid-Maxwell models arise from taking moments of the non-relativistic Boltzmann-Maxwell system. My simulations study the ability of non-relativistic two-fluid-Maxwell models to agree with the two-species non-relativistic Boltzmann-Maxwell system. In the relativistic regime one would instead prefer a fully relativistic two-fluid-Maxwell system. In the low-speed limit one would prefer an MHD system. I therefore discuss the equations and properties of MHD. Simulating with them would be a natural extension of this dissertation.

2.1.1 Kinetic models

We generally refer to models based on the evolving of particle states according to fundamental laws as **particle models**. *Particle-in-cell (PIC)* methods simulate plasma by a rescaling of the fundamental laws which leaves macroscopic physical quantities basically unchanged but reduces the number of particles to a computationally feasible number. At any given time the state of a particle is specified by its position in **phase space**, defined to be the pair (\mathbf{x}, \mathbf{v}) consisting of the particle's position \mathbf{x} and velocity \mathbf{v} .

Particle models are a type of kinetic model. **Kinetic models** evolve a representation of particle positions and velocities. Continuum kinetic models represent particles via *particle density functions* which specify the density of particles with a particular location and velocity. The simplest general continuum kinetic model is the [Boltzmann equation](#). The Boltzmann equation represents each species s with a particle mass density $f_s(t, \mathbf{x}, \mathbf{v})$ which is a function of time (t), spatial location (\mathbf{x}) and particle velocity (\mathbf{v}). The Boltzmann equation depends on the choice of a **collision operator** C_s , which specifies a model for how particles collide. If the collision operator is entirely neglected, then the Boltzmann equation is instead referred to as the **Vlasov equation**.

Simulation with kinetic models is highly expensive, because of the need to evolve a representation of the detailed distribution of particle velocities. Particle simulations typically track millions of particles, and a typical Vlasov simulation might be two orders of magnitude more expensive than a comparable particle simulation. The computational expensiveness of kinetic models is one of the motivations for developing *fluid models*.

2.1.2 Fluid models

Moments

Fluid models of plasma or gas allow simulation with greatly reduced expense. **Fluid models** assume that the distribution of particle velocities is characterized by a small set of parameters which are typically *moments* of the distribution. An n **th order moment** specifies at each time t and location \mathbf{x} the average value (averaged over all particles momentarily near \mathbf{x}) of a sum of products of n components of \mathbf{v} . The most important examples of moments are the (physically) **conserved moments**: mass density, momentum density, and energy density. The conserved moments are conserved in collisions. Collisions cause the velocity distribution to trend toward an equilibrium distribution characterized by its conserved moments. An equilibrium velocity distribution is bell-shaped and is known as a *Maxwellian distribution*. We refer to the conserved moments as *Maxwellian moments*.

Five-moment model.

The simplest and most well-justified model of a gas is the **five-moment model**, which represents the state of the gas in terms of the conserved moments. In the three-dimensional space of our physical world the conserved moments are the “first five moments”: the mass density $\rho_s := \int_{\mathbf{v} \in \mathbb{R}^3} f_s$ (which is the zeroth-order moment), the momentum density $\mathbf{M}_s := \rho_s \mathbf{u}_s := \int_{\mathbf{v} \in \mathbb{R}^3} f_s \mathbf{v}$ (three first-order moments, one for each component of the velocity/momentum), and the energy density $\mathcal{E}_s := \rho_s e_s := \int_{\mathbf{v} \in \mathbb{R}^3} f_s (v_1^2 + v_2^2 + v_3^2)/2$ (the conserved second-order moment). Here \mathbb{R} denotes the real numbers.

Primitive and conservation variables.

Note that the fluid velocity \mathbf{u}_s is defined to be the average velocity of particles of species s . We define the **thermal velocity** $\mathbf{c}_s := \mathbf{v} - \mathbf{u}_s$ to be the velocity of a particle in the reference frame defined by the local fluid velocity. The first moments of \mathbf{c}_s are by definition zero; other moments of the particle velocity \mathbf{v} are equivalent to moments of the thermal velocity \mathbf{c} . For example, $\rho_s e_s = \rho_s |\mathbf{u}_s|^2/2 + (3/2)p_s$, where $p_s := \int_{\mathbf{c} \in \mathbb{R}^3} f_s |\mathbf{c}|^2/3$ is the pressure. The fluid velocity \mathbf{u}_s and the non-first-order moments of \mathbf{c} (including density and pressure) are called **primitive variables**. In contrast, we refer to moments of \mathbf{v} as **conservation variables**, not because they are all conserved, but because they would be conserved except for nondifferentiated source terms that represent particle collisions and interaction with the electromagnetic field. I remark that fluid closures are naturally defined in terms of moments of \mathbf{c} ; closures thus defined in the reference frame of the fluid are by definition independent of reference frame.

Ten-moment model.

Extended-moment fluid models use additional moments of order two or higher to represent the particle velocity distribution more accurately. For plasmas with nonzero magnetic field, the simplest extended-moment fluid model is the **gyrotropic (six-moment) model**. Instead of evolving a single energy moment (or scalar pressure), the gyrotropic model evolves a pressure component parallel to the magnetic field and a pressure component perpendicular to the magnetic field. This representation is natural in a strongly magnetized plasma due to the rapid rotation of particles around field lines and the relatively slow trend to equilibrium of velocity components parallel to the magnetic field.

In unmagnetized regions of low-collisionality velocity distributions do not have a magnetic field to align with and trend slowly to equilibrium. In such regions pressure can become highly anisotropic or agyrotropic. The **ten-moment model** evolves all six independent second-order monomial moments, which define a full pressure tensor, allowing it to represent highly anisotropic and agyrotropic pressures.

Extended-moment models of plasma for reconnection

The use of ten-moment gas dynamics is particularly relevant for nearly collisionless magnetic reconnection near a magnetic null point or null line. In the general case of steady two-dimensional non-resistive magnetic reconnection symmetric under 180-degree rotations about an X-point, pressure cannot be gyrotropic in the vicinity of the X-point (see section 3.3.3). Moreover, in the special case of antiparallel reconnection with reflectional symmetry across both axes, simulations of the

GEM problem with a near-collisionless ten-moment model develop strong gyroviscosity in the vicinity of the X-point. A diffusive closure for the viscous pressure in terms of the fluid velocity gradient allows the five-moment (isotropic) model to accurately simulate small perturbations from isotropy and allows the six-moment (gyrotropic) model to accurately simulate small perturbations from gyroviscosity. But these diffusive closures are based on the assumption of high collisionality.

In contrast, the use of a ten-moment model with relaxation of the pressure tensor toward isotropy or gyroviscosity not only agrees with the viscous isotropic and gyroviscous models in the high-collisionality limit, but also allows the isotropization rate, equivalent to the collision rate, to be dialed over the full range between zero and infinity, making it appropriate for study and simulation of low-collisionality plasmas. In particular, *the ten-moment model seems to be the simplest fluid model for which one can study the dependence of magnetic reconnection on the collision operator as the collision rate is taken to zero*. This may give qualitative insight into the behavior of kinetic models as the collision operator is taken to zero.

In chapter 3 we argue that to simulate sustained magnetic reconnection it is necessary to admit heat flux at least in some cases. Therefore we derive a ten-moment heat flux closure in this chapter.

Chapter 3 also includes a ten-moment adiabatic simulation of a pair plasma version of the *GEM magnetic reconnection challenge problem* as the collision rate is dialed between zero and infinity. The absence of heat flux in the model results in instabilities when simulating the GEM problem past the time of the peak reconnection rate.

I propose doing a similar study of this problem for the Boltzmann equation using a *Gaussian-BGK* collision operator.

A study of vanishing collisionality using the ten-moment model is admittedly artificial from a physical perspective. In particular, as the collision rate goes to zero the heat flux must go to infinity unless one artificially takes the Prandtl number to infinity. In fact, to study the effects of vanishing entropy production in the low-collisionality limit it would be necessary to take the heat flux to *zero* as the collision rate goes to zero. This is highly unphysical.

In the zero-collisionality limit of the Boltzmann equation the rate of isotropization (i.e. the rate of decay of the deviatoric pressure) and the rate of decay of the heat flux both go to zero. The ten-moment model is able to study vanishing isotropization because it *evolves deviatoric pressure*. But it is not able to study vanishing heat flux decay because it uses a diffusive closure for the heat flux (in terms of spatially differentiated state variables).

To study vanishing heat flux decay requires a model which *evolves heat flux*. Heat flux is a third-order moment. Models which evolve such superquadratic moments are called *higher-moment models*.

The challenge in formulating a fluid moment model which evolves heat flux is to define a *hyperbolic closure* for the unevolved moments in the equations. For the ten-moment model a hyperbolic closure is to set the heat flux to zero. This closure guarantees that pressure and density will not go negative and that the equations remain hyperbolic (that is, well-posed, meaning that the solution depends continuously on the data) as the solution evolves. For higher-moment models, however, it is not clear how to define hyperbolic closures. In particular, in order to approach Galilean-invariance, hyperbolic higher-moment closures have to admit wave speeds that approach infinity for states arbitrarily close to equilibrium [44, 42].

In contrast, a *Lorentz-invariant hyperbolic higher-moment closure* would presumably bound wave speeds by the speed of light. A natural way to formulate such a closure is to choose an assumed form for the family of possible particle velocity distribution functions (just as one assumes a Maxwellian

distribution for the five-moment hyperbolic closure and a Gaussian distribution (equation (2.18)) for the ten-moment hyperbolic closure). It is not known how to choose such a distribution so that solutions remain hyperbolic and *realizable* (that is, the evolved moments are those of a distribution of the assumed form). To get a closure in explicit form one needs to be able to compute in closed form the integrals giving the unevolved moments in the equations. Torrilhon has used a Pearson-IV velocity distribution family to obtain closed-form closures for the Galilean-invariant Boltzmann equation [60], but for the Lorentz-invariant Boltzmann equation, except in the case of a Maxwellian distribution of proper velocities, which has the unique property that the distribution may be represented as the product of one-dimensional distributions, it seems highly unlikely that one can formulate an assumed family of distributions for which the integrals can be computed in closed form and for which solutions remain hyperbolic and the moments remain realizable by a distribution. One therefore would have to resort to numerical quadrature for these integrals over three-dimensional velocity space, which would be very expensive unless some simplifying technique can be identified.

The ten-moment model not only allows a fluid study of vanishing pressure isotropization (which generally implies that the pressure is *not* isotropic) but has the additional general benefit that one can study nonvanishing viscosity (i.e. nonvanishing deviatoric pressure) efficiently with an explicit numerical method.

Likewise, a higher-moment fluid model would not only allow a fluid study of vanishing heat flux decay (which generally implies that the heat flux is *nonvanishing*) but would have the additional general benefit that one could study nonvanishing heat conductivity (i.e. nonvanishing heat flux) efficiently with an explicit numerical method.

In summary, what I seek is a Lorentz-invariant higher-moment plasma model; it would serve as a fluid analog of the relativistic Boltzmann equation with Gaussian-BGK closure. The ultimate extension of this dissertation would be to simulate fast magnetic reconnection in the low-collisionality limit with a Lorentz-invariant higher-moment plasma model using an explicit numerical method. This is my dream.

2.2 Equations of kinetic models

2.2.1 Particle models (PIC)

Particle models of plasma are based on the fundamental laws of classical electrodynamics: **Newton's second law**,

$$m_p d_t \tilde{\mathbf{v}}_p = \mathbf{F}_p, \quad \mathbf{v}_p := d_t \mathbf{x}_p,$$

the **Lorentz force law**,

$$\mathbf{F}_p = q_p (\mathbf{E} + \mathbf{v} \times \mathbf{B}),$$

and **Maxwell's equations**,

$$\partial_t \mathbf{B} + \nabla \times \mathbf{E} = 0, \quad \nabla \cdot \mathbf{B} = 0, \quad (2.1)$$

$$\partial_t \mathbf{E} - c^2 \nabla \times \mathbf{B} = -\mathbf{J}/\epsilon_0, \quad \nabla \cdot \mathbf{E} = \sigma/\epsilon_0, \quad (2.2)$$

where \mathbf{B} is magnetic field, \mathbf{E} is electric field, and current \mathbf{J} and charge density ¹ σ are given by

$$\mathbf{J} = \sum_{\mathbf{p}} q_{\mathbf{p}} \mathbf{v}_{\mathbf{p}} \delta_{\mathbf{x}_{\mathbf{p}}}, \quad \sigma = \sum_{\mathbf{p}} q_{\mathbf{p}} \delta_{\mathbf{x}_{\mathbf{p}}};$$

here c is the speed of light, ϵ_0 is permittivity of space, \mathbf{p} is particle index, m_p is particle mass, q_p is particle charge, \mathbf{x}_p is particle position, \mathbf{v}_p is particle velocity, and $\tilde{\mathbf{v}}_p$ (i.e. $\gamma_p \mathbf{v}_p$) is the proper velocity, where $\gamma := (1 - (v/c)^2)^{-1/2}$, the Lorentz factor, is the rate of elapse of time with respect to proper time, where the elapse of proper time is defined in the reference frame of a particle moving with velocity \mathbf{v} .

In case $|v| \ll c$, $\gamma \approx 1$ and we can use the nonrelativistic approximation $\tilde{\mathbf{v}} \approx \mathbf{v}$.

2.2.2 Boltzmann/Vlasov equations

The **Boltzmann equation** or **kinetic equation** is written

$$\partial_t f_s + \nabla_{\mathbf{x}} \cdot (\mathbf{v} f_s) + \nabla_{\tilde{\mathbf{v}}} \cdot (\mathbf{a}_s f_s) = C_s / \gamma; \quad (2.3)$$

here $f_s(t, \mathbf{x}, \tilde{\mathbf{v}})$ is the particle density function of species s as a function of time and **phase space** $(\mathbf{x}, \tilde{\mathbf{v}})$, $\mathbf{a}_s = d_t \tilde{\mathbf{v}} = (q_s/m_s)(\mathbf{E} + \mathbf{v} \times \mathbf{B})$ is particle acceleration, and we recall that $\mathbf{v} = d_t \mathbf{x}$ is velocity and $\tilde{\mathbf{v}} = \gamma \mathbf{v}$ is proper velocity.

The Maxwell source terms are provided by the relations

$$\mathbf{J} = \sum_{\mathbf{s}} q_{\mathbf{s}} \int f_{\mathbf{s}} \mathbf{v} d\tilde{\mathbf{v}}, \quad \sigma := \sum_{\mathbf{s}} q_{\mathbf{s}} \int f_{\mathbf{s}} d\tilde{\mathbf{v}}.$$

The collision operator C_s specifies the rate of change of the particle distribution due to particle collisions and depends on the choice of collision model.

If we set $C_s = 0$ then we get the **Vlasov equation**. If we regard f_s as a linear superposition of spike functions then the Vlasov system with Maxwell's equations is equivalent to the fundamental equations of electrodynamics written in terms of individual particles. This is because at the microscale level particles do not actually collide; they interact with an electromagnetic field that becomes highly irregular in the vicinity of another particle.

Use of the Vlasov equation to resolve interaction of individual particles would require impossibly high resolution and would be enormously expensive computationally. (Actually, one would need a mechanism to maintain the singular electromagnetic field near individual particles, which would force it to be a particle method.) For this reason, we partition the electromagnetic field into a relatively large but smoothly varying *macro-scale* field that governs the interaction of particles with the plasma as a whole and a relatively small but highly irregular *microscale field* that mediates localized particle interactions. Rather than evolve the microscale electromagnetic field and microscale particle distribution function, we assume a smooth electromagnetic field and smooth particle distribution functions and model particle interactions via a collision operator. The *Coulomb collision operator* assumes that particle interactions occur pairwise and randomly (independently and in proportion to particle density) and are governed by the inverse square force law of electrostatics. Assuming

¹Electromagnetism books often use ρ for charge density, but I'm already using this for mass density, so I took the next letter of the alphabet, as does, for example, Balescu [2].

that the particle density function is smooth (reflecting a smooth estimate of the probability of the number of particles in a local region), the value of the collision operator will also be smooth.

Thus, while in (microscale) theory the Boltzmann equation is an approximation to the Vlasov equation, in (macro-scale) practice the Vlasov equation is an approximation to the Boltzmann equation under the assumption that particle collisions may be neglected for the phenomena or scales of interest.

2.3 Fluid balance equations of Galilean-invariant gas dynamics

Fluid equations are obtained from the Boltzmann equation by evaluating velocity moments and assuming closures for the unevolved moments that arise in terms of the evolved moments. In this section we evaluate velocity moments of the Boltzmann equation to obtain generic balance laws for mass, momentum, and various forms and consequences of energy evolution, including pressure, temperature, and entropy evolution. The fluid equations that we derive are Galilean-invariant rather than Lorentz-invariant. We do not consider closures in this section.

2.3.1 Notational conventions for fluid moments

Velocity-space integrals

Fluid quantities are functions of time and spatial location that are defined in terms of integrals of a particle distribution function over velocity space. By default integrals over velocity are taken over the full domain of possible velocities: $\int_{\mathbf{v}} := \int_{\mathbf{v} \in \mathbb{R}^3}$.

Let $f(t, \mathbf{x}, \mathbf{v})$ be the particle mass distribution of a gas. The primary fluid quantities that describe the gas are the density $\rho(t, \mathbf{x}) := \int_{\mathbf{v}} f$ and the velocity defined by $\rho \mathbf{u}(t, \mathbf{x}) := \int_{\mathbf{v}} \mathbf{v} f$. *Primitive variables* are most naturally defined in terms of moments of the thermal velocity $\mathbf{c}(t, \mathbf{x}, \mathbf{v}) := \mathbf{v} - \mathbf{u}(t, \mathbf{x})$. When integrating moments of \mathbf{c} , I typically write $\int_{\mathbf{c}}$ for $\int_{\mathbf{v}}$, since $\int_{\mathbf{c} \in \mathbb{R}^3} = \int_{\mathbf{v} \in \mathbb{R}^3}$.

Authors often use angle brackets to denote velocity-space integrals, following one of three conventions:

1. $\langle f\chi \rangle := \langle f\chi \rangle_f := \int_{\mathbf{v}} f\chi$. That is, $\langle \cdot \rangle$ simply denotes integration over velocities. In this notation the distribution is explicit and may thus be replaced with another distribution or the collision operator.
2. $\langle \chi \rangle := \langle \chi \rangle_f := \int_{\mathbf{v}} f\chi$. That is, $\langle \chi \rangle(t, \mathbf{x})$ denotes the density per volume of the quantity χ . This definition is intermediate between the other two.
3. $\rho \langle \chi \rangle := \rho \overline{\langle \chi \rangle} := \int_{\mathbf{v}} f\chi$. That is, $\langle \chi \rangle(t, \mathbf{x})$ denotes the statistical average value of χ at time t over all particles at point \mathbf{x} . It is a density per mass.

In this work we adopt convention (3) and simply write integrals for the other two cases.

Tensor products

In this document products of tensors are by default tensor products and powers of tensors are by default (unsymmetrized and uncontracted) tensor powers.

Let A be an n th order tensor and let B be an m th order tensor. Then by AB we mean the tensor product $A \otimes B$. In contrast, by \overline{AB} some authors mean the *symmetric* tensor product $\text{Sym}(AB)$, where Sym denotes the average over all permutations of subscripts. Except in section A.5 I always explicitly indicate symmetrization.

Some authors define the vee product by $A \vee B := \text{Sym}(AB)$, just as some authors define the wedge product by $A \wedge B := \text{Ant}(A \otimes B)$, where Ant denotes the average over all permutations of subscripts each multiplied by the sign of its permutation. Most authors, however, such as John Lee [36], define the wedge product by $A \wedge B := \frac{(n+m)!}{n!m!} \text{Ant}(A \otimes B)$; in case A and B are antisymmetric tensors this defines their wedge product to be the sum over all “distinguishable” signed permutations: specifically, there exists a partition of the $(n+m)!$ signed permutations of $A \otimes B$ into $\frac{(n+m)!}{n!m!}$ classes each containing $n!m!$ identical terms. For the antisymmetric product Lee instead uses the notation $A \bar{\wedge} B := \text{Ant}(A \otimes B)$.

Analogously, I define the vee product by

$$A \vee B := \frac{(n+m)!}{n!m!} \text{Sym}(A \otimes B); \quad (2.4)$$

in case A and B are symmetric tensors this defines their vee product to be the sum over all “distinguishable” permutations: specifically, there exists a partition of the $(n+m)!$ permutations of $A \otimes B$ into $\frac{(n+m)!}{n!m!}$ classes each containing $n!m!$ identical terms. For the symmetric product I instead use the notation $A \underline{\vee} B := \text{Sym}(A \otimes B)$.

Convective derivatives

It is natural to describe the evolution a fluid quantity $a(t, \mathbf{x})$ in terms of its rate of change as an observer moves with the fluid. Given a velocity field $\mathbf{u}(t, \mathbf{x})$, we define the **convective derivative** of a relative to \mathbf{u} to be $d_t^{\mathbf{u}} a := \partial_t a + \mathbf{u} \cdot \nabla_{\mathbf{x}} a$, the rate of change of a along a trajectory moving with the fluid. We write $d_t := d_t^{\mathbf{u}}$ when the relevant velocity field \mathbf{u} is clear; \mathbf{u} is generally understood to be the velocity of the fluid under consideration. Thus, when describing quantities defined in terms of an individual species, \mathbf{u} is by default taken to be the velocity of the species fluid, and when describing quantities summed over all species \mathbf{u} is by default taken to be the overall bulk fluid velocity including both species.

For convenience define the “**bulk derivative**” by $\bar{\delta}_t \alpha := \partial_t \alpha + \nabla \cdot (\mathbf{u} \alpha)$ for all α . Suppose that mass density $\rho(t, \mathbf{x})$ is conserved: $\bar{\delta}_t \rho = \partial_t \rho + \nabla \cdot (\rho \mathbf{u}) = 0$. Then the convective derivative of a is related to the bulk derivative of ρa :

$$\rho d_t a = \bar{\delta}_t (\rho a) = \partial_t (\rho a) + \nabla \cdot (\rho \mathbf{u} a).$$

Here a would be a density per mass and ρa would be a density per volume. While the convective derivative is conventional and widely used, the bulk derivative does not enjoy a common conventional name or notation. For this reason densities per mass (or per particle number) are often preferred.

2.3.2 Conservation moments

Our starting point for deriving Galilean-invariant fluid equations is the Galilean-invariant Boltzmann equation (equation (2.3) with γ taken as 1),

$$\partial_t f_s + \nabla_{\mathbf{x}} \cdot (\mathbf{v} f_s) + \nabla_{\mathbf{v}} \cdot (\mathbf{a}_s f_s) = C_s, \quad (2.5)$$

where $\mathbf{a}_s = (q_s/m_s)(\mathbf{E} + \mathbf{v} \times \mathbf{B})$ is acceleration due to the Lorentz force. In deriving fluid balance laws we take the electric field \mathbf{E} and the magnetic field \mathbf{B} as prescribed. To ensure that the Lorentz force is invariant under a Galilean transformation of inertial reference frame we assume (that is, pretend) that the electromagnetic field transforms according to

$$\begin{aligned} \mathbf{B}' &= \mathbf{B}, \\ \mathbf{E}' &= \mathbf{E} + d\mathbf{v} \times \mathbf{B}, \end{aligned}$$

where $d\mathbf{v} := \mathbf{v} - \mathbf{v}'$ is the velocity of the primed reference frame measured in the unprimed frame; this approximates the actual transformation of electromagnetic field and velocities when $d\mathbf{v}$ is much smaller than the speed of light.

Let $\chi(\mathbf{v})$ be a generic conservation velocity moment. Multiply both sides by χ and integrate by parts. Get the generic moment evolution equation

$$\partial_t \int_{\mathbf{v}} f_s \chi + \nabla \cdot \int_{\mathbf{v}} f_s \mathbf{v} \chi$$

Taking $\chi = 1$ gives an evolution equation for **density** $\rho_s := \int_{\mathbf{v}} f_s$,

$$\partial_t \rho_s + \nabla \cdot (\rho_s \mathbf{u}_s) = 0 \quad (2.6)$$

and taking $\chi = 1/m_s$ gives an evolution equation for **particle number density** $n_s := \rho_s/m_s$,

$$\partial_t n_s + \nabla \cdot (n_s \mathbf{u}_s) = 0. \quad (2.7)$$

Taking $\chi = \mathbf{v}$ gives an evolution equation for **momentum density**² $\mathbf{M}_s := \rho_s \mathbf{u}_s := \int_{\mathbf{v}} \mathbf{v} f_s$,

$$\partial_t (\rho_s \mathbf{u}_s) + \nabla \cdot (\rho_s \mathbf{u}_s \mathbf{u}_s + \mathbb{P}_s) = q_s n_s (\mathbf{E} + \mathbf{u}_s \times \mathbf{B}) + \mathbf{R}_s, \quad (2.8)$$

where $\mathbb{P}_s := \int_{\mathbf{c}} f_s \mathbf{c} \mathbf{c} = \rho_s (\mathbf{e}_s - \mathbf{u}_s \mathbf{u}_s)$ is the **pressure tensor** and $\mathbf{R}_s := \int_{\mathbf{v}} C_s \mathbf{v}$ is the (resistive) **drag force** due to collisions with other species. Taking $\chi = \mathbf{v} \mathbf{v}$ gives an evolution equation for the **energy tensor** $\mathbb{E}_s := \rho_s \mathbf{e}_s := \int_{\mathbf{v}} \mathbf{v} \mathbf{v} f_s$,

$$\partial_t (\rho_s \mathbf{e}_s) + \nabla \cdot (\rho_s \mathbf{u}_s \mathbf{e}_s) + \text{Sym}2(\nabla \cdot (\mathbb{P}_s \mathbf{u}_s)) + \nabla \cdot \mathbf{q}_s \quad (2.9)$$

$$= q_s n_s \text{Sym}2(\mathbf{u}_s \mathbf{E} + \mathbf{e}_s \times \mathbf{B}) + \text{Sym}2(\mathbf{u}_s \mathbf{R}_s) + \mathbb{R}_s + \mathbb{Q}_s, \quad (2.10)$$

where $\mathbf{q}_s := \int_{\mathbf{c}} f_s \mathbf{c} \mathbf{c} \mathbf{c}$ is the heat flux tensor, **Sym** denotes the symmetric part of its tensor argument, **Sym2** denotes twice the symmetric part of a second-order tensor, $\mathbb{R}_s + \mathbb{Q}_s := \int_{\mathbf{v}} \mathbf{v} \mathbf{v} C_s$ is collisional source of tensor energy, where the isotropization tensor $\mathbb{R}_s := \int_{\mathbf{v}} \mathbf{v} \mathbf{v} C_{ss}$ is the result of intraspecies collisions and the heating tensor $\mathbb{Q}_s := \sum_{p \neq s} \int_{\mathbf{v}} \mathbf{v} \mathbf{v} C_{sp}$ is the result of collisions with other species. Finally, taking half the trace of the energy tensor evolution equation (or taking $\chi = |\mathbf{v}|^2/2$) gives an evolution equation for the energy $\mathcal{E}_s := \rho_s e_s := \int_{\mathbf{v}} |\mathbf{v}|^2 f_s$,

$$\partial_t (\rho_s e_s) + \nabla \cdot (\rho_s \mathbf{u}_s e_s + \mathbf{u}_s \cdot \mathbb{P}_s + \mathbf{q}_s) = q_s n_s \mathbf{u}_s \cdot \mathbf{E} + Q_s, \quad (2.11)$$

where e_s is the energy per mass, $\mathbf{q}_s := \int_{\mathbf{c}} f_s \mathbf{c} |\mathbf{c}|^2/2 = \text{tr} \mathbf{q}_s/2$ is the heat flux, and $Q_s := \sum_{p \neq s} \int_{\mathbf{v}} C_{sp} |v|^2/2$ is the heat source due to collisions with other species.

²with apologies to the magnetization \vec{M} and to those who prefer to mind their p's and q's. The letter *P* has gotten out of hand. This dissertation is *not* brought to you by the letter “**P**” (nor “e”, nor “p”, nor “s”, nor “i”).

2.3.3 Pressure evolution

Multiplying the momentum evolution equation (2.8) by $2\mathbf{u}_s$, taking the symmetric part, and assuming a smooth solution gives the kinetic energy tensor evolution equation

$$\begin{aligned} & \partial_t(\rho_s \mathbf{u}_s \mathbf{u}_s) + \nabla \cdot (\rho_s \mathbf{u}_s \mathbf{u}_s \mathbf{u}_s) + \text{Sym}2(\mathbf{u}_s \nabla \cdot \mathbb{P}_s) \\ &= (q_s/m_s) \text{Sym}2(\rho_s \mathbf{u}_s \mathbf{E} + \rho_s \mathbf{u}_s \mathbf{u}_s \times \mathbf{B}) + \text{Sym}2(\mathbf{u}_s \mathbf{R}_s). \end{aligned}$$

Subtracting this kinetic energy tensor evolution equation from the energy tensor evolution equation (2.9) gives the pressure tensor evolution equation

$$\partial_t \mathbb{P}_s + \nabla \cdot (\mathbf{u}_s \mathbb{P}_s) + \text{Sym}2(\mathbb{P}_s \cdot \nabla \mathbf{u}_s) + \nabla \cdot \mathbf{q}_s = (q_s/m_s) \text{Sym}2(\mathbb{P}_s \times \mathbf{B}) + \mathbb{R}_s + \mathbb{Q}_s \quad (2.12)$$

(where we have used that $\text{Sym}2(\nabla \cdot (\mathbb{P}_s \mathbf{u}_s) - \mathbf{u}_s \nabla \cdot \mathbb{P}_s) = \text{Sym}2(\mathbb{P}_s \cdot \nabla \mathbf{u}_s)$). Alternatively, to obtain the pressure tensor evolution equation directly, multiply both sides of the Boltzmann equation by $\mathbf{c}\mathbf{c}$ and integrate by parts.

Scalar pressure evolution is half the trace of pressure tensor evolution:

$$(3/2)(\partial_t p_s + \nabla \cdot (\mathbf{u}_s p_s)) + p_s \nabla \cdot \mathbf{u}_s + \mathbb{P}^\circ : \nabla \mathbf{u}_s + \nabla \cdot \mathbf{q}_s = Q_s, \quad (2.13)$$

where $p_s := \text{tr } \mathbb{P}_s/3 = \int_{\mathbf{c}} f_s |\mathbf{c}|^2/3$ is the **scalar pressure**, $\mathbb{P}_s^\circ := \mathbb{P}_s - \mathbf{1} p_s$ is the deviatoric pressure tensor, and $:$ denotes contraction over two adjacent indices.

2.3.4 Temperature evolution

Conserved variables such as energy are volume densities which depend on the choice of reference frame. Pressure represents volume density of energy in the reference frame of the fluid. *Temperature* represents mass density of energy in the reference frame of the fluid. It is the natural quantity with which to represent energy evolution (1) in terms of convective derivatives and (2) independent of reference frame.

For a five-moment gas we define the **temperature** T_s to be the average thermal energy per particle, $T_s := p_s/n_s = m_s \langle |\mathbf{c}|^2 \rangle/3$, and we define the “**quasi**” **temperature** to be the thermal energy density per mass, $\theta_s := p_s/\rho_s = \langle |\mathbf{c}|^2 \rangle/3$. Note that $T_s = m_s \theta_s$.

For a ten-moment gas we define the **temperature tensor** by $\mathbb{T}_s := \mathbb{P}_s/n_s = m_s \langle \mathbf{c}\mathbf{c} \rangle$ and we define the “**quasi**” **temperature tensor** by $\Theta_s := \mathbb{P}_s/\rho_s = \langle \mathbf{c}\mathbf{c} \rangle$.

Using $n_s d_t \mathbb{T}_s = \bar{\delta}_t(n_s \mathbb{T}_s) = \bar{\delta}_t(\mathbb{P}_s)$, the pressure evolution equation (2.12) may also be regarded as a temperature evolution equation,

$$n_s d_t \mathbb{T}_s + \text{Sym}2(\mathbb{P}_s \cdot \nabla \mathbf{u}_s) + \nabla \cdot \mathbf{q}_s = (q_s/m_s) \text{Sym}2(\mathbb{P}_s \times \mathbf{B}) + \mathbb{R}_s + \mathbb{Q}_s. \quad (2.14)$$

Dividing by number density,

$$d_t \mathbb{T}_s + \text{Sym}2(\mathbb{T}_s \cdot \nabla \mathbf{u}_s) + n_s^{-1} \nabla \cdot \mathbf{q}_s = (q_s/m_s) \text{Sym}2(\mathbb{T}_s \times \mathbf{B}) + n_s^{-1} \mathbb{R}_s + n_s^{-1} \mathbb{Q}_s. \quad (2.15)$$

Scalar temperature evolution is half the trace of temperature tensor evolution. Equivalently, scalar pressure evolution (2.13) may be regarded as scalar temperature evolution using $n_s d_t T_s = \bar{\delta}_t(n_s T_s) = \bar{\delta}_t(p_s)$:

$$(3/2) n d_t T_s + n T_s \nabla \cdot \mathbf{u}_s + n \mathbb{T}^\circ : \nabla \mathbf{u}_s + \nabla \cdot \mathbf{q}_s = Q_s; \quad (2.16)$$

divided by number density,

$$(3/2) d_t T_s + T_s \nabla \cdot \mathbf{u}_s + \mathbb{T}_s^\circ : \nabla \mathbf{u}_s + n_s^{-1} \nabla \cdot \mathbf{q}_s = n_s^{-1} Q_s; \quad (2.17)$$

here $\mathbb{T}_s^\circ := \mathbb{T}_s - T_s \mathbf{1}$ (where $\mathbf{1}$ is the identity tensor) is the **deviatoric part** of the temperature tensor; we have separated it out in anticipation of the entropy-respecting five-moment closure.

2.4 Entropy evolution

2.4.1 Kinetic entropy evolution

The (statistical) **entropy density** of the particle density distribution $f_s(t, \mathbf{x}, \mathbf{v})$ is defined to be

$$S_s := \int_{\mathbf{v}} \eta_s, \quad \text{where} \quad \eta_s := -(\beta_s f_s \ln f_s + \alpha_s f_s);$$

S_s increases with randomness and measures the expected “surprise” or unlikelihood of the actual distribution of particles. The total gas-dynamic entropy is the sum of the entropies of the distributions. Collision operators are expected to cause the total statistical entropy to increase.

The constant α_s is arbitrary and may be freely chosen so that the entropy of equilibrium distributions has a simple formula. The constant β_s must be positive.

To ensure that interaction of particles of different species increases the total entropy, the scaling of β_s should be consistent among species. If f_s is taken to be a *number* density of particles in phase space then β_s should be equal (e.g. to 1) for all particle species; if f_s is taken to be a *mass* density then β_s should be proportional to m_s^{-1} .

One way to justify the definition of statistical entropy is to discretize state space and approximate the evolution of f_s by a Markov chain.

Recall the Boltzmann equation, which says that particles are conserved under flow in phase space. Since $\nabla_{\mathbf{x}} \cdot \mathbf{v} = 0$ and since $\nabla_{\mathbf{v}} \cdot \mathbf{a}_s = 0$ (because $\mathbf{a}_s = (q_s/m_s)(\mathbf{E} + \mathbf{v} \times \mathbf{B})$), flow in phase space is incompressible and can instead be written in terms of a material derivative in phase space:

$$\partial_t f_s + \mathbf{v} \cdot \nabla_{\mathbf{x}} f_s + \mathbf{a}_s \cdot \nabla_{\mathbf{v}} f_s = C_s;$$

this is not the natural form to use when deriving fluid conservation laws, but it is relevant in obtaining entropy evolution.

Multiply the Boltzmann equation by $\eta'_s := \frac{d\eta_s}{df_s}$. Using the chain rule,

$$\partial_t \eta_s + \mathbf{v} \cdot \nabla_{\mathbf{x}} \eta_s + \mathbf{a}_s \cdot \nabla_{\mathbf{v}} \eta_s = \eta'_s C_s.$$

Using phase space incompressibility to put it back into conservation form,

$$\partial_t \eta_s + \nabla_{\mathbf{x}} \cdot (\mathbf{v} \eta_s) + \nabla_{\mathbf{v}} \cdot (\mathbf{a}_s \eta_s) = \eta'_s C_s.$$

Integrate over velocity space. Get the entropy evolution equation

$$\partial_t S_s + \underbrace{\nabla_{\mathbf{x}} \cdot (\mathbf{v} \eta_s)}_{\text{Call } \Phi_s} = \underbrace{\int_{\mathbf{v}} \eta'_s C_s}_{\text{Call } \Psi_s};$$

Φ_s is the **entropy flux** and Ψ_s is the rate of **entropy production**. The content of Maxwell’s “H” theorem is that Ψ_s is zero precisely when f_s is a *Maxwellian* (equilibrium) velocity distribution; else it is strictly positive. Therefore, collisions cause distributions to trend toward equilibrium. In general we impose the H theorem as an assumption and a modeling requirement for collision operators.

To study properties and closure, we want to put entropy evolution in frame-invariant form. Define the molar entropy by $s_s := S_s/n_s$. Then

$$n_s d_t s_s + \nabla_{\mathbf{x}} \cdot \underbrace{\int_{\mathbf{c}} \mathbf{c} \eta_s}_{\text{Call } \Phi'_s} = \Psi_s.$$

We refer to Φ'_s as the **diffusive entropy flux**. It is the portion of the entropy flux that is not accounted for by fluid motion. We will see that it corresponds roughly to heat flux (divided by temperature).

2.4.2 Maxwellian limit

In the absence of other effects, collisions cause entropy to trend to a distribution that maximizes entropy subject to the constraint that mass, momentum, and energy must be conserved. Solving this constrained maximum problem by variational calculus shows (see equation (A.2)) that the equilibrium distribution is a Maxwellian,

$$f_{\mathcal{M}} := \frac{\rho}{(2\pi\theta)^{3/2}} \exp\left(\frac{-|\mathbf{v} - \mathbf{u}|^2}{2\theta}\right).$$

The **Gaussian distribution** is defined to be the entropy-maximizing distribution subject to the (not physically justified) constraint that all second-order velocity moments are conserved, and equals (see (A.5))

$$f_{\mathcal{G}} := \frac{\rho}{\sqrt{\det(2\pi\Theta)}} \exp(-\mathbf{c} \cdot \Theta^{-1} \cdot \mathbf{c}/2). \quad (2.18)$$

We say that f is an **even function of velocity** if $f(-\mathbf{v}) = f(\mathbf{v})$. Maxwellian and Gaussian distributions are even functions of thermal velocity. If f is even then so is $\eta(f)$. Odd moments of even functions are zero. In particular, *the diffusive entropy flux $\Phi' := \int_{\mathbf{c}} \mathbf{c} \eta$ and the heat flux $\mathbf{q} := \int_{\mathbf{c}} \mathbf{c} |\mathbf{c}|^2 f$ and tensor heat flux $\mathbf{q} := \int_{\mathbf{c}} \mathbf{c} \mathbf{c} \mathbf{c} f$ all vanish for Maxwellian and Gaussian distributions.*

2.4.3 Gas-dynamic entropy evolution

In a highly collisional gas, the distribution function f is close to Maxwellian. Assuming that the distribution is exactly Maxwellian gives the **hyperbolic five-moment model** of a gas; it is equivalent to the Boltzmann equation for a collision operator that instantaneously relaxes to equilibrium.

As obtained in equation A.9, the entropy density of a Maxwellian distribution is $S_{\mathcal{M}} = n s_{\mathcal{M}}$, where

$$s_{\mathcal{M}} := \ln\left(\frac{T^{3/2}}{n}\right)$$

is the molar entropy. We define the **five-moment gas-dynamic entropy** by this formula regardless of whether the distribution is actually Maxwellian.

Assuming that the distribution is exactly Gaussian gives the **hyperbolic ten-moment model** of a gas; it is equivalent to the Boltzmann equation for an (artificial and unphysical) collision operator that instantaneously relaxes to the entropy-maximizing distribution subject to the constraint that all ten moments are preserved.

As obtained in equation A.8, the entropy density of a Gaussian distribution is $S_G = ns_G$, where

$$s_G := \ln \left(\frac{\sqrt{\det \mathbb{T}}}{n} \right)$$

is the molar entropy. We define the **ten-moment gas-dynamic entropy** by this formula regardless of whether the distribution is actually Gaussian.

Note that

$$s \leq s_G \leq s_{\mathcal{M}},$$

with equality only when the assumed distributions match.

Five-moment entropy evolution

We can obtain an evolution equation for each gas-dynamic entropy analogous to our equation for the convective derivative of kinetic entropy. Taking the convective derivative of five-moment entropy and using the continuity equation $d_t n = -n \nabla \cdot \mathbf{u}$ gives $d_t s_{\mathcal{M}} = d_t((3/2) \ln T - \ln n) = (3/2)T^{-1}d_t T + \nabla \cdot \mathbf{u}$; using the temperature evolution equation (2.17) (divided by T) allows us to eliminate not only $d_t T$ but also the $\nabla \cdot \mathbf{u}$ term:

$$n d_t s_{\mathcal{M}} + T^{-1} \nabla \cdot \mathbf{q} + T^{-1} \mathbb{P}^\circ : \nabla \mathbf{u} = T^{-1} Q; \quad (2.19)$$

that is,

$$n d_t s_{\mathcal{M}} + \nabla \cdot (T^{-1} \mathbf{q}) = \mathbf{q} \cdot \nabla T^{-1} - T^{-1} \mathbb{P}^\circ : \text{Sym}(\nabla \mathbf{u}) + T^{-1} Q; \quad (2.20)$$

here we have separated out the *thermal entropy production* $\mathbf{q} \cdot \nabla T^{-1}$ from the divergence of the *diffusive entropy flux* $\Phi'_{\mathcal{M}} := T^{-1} \mathbf{q}$. The term $T^{-1} Q$ represents entropy source due to collisional exchange with other species (via thermal exchange and resistive drag force); since I am interested in non-resistive two-fluid plasmas I will generally ignore this term.

The entropy-evolution equations reveal that for smooth solutions entropy is conserved in the absence of heat flux.

Ten-moment entropy evolution

To get ten-moment entropy evolution we take the convective derivative of ten-moment entropy $s_G = \ln(\det \mathbb{T})/2 - \ln n$. Recall the Jacobi formula for the differential of the determinant, $d \det \underline{\underline{A}} = \text{tr}(\text{adj}(\underline{\underline{A}}) \cdot d\underline{\underline{A}})$, that is, $d \ln \det \underline{\underline{A}} = \text{tr}(\underline{\underline{A}}^{-1} \cdot d\underline{\underline{A}})$. Thus, $d_t \ln \det \mathbb{T} = \mathbb{T}^{-1} : d_t \mathbb{T}$. Again using the continuity equation $d_t \ln n = -\nabla \cdot \mathbf{u}$,

$$2d_t s_G = \mathbb{T}^{-1} : d_t \mathbb{T} + 2\nabla \cdot \mathbf{u}. \quad (2.21)$$

Recall the temperature evolution equation (2.15),

$$n_s d_t \mathbb{T}_s + n_s \text{Sym}2(\mathbb{T}_s \cdot \nabla \mathbf{u}_s) + \nabla \cdot \mathbf{q}_s = n_s (q_s/m_s) \text{Sym}2(\mathbb{T}_s \times \mathbf{B}) + \mathbb{R}_s + \mathbb{Q}_s.$$

Applying $\mathbb{T}^{-1} :$ to this equation, using the identities

$$\begin{aligned}\mathbb{T}^{-1} : d_t \mathbb{T} &= d_t \ln \det \mathbb{T}, \\ \mathbb{T}^{-1} : \text{Sym}(\mathbb{T} \cdot \nabla \mathbf{u}) &= \nabla \cdot \mathbf{u} = -d_t \ln n, \text{ and} \\ \mathbb{T}^{-1} : \text{Sym}(\mathbb{T} \times \mathbf{B}) &= 0,\end{aligned}$$

and substituting into equation (2.21) yields

$$2n d_t s_G + \mathbb{T}^{-1} : \nabla \cdot \mathbf{q}_s = \mathbb{T}^{-1} : \mathbb{R}_s + \mathbb{T}^{-1} : \mathbb{Q}_s; \quad (2.22)$$

that is,

$$2n d_t s_G + \nabla \cdot (\mathbb{T}^{-1} : \mathbf{q}_s) = \mathbf{q}_s : \nabla \mathbb{T}^{-1} + \mathbb{T}^{-1} : \mathbb{R}_s + \mathbb{T}^{-1} : \mathbb{Q}_s,$$

where $:$ denotes contraction over three adjacent indices. Here we have separated out the *thermal entropy production* $\mathbf{q}_s : \nabla \mathbb{T}^{-1}$ from the divergence of the *diffusive entropy flux* $\Phi'_G := \mathbb{T}^{-1} : \mathbf{q}_s$. The term $\mathbb{T}^{-1} : \mathbb{R}_s$ represents entropy production due to intraspecies collisional exchange (which effects relaxation toward a Maxwellian), and the term $\mathbb{T}^{-1} : \mathbb{Q}_s$ represents entropy production due to collisions with other species (via thermal exchange and resistive drag force); again, since I am interested in non-resistive two-fluid plasmas I will generally ignore this term.

2.5 Entropy-respecting forms for closure

While gas-dynamic entropy of a physical/kinetic gas can decrease, we may impose the assumption that gas-dynamic entropy cannot decrease as a requirement that closure relations must satisfy. For the five-moment gas dynamic equations, when collisions are sufficiently predominant to keep velocity distributions near Maxwellian, closures can be well-justified, and in particular the requirement that gas-dynamic entropy must increase can be justified as follows. Since Maxwellian distributions maximize entropy subject to *physical* constraints, if the deviation from the Maxwellian distribution is of order ϵ the deviation of the entropy will merely be of order ϵ^2 . Therefore, gas-dynamic entropy is an accurate approximation to kinetic entropy, and for a collisional gas we expect it to increase.

In contrast, closures of the ten-moment equations which do not cause it to approximate the five-moment model are difficult to justify unless one assumes an idiosyncratic collision operator which kills deviations from a Gaussian much faster than it relaxes a Gaussian distribution to a Maxwellian. For such a model heat flux is negligible in comparison to viscosity, i.e., the Prandtl number is much larger than 1. For a monatomic gas the Prandtl number is approximately 2/3; for other gases and fluids the Prandtl number is smaller, often much smaller.

Given a deviation of order ϵ from a Gaussian distribution, to conclude that the deviation of the ten-moment entropy is of order ϵ^2 we would need to assume that the deviation from the artificial constraint (that the tensor pressure is invariant) is of order ϵ^2 . Regardless of how artificially high a finite Prandtl number is, for sufficiently small ϵ this artificial constraint does not hold. The requirement that ten-moment gas-dynamic entropy should be nondecreasing for ten-moment closures thus lacks adequate physical justification except in the adiabatic case where the Prandtl number is infinite.

Having stated these prefatory caveats, we now proceed to derive the form of entropy-respecting 5-moment and 10-moment closures.

2.5.1 Five-moment closure

Recall the five-moment entropy evolution equation (2.20), which we now rewrite as:

$$n d_t s_{\mathcal{M}} + \nabla \cdot (T^{-1} \mathbf{q}) = \mathbf{q} \cdot \nabla T^{-1} - n \boldsymbol{\pi}^\circ : \mathbf{e}^\circ + T^{-1} Q; \quad (2.23)$$

here $\boldsymbol{\pi}^\circ := T^{-1} \mathbb{T}^\circ$ is the deviatoric part of the “shape” of the temperature tensor and $\mathbf{e}^\circ := \text{Sym}(\nabla \mathbf{u})^\circ := \text{Sym}(\nabla \mathbf{u}) - \mathbb{1} \nabla \cdot \mathbf{u} / 3$ is called the **deviatoric strain rate** and is the traceless part of the **strain rate** tensor $\mathbf{e} := \text{Sym}(\nabla \mathbf{u})$. We now require the intraspecies entropy source terms $\mathbf{q} \cdot \nabla T^{-1}$ and $-\boldsymbol{\pi}^\circ : \mathbf{e}^\circ$ to be nonnegative as a closure requirement and deduce the form of the closure.

Isotropic linearized heat flux closure

To ensure that $\mathbf{q} \cdot \nabla T^{-1}$ is nonnegative we make \mathbf{q} a function of ∇T^{-1} . We will approximate the function as linear (with state-dependent coefficients). Since \mathbf{q} should be zero in equilibrium (for which $\nabla T^{-1} = 0$), and assuming that the derivative of the map $\nabla T^{-1} \mapsto \mathbf{q}$ is nonzero, in the near-Maxwellian limit such a linearized closure is rigorously justifiable.

Physical laws should be invariant under rotation for closed systems. In the absence of a magnetic field (or other external influence) sufficiently strong to break this fundamental symmetry we expect intraspecies closure relations to be isotropic. The general form of a linear isotropic closure is

$$\mathbf{q}_s = \bar{\kappa}_s \nabla T^{-1}_s = -k_s \nabla T_s, \quad (2.24)$$

where k is called the **heat conductivity** and we infer that

$$\bar{\kappa}_s = T_s^2 k_s. \quad (2.25)$$

Nonnegativity of $\mathbf{q}_s \cdot \nabla T^{-1}_s = \bar{\kappa}_s \|\nabla T^{-1}_s\|^2$ is ensured as long as $\bar{\kappa}$ is nonnegative.

Gyrotropic heat flux closure.

In the presence of a sufficiently strong magnetic field $\mathbf{B} = \|\mathbf{B}\| \mathbf{b}$ we cannot assume that intraspecies collisions are governed by isotropic physics, and instead we can merely assume a gyrotropic linear closure $\mathbf{q} = -\mathbf{k} \cdot \nabla T$, where \mathbf{k} is a **gyrotropic tensor**; that is, \mathbf{k} is invariant under rotations around an axis aligned with the magnetic field. In particular,

$$\mathbf{q} = -(\kappa_\perp \mathbb{1}_\perp + \kappa_\wedge \mathbb{1}_\wedge + \kappa_\parallel \mathbb{1}_\parallel) \cdot \nabla T_s, \quad (2.26)$$

where we have used that since \mathbf{k} is gyrotropic second-order tensor it is therefore a linear combination of the perpendicular, skew, and parallel gyrotropic tensors

$$\mathbb{1}_\perp := \mathbb{1} - \mathbf{b}\mathbf{b}, \quad \mathbb{1}_\wedge := \mathbb{1} \times \mathbf{b}, \quad \mathbb{1}_\parallel := \mathbf{b}\mathbf{b}.$$

For this closure, to ensure that $\mathbf{q} \cdot \nabla T^{-1} = T^{-2} \nabla T \cdot \mathbf{k} \cdot \nabla T \geq 0$, \mathbf{k} must be positive definite; that is, the parallel and perpendicular heat conductivities must be nonnegative,

$$\kappa_\perp \geq 0, \quad \kappa_\parallel \geq 0. \quad (2.27)$$

Isotropic viscous stress closure

To ensure that the viscous entropy production term $-\boldsymbol{\pi}^\circ : \mathbf{e}^\circ$ in equation (2.23) is nonnegative, we make $\boldsymbol{\pi}^\circ$ a function of \mathbf{e}° . The simplest such closure is to make $\boldsymbol{\pi}^\circ$ a linear isotropic function of \mathbf{e}° . Then the facts that \mathbf{e}° is symmetric and that $\boldsymbol{\pi}^\circ$ must be symmetric and traceless imply that $\boldsymbol{\pi}^\circ$ is proportional to \mathbf{e}° ,

$$-\boldsymbol{\pi}^\circ = 2\tau \mathbf{e}^\circ, \quad (2.28)$$

where we will see that τ is a relaxation period; equivalently, the deviatoric stress $-\mathbb{P}^\circ := -n\mathbb{T}^\circ$ is proportional to the deviatoric strain,

$$-\mathbb{P}^\circ = 2\mu \mathbf{e}^\circ, \quad (2.29)$$

where the **viscosity** $\mu := p\tau$ must be positive to respect entropy. In the absence of a symmetry-breaking magnetic field, in the near-Maxwellian-limit, assuming that the function $\mathbf{e}^\circ \mapsto \mathbb{P}^\circ$ has nonzero derivative at $\mathbf{e}^\circ = 0$, such a closure can be rigorously justified.

Gyrotropic viscous stress closure

In the presence of a sufficiently strong magnetic field, we might merely assume that $\boldsymbol{\pi}^\circ$ is a *gyrotropic* function of \mathbf{e}° :

$$-\boldsymbol{\pi}^\circ = 2\tau \tilde{\boldsymbol{\mu}} : \mathbf{e}^\circ, \quad \text{that is,} \quad -\mathbb{P}^\circ = 2\boldsymbol{\mu} : \mathbf{e}^\circ, \quad (2.30)$$

where $\boldsymbol{\mu} := \tilde{\boldsymbol{\mu}}\mu$ is the viscosity tensor and $\tilde{\boldsymbol{\mu}}$ is its nondimensional shape; $\tilde{\boldsymbol{\mu}}$ is a gyrotropic tensor which evidently must be symmetric and traceless in its first two coefficients and which is without loss of generality symmetric in its last two coefficients. This leads to five distinct coefficients of viscosity. To ensure that entropy production $T^{-1} \mathbf{e}^\circ : 2\boldsymbol{\mu} : \mathbf{e}^\circ$ is strictly positive for a non-Maxwellian distribution, we impose the positive-definiteness (and invertibility) criterion $\underline{\underline{\mathbf{A}}} : \tilde{\boldsymbol{\mu}} : \underline{\underline{\mathbf{A}}} > 0$ for any $\underline{\underline{\mathbf{A}}} \neq 0$. In the isotropic case $\tilde{\boldsymbol{\mu}}$ is the identity tensor $\mathbf{1} \diamond \mathbf{1}$ for linear transformations on the space of second-order tensors, whose components are $\delta_{ijkl} = \delta_{ik}\delta_{jl}$.

2.5.2 Ten-moment closure

Recall the ten-moment entropy evolution equation (2.31), which we now write as

$$2n d_t s_G + \nabla \cdot (\mathbb{T}^{-1} : \mathbf{q}) = \mathbf{q} : \text{Sym}(\nabla \mathbb{T}^{-1}) + (\mathbb{T}^{-1})^\circ : \mathbb{R} + \mathbb{T}^{-1} : \mathbb{Q}; \quad (2.31)$$

here we have used that $\text{tr}(\mathbb{R}) = 0$ (because $\mathbb{R} := \int_{\mathbf{v}} \mathbf{v}\mathbf{v}C$ and $\int_{\mathbf{c}} |\mathbf{v}|^2 C = 0$ by conservation of energy) to replace \mathbb{T}^{-1} with its deviatoric part $(\mathbb{T}^{-1})^\circ := \mathbb{T}^{-1} - \mathbf{1} \text{tr}(\mathbb{T}^{-1})/3$.

We impose the closure requirement that the intraspecies entropy source terms must be nonnegative and zero at equilibrium.

Intraspecies collision closure

By selecting an artificial collision operator that instantaneously relaxes to a Gaussian distribution we may justify the requirement that the entropy production of the intraspecies collision term $(\mathbb{T}^{-1})^\circ : \mathbb{R}$ should be positive. Clearly we can ensure positivity by making \mathbb{R} a function of $(\mathbb{T}^{-1})^\circ$. However,

to keep the closure simple we instead prefer to make \mathbb{R} a function of \mathbb{T}° ; this is equivalent for small deviations from isotropy (i.e. equilibrium), which is when we can justify linearized closures anyway.

Isotropic intraspecies collision closure. Imposing that \mathbb{R} is a linear isotropic function of \mathbb{T}° , equivalently of \mathbb{P}° , yields the closure

$$\mathbb{R} = -\tau^{-1}\mathbb{P}^\circ, \quad (2.32)$$

where τ is the *relaxation period* and τ^{-1} is called the *relaxation rate*. Then

$$\begin{aligned} (\mathbb{T}^{-1})^\circ : \mathbb{R}/n &= \mathbb{T}^{-1} : \mathbb{R}/n \\ &= \mathbb{T}^{-1} : (T \mathbb{1} - \mathbb{T})/\tau \\ &= (\text{tr}(\mathbb{T}^{-1})\text{tr}(\mathbb{T})/3 - 3)/\tau \\ &= 3 \tan^2(\theta)/\tau, \end{aligned}$$

where θ is the angle between the vector $\mathbf{V} := (\sqrt{T_1}, \sqrt{T_2}, \sqrt{T_3})^T$ and the vector $\mathbf{W} := (\sqrt{T_1}^{-1}, \sqrt{T_2}^{-1}, \sqrt{T_3}^{-1})^T$, where T_1 , T_2 , and T_3 are the eigenvalues of the temperature tensor. Indeed, $\mathbf{V} \cdot \mathbf{V} = \text{tr} \mathbb{T}$, $\mathbf{W} \cdot \mathbf{W} = \text{tr}(\mathbb{T}^{-1})$, and $\mathbf{V} \cdot \mathbf{W} = 3$; since $\cos^2 \theta = \frac{(\mathbf{V} \cdot \mathbf{W})^2}{\|\mathbf{V}\|^2 \|\mathbf{W}\|^2}$, $\tan^2 \theta = \sec^2 \theta - 1 = \frac{(\text{tr} \mathbb{T})\text{tr}(\mathbb{T}^{-1})}{9} - 1$, which is strictly greater than 0 unless $\mathbf{V} \times \mathbf{W} = \mathbf{0}$ (which says that the temperature tensor is isotropic).

Gyrotropic intraspecies collision closure. More generally, we assume that \mathbb{R} is a linear *gyrotropic* function of \mathbb{T}° , equivalently, of \mathbb{P}° :

$$\mathbb{R} = -\tau^{-1}C^{\mathbb{R}} : \mathbb{P}^\circ, \quad (2.33)$$

where $C^{\mathbb{R}}$ is a nondimensional gyrotropic tensor of coefficients. To respect entropy, based on equation (2.31), we require that

$$(\mathbb{T}^{-1})^\circ : \mathbb{R} = -(\mathbb{T}^{-1})^\circ : C^{\mathbb{R}} : \mathbb{T}^\circ > 0 \quad (2.34)$$

whenever $\mathbb{T}^\circ \neq 0$, that is, whenever the pressure is not isotropic. Recall that $\boldsymbol{\pi}^\circ := T^{-1}\mathbb{T}^\circ$. In the limit $\|\boldsymbol{\pi}^\circ\| \rightarrow 0$, $(\boldsymbol{\pi}^{-1})^\circ \approx -\boldsymbol{\pi}^\circ$. Therefore, for small $\|\boldsymbol{\pi}^\circ\|$, equation (2.34) implies that for all $\boldsymbol{\pi}^\circ$

$$\boldsymbol{\pi}^\circ : C^{\mathbb{R}} : \boldsymbol{\pi}^\circ > 0, \quad (2.35)$$

which implies that $C^{\mathbb{R}}$ has an inverse when regarded as a linear transformation relating traceless tensors. We impose invertibility as a minor auxiliary closure requirement, which we justify by showing in section 2.5.3 the asymptotic equivalence of the five-moment and ten-moment closures.

Entropy-respecting closure for tensor heat flux

The requirement that the entropy production of the intraspecies heat flux tensor be positive is difficult to justify. One could try to justify it with a sequence of collision operators which relax to a Gaussian increasingly rapidly, but in such a limit there is no heat flux anyway. Nevertheless, we work out the consequences of this requirement.

The local production of ten-moment gas-dynamic entropy due to heat flux is seen in equation (2.31) to be

$$\mathbf{q} : \text{Sym}(\nabla \mathbb{T}^{-1}). \quad (2.36)$$

To ensure that this quantity is positive, we posit that \mathbf{q} is a linear gyrotropic function of its complement in this inner product,

$$\mathbf{q} = K_{[6]} \vdash \text{Sym}(\nabla \mathbb{T}^{-1}), \quad (2.37)$$

where $K_{[6]}$ is a gyrotropic tensor which must be symmetric in its first three indices and which without loss of generality we require to be symmetric in its last three indices; the entropy production (2.38) is then

$$\text{Sym}(\nabla \mathbb{T}^{-1}) \vdash K_{[6]} \vdash \text{Sym}(\nabla \mathbb{T}^{-1}), \quad (2.38)$$

which is guaranteed to be positive if $K_{[6]}$ satisfies the positive-definiteness criterion

$$A \vdash K_{[6]} \vdash A > 0 \quad (2.39)$$

for all $A \neq 0$.

Isotropic case. In the absence of a magnetic field $K_{[6]}$ should be isotropic. Recall that in three-dimensional space (or any odd-dimensional space) every even-order isotropic tensor is a linear combination of tensor products of the identity tensor [31]. So if A and B are symmetric third-order tensors and A is a linear isotropic function of B , then $A = \bar{\kappa}_1 B + \bar{\kappa}_2 \mathbf{1} \vee \text{tr} B$ for some μ and λ , where recall the definition of the vee product \vee from (2.4). Therefore, we can write the general form of a linear isotropic entropy-respecting heat flux closure,

$$\mathbf{q}_L = \bar{\kappa}_1 \nabla \vee \mathbb{T}^{-1} + \bar{\kappa}_2 \mathbf{1} \vee \text{tr}(\nabla \vee \mathbb{T}^{-1}), \quad (2.40)$$

where \mathbf{q}_L denotes the entropy-respecting heat flux closure proposed by Levermore for ten-moment gas dynamics (C.D. Levermore, presented in talk slides e.g. at Kinetic FRG Young Researchers Workshop: *Kinetic Description of Multiscale Phenomena: Modeling, Theory, and Computation*, University of Maryland, College Park, 5 March 2009). To determine for what coefficients the entropy production given by (2.38) is positive, we compute:

$$\begin{aligned} \text{Sym}3(\nabla \mathbb{T}^{-1}) \vdash \mathbf{q}_L &= (\nabla \vee \mathbb{T}^{-1}) \vdash \mathbf{q}_L \\ &= (\nabla \vee \mathbb{T}^{-1}) \vdash (\bar{\kappa}_1 3 \nabla \vee \mathbb{T}^{-1} + \bar{\kappa}_2 9 \mathbf{1} \vee \text{tr}(\nabla \vee \mathbb{T}^{-1})) \\ &= 3\bar{\kappa}_1 \|\nabla \vee \mathbb{T}^{-1}\|^2 + 9\bar{\kappa}_2 \|\text{tr}(\nabla \vee \mathbb{T}^{-1})\|^2; \end{aligned}$$

here we have used that

$$\begin{aligned} &(\nabla \vee \mathbb{T}^{-1}) \vdash (\mathbf{1} \vee \text{tr}(\nabla \vee \mathbb{T}^{-1})) \\ &= (\nabla \vee \mathbb{T}^{-1}) \vdash (\mathbf{1} \otimes \text{tr}(\nabla \vee \mathbb{T}^{-1})) \\ &= (\nabla \vee \mathbb{T}^{-1})_{ijk} \delta_{ij} (\nabla \vee \mathbb{T}^{-1})_{mmk} \\ &= \text{tr}(\nabla \vee \mathbb{T}^{-1}) \cdot \text{tr}(\nabla \vee \mathbb{T}^{-1}) \\ &= \|\text{tr}(\nabla \vee \mathbb{T}^{-1})\|^2. \end{aligned}$$

So to ensure that entropy is respected we would require that $\bar{\kappa}_1 \geq 0$ and $\bar{\kappa}_2 \geq 0$.

To compare with other closures, we express $\nabla \mathbb{T}^{-1}$ in terms of $\nabla \mathbb{T}$. Taking the differential of the identity $\mathbb{T}^{-1} \cdot \mathbb{T} = \mathbf{1}$ and solving yields

$$d\mathbb{T}^{-1} = -\mathbb{T}^{-1} \cdot d\mathbb{T} \cdot \mathbb{T}^{-1} = -T^{-2} \boldsymbol{\pi}^{-1} \cdot d\mathbb{T} \cdot \boldsymbol{\pi}^{-1} = -T^{-2} d\mathbb{T} : (\boldsymbol{\pi}^{-1} \diamond \boldsymbol{\pi}^{-1}).$$

In particular,

$$\nabla \mathbb{T}^{-1} = -T^{-2} \nabla \mathbb{T} : (\boldsymbol{\pi}^{-1} \diamond \boldsymbol{\pi}^{-1})$$

and

$$\nabla \vee \mathbb{T}^{-1} = -T^{-2} \text{Sym}3(\nabla \mathbb{T} : (\boldsymbol{\pi}^{-1} \diamond \boldsymbol{\pi}^{-1})). \quad (2.41)$$

In the isotropic case, where $\boldsymbol{\pi} = \mathbb{1}$, $\mathbb{T} = \mathbb{1} T$ and

$$\nabla \vee \mathbb{T}^{-1} = \mathbb{1} \vee \nabla T^{-1}, \quad \text{tr}(\nabla \vee \mathbb{T}^{-1}) = 5 \nabla T^{-1}, \quad (2.42)$$

and the expressions above simplify. We then have

$$\begin{aligned} \mathbf{q}_L &= \bar{\kappa}_1 \nabla \vee \mathbb{T}^{-1} + \bar{\kappa}_2 \mathbb{1} \vee \text{tr}(\nabla \vee \mathbb{T}^{-1}) \\ &= \bar{\kappa}_1 \mathbb{1} \vee \nabla T^{-1} + 5 \bar{\kappa}_2 \mathbb{1} \vee \nabla T^{-1} \\ &= (\bar{\kappa}_1 + 5 \bar{\kappa}_2) \mathbb{1} \vee \nabla T^{-1}. \end{aligned} \quad (2.43)$$

So the entropy production is

$$\begin{aligned} (\nabla \vee \mathbb{T}^{-1}) : \mathbf{q}_L &= \mathbb{1} \vee \nabla T^{-1} : (\bar{\kappa}_1 + 5 \bar{\kappa}_2) \mathbb{1} \vee \nabla T^{-1} \\ &= 5(\bar{\kappa}_1 + 5 \bar{\kappa}_2) \|\nabla T^{-1}\|^2, \end{aligned}$$

where we have used that $\mathbb{1} \vee \nabla T^{-1} : \mathbb{1} \vee \nabla T^{-1} = \mathbb{1} \nabla T^{-1} : \mathbb{1} \vee \nabla T^{-1} = (\delta_{ij} \partial_k T^{-1})(\delta_{ij} \partial_k T^{-1} + 2\delta_{ik} \partial_j T^{-1}) = 5 \partial_k T^{-1} \partial_k T^{-1} = 5 \|\nabla T^{-1}\|^2$.

2.5.3 Equivalence of ten-moment and five-moment stress closure for near-isotropy

In the near-Maxwellian limit, that is, in case pressure anisotropy is small (as is generally the case if isotropization is rapid) we can show that the ten-moment viscous stress closure for the relaxation tensor \mathbb{R} given by equation (2.33), equivalently,

$$-\tau \mathbb{R}/p = C^{\mathbb{R}} : \boldsymbol{\pi}^\circ,$$

is asymptotically equivalent to the five-moment viscous stress closure for the deviatoric pressure \mathbb{P}° given by equation (2.30), equivalently,

$$-2\tau e^\circ = \tilde{\boldsymbol{\mu}}^{-1} : \boldsymbol{\pi}^\circ.$$

(So evidently we need $\mathbb{R}/p = 2e^\circ$.)

The strategy is to match up the ten-moment pressure tensor evolution equation with the five-moment closure for the viscous stress. Since the five-moment closure is expressed in terms of the deviatoric pressure, it is natural to proceed by writing an evolution equation for the deviatoric part of the pressure. We will instead write an evolution equation for the *shape* of the pressure tensor where (recall that) the nondimensional shape of the pressure (or temperature) tensor $\boldsymbol{\pi}$ and its deviatoric part $\boldsymbol{\pi}^\circ$ are defined by

$$\boldsymbol{\pi} := \frac{\mathbb{T}}{T} = \frac{\mathbb{P}}{p}, \quad \boldsymbol{\pi} =: \mathbb{1} + \boldsymbol{\pi}^\circ, \quad \text{so} \quad \boldsymbol{\pi}^\circ := \frac{\mathbb{T}^\circ}{T} = \frac{\mathbb{P}^\circ}{p},$$

where \mathbb{P}° is of course the deviatoric part of the pressure tensor. This formulation is convenient because we expect the ten-moment closure to agree with the five-moment closure when the deviatoric pressure is small, that is, when $\boldsymbol{\pi}^\circ$ is much smaller than the identity tensor $\mathbb{1}$.

Recall temperature tensor evolution (2.15):

$$d_t \mathbb{T} + \text{Sym}2(\mathbb{T} \cdot \nabla \mathbf{u}) + n^{-1} \nabla \cdot \mathbf{q} = (q/m) \text{Sym}2(\mathbb{T} \times \mathbf{B}) + \mathbb{R}/n,$$

where we assume a single species and neglect heating due to interaction with other species. Divide temperature tensor evolution by T and get

$$T^{-1} d_t \mathbb{T} + \text{Sym}2(\boldsymbol{\pi} \cdot \nabla \mathbf{u}) + p^{-1} \nabla \cdot \mathbf{q} = \text{Sym}2(\boldsymbol{\pi} \times q\mathbf{B}/m) + \mathbb{R}/p.$$

Using that $\boldsymbol{\pi} = \mathbb{1} + \boldsymbol{\pi}^\circ$, and that $T^{-1} d_t \mathbb{T} = T^{-1} d_t (T\boldsymbol{\pi}) = d_t \boldsymbol{\pi}^\circ + \boldsymbol{\pi} d_t \ln T$, we get an evolution equation for the deviatoric part of the shape of the pressure tensor,

$$\begin{aligned} d_t \boldsymbol{\pi}^\circ + (\mathbb{1} + \boldsymbol{\pi}^\circ) d_t \ln T + \text{Sym}2(\nabla \mathbf{u}) + \text{Sym}2(\boldsymbol{\pi}^\circ \cdot \nabla \mathbf{u}) + p^{-1} \nabla \cdot \mathbf{q} \\ = \frac{q}{m} \text{Sym}2(\boldsymbol{\pi}^\circ \times \mathbf{B}) + \mathbb{R}/p. \end{aligned} \quad (2.44)$$

Half the trace of this equation gives

$$(3/2) d_t \ln T + \nabla \cdot \mathbf{u} + \boldsymbol{\pi}^\circ : \nabla \mathbf{u} + p^{-1} \nabla \cdot \mathbf{q} = 0, \quad (2.45)$$

which incidently we can rewrite as evolution of the five-moment entropy, $s_{\mathcal{M}} := \ln(T^{3/2}/n)$,

$$d_t s_{\mathcal{M}} = (3/2) d_t \ln T + \nabla \cdot \mathbf{u} = -\boldsymbol{\pi}^\circ : \nabla \mathbf{u} - p^{-1} \nabla \cdot \mathbf{q} \quad (2.46)$$

(compare (2.19)). We could simplify the analysis at this point by identifying the assumptions which imply that entropy is conserved on the relaxation time scale τ , but instead we delay making approximating assumptions in order to reap the benefit of writing an exact evolution equation for $\boldsymbol{\pi}^\circ$ which allows us to more sharply match up the closures and identify the domain of agreement.

Solving equation (2.45) for $d_t \ln T$ and substituting back into equation (2.44), which we first rewrite as

$$\begin{aligned} \mathbb{R}/p = \mathbb{1} d_t \ln T + \text{Sym}2(\nabla \mathbf{u}) + \text{Sym}2(\boldsymbol{\pi}^\circ \cdot \nabla \mathbf{u}) + p^{-1} \nabla \cdot \mathbf{q} \\ + \boldsymbol{\pi}^\circ d_t \ln T + d_t \boldsymbol{\pi}^\circ - \text{Sym}2(\boldsymbol{\pi}^\circ \times q\mathbf{B}/m) \end{aligned}$$

gives a manifestly traceless equation (which as it happens can be interpreted as an evolution equation for $\boldsymbol{\pi}^\circ$):

$$\begin{aligned} \mathbb{R}/p = 2\mathbf{e}^\circ + \text{Sym}2(\boldsymbol{\pi}^\circ \cdot \nabla \mathbf{u})^\circ + p^{-1} \nabla \cdot \mathbf{q}^\circ \\ - (2/3) \boldsymbol{\pi}^\circ (\nabla \cdot \mathbf{u} + \boldsymbol{\pi}^\circ : \nabla \mathbf{u} + p^{-1} \nabla \cdot \mathbf{q}) \\ + d_t \boldsymbol{\pi}^\circ - \text{Sym}2(\boldsymbol{\pi}^\circ \times q\mathbf{B}/m), \end{aligned} \quad (2.47)$$

where $\mathbf{e}^\circ := \text{Sym}(\nabla \mathbf{u})^\circ$ is the strain deviator, $\mathbf{q}^\circ := \mathbf{q} - (2/5) \text{Sym}3(\mathbb{1} \mathbf{q})$ is the **deviatoric heat flux tensor**, and $\text{Sym}2(\boldsymbol{\pi}^\circ \cdot \nabla \mathbf{u})^\circ = \text{Sym}2(\boldsymbol{\pi}^\circ \cdot \nabla \mathbf{u}) - (2/3) \mathbb{1} \boldsymbol{\pi}^\circ : \nabla \mathbf{u}$ denotes the deviatoric part of $\text{Sym}(\boldsymbol{\pi}^\circ \cdot \nabla \mathbf{u})$. Note that **Sym3** denotes thrice the symmetric part of a third-order tensor.

Recall the gyrotropic closure (2.33), i.e.

$$-\tau \mathbb{R}/p = C^{\mathbb{R}} : \boldsymbol{\pi}^\circ.$$

Multiplying (2.47) by τ gives an equation in terms of the nondimensional quantities $C^{\mathbb{R}} : \boldsymbol{\pi}^\circ$ and

$$\tau \nabla \mathbf{u}, \quad \tau p^{-1} \nabla \cdot \mathbf{q}, \quad d_{(t/\tau)} \boldsymbol{\pi}^\circ, \quad \text{and} \quad \tau q \mathbf{B}/m$$

which reads

$$\begin{aligned} -C^{\mathbb{R}} : \boldsymbol{\pi}^\circ &= 2\tau \mathbf{e}^\circ + \text{Sym}2(\boldsymbol{\pi}^\circ \cdot \tau \nabla \mathbf{u})^\circ + \tau p^{-1} \nabla \cdot \mathbf{q}^\circ \\ &\quad - (2/3) \boldsymbol{\pi}^\circ (\tau \nabla \cdot \mathbf{u} + \boldsymbol{\pi}^\circ : \tau \nabla \mathbf{u} + \tau p^{-1} \nabla \cdot \mathbf{q}) \\ &\quad + d_{(t/\tau)} \boldsymbol{\pi}^\circ - \text{Sym}2(\boldsymbol{\pi}^\circ \times \tau q \mathbf{B}/m). \end{aligned} \quad (2.48)$$

We want to show that this agrees with the five-moment closure (2.30),

$$-\tilde{\boldsymbol{\mu}}^{-1} : \boldsymbol{\pi}^\circ = 2\tau \mathbf{e}^\circ; \quad (2.49)$$

since we do not want closure coefficients that depend on differentiated quantities, we will discard all terms after the first plus sign except for the magnetic field term.

We will need to assume that the deviatoric pressure is small, that is, $\|\boldsymbol{\pi}^\circ\| \ll 1$.

Let τ_0 designate the time scale defined by $\nabla \mathbf{u}$. That is, $\|\nabla \mathbf{u}\| = \mathcal{O}(\tau_0^{-1})$. The five-moment closure (2.49) then implies that $\boldsymbol{\pi}^\circ = \mathcal{O}(\tau/\tau_0)$. To discard terms such as $\boldsymbol{\pi}^\circ \tau \nabla \cdot \mathbf{u}$ we need that $\tau/\tau_0 \ll 1$. To discard the heat flux terms we need that the divergence of the deviatoric heat flux is very small,

$$\|\tau p^{-1} \nabla \cdot \mathbf{q}^\circ\| \ll \|\boldsymbol{\pi}^\circ\|, \quad \text{i.e.} \quad \|p^{-1} \nabla \cdot \mathbf{q}^\circ\| \ll 1/\tau_0, \quad \text{i.e.} \quad \|p^{-1} \nabla \cdot \mathbf{q}^\circ\| \ll \|\nabla \mathbf{u}\|$$

and that the divergence of the nondeviatoric part is small,

$$\|\boldsymbol{\pi}^\circ \tau p^{-1} \nabla \cdot \mathbf{q}\| \ll \|\boldsymbol{\pi}^\circ\|, \quad \text{i.e.} \quad \|p^{-1} \nabla \cdot \mathbf{q}\| \ll 1/\tau.$$

Of the unwanted terms in equation (2.48) it remains to discard the term $d_{(t/\tau)} \boldsymbol{\pi}^\circ$. We need that

$$\|d_{(t/\tau)} \boldsymbol{\pi}^\circ\| \ll \|\boldsymbol{\pi}^\circ\| = \mathcal{O}(\tau/\tau_0).$$

This says that the shape of the stress (or strain) deviator changes little on the time scale of a relaxation period.

We now consider the magnetic field term $\text{Sym}2(\boldsymbol{\pi}^\circ \times \tau q \mathbf{B}/m)$ in equation (2.48). Define the **gyrofrequency** $\omega_c := q\|\mathbf{B}\|/m$ and the nondimensionalized gyrofrequency $\varpi := \tau\omega_c$, which is the rate of gyration divided by the rate of relaxation. We can neglect the magnetic field term and use the same closure coefficients for both closures if the magnetic field is sufficiently small so that

$$\text{Sym}2(\boldsymbol{\pi}^\circ \times \tau q \mathbf{B}/m) \ll \boldsymbol{\pi}^\circ, \quad \text{i.e.,} \quad \varpi \ll 1,$$

which says that the gyrofrequency is much smaller than the relaxation period. If the effect of the magnetic field is negligible then $\tilde{\boldsymbol{\mu}}^{-1}$ and $C^{\mathbb{R}}$ should be the identity and we might as well have restricted our study to isotropic closures.

What if the magnetic field is large? Then we need the approximate closure identity

$$\boxed{-C^{\mathbb{R}} : \boldsymbol{\pi}^\circ = 2\tau \mathbf{e}^\circ - \text{Sym}2(\boldsymbol{\pi}^\circ \times \varpi \mathbf{b})} \quad (2.50)$$

(from (2.48), where $\mathbf{b} := \mathbf{B}/\|\mathbf{B}\|$ is the magnetic field direction vector) to match up with the five-moment closure of equation (2.49),

$$-\tilde{\boldsymbol{\mu}}^{-1} : \boldsymbol{\pi}^\circ = 2\tau \mathbf{e}^\circ.$$

Evidently we need that

$$\tilde{\boldsymbol{\mu}}^{-1} : \boldsymbol{\pi}^\circ = C^{\mathbb{R}} : \boldsymbol{\pi}^\circ - \text{Sym}2(\boldsymbol{\pi}^\circ \times \varpi \mathbf{b}). \quad (2.51)$$

We rewrite the last term as

$$\text{Sym}2(\boldsymbol{\pi}^\circ \times \varpi \mathbf{b}) = \text{Sym}2(\mathbb{1} \cdot \boldsymbol{\pi}^\circ \cdot \mathbb{1} \times \varpi \mathbf{b}) = \text{Sym}2(\mathbb{1} \cdot \boldsymbol{\pi}^\circ \cdot \mathbb{1}_\wedge \varpi), \quad (2.52)$$

where we define $\mathbb{1}_\wedge := \mathbb{1} \times \mathbf{b} = \mathbf{b} \times \mathbb{1}$, which projects onto the plane orthogonal to \mathbf{b} and then rotates 90 degrees in this plane. Define the **diamond product** of two tensors with the convention that $(\underline{M} \diamond \underline{N}) : \underline{A} = \underline{M} \cdot \underline{A} \cdot \underline{N}$. Using that $\mathbb{1}_\wedge$ is antisymmetric,

$$\text{Sym}2(\mathbb{1} \cdot \boldsymbol{\pi}^\circ \cdot \mathbb{1}_\wedge) = \text{Sym}2(\mathbb{1} \diamond \mathbb{1}_\wedge : \boldsymbol{\pi}^\circ) = (\mathbb{1} \diamond \mathbb{1}_\wedge - \mathbb{1}_\wedge \diamond \mathbb{1}) : \boldsymbol{\pi}^\circ. \quad (2.53)$$

So (2.51) becomes

$$\tilde{\boldsymbol{\mu}}^{-1} : \boldsymbol{\pi}^\circ = (C^{\mathbb{R}} + \varpi(\mathbb{1}_\wedge \diamond \mathbb{1} - \mathbb{1} \diamond \mathbb{1}_\wedge)) : \boldsymbol{\pi}^\circ.$$

We infer that $\tilde{\boldsymbol{\mu}}^{-1} = C^{\mathbb{R}} + \varpi(\mathbb{1}_\wedge \diamond \mathbb{1} - \mathbb{1} \diamond \mathbb{1}_\wedge)$, that is,

$$\boxed{\tilde{\boldsymbol{\mu}}^{-1} = C^{\mathbb{R}} + (\mathbb{1} \times \varpi \mathbf{b}) \diamond \mathbb{1} - \mathbb{1} \diamond (\varpi \mathbf{b} \times \mathbb{1})}, \quad (2.54)$$

where we have used that $\mathbf{b} \times \mathbb{1} = \mathbb{1} \times \mathbf{b}$.

As we will see in section 2.6.3, for $C^{\mathbb{R}}$ the closure coefficients are quite simple (the identity four-tensor) whereas the closure coefficients for $\tilde{\boldsymbol{\mu}}$ must take into account the rotational effects of the magnetic field because it defines a closure in terms of a differentiated quantity. Equation (2.50) agrees with equation (5.122) in the book [62] by Woods if one simply takes $C^{\mathbb{R}} = \mathbb{1} \diamond \mathbb{1}$. He arrives at this form by assuming that the response of the viscous stress to the deviatoric strain is delayed by a collision period. During this time the affect of the magnetic field is to rotate the deviatoric strain.

I remark that to compare the five- and ten-moment closures one must use equation (2.54) to translate closure coefficients (or just (2.50) if all one wants to do is test the agreement of the models).

2.6 Perturbative closure

In section 2.5 we deduced forms of closure by requiring entropy to increase. This gave the functional form of the closure, but it did not give any estimate of the closure coefficients. A method that determines closure coefficients is to use a Chapman-Enskog perturbative expansion.

2.6.1 BGK and Gaussian-BGK collision operators

To perform a Chapman-Enskog expansion we have to assume the form of the collision operator. The simplest choice of collision operator which satisfies the physical constraints that it (1) conserves the conserved moments (mass, momentum, and energy) and (2) respects entropy is a collision operator which relaxes the distribution toward an entropy-maximizing distribution. Appendix A.1 calculates that distribution which maximizes entropy subject only to these physical constraints is a **Maxwellian distribution**, of the form (A.2)

$$f_\theta = \frac{\rho}{(2\pi\theta)^{3/2}} \exp\left(\frac{-|\mathbf{v} - \mathbf{u}|^2}{2\theta}\right),$$

where f_θ is mass density in velocity space and $\theta := \langle |\mathbf{c}|^2/2 \rangle = T/m$ defines the *pseudo-temperature*. A distribution which maximizes entropy subject to the additional constraint that all quadratic velocity moments are conserved is a **Gaussian distribution**, of the form (A.5)

$$f_G = \frac{\rho}{\sqrt{\det(2\pi\Theta)}} \exp\left(-(\mathbf{v} - \mathbf{u}) \cdot \Theta^{-1} \cdot (\mathbf{v} - \mathbf{u})/2\right),$$

where $\Theta := \langle \mathbf{c}\mathbf{c} \rangle$ is the **pseudo-temperature tensor**. The distribution f_G is a normal distribution along any axis through the origin and is the product of independent normal distributions defined along three orthogonal principal axes. It agrees with the Maxwellian distribution in the isotropic case $\Theta = \mathbf{1}\theta$.

Recall the Galilean-invariant Boltzmann equation (equation (2.5) assuming a single default species),

$$\partial_t f + \nabla_{\mathbf{x}} \cdot (\mathbf{v}f) + \nabla_{\mathbf{v}} \cdot (\mathbf{a}f) = C. \quad (2.55)$$

The BGK collision operator is

$$C_\theta = \frac{f_\theta - f}{\tau},$$

where τ is the **relaxation period**. For the BGK collision operator, the *Prandtl number* (i.e. the ratio of the rate of thermal diffusion to momentum diffusion, see Appendix section A.4) is $\text{Pr} = 1$ (for a monatomic gas), as we will see.

In order to admit a tunable Prandtl number, the *Gaussian-BGK* collision operator $C_{\tilde{\Theta}}$, also called the *Ellipsoidal-Statistical BGK* collision operator, was introduced by Holway [26] and is often used instead. This model relaxes to a Gaussian distribution for a temperature tensor which is an affine combination of the isotropized temperature tensor (of the Maxwellian distribution) and the temperature tensor (of the Gaussian distribution with the same quadratic moments). The Gaussian-BGK collision operator is

$$C_{\tilde{\Theta}} = \frac{f_{\tilde{\Theta}} - f}{\tilde{\tau}}, \quad (2.56)$$

where $\tilde{\tau}$ is the Gaussian-BGK relaxation period, $f_{\tilde{\Theta}}$ is the Gaussian distribution for the temperature tensor

$$\tilde{\Theta} := (1 - \nu)\theta \mathbf{1} + \nu\Theta, \quad (2.57)$$

and ν is a tunable parameter which corresponds to the Prandtl number, as we will see, according to the relation $\text{Pr}(1 - \nu) = 1$. Define τ by the requirement that the viscosity satisfies $\mu = p\tau$. Then $\tau = \text{Pr}\tilde{\tau}$; τ is considered to be the relaxation period of the standard BGK collision operator. The collision operator $C_{\tilde{\Theta}}$ respects entropy over the full range of ν values for which $\Theta \geq 0$ (is positive definite) implies $\tilde{\Theta} \geq 0$, that is, for $0 \leq (1 - \nu) \leq 3/2$, corresponding to the range of Prandtl numbers $2/3 \leq \text{Pr} \leq \infty$, which is surprising since in the case $(1 - \nu) > 1$ (where $\theta \mathbf{1}$ is “super-weighted”) the affine combination (2.57) is nonconvex [1]. The Gaussian-BGK model thus gives an entropy-respecting collision operator which allows the heat flux to be tuned from zero ($\text{Pr} = \infty$) essentially up to the full heat flux for a monatomic gas: for a monatomic gas with Maxwell molecules $\text{Pr} = 2/3$, and this is a good approximation for a broad range of physical collision operators including hard spheres and Coulomb collisions (in particular, $\text{Pr} \approx .61$ for ions and $\text{Pr} \approx .58$ for electrons in the Braginskii closure [10]).

Henceforth in this section 2.6 we take as our standard of truth the Galilean-invariant Boltzmann equation (2.55) with Gaussian-BGK collision operator (2.56)

$$\partial_t f + \nabla_{\mathbf{x}} \cdot (\mathbf{v}f) + \nabla_{\mathbf{v}} \cdot (\mathbf{a}f) = C_{\tilde{\Theta}} := \frac{f_{\tilde{\Theta}} - f}{\tilde{\tau}}, \quad (2.58)$$

where $f_{\tilde{\Theta}}$ is given by the Gaussian distribution equation for $\tilde{\Theta}$,

$$f_{\tilde{\Theta}} = \frac{\rho}{\sqrt{\det(2\pi\tilde{\Theta})}} \exp\left(-(\mathbf{v} - \mathbf{u}) \cdot \tilde{\Theta}^{-1} \cdot (\mathbf{v} - \mathbf{u})/2\right),$$

and $\tilde{\Theta}$ is given by equation (2.57),

$$\tilde{\Theta} := (1 - \nu)\theta \mathbf{1} + \nu\Theta.$$

2.6.2 Chapman-Enskog expansion

Consider the Boltzmann equation

$$Df = C[f],$$

where $D = \partial_t f + \nabla_{\mathbf{x}} \cdot (\mathbf{v}f) + \nabla_{\mathbf{v}} \cdot (\mathbf{a}f)$ is the convective derivative in phase space and C is the collision operator. Assume the BGK collision operator

$$C = \frac{f_{\theta} - f}{\tau}.$$

This collision operator is linear and satisfies $C[f_{\theta}] = 0$. (In contrast, the general Gaussian-BGK collision operator causes $\tilde{\Theta}$ to be modified over time, resulting in nonlinear evolution of f .)

The idea of the Chapman-Enskog expansion is to begin with a guess f_0 (which is the distribution about which one is expanding, e.g. a Maxwellian), and solve by successive approximations:

$$\begin{aligned} Df_0 &= Cf_1 \\ Df_1 &= Cf_2 \\ Df_2 &= Cf_3 \\ &\vdots \end{aligned}$$

where it is assumed that one can solve e.g. for f_1 in terms of f_0 . Hopefully the sequence f_n converges rapidly to a solution f .

A formalism which effects such a sequence is as follows. Expand f as

$$f = f^{(0)} + \epsilon \bar{f}^{(1)} + \epsilon^2 \bar{f}^{(2)} + \dots,$$

where ϵ is a formal smallness parameter. Let $C = \bar{C}/\epsilon$:

$$Df = \frac{\bar{C}[\bar{f}]}{\epsilon}. \quad (2.59)$$

Substituting the expansion of f and matching powers of ϵ yields the infinite sequence

$$\begin{aligned} \epsilon^{-1} : & & 0 &= \bar{C}[f^{(0)}], \\ \epsilon^0 : & & Df^{(0)} &= \bar{C}[\bar{f}^{(1)}], \\ \epsilon^1 : & & D\bar{f}^{(1)} &= \bar{C}[\bar{f}^{(2)}], \\ \epsilon^2 : & & & \vdots \end{aligned}$$

Multiplying each equation by its ϵ^n factor and summing yields equation (2.59) (assuming convergence). Choosing $f^{(0)} = f_\theta$ means that $C[f^{(0)}] = 0$ and we can get the chain of approximations started.

To map onto the description in terms of successive approximations, $f_n = \sum_{k=0}^n f^{(k)}$, where $f^{(k)} := \epsilon^k \bar{f}^{(k)}$.

The formal smallness parameter ϵ serves two purposes. First, it specifies how to match up terms (to determine which terms are used for the correction and which for the previous estimate). Second, it signifies that the corrections are expected to decay; otherwise the series would not converge. Once we have used ϵ to match up terms and get an approximate closure we can set $\epsilon = 1$ as a shortcut to restoring the original collision operator and making the replacements $f^{(n)} := \epsilon^n \bar{f}^{(n)}$.

2.6.3 Perturbative stress closure

To derive the five-moment closure for the deviatoric pressure we take the deviatoric part of the pressure tensor evolution equation. Neglecting collisions with other species, the pressure tensor evolution equation (2.12) reads

$$\partial_t \mathbb{P} + \nabla \cdot (\mathbf{u}\mathbb{P}) + \text{Sym}2(\mathbb{P} \cdot \nabla \mathbf{u}) + \nabla \cdot \mathbf{q} = (q/m) \text{Sym}2(\mathbb{P} \times \mathbf{B}) + \mathbb{R}, \quad (2.60)$$

where recall that $\mathbb{R} := \int_{\mathbf{v}} \mathbf{v}\mathbf{v}C$. Note that $\mathbb{R} = \int_{\mathbf{c}} \mathbf{c}\mathbf{c}C$, by conservation of mass ($\int_{\mathbf{v}} C = 0$ and momentum ($\int_{\mathbf{c}} \mathbf{c}C = 0$). Also, \mathbb{R} is traceless by conservation of energy ($\int_{\mathbf{v}} |\mathbf{c}|^2 C = 0$). To prepare to take the deviatoric part we separate into isotropic and traceless parts:

$$\begin{aligned} \text{Sym}2(\mathbb{P} \cdot \nabla \mathbf{u}) &= \text{Sym}2((p \mathbf{1} + \mathbb{P}^\circ) \cdot \nabla \mathbf{u}) \\ &= p \text{Sym}2(\nabla \mathbf{u}) + \text{Sym}2(\mathbb{P}^\circ \cdot \nabla \mathbf{u}) \\ &= p \text{Sym}2(\nabla \mathbf{u})^\circ + 2p \nabla \cdot \mathbf{u} \mathbf{1} + \text{Sym}2(\mathbb{P}^\circ \cdot \nabla \mathbf{u}) \end{aligned}$$

Taking the deviatoric part of (2.12) thus gives

$$\partial_t \mathbb{P}^\circ + \nabla \cdot (\mathbf{u}\mathbb{P}^\circ) + p \text{Sym}2(\nabla \mathbf{u})^\circ + \text{Sym}2(\mathbb{P}^\circ \cdot \nabla \mathbf{u}) + \nabla \cdot \mathbf{q}^\circ = \frac{q}{m} \text{Sym}2(\mathbb{P}^\circ \times \mathbf{B}) + \mathbb{R}, \quad (2.61)$$

where recall that $\mathbf{q}^\circ := \mathbf{q} - (2/5) \text{Sym}3(\mathbf{1} \mathbf{q})$ is the *deviatoric heat flux tensor*.

If a BGK or Gaussian-BGK collision operator is used then we can calculate the relaxation term:

$$\mathbb{R} = \int_{\mathbf{c}} \mathbf{c}\mathbf{c}C_{\tilde{\Theta}} = \int_{\mathbf{c}} \mathbf{c}\mathbf{c} \frac{f_{\tilde{\Theta}} - f}{\tilde{\tau}} = \tilde{\tau}^{-1}((1 - \nu)p \mathbf{1} + \nu \mathbb{P} - \mathbb{P}) = \frac{1 - \nu}{\tilde{\tau}}(p \mathbf{1} - \mathbb{P}).$$

That is, using $\tau := \tilde{\tau}/(1 - \nu)$,

$$\mathbb{R} = -\mathbb{P}^\circ/\tau. \quad (2.62)$$

Note that this agrees with (2.33) in case $C^{\mathbb{R}} = \mathbf{1} \diamond \mathbf{1}$.

To perform a Chapman-Enskog expansion we assume an initial guess (a Maxwellian) for the velocity distribution and substitute into the pressure tensor evolution equation (2.60). The right side will be zero but the left side will not. So we modify the solution used on the right hand side so that it agrees with value assumed by the left hand side for the original guess. One could then substitute the modified distribution into the left hand side to obtain yet another correction from the right hand side. Hopefully this process would converge to a solution of the equation.

Formally, we assume a velocity distribution expansion of the form

$$f = f^{(0)} + \epsilon f^{(1)} + \epsilon^2 f^{(2)} + \dots,$$

where ϵ is a formal smallness parameter which conveys the expectation that the series is intended to converge and which will indicate how to match up terms. We seek a near-Maxwellian stress closure, so we assume that $f^{(0)}$ is Maxwellian (with the same conserved moments as f). The expansion of f implies moment expansions such as

$$\begin{aligned} \mathbb{P} &= p \mathbf{1} + \epsilon \mathbb{P}^{(1)} + \epsilon^2 \mathbb{P}^{(2)} + \dots, \\ \mathbf{q} &= \epsilon \mathbf{q}^{(1)} + \epsilon^2 \mathbf{q}^{(2)} + \dots. \end{aligned}$$

Using the closure equation (2.62) $\mathbb{R} = -\mathbb{P}^\circ/\tau$, the right hand side of the pressure tensor evolution equation is

$$\partial_t \mathbb{P} + \nabla \cdot (\mathbf{u} \mathbb{P}) + \text{Sym}2(\mathbb{P} \cdot \nabla \mathbf{u}) + \nabla \cdot \mathbf{q} = (q/m) \text{Sym}2\left(\frac{\mathbb{P} \times \mathbf{B}}{\epsilon}\right) - \frac{\mathbb{P}^\circ}{\epsilon \tau},$$

where we have replaced \mathbf{B} with \mathbf{B}/ϵ and τ^{-1} with τ^{-1}/ϵ firstly as a way of indicating that τ is expected to be large and \mathbf{B} could be large and secondly in order to show how to match up terms when we substitute the expansions in ϵ . The evolution equation for the deviatoric pressure (2.61) now reads

$$\begin{aligned} \partial_t \mathbb{P}^\circ + \nabla \cdot (\mathbf{u} \mathbb{P}^\circ) + p \text{Sym}2(\nabla \mathbf{u})^\circ + \text{Sym}2(\mathbb{P}^\circ \cdot \nabla \mathbf{u}) + \nabla \cdot \mathbf{q}^\circ \\ = (q/m) \text{Sym}2\left(\frac{\mathbb{P}^\circ \times \mathbf{B}}{\epsilon}\right) - \frac{\mathbb{P}^\circ}{\epsilon \tau}. \end{aligned} \quad (2.63)$$

Since the right hand side vanishes for $f^{(0)}$ (a Maxwellian) we can match up powers of ϵ . For ϵ^0 we obtain

$$p \text{Sym}2(\nabla \mathbf{u})^\circ = (q/m) \text{Sym}2(\mathbb{P}^{\circ(1)} \times \mathbf{B}) - \mathbb{P}^{\circ(1)}/\tau. \quad (2.64)$$

At this point we can “eliminate” ϵ either by replacing $\epsilon \mathbb{P}^{\circ(1)}$ with $\mathbb{P}^{\circ(1)}$, \mathbf{B}/ϵ with the original expression \mathbf{B} , and $\tau\epsilon$ with the original expression τ , all of which leaves equation (2.64) unchanged in appearance, or (more simply) we can just set the formal smallness parameter ϵ to 1. Multiply (2.64) by τ . Assume $\mathbb{P}^{\circ(1)} \approx \mathbb{P}^\circ$. Get the following implicit closure for the deviatoric stress:

$$\boxed{p\tau 2e^\circ = \text{Sym}2(\mathbb{P}^\circ \times \varpi \mathbf{b}) - \mathbb{P}^\circ}, \quad (2.65)$$

where recall that $\varpi := \tau q |\mathbf{B}|/m = \tau \omega_c$, which agrees with the Stokes closure (2.50) in case $C^{\mathbb{R}} = \mathbf{1} \diamond \mathbf{1}$.

2.6.4 Perturbative heat flux closure

McDonald and Groth have obtained a heat flux closure using a Chapman-Enskog expansion. This section follows their derivation in section III.A in [43], generalizing to the case of nonzero magnetic field.

Multiplying the Boltzmann equation (2.58) by $\mathbf{c}\mathbf{c}\mathbf{c}$ and integrating by parts gives the evolution equation

$$\begin{aligned} \partial_t \mathbf{q} + \nabla \cdot (\mathbf{u}\mathbf{q}) + \text{Sym3}(\mathbf{q} \cdot \nabla \mathbf{u}) - \text{Sym3}(\mathbb{P}(\nabla \cdot \mathbb{P})/\rho) + \nabla \cdot \mathbf{q}^{[4]} \\ = \text{Sym3}(\mathbf{q} \times q\mathbf{B}/m) + \int_{\mathbf{c}} \mathbf{c}\mathbf{c}\mathbf{c}C, \end{aligned} \quad (2.66)$$

where $\mathbf{q}^{[4]} := \int_{\mathbf{c}} \mathbf{c}\mathbf{c}\mathbf{c}\mathbf{c}f$ is the fourth-order primitive moment. For the Gaussian-BGK collision operator we compute that

$$\int_{\mathbf{c}} \mathbf{c}\mathbf{c}\mathbf{c}C = \int_{\mathbf{c}} \mathbf{c}\mathbf{c}\mathbf{c} \frac{f_{\tilde{\Theta}} - f}{\tilde{\tau}} = \frac{0 - \mathbf{q}}{\tilde{\tau}} = \frac{-\mathbf{q}}{\tilde{\tau}} = \frac{-\text{Pr}}{\tau} \mathbf{q}.$$

In a Chapman-Enskog expansion we assume a velocity distribution expansion

$$f = f^{(0)} + \epsilon f^{(1)} + \epsilon^2 f^{(2)} + \dots,$$

where $f^{(0)}$ is assumed to be the Gaussian distribution f_{Θ} of f . This implies moment expansions such as

$$\begin{aligned} \mathbf{q} &= \epsilon \mathbf{q}^{(1)} + \epsilon^2 \mathbf{q}^{(2)} + \dots, \\ \mathbf{q}^{[4]} &= \mathbf{q}^{[4](0)} + \epsilon \mathbf{q}^{[4](1)} + \epsilon^2 \mathbf{q}^{[4](2)} + \dots. \end{aligned}$$

For a Gaussian distribution we compute (see equation (A.6)) that $\mathbf{q}^{[4]} = \text{Sym3}(\mathbb{P}\mathbb{P})/\rho$. Following [43], Let

$$K^{[4]} := \int_{\mathbf{c}} \mathbf{c}\mathbf{c}\mathbf{c}\mathbf{c}(f - f_{\Theta}) = \mathbf{q}^{[4]} - \text{Sym3}(\mathbb{P}\mathbb{P})/\rho$$

denote the deviation of the fourth moment from the value for the Gaussian distribution. Using $\text{Sym3}(\nabla \cdot (\mathbb{P}\mathbb{P}/\rho)) - \text{Sym3}(\mathbb{P}(\nabla \cdot \mathbb{P})/\rho) = \text{Sym3}\left(\mathbb{P} \cdot \nabla \left(\frac{\mathbb{P}}{\rho}\right)\right)$, equation (2.66) becomes

$$\begin{aligned} \partial_t \mathbf{q} + \nabla \cdot (\mathbf{u}\mathbf{q}) + \text{Sym3}(\mathbf{q} \cdot \nabla \mathbf{u}) + \text{Sym3}\left(\mathbb{P} \cdot \nabla \left(\frac{\mathbb{P}}{\rho}\right)\right) + \nabla \cdot K^{[4]} \\ = \frac{1}{\epsilon} \left(\text{Sym3}(\mathbf{q} \times q\mathbf{B}/m) - \frac{\mathbf{q}}{\tilde{\tau}} \right), \end{aligned} \quad (2.67)$$

where we have rescaled the collision operator (including the magnetic field) on the right hand side by a factor of ϵ by replacing \mathbf{B} with \mathbf{B}/ϵ and τ with $\tau\epsilon$. Substituting the expansions

$$\begin{aligned} \mathbf{q} &= \epsilon \mathbf{q}^{(1)} + \epsilon^2 \mathbf{q}^{(2)} + \dots, \\ K^{[4]} &= \epsilon K^{[4](1)} + \epsilon^2 K^{[4](2)} + \dots \end{aligned}$$

and matching powers of epsilon yields the implicit heat flux closure equation

$$\text{Sym3}\left(\mathbb{P} \cdot \nabla \left(\frac{\mathbb{P}}{\rho}\right)\right) = \text{Sym3}(\mathbf{q} \times q\mathbf{B}/m) - \frac{\mathbf{q}^{(1)}}{\tilde{\tau}}.$$

Set the formal smallness parameter ϵ to 1. Multiply by $\tilde{\tau} = \tau/\text{Pr}$. Take $\mathbf{q} \approx \mathbf{q}^{(1)}$. Get the following implicit closure for the heat flux tensor:

$$\frac{\tau}{m \text{Pr}} \text{Sym3} \left(\mathbb{P} \cdot \nabla \left(\frac{\mathbb{P}}{\rho} \right) \right) = \text{Sym3}(\mathbf{q} \times \tilde{\omega} \mathbf{b}) - \mathbf{q}, \quad (2.68)$$

which by setting $\tilde{\omega} = 0$ is observed to be a generalization of the heat flux closure given by McDonald and Groth in equation (23) of [43]; here we define

$$\tilde{\omega} := \frac{\varpi}{\text{Pr}} = \frac{\tau \omega_c}{\text{Pr}} = \tilde{\tau} \omega_c = \tilde{\tau} q |\mathbf{B}|/m.$$

We rewrite (2.68) in the form

$$\boxed{\mathbf{q} + \text{Sym3}(\tilde{\omega} \mathbf{b} \times \mathbf{q}) = -\frac{2}{5} k \text{Sym3}(\boldsymbol{\pi} \cdot \nabla \mathbb{T})}, \quad (2.69)$$

where k is the *heat conductivity*, related to the Prandtl number by the formula (A.15)

$$\text{Pr} = \frac{5}{2} \frac{p\tau}{mk},$$

and we have used that $\mathbb{P}/\rho = \mathbb{T}/m$ and $\boldsymbol{\pi} := \mathbb{P}/p$. The explicit solution to equation (2.69) is obtained in the appendix as equation (A.38).

Half the trace of equation (2.69) will give an implicit closure for the heat flux. Using that $\text{tr Sym3}(\mathbf{q} \times \mathbf{b}) = 2\mathbf{q} \times \mathbf{b}$ and that $\text{tr Sym3}(\boldsymbol{\pi} \cdot \nabla \mathbb{T}) = 3\boldsymbol{\pi} \cdot \nabla T + 2\boldsymbol{\pi} : \nabla \mathbb{T} = 5\boldsymbol{\pi} \cdot \nabla T + 2\boldsymbol{\pi} \cdot \nabla \mathbb{T}^\circ$, half the trace of (2.69) is

$$\mathbf{q} + \tilde{\omega} \mathbf{b} \times \mathbf{q} = -k \left(\boldsymbol{\pi} \cdot \nabla T + \frac{2}{5} \boldsymbol{\pi} \cdot \nabla \mathbb{T}^\circ \right). \quad (2.70)$$

Neglecting deviatoric parts (which would be of order ϵ in a Chapman-Enskog expansion about a Maxwellian distribution) and recalling that $\boldsymbol{\pi} = \mathbb{1} + \boldsymbol{\pi}^\circ$ yields

$$\boxed{\mathbf{q} + \tilde{\omega} \mathbf{b} \times \mathbf{q} = -k \nabla T}, \quad (2.71)$$

which agrees with the implicit heat flux closure equation (5.107) in [62] in case $\text{Pr} = 1$.

To get an explicit heat flux closure we need to solve the implicit closures for the heat flux. In section A.5.5 we solve this equation for \mathbf{q} to obtain the heat flux closure (A.27),

$$\mathbf{q} = -k \left(\mathbf{b}\mathbf{b} + \frac{1}{1 + \tilde{\omega}^2} \left((\mathbb{1} - \mathbf{b}\mathbf{b}) - \tilde{\omega} \mathbf{b} \times \mathbb{1} \right) \right) \cdot \nabla T, \quad (2.72)$$

I remark that this closure satisfies the form of an entropy-respecting closure specified in equations (2.26) and (2.27).

2.6.5 Comparison of heat flux closures

In the absence of a magnetic field, the McDonald-Groth (Chapman-Enskog Gaussian-BGK) heat flux closure (2.69) is

$$\mathbf{q}_M = -\frac{2}{5} k \text{Sym3}(\boldsymbol{\pi} \cdot \nabla \mathbb{T}),$$

whereas the entropy-respecting closure (2.40) is

$$\mathbf{q}_L = \bar{\kappa}_1 \nabla \vee \mathbb{T}^{-1} + \bar{\kappa}_2 \mathbb{1} \vee \text{tr}(\nabla \vee \mathbb{T}^{-1}). \quad (2.73)$$

In the isotropic case (see (2.42)),

$$\nabla \vee \mathbb{T}^{-1} = T^{-2} \mathbb{1} \vee \nabla T \text{ and } \mathbb{1} \vee \text{tr}(\nabla \vee \mathbb{T}^{-1}) = 5T^{-2} \mathbb{1} \vee \nabla T,$$

and these closures simplify to (see (2.43))

$$\mathbf{q}_L = -T^{-2}(\bar{\kappa}_1 + 5\bar{\kappa}_2) \mathbb{1} \vee \nabla T \quad \text{and} \quad \mathbf{q}_M = -\frac{2}{5}k \mathbb{1} \vee \nabla T.$$

So for consistent closure coefficients we require that

$$\bar{\kappa}_1 + 5\bar{\kappa}_2 = \frac{2}{5}T^2 k,$$

which is analogous to equation (2.25). In general, however, the two closures disagree. Recall from (2.41) that

$$\nabla \vee \mathbb{T}^{-1} = -T^{-2} \text{Sym3}(\nabla \mathbb{T} : (\boldsymbol{\pi}^{-1} \diamond \boldsymbol{\pi}^{-1})).$$

The entropy-respecting closures with consistent closure coefficients are thus

$$\begin{aligned} \mathbf{q}_1 &= -\frac{2}{5}k \underbrace{\text{Sym3}(\nabla \mathbb{T} : \boldsymbol{\pi}^{-1} \diamond \boldsymbol{\pi}^{-1})}_{\mathbb{1} \vee \nabla T \text{ if } \boldsymbol{\pi} = \mathbb{1}} && \text{(if } \bar{\kappa}_2 = 0) \text{ and} \\ \mathbf{q}_2 &= -\frac{2}{25}k \underbrace{\mathbb{1} \vee \text{tr}(\text{Sym3}(\nabla \mathbb{T} : \boldsymbol{\pi}^{-1} \diamond \boldsymbol{\pi}^{-1}))}_{5\nabla T \text{ if } \boldsymbol{\pi} = \mathbb{1}} && \text{(if } \bar{\kappa}_1 = 0) \end{aligned}$$

and convex combinations thereof, in contrast to the McDonald-Groth closure

$$\mathbf{q}_M = -\frac{2}{5}k \text{Sym3}(\boldsymbol{\pi} \cdot \nabla \mathbb{T}).$$

In the isotropic limit $\boldsymbol{\pi} \approx \mathbb{1}$ and the two closures agree. If $\boldsymbol{\pi} \approx \mathbb{1}$ and if $\nabla \mathbb{T}^\circ$ is small (i.e. $|\nabla \boldsymbol{\pi}^\circ| \ll |\nabla \ln T|$) then the closures simplify to

$$\mathbf{q}_M \approx \mathbf{q}_L \approx \mathbf{q}_1 := -\frac{2}{5}k \mathbb{1} \vee \nabla T.$$

I remark that the entropy-respecting constraint assumed by the Levermore closure is not physically justified except in the near-Maxwellian limit, whereas the McDonald-Groth closure is physically justifiable in the near-Gaussian limit. One wonders whether the closures \mathbf{q}_L and \mathbf{q}_1 are well-posed.

2.7 Intraspecies closure coefficients

The five-moment and ten-moment gas-dynamic closures are determined by the relaxation period τ of the deviatoric stress and the relaxation period $\tilde{\tau}$ of the heat flux, related to τ by $\tilde{\tau} = \tau / \text{Pr}$. The viscosity is given by $\mu = p\tau$ and the thermal conductivity by $k = \frac{5}{2} \frac{\mu}{\text{Pr}}$.

To obtain full closure we need to specify τ in terms of the evolved moments. We therefore assume that τ is a function of the evolved moments, that is, of the Maxwellian or Gaussian distribution which is in bijective correspondence with the evolved moments. This is a simplifying assumption, since for physical collision operators τ and $\tilde{\tau}$ actually depend on the details of the distribution. So in general we write, e.g., $\tau(f)$.

2.7.1 Viscosity and heat conductivity are functions of temperature independent of density.

By Galilean relativity τ is a function of the density and the primitive moments of order greater than 1 (e.g. the pressure). In the five-moment case we can write $\tau(n, T)$ and in the ten-moment case $\tau(n, \mathbb{T})$. We want to characterize these functions.

Most classical collision operators satisfy

$$C(\lambda f) = \lambda^2 C(f). \quad (2.74)$$

We will argue that, for such collision operators, closures for μ and k depend only on temperature.

Property 2.74 essentially says that doubling the number of particles doubles the rate of collisions experienced by a particle and thus doubles the rate of evolution of the shape of the distribution without otherwise altering its shape. Formally, if f satisfies the spatially homogeneous Boltzmann equation

$$\partial_t f = C(f)$$

then so does $\tilde{f}(t) = \lambda f(\lambda t)$.

Therefore, the relaxation periods scale according to $\tau(\lambda f) = \lambda^{-1} \tau(f)$. The moments are a function of f and scale as: $n(\lambda f) = \lambda n(f)$, $T(\lambda f) = T(f)$, and $\mathbb{T}(\lambda f) = \mathbb{T}(f)$.

Therefore, the viscosity $\mu = nT\tau$ and the thermal conductivity scale as $\mu(\lambda f) = \mu(f)$ and $k(\lambda f) = k(f)$.

We now invoke the simplifying assumption e.g. that $\mu(n, \mathbb{T})$. This says that μ is the same for any two distributions which share the same moments. We show that μ is actually independent of n by differentiating the constant map $\lambda \mapsto \mu(\lambda f) = \mu(f)$ with respect to λ : $0 = d_\lambda \mu(\lambda f) = d_\lambda \mu(n(\lambda f), \mathbb{T}(\lambda f)) = d_\lambda \mu(\lambda n(f), \mathbb{T}(f)) = n \partial_n \mu$, as needed.

In conclusion, for the ten-moment model

$$\tau(n, \mathbb{T}) = \frac{\mu(\mathbb{T})}{nT}, \quad \tilde{\tau} = \tau / \text{Pr}. \quad k(\mathbb{T}) = \frac{5}{2} \frac{\mu(\mathbb{T})}{m \text{Pr}}.$$

2.7.2 Positivity-preserving heat conductivity closure

Contrary to the case for five-moment entropy evolution, in the ten-moment case a local minimum can decrease if a nonzero heat flux closure is used. The closure for k is critically important in maintaining positivity.

To ensure that the heat flux closure maintains positivity of the temperature, the heat conductivity k should go to zero as $\det(\mathbb{T})$ goes to zero. This effectively shuts down heat flow to prevent positivity violations. Five-moment closures for k naturally are specified in terms of the scalar temperature T . When using such a closure formula in the ten-moment model, T (i.e. $\text{tr } \mathbb{T} / 3$, the arithmetic average of the eigenvalues of \mathbb{T}) should be replaced with $(\det \mathbb{T})^{1/3}$ (i.e. the geometric average of the eigenvalues of \mathbb{T}) [38].

For the pressure tensor relaxation period τ one can choose to define τ in terms of $\text{tr } \mathbb{T}$ or $\det \mathbb{T}$.

In particular, the Braginskii five-moment closure (discussed in the next subsection) is of the form

$$\tau = \tau_0 \sqrt{m} \frac{T^{3/2}}{n}. \quad (2.75)$$

In the ten-moment model one could use

$$\tau = \tau_0 \sqrt{m} \frac{(\det \mathbb{T})^{1/2}}{n}.$$

The viscosity is then

$$\mu = p\tau = \tau_0 \sqrt{m} T (\det \mathbb{T})^{1/2}$$

2.7.3 Braginskii closure coefficients

In the absence of a magnetic field the viscosities given by Braginskii [10] are³

$$\begin{aligned} \mu_i &= .96\tau_i^{\text{Br}} p_i = .96\tau'_{ii} p_i, & \tau_i^{\text{Br}} &:= \tau'_{ii}, & \tau'_{ii} &:= \tau_0 \sqrt{m_i} \frac{T_i^{3/2}}{n_i}, \\ \mu_e &= .73\tau_e^{\text{Br}} p_e = .52\tau'_{ee} p_e, & \tau_e^{\text{Br}} &:= \frac{\tau'_{ee}}{\sqrt{2}}, & \tau'_{ee} &:= \tau_0 \sqrt{m_e} \frac{T_e^{3/2}}{n_e}, \end{aligned} \quad (2.76)$$

where the base isotropization period is

$$\tau_0 = \frac{12\pi^{3/2}}{\ln \Lambda} \left(\frac{\epsilon_0}{e^2} \right)^2, \quad (2.77)$$

where $\ln \Lambda$ is the Coulomb logarithm, discussed below.

In a one-species charged gas the ion viscosities would be

$$\begin{aligned} \mu_i &= \tau'_{ii} p_i, \\ \mu_e &= \tau'_{ee} p_e. \end{aligned}$$

In the two-species gas, however, isotropization of each species is accelerated by interspecies collisions. Therefore, the viscosities are given by

$$\begin{aligned} \mu_i &= \tau_i p_i, \\ \mu_e &= \tau_e p_e, \end{aligned}$$

where the overall isotropization rates are given by

$$\begin{aligned} \tau_i^{-1} &\approx \tau_{ii}^{-1} + \tau_{ie}^{-1}, \\ \tau_e^{-1} &\approx \tau_{ee}^{-1} + \tau_{ei}^{-1}. \end{aligned}$$

³ I have used the symbols τ_i^{Br} and τ_e^{Br} to distinguish them from τ_i and τ_e , which are defined in this document to be the isotropization period of the pressure tensor, equivalently the collision period taking all species into account.

My understanding is that τ_i^{Br} is intended to be the ion-ion collision period (which approximates the ion collision period), whereas τ_e^{Br} is intended to be the electron-ion collision period in a Lorentzian plasma; the factor of $\sqrt{2}$ evidently arises from the fact that the reduced mass in an ion-ion collision is half the ion mass. See [10] pages 220 and 277.

Balescu objects to the artificial dissimilarity between ions and electrons that this convention introduces into the formulas and instead redefines τ_i so that its formula agrees with the formula for τ_e (see his footnote on page 274 of [2]), but Braginskii's definitions seem to have become fairly standard.

Since the mass ratio is large,

$$\begin{aligned}\tau_i^{-1} &\approx \tau_{ii}^{-1} \gg \tau_{ie}^{-1}, \\ \frac{1}{2}\tau_e^{-1} &\approx \tau_{ee}^{-1} \approx \tau_{ei}^{-1}\end{aligned}$$

explaining the differing coefficients in equation (2.76). In a pair plasma we expect that $\tau_i^{-1} = 2\tau_{ii}^{-1}$.

The Coulomb logarithm is the logarithm of the plasma parameter Λ which is on the order of the number of particles in a Debye sphere, roughly

$$\Lambda = n\lambda_D^3,$$

where the Debye length (see section A.2) is given by

$$\lambda_D = \sqrt{\frac{\epsilon_0 T_e}{n_e e^2}};$$

typically $10 \lesssim \ln \Lambda \lesssim 20$.

Note that these collision periods are not identical to the isotropization periods τ_s appearing elsewhere in this dissertation, which I define to be the viscosity divided by the pressure: $\mu = p\tau$.

Comparing Braginskii's viscosities and heat conductivities,

$$\begin{aligned}\mu_e &= 0.73 p_e \tau_e^{\text{Br}}, & \mu_i &= 0.96 p_i \tau_i^{\text{Br}}, \\ k_e &= 3.16 p_e \tau_e^{\text{Br}} / m_e, & k_i &= 3.91 p_i \tau_i^{\text{Br}} / m_i,\end{aligned}$$

the Prandtl numbers for the unmagnetized Braginskii closure are

$$\text{Pr}_e = .58, \quad \text{Pr}_i = .61,$$

where we have used the definition (A.15)

$$\text{Pr}_s := \frac{5}{2} \frac{\mu_s}{m k_s}.$$

Recall that for a monatomic gas the Prandtl number should be close to $2/3 = \overline{.66}$.

2.8 Interspecies collisional closures

Interspecies collisions are generally ignored in this work, on the assumption that in a weakly collisional plasma we can lump the large majority of the microscale effects into the intraspecies collision operators. That is, we are assuming that momentum and energy are largely conserved within each species. As an illustration of this principle, note that even in the case of Coulomb collisions one of the chief effects of electron-ion collisions is to increase the rate of isotropization of the electrons. Our Gaussian-BGK ‘‘intraspecies’’ collision operator really includes the interspecies particle interactions to the degree that these interactions conserve momentum and energy within each species.

Nevertheless, it would be of interest to incorporate an interspecies collision operator. To obtain a form for the interspecies collision operator one can require interspecies collisions not to decrease entropy.

For an interspecies BGK collision operator $C_{ie}(f_i, f_e)$, one could make the loss term proportional to the distribution function and define the gain term so as to satisfy the following requirements:

- conservation of total mass, momentum, and energy:

$$\begin{aligned}\int_{\mathbf{v}} (C_{ie}) &= 0, \\ m_i \int_{\mathbf{v}} (\mathbf{v} C_{ie}) + m_e \int_{\mathbf{v}} (\mathbf{v} C_{ei}) &= 0, \\ m_i \int_{\mathbf{v}} (|\mathbf{v}|^2 C_{ie}) + m_e \int_{\mathbf{v}} (|\mathbf{v}|^2 C_{ei}) &= 0,\end{aligned}$$

- bilinearity of $C_{ie}(f_i, f_e)$ and $C_{ei}(f_e, f_i)$,
- total entropy is nondecreasing in the near-Maxwellian limit,

$$\int_{\mathbf{v}} (C_{ie} \log f_i) + \int_{\mathbf{v}} (C_{ei} \log f_e) \gtrsim 0,$$

- agreement with Gaussian-BGK for agreeing distributions, e.g., if $f_i = f_e$ and $m_i = m_e$ then $C_{ii}(f_i, f_i) = C_{ie}(f_i, f_e)$, and
- Galilean invariance.

A heuristic to design such an interspecies collision operator is first to specify a “driftless interspecies collision operator” for the case that the interspecies drift velocity is zero. For the simple BGK case (relaxation to a Maxwellian) one could calculate the Maxwellian distributions that the two distributions would have in equilibrium and relax the distributions of the two species toward their respective equilibrium Maxwellians at the same rate.

To handle drifting distributions one can independently relax the drift velocity to zero and relax the distribution shapes toward an average. For the ten-moment model this leads to a fluid closure which relaxes toward a common temperature tensor.

So for the Maxwellian case the driftless collision operators would be:

$$\begin{aligned}C'_{ie} &= (\mathcal{M}(n_i, \mathbf{u}_i, T) - f_i)/\tau, \\ C'_{ei} &= (\mathcal{M}(n_e, \mathbf{u}_e, T) - f_e)/\tau,\end{aligned}$$

where \mathcal{M} denotes a Maxwellian distribution and (for monatomic species)

$$T = (n_i T_i + n_e T_e)/(n_i + n_e)$$

to conserve total thermal energy.

To generalize to the Gaussian-BGK case, one would instead use

$$\begin{aligned}C_{ie} &= (\mathcal{G}(n_i, u_i, \tilde{\mathbb{T}}) - f_i)/\tau, \\ C_{ei} &= (\mathcal{G}(n_e, u_e, \tilde{\mathbb{T}}) - f_e)/\tau,\end{aligned}$$

where

$$\begin{aligned}\tilde{\mathbb{T}} &= (n_i \tilde{\mathbb{T}}_i + n_e \tilde{\mathbb{T}}_e)/(n_i + n_e), \\ \tilde{\mathbb{T}}_i &= \nu \mathbb{T}_i + (1 - \nu) T_i \mathbf{1}, \\ \tilde{\mathbb{T}}_e &= \nu \mathbb{T}_e + (1 - \nu) T_e \mathbf{1}.\end{aligned}$$

This should respect entropy for near-Maxwellian distributions.

To generalize to the case $\mathbf{u}_i \neq 0 \neq \mathbf{u}_e$, we can use the same collision operators specified above for the thermal equilibration part and handle the resistive drag separately. The constraints above on the collision operator are satisfied if the resistive drag force on the species is equal and opposite, so there is essentially complete freedom in specifying the magnitude and direction of resistive drag and the allocation of resistive heating among species and spatial directions. Closures such as Braginskii's would imply the value of the drag force, and one would expect heating to be allocated among species in inverse proportion to particle mass. I am inclined to allocate resistive heating primarily perpendicular to the direction of drift velocity, although for some reason Miura and Groth [46] allocate it primarily parallel to the drift velocity in their ten-moment closure.

2.9 MHD equations

A **magnetohydrodynamic (MHD) fluid** is a fluid that conducts electricity. In this document we use MHD to refer to models of plasma that evolve a single-fluid description of mass density and momentum density.

MHD allows us to write a description of plasma evolution that is fully Galilean-invariant. Although Lorentz-invariant formulations of MHD have also been formulated, in this discussion we take MHD to mean Galilean-invariant MHD. Consider Maxwell's equations (2.1) in the form

$$\begin{aligned} \partial_t \mathbf{B} + \nabla \times \mathbf{E} &= 0, & \nabla \cdot \mathbf{B} &= 0, \\ -c^{-2} \partial_t \mathbf{E} + \nabla \times \mathbf{B} &= \mu_0 \mathbf{J}, & c^{-2} \nabla \cdot \mathbf{E} &= \mu_0 \sigma, \end{aligned}$$

where $\mu_0 := 1/(c^2 \epsilon_0)$. In the limit $c \rightarrow \infty$ the displacement current $\partial_t \mathbf{E}$ and the net charge σ go to zero and we get the Galilean-invariant system

$$\begin{aligned} \partial_t \mathbf{B} + \nabla \times \mathbf{E} &= 0, & \nabla \cdot \mathbf{B} &= 0, \\ \nabla \times \mathbf{B} &= \mu_0 \mathbf{J}, & 0 &= \mu_0 \sigma. \end{aligned} \tag{2.78}$$

Note that this does *not* imply that $\nabla \cdot \mathbf{E} = 0$. (In fact, $\nabla \cdot \mathbf{E}$ is not a Galilean-invariant quantity and in the Galilean limit transforms according to $\nabla \cdot \mathbf{E}' = \nabla \cdot \mathbf{E} + d\mathbf{v} \cdot \mathbf{J}/\mu_0$, where $d\mathbf{v} = \mathbf{v} - \mathbf{v}'$.) For this reason, in the MHD limit people often speak of the assumption of charge **quasineutrality** rather than charge neutrality. This should not be misunderstood. The MHD model constitutes a self-consistent Galilean-invariant model that assumes exact charge neutrality.

The MHD limit fundamentally alters the ‘‘causal’’ relationship of electromagnetic quantities. In the Lorentz-invariant Maxwell equations a prescribed \mathbf{J} and σ (and initial conditions) determine \mathbf{E} and \mathbf{B} . In the Galilean-invariant limit \mathbf{J} is determined from \mathbf{B} , and \mathbf{E} must be externally supplied from a fluid equation called *Ohm's law*.

2.9.1 Ohm's law

Ohm's law is the evolution equation for current density \mathbf{J} , solved for the electric field \mathbf{E} . The evolution equation for \mathbf{J} is obtained by summing current evolution for each species over all species. Current evolution for a single species s is momentum evolution (2.8) times its charge-to-mass ratio q_s/m_s :

$$\partial_t \mathbf{J}_s + \nabla \cdot (\mathbf{u}_s \mathbf{J}_s + (q_s/m_s) \mathbb{P}_s) = (q_s^2/m_s) n_s (\mathbf{E} + \mathbf{u}_s \times \mathbf{B}) + (q_s/m_s) \mathbf{R}_s,$$

where $\mathbb{P}_s^q := (q_s/m_s)\mathbb{P}_s$ is the *electrokinetic pressure tensor*. Summing over all species gives net current evolution,

$$\begin{aligned} \partial_t \mathbf{J} + \nabla \cdot (\mathbf{u}\mathbf{J} + \mathbf{J}\mathbf{u} - \sigma \mathbf{u}\mathbf{u} + \sum_s \sigma_s \mathbf{w}_s \mathbf{w}_s) + \sum_s (q_s/m_s) \nabla \cdot \mathbb{P}_s \\ = \sum_s (q_s^2/m_s) n_s (\mathbf{E} + (\mathbf{u} + \mathbf{w}_s) \times \mathbf{B}) + \sum_s (q_s/m_s) \mathbf{R}_s, \end{aligned}$$

where the total momentum density $\rho \mathbf{u} := \sum_s \rho_s \mathbf{u}_s$ defines the net fluid velocity \mathbf{u} and the *species drift velocity* is defined by $\mathbf{w}_s := \mathbf{u}_s - \mathbf{u}$. To infer the species drift velocities \mathbf{w}_s from current, for a multispecies fluid one must impose constitutive assumptions, but for a two-species fluid e.g. of ions i and electrons e the assumption of charge neutrality

$$n_i = n_e =: n$$

allows one to infer species drift velocity from current. Charge neutrality says that net current is independent of reference frame. In the reference frame of the fluid we can solve the definitions of charge density and momentum density

$$\begin{aligned} \mathbf{J} &= \mathbf{J}_i + \mathbf{J}_e, \\ 0 &= \frac{m_i}{q_i} \mathbf{J}_i + \frac{m_e}{q_e} \mathbf{J}_e \end{aligned}$$

for the drift velocities in terms of the current and the ratios of mass to charge of the species. For simplicity we take $q_i = e$ and $q_e = -e$, where e is the charge on a proton. Then

$$\mathbf{J}_s = \frac{\check{\mu}}{m_s} \mathbf{J} \quad \text{and} \quad \mathbf{w}_s = \frac{\mathbf{J}_s}{n q_s}. \quad (2.79)$$

Current evolution simplifies to

$$\partial_t \mathbf{J} + \nabla \cdot \left(\mathbf{u}\mathbf{J} + \mathbf{J}\mathbf{u} - \frac{d\tilde{m}}{\rho} \mathbf{J}\mathbf{J} \right) + \nabla \cdot \left(\frac{\mathbb{P}_i}{\tilde{m}_i} - \frac{\mathbb{P}_e}{\tilde{m}_e} \right) = \frac{en}{\check{\mu}} \left(\mathbf{E} + \left(\mathbf{u} - \frac{d\tilde{m}}{\rho} \mathbf{J} \right) \times \mathbf{B} - \boldsymbol{\eta} \cdot \mathbf{J} \right);$$

here the reduced mass $\check{\mu}$ is defined by $\check{\mu}^{-1} := m_i^{-1} + m_e^{-1}$, the mass difference is defined by $dm = m_i - m_e$, and we use tilde to indicate division by e , so $\tilde{\mu} := \check{\mu}/e$, $d\tilde{m} := dm/e$, $\tilde{m}_i := m_i/e$, and $\tilde{m}_e := m_e/e$. The resistivity $\boldsymbol{\eta}$ is related to the interspecies drag force by $-\mathbf{R}_i = \mathbf{R}_e = n\boldsymbol{\eta} \cdot \mathbf{J}$. The quantity $-\frac{d\tilde{m}}{\rho} \mathbf{J} = \mathbf{w}_i + \mathbf{w}_e$ is twice the velocity of the charges relative to the fluid.

Solving for \mathbf{E} gives Ohm's law,

$$\mathbf{E} = \boldsymbol{\eta} \cdot \mathbf{J} + \mathbf{B} \times \left(\mathbf{u} - \frac{d\tilde{m}}{\rho} \mathbf{J} \right) + \frac{\check{\mu}}{en} \left[\nabla \cdot \left(\frac{\mathbb{P}_i}{\tilde{m}_i} - \frac{\mathbb{P}_e}{\tilde{m}_e} \right) + \partial_t \mathbf{J} + \nabla \cdot \left(\mathbf{u}\mathbf{J} + \mathbf{J}\mathbf{u} - \frac{d\tilde{m}}{\rho} \mathbf{J}\mathbf{J} \right) \right]. \quad (2.80)$$

We write Ohm's law in the form

$$\mathbf{E} = \mathbf{B} \times \mathbf{u}_c + \mathbf{E}', \quad (2.81)$$

where

$$\mathbf{u}_c := \mathbf{u} - \frac{d\tilde{m}}{\rho} \mathbf{J} \quad (2.82)$$

is the **charge velocity** (defined to be the fluid velocity plus the sum of the drift velocities of both species) and where

$$\mathbf{E}' := \boldsymbol{\eta} \cdot \mathbf{J} + \frac{\tilde{\mu}}{en} \left[\nabla \cdot \left(\frac{\mathbb{P}_i}{\tilde{m}_i} - \frac{\mathbb{P}_e}{\tilde{m}_e} \right) + \partial_t \mathbf{J} + \nabla \cdot \left(\mathbf{u} \mathbf{J} + \mathbf{J} \mathbf{u} - \frac{d\tilde{m}}{\rho} \mathbf{J} \mathbf{J} \right) \right]$$

is the nonideal component of the electric field. The expression $\mathbf{B} \times \mathbf{u}_c$ is the ideal electric field of Hall MHD.

In the MHD model the Ohm's law expression for electric field is used in the evolution equation $\partial_t \mathbf{B} + \nabla \times \mathbf{E} = 0$ for the magnetic field, and Ampere's law (from (2.78))

$$\mathbf{J} = \mu_0^{-1} \nabla \times \mathbf{B} \tag{2.83}$$

is used to define the current. Thus the full evolution equation for the magnetic field is

$$\begin{aligned} \partial_t \mathbf{B} + \nabla \times \left(\boldsymbol{\eta} \cdot (\mu_0^{-1} \nabla \times \mathbf{B}) + \mathbf{B} \times \left(\mathbf{u} - \frac{d\tilde{m}}{\rho} \mu_0^{-1} \nabla \times \mathbf{B} \right) + \frac{\tilde{\mu}}{en} \nabla \cdot \left(\frac{\mathbb{P}_i}{\tilde{m}_i} - \frac{\mathbb{P}_e}{\tilde{m}_e} \right) \right. \\ \left. + \frac{\tilde{\mu}}{en} \left[\mu_0^{-1} \nabla \times \partial_t \mathbf{B} + \mu_0^{-1} \nabla \cdot \left(\mathbf{u} \nabla \times \mathbf{B} + (\nabla \times \mathbf{B}) \mathbf{u} - \mu_0^{-1} \frac{d\tilde{m}}{\rho} (\nabla \times \mathbf{B}) \nabla \times \mathbf{B} \right) \right] \right) = 0. \end{aligned}$$

This is an implicit differential equation for \mathbf{B} and requires an implicit numerical method. Use of an explicit method requires some sort of simplification. Ideal MHD simplifies magnetic field evolution to

$$\partial_t \mathbf{B} + \nabla \times (\mathbf{B} \times \mathbf{u}) = 0,$$

discarding all other terms; this is a hyperbolic system and is naturally suited to an explicit method. The Hall term

$$\nabla \times \left(\mathbf{B} \times \left(\frac{d\tilde{m}}{\rho} \mu_0^{-1} \nabla \times \mathbf{B} \right) \right)$$

is strongly dispersive, especially if the $\partial_t \mathbf{B}$ terms is left out, and calls for an implicit method.

2.9.2 Mass density evolution

Since MHD assumes charge neutrality, its representation of species densities should enforce this constraint. In a charge-neutral two-species fluid the density of each species can be inferred from the total mass density. Therefore we evolve the total mass density. The evolution equation of (total) mass density is the sum of the evolution equations (2.6) for the mass density of the individual species. It reads

$$\partial_t \rho + \nabla \cdot (\rho \mathbf{u}) = 0, \tag{2.84}$$

where $\rho = \rho_i + \rho_e$ and the total fluid velocity is defined by the conservation requirement that the total momentum density be the sum of the momentum densities of the individual species, $\rho \mathbf{u} := \rho_i \mathbf{u}_i + \rho_e \mathbf{u}_e$.

We can infer the mass density and number density of each species from the total mass density using the relations

$$\rho = (m_i + m_e)n, \quad \rho_i = nm_i, \quad \rho_e = nm_e.$$

Recall from equation (2.79) that we can infer the species drift velocity $\mathbf{w}_s := \mathbf{u}_s - \mathbf{u}$ from the current:

$$\mathbf{w}_s = \frac{\check{\mu}}{m_s n q_s} \mathbf{J}. \quad (2.85)$$

With this we may check that mass evolution, equivalently number density evolution (2.7)

$$\partial_t n_s + \nabla \cdot (n_s \mathbf{u}_s), \quad (2.86)$$

is satisfied for each species. Indeed, $n_s = n$ and $\nabla \cdot (n \mathbf{u}_s) = \nabla \cdot (n \mathbf{u}) + \nabla \cdot (n \mathbf{w}_s)$ and $\nabla \cdot (n \mathbf{w}_s) = 0$ by equation (2.85) because by the Galilean-invariant Ampere's law $\nabla \cdot \mathbf{J} = \mu_0^{-1} \nabla \cdot \nabla \times \mathbf{B} = 0$. So number density evolution for each species reduces to the same assertion,

$$\partial_t n + \nabla \cdot (\mathbf{u} n) = 0, \quad (2.87)$$

which is equivalent to the evolution equation (2.84) for total mass density.

2.9.3 Momentum density evolution

MHD evolves an evolution equation for the net momentum density. It is derived by summing the density evolution equations of the individual species. Knowledge of number density n , net momentum density $\rho \mathbf{u}$, and current density \mathbf{J} is sufficient to infer the momentum density $\rho_s \mathbf{u}_s$ of each species. Indeed, $\rho_s \mathbf{u}_s = m_s (\mathbf{u} + \mathbf{w}_s)$ where $\mathbf{w}_s = \frac{\check{\mu}}{m_s n q_s} \mathbf{J}$ (equation (2.85)). Therefore, there is no need to evolve separate momentum evolution equations for each species (and doing so would result in inconsistency due to numerical error or use of an approximate Ohm's law).

From another viewpoint, recall that Ohm's law is current evolution solved for electric field. Exact current evolution is a linear combination (with weights e/m_i and $-e/m_e$) of the momentum evolution equations of the two species. Total momentum evolution is the sum of the momentum evolution equations. So we again see that momentum evolution plus Ohm's law is equivalent to specifying momentum evolution for each species.

Summing the species momentum evolution equations (2.8),

$$\partial_t (\rho_s \mathbf{u}_s) + \nabla \cdot (\rho_s \mathbf{u}_s \mathbf{u}_s + \mathbb{P}_s) = q_s n_s (\mathbf{E} + \mathbf{u}_s \times \mathbf{B}) + \mathbf{R}_s,$$

over ions i and electrons e gives net momentum evolution

$$\partial_t (\rho \mathbf{u}) + \nabla \cdot (\rho \mathbf{u} \mathbf{u} + \mathbb{P}^d + \mathbb{P}) = \mathbf{J} \times \mathbf{B}, \quad (2.88)$$

where we will call

$$\mathbb{P}^d := \rho_i \mathbf{w}_i \mathbf{w}_i + \rho_e \mathbf{w}_e \mathbf{w}_e$$

the **drift pressure** tensor; here \mathbf{E} has disappeared because of charge neutrality and we have used that $\mathbf{R}_i + \mathbf{R}_e = 0$ by conservation of momentum.

We can compute the diffusion pressure in terms of the current using equation (2.85),

$$\mathbf{w}_s = \frac{\check{\mu}}{m_s n q_s} \mathbf{J}.$$

We get

$$\mathbb{P}^d = \tilde{m}_e \tilde{m}_i \mathbf{J} \mathbf{J} / \rho \quad (2.89)$$

In addition to assuming [quasineutrality](#), MHD models typically neglect second-order terms in \mathbf{w}_s such as \mathbb{P}^d . A physical justification for doing so is the assumption that interspecies drift velocity is dominated by the fluid velocity \mathbf{u} and the thermal velocity \mathbf{c} of particles. We wish to drop such second-order terms in \mathbf{w}_s because they are numerically difficult: since \mathbf{w}_s is defined in terms of $\nabla \times \mathbf{B}$, second-order terms give rise to nonlinear higher-order differential operators.

2.9.4 Energy density evolution

In contrast to the situation for mass and momentum, the neutrality assumption of MHD does not require that one replace the evolution equations for energy density of the individual species with a net energy density.

Models which evolve separate energy evolution equations for two species are called **two-fluid MHD** models. Models which evolve a total energy equation are **one-fluid MHD models**.

In this document we are chiefly interested in two-fluid MHD. If we evolve a single energy equation then we must use a constitutive assumption to infer the energy of the individual species in order to define the pressure tensors that appear in Ohm's law (2.80). A single energy evolution equation is most often used when the pressure terms are neglected in Ohm's law. A primary goal of this dissertation is to determine minimal modeling requirements to simulate fast magnetic reconnection with a fluid model without invoking resistive drag force (which is found to be insufficient for fast reconnection unless resistivity is defined anomalously). In the absence of resistivity the pressure term is necessary to support steady magnetic reconnection. We seek a model which supports fast reconnection even for pair plasma. But in the case of pair plasma, if we evolve a combined pressure tensor and assume that pressure is equally distributed among both species then the pressure term disappears from Ohm's law and steady reconnection cannot be supported. If we evolve separate evolution equations for the pressure of each species, however, even in the case of *symmetric pair plasma* we will see that the contributions of the pressure tensors of the two species to the reconnection electric field will add instead of cancel.

2.9.5 Incompressible MHD

Incompressible MHD assumes that the number density n is conserved along particle paths. Recall number density evolution (2.87), which we here write in the form

$$d_t n = -n \nabla \cdot \mathbf{u}.$$

So incompressibility means that $\nabla \cdot \mathbf{u} = 0$.

In the compressible case we need to evolve energy in order to infer the scalar pressure in the momentum evolution equation. In the incompressible case one instead infers the scalar pressure from the incompressibility equation as a constraint. The deviatoric pressure can be obtained either from deviatoric strain (for the five-moment closure) or by evolving a deviatoric pressure tensor.

Again, we may check that the evolution equation (2.86) for number density of each species is exactly satisfied when the assumption of incompressibility is imposed. As before, we need that

$\nabla \cdot (n_s \mathbf{w}_s) = 0$. The proof goes through without change, since it is simply based on the definition of \mathbf{w}_s in terms of \mathbf{J} .

Incompressibility is justified in the presence of a strong, slowly varying magnetic field if quantities vary slowly in the direction of the magnetic field (see equation (6.157) in [21]).

2.9.6 Entropy evolution for two-fluid MHD

While neglect of the drift pressure means that the momentum equation of two-fluid MHD usually differs from the momentum equation of two-fluid Maxwell, two-fluid MHD, whether compressible or not, satisfies the exact same equations as two-fluid Maxwell for density evolution and pressure evolution. Since entropy evolution is derived based only on density evolution and pressure evolution and not on momentum evolution, the entropy evolution equations hold unchanged for both incompressible and compressible two-fluid MHD.

2.10 Summary

For a summary of the results of this chapter, we refer the reader back to the systems of equations immediately preceding this chapter.

Chapter 3

Steady Magnetic Reconnection

3.1 Definition of rotationally symmetric 2D magnetic reconnection

3.1.1 Translational symmetry

We define a problem to be **two-dimensional (2D)** if the problem is invariant under translation parallel to an axis which we momentarily call the translational axis. Choose a plane perpendicular to the translational axis. We will call it **the plane**. The solution is fully represented by its value on the plane. So we can solve the problem on the plane, that is, on a two-dimensional spatial domain rather than on three-dimensional space.

3.1.2 Rotational symmetry

Suppose that the problem is also invariant under 180-degree rotation around an axis parallel to the translational axis, which we will call the **out-of-plane axis**. Then we say that the problem is **rotationally symmetric**. This chapter is concerned with 2D rotationally symmetric problems.

We refer to the intersection of the plane and the out-of-plane axis as the **origin**, which we designate as $\mathbf{0}$; we choose a cartesian coordinate system whose origin is at this point and one of whose coordinate axes coincides with the out-of-plane axis. We will take the out-of-plane axis to be the z **axis**. The other two axes lie in the plane.

The alignment of the other two axes is based on the symmetries of the initial conditions and of the imposed boundary conditions. We conform to the general convention that the x axis should be the “outflow” axis. The y axis will then be the “inflow” axis.¹ The inflow axis is so-named because fluid flow approaches the origin along the inflow axis and diverges from the origin along the outflow axis.

Rotational symmetry implies that the in-plane component of any vector (including the magnetic field) must be zero at the origin. Therefore, the origin is a 2D null point of the in-plane component of the magnetic field. In the remainder of this paragraph ignore the out-of-plane component of the magnetic field and take the phrase *magnetic field* to refer to the in-plane component of the magnetic field \mathbf{B}^\perp . By linearizing the magnetic field near the origin we can classify the origin as an *X-point* or an *O-point*. Let $\underline{\underline{A}} := \nabla \mathbf{B}|_0$ denote the derivative of the in-plane component of the magnetic field at the origin. Then $\nabla \cdot \mathbf{B} = 0$ says that $\text{tr } \underline{\underline{A}} = 0$. We classify the point based on the eigenvalues and eigenvectors of $\underline{\underline{A}}$.

¹ It is more common in the reconnection literature to use **geocentric coordinates**, in which y is the out-of-plane axis and z is the inflow axis. The convention of geocentric coordinates is that the x axis connects Earth and Sun and z is perpendicular to the ecliptic [8]

- *X-point case.* If \underline{A} has real eigenvalues then they are equal and opposite. If the real eigenvalues are nonzero then the eigenvectors define a pair of **separatrices**. The separatrices are magnetic field lines which intersect the origin. The *in-coming separatrix* is tangent to the eigenvector with negative eigenvalue, and the *out-going separatrix* is tangent to the eigenvector with positive eigenvalue. In this case we refer to the origin as an **X-point**.
- *Antiparallel case.* If the eigenvalues are both zero, then \underline{A} is either zero or nilpotent. If \underline{A} is nilpotent then near the origin the magnetic field lines are antiparallel and are aligned with the eigenvector of \underline{A} . (If \underline{A} is zero then linearization is insufficient to classify the topology of the magnetic field near the origin.)
- *O-point case.* If the eigenvalues are complex then their real part is zero and their imaginary parts are opposite, so magnetic field lines near the origin are approximately ellipses. In this case we refer to the origin as an **O-point**.

In this document we are chiefly concerned with rotationally symmetric 2D problems where the origin is an X-point.

Symmetry about the origin means that the in-plane component of the fluid velocity vectors \mathbf{u}_s^\perp is also zero at the origin. We can use the same type of eigenstructure analysis that we used to classify magnetic field structure at the origin in order to classify fluid flow near the origin. For steady solutions conservation of particles (i.e. $d_t n_s := -n_s \nabla \cdot \mathbf{u}_s$, where recall that $d_t := \partial_t + \mathbf{u}_s \cdot \nabla$) implies at the origin (where $d_t = 0$) that $\nabla \cdot \mathbf{u}_s^\perp = 0$, so the classification of fluid flow lines is exactly like the classification of magnetic field lines. Regardless of whether incompressibility holds, by transforming into a rotating frame of reference we can assume that $\nabla \cdot \mathbf{u}_s^\perp = \text{Sym}(\nabla \cdot \mathbf{u}_s^\perp)$; in this case eigenvalues are real and eigenvectors are orthogonal. In the incompressible case the sum of the eigenvalues is zero. So we can define inflow and outflow separatrices for each species fluid (for irrotational flow or in a frame of reference rotating with the fluid). (Note, however, that when transforming into a rotating reference frame steady solutions become periodic solutions.)

3.1.3 Consequences of symmetries for tensor components

We also consider problems that are symmetric under reflection across a plane containing the out-of-plane axis. Reflection across the y - z plane is effected by negation of the x coordinate, so we refer to this reflection as a *reflection in x* .

We say that a tensor is a **proper tensor** if it is invariant under reflections. A tensor that is negated under reflections is called a **pseudo-tensor**. Pseudo-tensors are negated under reflections because reflections reverse the orientation of space. Vectors which are pseudo-tensors are called pseudo-vectors and vectors which are proper tensors are called proper vectors. The magnetic field \mathbf{B} is a pseudo-vector. So is the curl of any proper vector (for example, the vorticity). The curl of a pseudo-vector is a proper vector.

Under a reflection in x , a component of a proper tensor with an odd number of x indices is negated; other components remain unchanged. (Therefore a component of a pseudo-tensor with an odd number of x indices remains unchanged and other components are negated.) Reflection in x followed by reflection in y effects 180-degree rotation in the x - y plane, i.e. around the z axis. Therefore, under rotation about the z axis, a component of a tensor with an odd number of non- z indices is negated; other components remain unchanged. Rotations do not reverse the orientation of space, so pseudo-tensors and proper tensors transform in the same way under a rotation.

Invariance under rotation (or reflection) means that negated components must be zero.

The assumption of 180-degree rotational symmetry implies at the origin that tensor components with an odd number of out-of-plane indices must be zero. For example, vectors at the origin must be parallel to the out-of-plane axis. In particular, the magnetic field at the origin must be out-of-plane and is called the **guiding magnetic field** or **guide field**.

3.1.4 Reflectional symmetry

We will also consider problems where there is symmetry under reflection across the in-plane axes (the x axis and the y axis). This implies 180-degree rotational symmetry about the out-of-plane axis. More generally, for reflection in x , reflection in y , and 180-degree rotation around z , any two of these transformations is sufficient to generate the third. We refer to symmetry under this set of transformations as **reflectional symmetry**.

Assume in the remainder of this subsection 3.1.4 that reflectional symmetry holds.

Symmetry under reflection in the y axis means that on the x axis the only nonzero component of the magnetic field is B_y ; likewise, on the y axis the only nonzero component of the magnetic field is B_x . So at the origin the magnetic field must be zero, i.e., there is no guide field.

The fluid velocity is a proper vector. Symmetry under reflection in the y axis means that on the x axis $u_y = 0$, and symmetry under reflection in the x axis means that on the y axis $u_x = 0$. Therefore the fluid velocity must be irrotational when linearized about the origin, i.e. $\nabla \mathbf{u}_s^\perp|_0$ must be symmetric, and the in-plane standard basis vectors must be eigenvectors. Assuming that $\nabla \mathbf{u}_s^\perp|_0 \neq 0$, one in-plane axis (by convention the x axis) must be an outflow axis and the other (the y axis) must be the inflow axis.

If the origin is an X-point for the magnetic field, then the separatrices must of course be symmetric with respect to the axes. But note that because \mathbf{B} is a pseudovector, in the case of reflectional symmetry it is still possible for the origin to be a magnetic O-point.

If there is symmetry under reflection across e.g. the y axis, then the \mathbf{B}_y component of the magnetic field must be zero on the y axis. If there is also symmetry under reflection across the x axis then the \mathbf{B}_x component of the magnetic field must be zero on the y axis. Under 180-degree rotation the magnetic field must be invariant, and so we can conclude that on the y axis the magnetic field satisfies $\mathbf{B}(y\mathbf{e}_y) = \mathbf{B}_x(y)\mathbf{e}_x$ and $\mathbf{B}(-y\mathbf{e}_y) = -\mathbf{B}_x(y)\mathbf{e}_x$. (Of course the same sort of statements can be made regarding the x axis.) In other words, in the case of reflectional symmetry the magnetic field lines are antiparallel on the y axis. By smoothness and symmetry the magnetic field is parallel to the x axis near the y axis. It is thus common to refer to reflectionally symmetric reconnection problems with X-point magnetic field geometry at the origin as **antiparallel reconnection**. (Note, however, that in general antiparallel magnetic field implies magnetic field uniformly aligned e.g. with the x axis.)

3.2 2D magnetic reconnection

Recall that the ideal MHD model of plasma assumes the ideal Ohm's law, which says that the electric field is $\mathbf{E} = \mathbf{B} \times \mathbf{u}$, that is, zero in the reference frame of the fluid. Inserting this into Faraday's law $\partial_t \mathbf{B} + \nabla \times \mathbf{E} = 0$ gives the evolution equation

$$\partial_t \mathbf{B} + \nabla \times (\mathbf{B} \times \mathbf{u}) = 0.$$

This equation says that \mathbf{u} is a *flux-transporting flow* for \mathbf{B} . It implies that magnetic flux and magnetic field lines are transported with the fluid and that the topology of the magnetic field therefore cannot change.

More generally, ideal Hall MHD assumes that the electric field is zero in the reference frame of the *charge velocity* \mathbf{u}_c . Recall the full Ohm's law,

$$\partial_t \mathbf{B} + \nabla \times (\mathbf{B} \times \mathbf{u}_c + \mathbf{E}') = 0,$$

where \mathbf{E}' is the nonideal electric field. If \mathbf{E}' is zero then \mathbf{u}_c is a flux transporting flow for the magnetic field and the topology of magnetic field lines cannot change. When $\mathbf{E}' \neq 0$ magnetic field lines can change their topology or *reconnect*.

This raises the question, “How should one define the *rate of magnetic reconnection*?” A full answer to this question reconnection in three-dimensional space would really entail a covariant (Lorentz-invariant) definition in space-time, but for two-dimensional reconnection we can give elementary definitions. In the case of 180-degree rotational symmetry we will be able to define the rate of reconnection to be the out-of-plane component of the electric field at the origin. A reasoned account of this definition follows.

Faraday's law of magnetic induction $\partial_t \mathbf{B} + \nabla \times \mathbf{E} = 0$ implies that the rate of change of magnetic flux through any line segment in the plane is the difference of the out-of-plane electric field values at its endpoints. For the *GEM magnetic reconnection challenge problem* conducting wall boundaries exist, at which the out-of-plane component of the electric field must be zero. Magnetic field lines cannot pass through conducting wall boundaries (see section 4.1.1). We therefore can define the reconnected flux to be the change in magnetic flux through a line segment extending from the origin to the conducting wall boundary. Then by Faraday's law the out-of-plane component of the electric field at the origin is the rate of magnetic reconnection.

For 2D steady state, Faraday's law implies that the out-of-plane component of the electric field must be constant (so the presence of conducting wall boundaries would not allow steady 2D reconnection). Thus, to given a definition of reconnection which incorporates steady driven reconnection we seek a more general definition of reconnection based on Ohm's law (2.81)

$$\mathbf{E} = \mathbf{B} \times \mathbf{u}_c + \mathbf{E}'$$

and its out-of-plane component $\mathbf{E}^{\parallel} = \mathbf{B}^{\perp} \times \mathbf{u}_c^{\perp} + \mathbf{E}'^{\parallel}$, where \mathbf{E}' denotes non-ideal electric field, and \mathbf{B}^{\perp} and \mathbf{u}_c^{\perp} are the in-plane components of the magnetic field and the charge velocity. At the origin the ideal term disappears (because \mathbf{B} and \mathbf{u}_c must be parallel). Assume that \mathbf{E}' vanishes in the *ideal region*, which includes the whole domain except for a region containing the origin called the *diffusion region*. Outside the diffusion region, Faraday's law $\partial_t \mathbf{B} + \nabla \times \mathbf{E} = 0$ and its projection into the plane $\partial_t \mathbf{B}^{\perp} + \nabla \times (\mathbf{E}^{\parallel}) = 0$ imply that \mathbf{u}_c (or $\mathbf{u}_{c\perp} = \frac{\mathbf{E} \times \mathbf{B}}{\mathbf{B} \cdot \mathbf{B}}$, where $\mathbf{u}_{c\perp} := \mathbf{u}_c - \mathbf{u}_c \cdot \mathbf{b}\mathbf{b}$, and $\mathbf{b} := \mathbf{B}/B$) is a *flux-transporting flow* for \mathbf{B} and that the in-plane component \mathbf{u}_c^{\perp} (or $(\mathbf{u}_c^{\perp})_{\perp} = \frac{\mathbf{E}^{\parallel} \times \mathbf{B}^{\perp}}{\mathbf{B}^{\perp} \cdot \mathbf{B}^{\perp}}$) is a flux-transporting flow for \mathbf{B}^{\perp} . Therefore, *the rate at which in-plane magnetic flux is convected across a point in the ideal region is $\|\mathbf{E}^{\parallel}\|$ (i.e. $\|(\mathbf{u}_c^{\perp})_{\perp}\| \cdot \|\mathbf{B}^{\perp}\|$)*. In steady state \mathbf{E}^{\parallel} is constant. So in general we say that *the rate of reconnection is the magnitude of the out-of-plane component of the electric field at the origin*.

3.3 Ohm's law (current evolution) at the origin

3.3.1 MHD

For MHD Ohm's law (equations 2.80, 2.82) is assumed,

$$\begin{aligned}
 \mathbf{E} = & \boldsymbol{\eta} \cdot \mathbf{J} && \text{(resistive term)} && (3.1) \\
 & + \mathbf{B} \times \mathbf{u}_c && \text{(ideal Hall term)} \\
 & + \frac{\tilde{\mu}}{en} \left[\nabla \cdot \left(\frac{\mathbb{P}_i}{\tilde{m}_i} - \frac{\mathbb{P}_e}{\tilde{m}_e} \right) \right] && \text{(pressure term)} \\
 & + \frac{\tilde{\mu}}{en} \left[\partial_t \mathbf{J} + \nabla \cdot \left(\mathbf{u} \mathbf{J} + \mathbf{J} \mathbf{u} - \frac{d\tilde{m}}{\rho} \mathbf{J} \mathbf{J} \right) \right] && \text{(inertial term).}
 \end{aligned}$$

Each of these terms represents a component of the electric field and thus may also be referred to as e.g. the resistive electric field. The ideal term of Hall MHD is usually decomposed as

$$\mathbf{B} \times \mathbf{u}_c = \underbrace{\mathbf{B} \times \mathbf{u}}_{\text{(ideal term)}} + \underbrace{\frac{d\tilde{m}}{\rho} \mathbf{J} \times \mathbf{B}}_{\text{(Hall term)}}.$$

Assuming symmetry under 180-degree rotation in the plane, at the origin only the out-of-plane component of the electric field $\mathbf{E}^{\parallel} := \mathbf{E} \cdot \mathbf{e}^{\parallel}$ survives and the Hall term $\mathbf{B} \times \mathbf{u}_c$ disappears:

$$\mathbf{E}^{\parallel} = (\boldsymbol{\eta} \cdot \mathbf{J})^{\parallel} + \underbrace{\frac{\tilde{\mu}}{en} \left[\nabla \cdot \left(\frac{\mathbb{P}_i}{\tilde{m}_i} - \frac{\mathbb{P}_e}{\tilde{m}_e} \right) \right]^{\parallel}}_{\text{pressure term}} + \underbrace{\frac{\tilde{\mu}}{en} \left[\partial_t \mathbf{J}^{\parallel} + \nabla \cdot \left(\mathbf{u} \mathbf{J} + \mathbf{J} \mathbf{u} - \frac{d\tilde{m}}{\rho} \mathbf{J} \mathbf{J} \right) \right]^{\parallel}}_{\text{inertial term}} \quad \text{at 0.}$$

Since $\mathbf{E}^{\parallel}|_0$ is the rate of reconnection, this says that at the origin reconnection must be supported by the resistive term, the pressure term, or the inertial term.

In steady state the inertial term disappears, since $\nabla \cdot \mathbf{J} = 0$ and since in steady state at the origin $\nabla \cdot \mathbf{u} = 0$:

$$\mathbf{E}^{\parallel} = (\boldsymbol{\eta} \cdot \mathbf{J})^{\parallel} + \frac{\tilde{\mu}}{en} \left[\nabla \cdot \left(\frac{\mathbb{P}_i}{\tilde{m}_i} - \frac{\mathbb{P}_e}{\tilde{m}_e} \right) \right]^{\parallel} \quad \text{at 0 for } \partial_t = 0.$$

Therefore *steady reconnection must be supported by the resistive term or the pressure term* [61].

3.3.2 Two-fluid-Maxwell

For a two-fluid-Maxwell model neutrality does not necessarily hold and therefore the Ohm's law assumed by MHD (which assumes neutrality) cannot be assumed to strictly hold. To analyze the constraints on the reconnecting electric field we therefore revert to the one-species current evolution equations from which Ohm's law is derived. Equivalently, we consider one-species momentum evolution.

Recall the momentum evolution equation (2.8)

$$\rho_s d_t \mathbf{u}_s + \nabla \cdot \mathbb{P}_s = q_s n_s (\mathbf{E} + \mathbf{u}_s \times \mathbf{B}) + \mathbf{R}_s,$$

Solving for the electric field gives a single-species proxy “Ohm’s law”,

$$\begin{aligned}
\mathbf{E} &= - (q_s n_s)^{-1} \mathbf{R}_s && \text{(resistive term)} \\
&+ \mathbf{B} \times \mathbf{u}_s && \text{(ideal term)} \\
&+ (q_s n_s)^{-1} \nabla \cdot \mathbb{P}_s && \text{(pressure term)} \\
&+ (m_s/q_s) d_t \mathbf{u}_s && \text{(inertial term)}
\end{aligned} \tag{3.2}$$

Assuming symmetry under 180-degree rotation in the plane, at the origin only the out-of-plane component of the electric field \mathbf{E}^\parallel survives:

$$\mathbf{E}^\parallel = - (q_s n_s)^{-1} \mathbf{R}_s^\parallel + (q_s n_s)^{-1} (\nabla \cdot \mathbb{P}_s)^\parallel + (m_s/q_s) d_t \mathbf{u}_s^\parallel \quad \text{at } 0. \tag{3.3}$$

In steady state the inertial term disappears:

$$\mathbf{E}^\parallel = - (q_s n_s)^{-1} \mathbf{R}_s^\parallel + (q_s n_s)^{-1} (\nabla \cdot \mathbb{P}_s)^\parallel \quad \text{at } 0 \text{ for } \partial_t = 0.$$

3.3.3 Implications of Ohm’s law at the origin

In the following discussion “Ohm’s law” may be taken as the MHD Ohm’s law (3.1) or the two-fluid-Maxwell quasi-Ohm’s law (3.2). Assume 2D 180-degree rotational symmetry.

Since the out-of-plane component of the electric field at the origin is the rate of reconnection, Ohm’s law at the origin implies a set of constraints on magnetic reconnection.

Note that the resistive term represents a frictional drag force and results in heating (and thus entropy production) in an energy-conserving model. In a model that conserves energy and respects entropy but lacks diffusive entropy flux this means that steady state is possible only if the resistive electric field is zero at the origin.

If the electric field is zero at the origin then the pressure term must be nonzero to support steady reconnection [61]. That is, the divergence of the pressure must be nonzero.

Note that if z is the out-of-plane axis then for $\mathbb{P} = \mathbb{P}_s$

$$(\nabla \cdot \mathbb{P})^\parallel = \partial_x \mathbb{P}_{xz} + \partial_y \mathbb{P}_{yz} \quad \text{at } 0.$$

Note that in deriving Ohm’s law one of our implicit regularity assumptions was that the fluid density is nonzero.

Agyrotropy is necessary for $\nabla \cdot \mathbb{P}|_0 \neq 0$.

We say that a pressure tensor is **isotropic** if $\mathbb{P} = p \mathbf{1}$. If the pressure is isotropic near the origin (that is, in a neighborhood containing the origin) then $\nabla \cdot \mathbb{P}_s = \nabla \cdot (p_s \mathbf{1}) = \nabla p_s$, which by symmetry is zero at the origin.

We say that a pressure tensor is **gyrotropic** if it is invariant under rotation around the direction vector $\mathbf{b} := \mathbf{B}/|\mathbf{B}|$ aligned with the magnetic field. Then we can write

$$\begin{aligned}
\mathbb{P} &= p_\parallel \mathbf{b}\mathbf{b} + p_\perp (\mathbf{1} - \mathbf{b}\mathbf{b}) \\
&= p_\perp \mathbf{1} + (p_\parallel - p_\perp) \mathbf{b}\mathbf{b},
\end{aligned} \tag{3.4}$$

where p_{\parallel} is called the **parallel pressure** and p_{\perp} is called the **perpendicular pressure**. At a point where the magnetic field is nonzero,

$$\nabla \cdot \mathbb{P} = \nabla p_{\perp} + \underbrace{\mathbf{B} \cdot \nabla [(p_{\parallel} - p_{\perp})\mathbf{b}/|\mathbf{B}|]}_{\text{if differentiable}},$$

where we have used that $\nabla \cdot \mathbf{B} = 0$. But $\mathbf{B} \cdot \nabla = 0$ at 0, and since p_{\perp} is a scalar, $\nabla p_{\perp} = 0$ at 0. So $\nabla \cdot \mathbb{P} = 0$ at the origin in the case of a nonzero guide field. (This argument was given in [23].)

We can extend the notion of gyrotropy to include points where the magnetic field is zero if isotropy holds when the magnetic field is zero (i.e. $p_{\parallel} = p_{\perp}$ when $\mathbf{B} = 0$) and equation (3.4) defines a smooth function. This is perhaps not enough to imply that the expression marked *if differentiable* is differentiable. We could simply impose this assumption as an additional condition for a gyrotropic function.

But I claim that gyrotropy implies $\nabla \cdot \mathbb{P}|_0 = 0$ even without imposing this extra assumption. Let $\underline{\underline{A}} = \nabla^{\perp} \mathbf{B}^{\perp}|_0$, that is, the two-dimensional matrix which is the gradient of the projection of the magnetic field onto the plane. Note that $\text{tr} \underline{\underline{A}} = 0$. There are two orthogonal directions \mathbf{n} in the plane such that $\mathbf{n} \cdot \underline{\underline{A}} \cdot \mathbf{n} = 0$. Call the axes aligned with these directions x and y . Since $\nabla \cdot \mathbb{P}|_0$ is aligned with the out-of-plane axis, it is invariant under reflections, so by averaging the data over reflections across x and y we can assume without loss of generality that symmetry holds under reflections across x and y . *[There is a hole in the proof at this point because the condition (3.4) that defines gyrotropy is nonlinear and therefore not invariant under averaging of data (otherwise I could choose any orthogonal axes). If $\nabla \mathbf{B}|_0 \neq 0$ probably I can patch this up by using an estimate on the violation of symmetry and an estimate of violation of agyrotropy, but I don't think that I care enough about this proof to do that; instead, I think I'll just limit my results to the symmetric case.]*

Assume that symmetry holds under reflections across x and y .

On the x axis \mathbf{B} is parallel to y or zero (zero can occur in an arbitrarily small neighborhood of 0 only in case $\nabla \mathbf{B}|_0$ is zero or nilpotent), and likewise on the y axis \mathbf{B} is parallel to x . Thus, gyrotropy implies that along the x -axis $\mathbb{P}_{xx} = \mathbb{P}_{zz}$ and $\mathbb{P}_{xz} = 0$ and along the y -axis $\mathbb{P}_{yy} = \mathbb{P}_{zz}$ and $\mathbb{P}_{yz} = 0$ (using that \mathbb{P} is isotropic at any points where $\mathbf{B} = 0$). Recall that at the origin only the out-of-plane component $\nabla \cdot \mathbb{P}$ survives and thus

$$\nabla \cdot \mathbb{P} = \partial_x P_{xz} + \partial_y P_{yz} \quad \text{at } 0.$$

Therefore $\nabla \cdot \mathbb{P} = 0$ at 0.

So we can say in general that if the pressure is gyrotropic near the origin then $\nabla \cdot \mathbb{P}_s = 0$. That is, *pressure cannot support reconnection without agyrotropy in the vicinity of the origin.*

3.4 Steadily rotationally symmetric 2D reconnection requires heat flux.

The purpose of this section is to justify the following assertion, which is one of the main results of this dissertation:

In a 2D problem invariant under 180-degree rotation nonsingular steady reconnection is impossible in a plasma model which conserves mass, momentum, and energy if the model implies that entropy production is zero in the vicinity of the origin or if the model implies that diffusive entropy flux (or heat flux) is zero in the vicinity of the origin.

We attempt to make this statement precise and justify it as fully as possible. The idea is to show that friction is necessary. Friction produces heat, so if energy is conserved then the heat must have a way to diffuse away from the stagnation point at the origin.

In any gas model physical solutions must satisfy a set of **positivity conditions**. In a Boltzmann gas model the particle density f_s must be positive. In a five-moment gas model the density ρ_s and pressure p_s must be positive. In a ten-moment gas model the density ρ_s must be positive and the pressure tensor \mathbb{P}_s must be positive definite.

In general, we say that a set of moments *satisfies positivity* or is *physically realizable* if there exists a distribution function with the specified moments. For a given collection of moments the set of physically realizable values of the moments is a convex set.

We define a solution to be singular if it at some point the state is not in the interior of the set of states that satisfy positivity. In particular, a distribution is singular if it is zero anywhere, a five-moment solution is singular if the density or pressure is not strictly positive anywhere, and a ten-moment solution is singular if the pressure tensor fails to be strictly positive definite anywhere or if the density fails to be strictly positive. In the argument we will assume that solutions are smooth. By convolution with a smooth approximate identity we can make this assumption without loss of generality.

We first lay out the high-level argument.

3.4.1 Outline of the physical argument

Before analyzing models we study the physics itself, taking the Boltzmann equation as our standard of truth. We consider the the possibilities at the origin for the physical solution based on the constraints implied by the entropy evolution equation and the momentum evolution equation and by the problem symmetries. We then consider implications of the analysis for models in light of the relationships assumed in our reasoning.

The outline of the argument is as follows. The argument focuses attention on a single species and analyzes its entropy evolution.

If the collision operator C is zero then the physics is governed by the Vlasov equation. We assume a steady state solution of the Vlasov equation at the origin and conclude that it must be singular.

If the collision operator is nonzero then we consider entropy evolution in the vicinity of the origin. Either there is entropy production at the origin or there is not. If so, then entropy and heat are produced at the origin and so there must also be diffusive entropy flux and heat flux to balance the production by dispersing the entropy and heat. (Note that entropy flux approximately equal heat flux divided by temperature for near-Maxwellian distributions.)

If there is no entropy production at the origin, then since the collision operator is nonzero, the Boltzmann H theorem implies that the solution at the origin is Maxwellian. In this case 5-moment gas dynamics applies near the origin. Assuming 5-moment gas dynamics, if the deviatoric strain rate is nonzero at the origin then we show that there is entropy production, contrary to hypothesis. *As we will show, if the deviatoric strain rate is zero and if the heat flux is zero in the vicinity of the origin then so is the divergence of the pressure tensor.* But in steady state at the origin the only terms in the momentum equation that can support a reconnection electric field are the divergence of the pressure tensor and the resistive drag force. If there is resistive drag force then there is entropy production at the origin, contrary to hypothesis. So we may conclude that if there

is steady reconnection then there must be heat flux in the vicinity of the origin even if there is no entropy production at the origin.

The previous paragraph begins with two assertions that the reader might question.

The first questionable assertion is that the only type of distribution for which there is no entropy production is a Maxwellian. The Boltzmann H theorem asserts that entropy production is nonnegative and is zero precisely when the velocity distribution is Maxwellian. This holds for a large class of collision operators and is generally taken as a requirement for nonzero collision operators. Nevertheless, one may conceive of a collision operator for which states other than Maxwellian are equilibria. In particular, the hyperbolic ten-moment model with no heat flux or isotropization can be regarded as assuming an idiosyncratic collision operator which instantaneously relaxes to a Gaussian distribution; for this model Gaussian distributions are equilibria.

The second questionable assertion is that if the solution at the origin is Maxwellian then 5-moment gas dynamics applies near the origin. The justification for this assertion is as follows. First, five-moment gas dynamics holds rigorously in the asymptotic limit as the solution approaches a Maxwellian distribution. Second, since the velocity at the origin is zero, the fluid near the origin stays near the origin for a long time and has time to equilibrate with conditions at the origin; in particular, flow along an inflow separatrix takes forever to approach the origin. These statements hold to even higher order in case the deviatoric strain rate is zero at the origin.

3.4.2 Consequences of the argument for models

We now identify the modeling consequences of the argument in section 3.4.1 by carefully identifying the assumptions of the argument and considering in what models these assumptions hold.

The essential assumptions of the argument relevant to fluid models are that the entropy evolution equation (2.20) holds for each species and that (1) the momentum evolution equation holds for each species (as in the two-fluid-Maxwell case) or more generally, that (2) Ohm's law holds (as needed in the analysis of two-fluid MHD).

The following models cannot support nonsingular steady magnetic reconnection for 2D problems with rotational symmetry:

- Models which evolve a form of the Vlasov equation.
- Adiabatic two-fluid models:
 - whether two-fluid-Maxwell or two-fluid MHD,
 - whether 5-moment (viscid or inviscid) or 10-moment (isotropizing or not),
 - whether compressible or incompressible (although in the incompressible case one typically does not evolve energy and therefore steady reconnection is possible).
- Ideal MHD or ideal Hall MHD.

I remark that Chacón et al. in [12] simulate steady fast reconnection in magnetized pair plasma using an incompressible five-moment two-fluid model without any heat flux in their equations. This does not contradict the results of this section. They do not have heat flux in their equations because they do not solve an energy evolution equation. They do not need explicit energy evolution because their model is incompressible. The scalar pressure is inferred from the incompressibility constraint,

and the deviatoric pressure is the viscosity times the deviatoric strain rate. So one may pretend that an energy evolution equation (e.g. with nonzero heat flux) is being evolved, but the rest of the equations do not depend on it.

For the incompressible two-fluid *ten*-moment model assumed in [9], however, the pressure tensor *is* evolved adiabatically in accordance with (2.12), and we can conclude that steady reconnection should not be possible for the antiparallel case at least.

3.4.3 Vlasov model

We first consider the case that the collision operator is zero. We argue that kinetic models require entropy production for nonsingular rotationally symmetric steady reconnection. Heuristically this holds because without collisions particles sitting at the origin will be accelerated without bound by the electric field.

Recall the Boltzmann equation,

$$\partial_t f_s + \mathbf{v} \cdot \nabla_{\mathbf{x}} f_s + \mathbf{a}_s \cdot \nabla_{\mathbf{v}} f_s = C_s,$$

where $f = f_s(t, \mathbf{x}, \mathbf{v})$ is particle density of species s , \mathbf{v} is particle velocity, $\mathbf{a}_s = (q_s/ms)(\mathbf{E} + \mathbf{v} \times \mathbf{B})$ is particle acceleration, and C_s is the collision operator. Drop the species subscript s . We claim that without the collision operator steady reconnection is singular.

Assume rotational symmetry about the z -axis. Then at the origin the Boltzmann equation simplifies to $\partial_t f + (q/m)E_z \partial_{v_z} f = C$. Assume steady state ($\partial_t = 0$) and no collisions ($C = 0$). If $E_z = 0$ then there is no magnetic reconnection. Otherwise $\partial_{v_z} f = 0$, which says that f is independent of v_z when \mathbf{v} is parallel to the z -axis. But nonsingular distributions should go to 0 as z goes to infinity. So f is 0 when \mathbf{v} is parallel to the z -axis, which is a type of singularity.

3.4.4 Quadratic moment models need heat flux

To complete the argument of section 3.4.1 we first prove the following theorem.

Theorem 3.1 *Assume a rotationally symmetric 2D problem in which a fluid species satisfies a steady-state entropy evolution equation of the form*

$$\mathbf{u} \cdot \nabla s = \underline{\underline{\tilde{p}}}^\circ : \underline{\underline{\tilde{C}}} : \underline{\underline{p}}^\circ - \underline{\underline{A}} : \nabla \cdot \mathbf{q} + \text{error} \quad (3.5)$$

in the vicinity of the origin, where $\underline{\underline{p}}^\circ$ and $\underline{\underline{\tilde{p}}}^\circ$ are deviatoric tensors and where the coefficients $\underline{\underline{\tilde{C}}}$ satisfy the positive-definiteness criterion $\underline{\underline{\tilde{p}}}^\circ : \underline{\underline{\tilde{C}}} : \underline{\underline{p}}^\circ > 0$ for all $\underline{\underline{p}}^\circ \neq 0$.

Suppose that $\nabla \cdot \mathbf{q}$, $\nabla \nabla \cdot \mathbf{q}$, $\nabla^2 \nabla \cdot \mathbf{q}$, error, ∇ error, $\nabla \nabla$ error, and $\text{Sym}(\nabla \mathbf{u})$ are all zero at the origin.

Then $\nabla \underline{\underline{p}}^\circ = 0$ at the origin.

Proof of theorem. Note that ∇^2 denotes the laplacian. At 0 the left hand side is zero. Since $\nabla \cdot \mathbf{q} = 0$ at 0, $\underline{\underline{p}}^\circ = 0$ at 0.

For convenience use $'$ to denote ∂_x . We apply ∂_x^2 to the entropy evolution equation and evaluate at the origin. Using that $\underline{\underline{p}}^\circ = 0$ at 0,

$$(\mathbf{u} \cdot \nabla s)'' = \underline{\underline{\tilde{p}}}^{\circ'} : \underline{\underline{\tilde{C}}} : \underline{\underline{p}}^{\circ'} - (\underline{\underline{A}} : \nabla \cdot \mathbf{q})'' \quad \text{at 0.} \quad (3.6)$$

For the remainder of this proof all expressions and statements are evaluated at the origin. I claim that the left hand side is zero. The left hand side expands to $\mathbf{u}'' \cdot \nabla s + \mathbf{u}' \cdot \nabla s' + \mathbf{u} \cdot \nabla s''$. The outer expressions are easily seen to be zero. For the first, $\mathbf{u}'' \cdot \nabla s = 0$ because ∇s is zero. For the last, $\mathbf{u} \cdot \nabla s'' = 0$ because $\mathbf{u} \cdot \nabla$ is zero. It remains to show that $\mathbf{u}' \cdot \nabla s' = 0$, that is, $\partial_x \mathbf{u} \cdot \nabla \partial_x s = 0$, that is, $\partial_x \mathbf{u}_x \partial_x^2 s + \partial_x \mathbf{u}_y \partial_y \partial_x s = 0$. But $\partial_x \mathbf{u}_x = 0$ because $\text{Sym}(\nabla \mathbf{u}) = 0$, and $\partial_y \partial_x s = 0$ because by rotational symmetry s is even in x and even in y .

For the right hand side, since $\mathbf{q} = 0$ and $\nabla \mathbf{q} = 0$, it follows that $(\underline{\underline{A}} : \nabla \cdot \mathbf{q})'' = \underline{\underline{A}} : \nabla \cdot \mathbf{q}''$. So we have shown that $\underline{\underline{\tilde{p}}}^{\circ'} : \underline{\underline{\tilde{C}}} : \underline{\underline{p}}^{\circ'} = \underline{\underline{A}} : \nabla \cdot \mathbf{q}''$. That is,

$$\begin{aligned} \partial_x \underline{\underline{\tilde{p}}}^{\circ} : \underline{\underline{\tilde{C}}} : \partial_x \underline{\underline{p}}^{\circ} &= \underline{\underline{A}} : \nabla \cdot \partial_x^2 \mathbf{q} \quad \text{and} \\ \partial_y \underline{\underline{\tilde{p}}}^{\circ} : \underline{\underline{\tilde{C}}} : \partial_y \underline{\underline{p}}^{\circ} &= \underline{\underline{A}} : \nabla \cdot \partial_y^2 \mathbf{q}, \end{aligned}$$

where we have used that the choice of axes is arbitrary. By the positive-definiteness assumption the left hand sides (and thus the right hand sides) must be nonnegative. But the hypothesis $\nabla^2 \nabla \cdot \mathbf{q} = 0$ says that $\nabla \cdot \partial_x^2 \mathbf{q} = -\nabla \cdot \partial_y^2 \mathbf{q}$. So the right hand sides are zero. So by the strict positive-definiteness assumption on $\underline{\underline{\tilde{C}}}$ we conclude that $\partial_x \underline{\underline{p}}^{\circ} = 0 = \partial_y \underline{\underline{p}}^{\circ}$, that is, $\nabla \underline{\underline{p}}^{\circ} = 0$. Q.E.D.

Corollary 3.2 *Assume a rotationally symmetric 2D problem in which a fluid species satisfies the steady-state five-moment entropy evolution equation (2.46)*

$$\mathbf{u} \cdot \nabla s_{\mathcal{M}} = -\mathbf{e}^\circ : \boldsymbol{\pi} - p^{-1} \nabla \cdot \mathbf{q} + \text{error}$$

with stress closure (2.30)

$$-\boldsymbol{\pi}^\circ = 2\tau \tilde{\boldsymbol{\mu}} : \mathbf{e}^\circ \quad (3.7)$$

in the vicinity of the origin, where the (gyrotropic) coefficients $\underline{\underline{\tilde{C}}}$ satisfy the positive-definiteness (entropy-respecting) criterion $\mathbf{e}^\circ : \tilde{\boldsymbol{\mu}} : \mathbf{e}^\circ > 0$ for all $\mathbf{e}^\circ \neq 0$.

Suppose that $\nabla \cdot \mathbf{q}$, $\nabla^2 \nabla \cdot \mathbf{q}$, error, ∇ error, and $\nabla \nabla$ error are all zero at the origin.

Then $\nabla \cdot \mathbb{P} = 0$ at the origin.

Proof. To map onto the theorem, take $\underline{\underline{\tilde{p}}}^\circ := \underline{\underline{p}}^\circ := \mathbf{e}^\circ$ and take $\underline{\underline{\tilde{C}}} := 2\tau \tilde{\boldsymbol{\mu}}$. Take $\mathbf{q} := (2/5) \text{Sym}3(\mathbf{q} \mathbf{1})$. Take $\underline{\underline{A}} := (2p)^{-1} \mathbf{1}$.

$\nabla \cdot \mathbf{q}$ is a scalar and therefore $\nabla \nabla \cdot \mathbf{q} = 0$ at 0. At the origin, $\mathbf{u} \cdot \nabla s_{\mathcal{M}} = 0$, so if $\nabla \cdot \mathbf{q} = 0$ at 0 then $\mathbf{e}^\circ = 0$ at 0. But steady state conservation of mass says that $\nabla \cdot \mathbf{u} = 0$ at 0. So $\text{Sym}(\nabla \mathbf{u}) = 0$ at 0, which is the remaining needed hypothesis of the theorem.

The conclusion of the theorem says that $\nabla \mathbf{e}^\circ = 0$ at 0. I claim that this implies that $\nabla \mathbb{P} = 0$. This follows from the stress closure (3.7), i.e. $-\boldsymbol{\pi}^\circ = 2\boldsymbol{\mu} : \mathbf{e}^\circ$, since at 0 $\mathbf{e}^\circ = 0$ and $\nabla \mathbf{e}^\circ = 0$. Taking the trace, $\nabla \cdot \mathbb{P} = 0$. Q.E.D.

Corollary 3.3 *Assume a rotationally symmetric 2D problem in which a fluid species satisfies the steady state ten-moment temperature tensor evolution equation (see (2.12))*

$$n\partial_t\mathbb{T} + \text{Sym}2(\mathbb{P} \cdot \nabla \mathbf{u}) + \nabla \cdot \mathbf{q} = (q/m) \text{Sym}2(\mathbb{P} \times \mathbf{B}) + \mathbb{R} \quad (3.8)$$

and the continuity equation

$$\partial_t n + \nabla \cdot (n\mathbf{u}) = 0$$

with isotropization closure (2.33)

$$\mathbb{R}/n = -\tau^{-1}C^{\mathbb{R}} : \mathbb{T}^\circ, \quad (3.9)$$

in the vicinity of the origin, where the (gyrotropic) coefficients $C^{\mathbb{R}}$ satisfy the positive-definiteness (entropy-respecting) criterion (2.34)

$$-(\mathbb{T}^{-1})^\circ : C^{\mathbb{R}} : \mathbb{T}^\circ > 0.$$

Suppose that $n \neq 0$ at the origin. Suppose that $\nabla \cdot \mathbf{q}$, $\nabla \nabla \cdot \mathbf{q}$, and $\nabla^2 \nabla \cdot \mathbf{q}$ are all zero at the origin.

Then $\nabla \cdot \mathbb{P} = 0$ at the origin.

Proof.

Recall that assuming the continuity equation and the pressure tensor evolution equation we derived equation (2.22) for ten-moment entropy, which by (3.9) is

$$2n\mathbf{u} \cdot \nabla s_{\mathcal{G}} = -\mathbb{T}^{-1} : (\tau^{-1}C^{\mathbb{R}}) : \mathbb{T}^\circ - \mathbb{P}^{-1} : \nabla \cdot \mathbf{q}. \quad (3.10)$$

First assume that $\text{Sym}(\nabla \mathbf{u}) = 0$ at the origin. To map onto the hypotheses of the theorem take $\underline{\underline{p}}^\circ = \mathbb{T}^\circ$, $\underline{\underline{p}}^\circ = -(\mathbb{T}^{-1})^\circ$, $\underline{\underline{C}}^\circ = (2\tau)^{-1}C^{\mathbb{R}}$, $\mathbf{q} = \mathbf{q}$, and $\underline{\underline{A}} = \mathbb{P}^{-1}/2$. The conclusion of the theorem says that $\nabla \mathbb{T}^\circ = 0$ at 0. But \mathbb{P}° is a scalar multiple of \mathbb{T}° . So $\nabla \mathbb{P}^\circ = 0$ at 0. So $\nabla \cdot \mathbb{P} = 0$ at 0.

Now suppose that $\text{Sym}(\nabla \mathbf{u}) \neq 0$ at the origin. That is, $\mathbf{e}^\circ \neq 0$ at 0 (since steady state says $\nabla \cdot \mathbf{u} = 0$ at 0). Then we will show using the hypotheses of the theorem that entropy production is nonzero at the origin (contradicting the assumption of steady state). By entropy evolution it will be enough to show that $\mathbb{R} \neq 0$ at 0, that is (by the closure hypotheses (3.9)), $\mathbb{T}^\circ \neq 0$ at 0.

Henceforth in this proof all statements are evaluated at zero. In steady state $d_t = 0$. Suppose that $\mathbb{T}^\circ = 0$. That is, $\boldsymbol{\pi}^\circ = 0$. $\nabla \cdot \mathbf{q} = 0$ implies $\nabla \cdot \mathbf{q} = 0$ and $\nabla \cdot \mathbf{q}^\circ = 0$. So at the origin equation (3.8) reduces to

$$2pe^\circ = \mathbb{R}. \quad (3.11)$$

But $\mathbf{e}^\circ \neq 0$. So $\mathbb{R} \neq 0$, contrary to hypothesis. So we may generally conclude that $\nabla \cdot \mathbb{P} = 0$ at the origin. Q.E.D.

3.4.5 Steady reconnection requires heat flux.

Section 3.4.1 promised that we would show that if the deviatoric strain rate is zero and if the heat flux is zero in the vicinity of the origin then so is the divergence of the pressure tensor.

To complete the verification of this claim for the five-moment model it remains to consider the hyperbolic case, where the closure $\mathbb{P}^\circ = 0$ is used; this closure is *non*strictly positive-definite, so the theorems in the previous section do not apply. But in this case isotropy holds and $\nabla \cdot \mathbb{P} = \nabla p$, which must be zero at the origin. So steady reconnection is generally not possible in the five-moment model without heat flux.

[I worry that the following argument is not completely valid. For a Coulomb collision operator deviations from a Maxwellian consisting e.g. of fast-moving electrons can decay arbitrarily slowly, so the assumption that 5-moment gas-dynamics holds in the Maxwellian limit seems dubious. Maybe I have to limit my conclusions to collision operators for which there is a uniform estimate on the rate of decay of perturbations. Are there other subtle assumptions? At least this should go through for collision operators which share the properties of the Gaussian-BGK collision operator that I perhaps implicitly assume.]

We now argue that the same claim holds for the Boltzmann equation with a collision operator which is strictly positive for non-Maxwellian distributions and for which 5-moment gas dynamics with linearized deviatoric stress closure applies in the Maxwellian limit. This should hold for physically reasonable collision operators.

In steady state the entropy production at the origin should be zero and therefore the velocity distribution at the origin should be a Maxwellian $f^{(0)}$. Let ϵ be a smooth even function equal to 0 at the origin such that $|f - f^{(0)}| \leq \epsilon$. Then $\epsilon = \mathcal{O}(|\mathbf{x}|^2)$. Near the origin we can define a Chapman-Enskog expansion $f = f^{(0)} + \epsilon \bar{f}^{(1)} + f_{\text{remainder}}$ where $f_{\text{remainder}} = \mathcal{O}(\epsilon^2)$. *[Can I fully justify this assumption?]* Note that in a normal Chapman-Enskog expansion ϵ is assumed independent of space; so for each position \mathbf{x} we perform a Chapman-Enskog expansion using $\epsilon(\mathbf{x})$ and then evaluate it at \mathbf{x} . In the Gaussian-BGK model we used a Chapman-Enskog expansion to show that (see equation (2.65))

$$\mathbb{P} = p \mathbf{1} + 2\mu C^{\mathbb{R}} : \mathbf{e}^\circ + \mathbb{P}_{\text{error}} \quad (3.12)$$

where $\mathbb{P}_{\text{error}} = \mathcal{O}(\epsilon^2)$ and is smooth assuming the other quantities in this equation are smooth. In section 2.5.1 we obtained this closure by using (1) that if the solution is within $\mathcal{O}(\epsilon)$ of a Maxwellian then within $\mathcal{O}(\epsilon^2)$ five-moment entropy is nondecreasing and (2) that five-moment entropy must be approximately nondecreasing for any small \mathbf{e}° . For the five-moment closure μ is determined by temperature and the coefficients $C^{\mathbb{R}}$ are functions of the five-moment state, but for a Boltzmann model the coefficients $\mu C^{\mathbb{R}}$ would also depend on the *shape* of the deviation of the distribution from a Maxwellian.

Since ϵ is smooth and even at \mathbf{x} , we can write $\epsilon = \mathcal{O}(|\mathbf{x}|^2)$. Therefore, near the origin the entropy evolution equation (3.2) holds to within $\mathcal{O}(\epsilon^2) = \mathcal{O}(|\mathbf{x}|^4)$. This is true even when the stress closure (3.7) is used, since the error in the deviatoric pressure closure is $\mathbb{P}_{\text{error}} = \mathcal{O}(\epsilon^2) = \mathcal{O}(|\mathbf{x}|^4)$. So the assumptions of corollary 3.2 are satisfied.

We conclude that for the Boltzmann equation with a “reasonable” collision operator steady reconnection requires that $\nabla \cdot \mathbf{q} \neq 0$ at the origin. The same conclusion holds for fluid models which evolve a temperature evolution equation that agrees with the five-moment model sufficiently well near a Maxwellian distribution.

3.4.6 The ten-moment hyperbolic model does not support steady reconnection (at least for reflectional symmetry)

We have shown that without heat flux the ten-moment model with nonzero isotropization cannot support steady reconnection. For the hyperbolic case the closure $\mathbb{R}_s = 0$ is used, which is *non*strictly positive-definite, so Corollary 3.3 does not directly apply.

We argue that in the case of reflectional symmetry the hyperbolic ten-moment model does not support regular steady reconnection if $\partial_z^n(\mathbf{u}_s)_z \neq 0$ for some n . By convolution with an approximate identity we can assume smoothness at the origin.

Consider the case of reflectional symmetry . Assume that the y axis is the inflow axis. On the y axis \mathbf{B} is aligned with the x axis. Along the y axis the temperature evolution equation (2.15) for the \mathbb{T}_{xx} component simplifies to

$$u_y \partial_y \mathbb{T}_{xx} = -2\mathbb{T}_{xx} \partial_x u_x. \quad (3.13)$$

Look at the continuity equation on the y axis,

$$u_{x,x} + u_{y,y} = u_y \partial_y \ln n.$$

Suppose that $u_y = \Omega(y^{n+1})$. That is, $u_{y,y} = \Omega(y^n)$. Then $u_{y,y} + u_{x,x} = \nabla \cdot \mathbf{u} = u_y \partial_y \ln n = \Omega(y^{n+1})\mathcal{O}(y^2) = \mathcal{O}(y^{n+3}) = \mathcal{O}(y^{n+1})$. So $u_{y,y}$ and $u_{x,x}$ have leading coefficients of the same magnitude but opposite sign of order n in y . So we can write

$$u_{x,x} = Cy^n + \mathcal{O}(y^{n+1}) \quad (3.14)$$

and

$$u_{y,y} = -Cy^n + \mathcal{O}(y^{n+1}). \quad (3.15)$$

Note that \mathbb{T}_{xx} is even. Assume that it is also smooth. Evaluate the n th derivative of both sides of (3.4.6) at the origin and get $0 = -2\mathbb{T}_{xx}Cn!$. This contradicts the assumption that \mathbb{T}_{xx} is strictly positive. So no such smooth steady solution exists.

We can gain insight into why no smooth steady solution exists if we substitute equations (3.14) and (3.15) into (3.4.6). We get

$$y \partial_y \mathbb{T}_{xx} = 2(n+1)\mathbb{T}_{xx} + \mathcal{O}(y).$$

Near the origin we can ignore the $\mathcal{O}(y)$ term; separating and integrating gives

$$\mathbb{T}_{xx} = C_1 y^{2(n+1)}. \quad (3.16)$$

Since n must be nonnegative, this says that \mathbb{T}_{xx} must be zero at the X-point. This is physically what we would expect, since there is expansion in the x axis as the flow approaches the origin along the y axis.

To treat the general case of rotational symmetry we could transform into a rotating reference frame. In this case we would have an oscillatory solution rather than a steady state solution. I am not sufficiently interested to pursue the hyperbolic case further.

3.4.7 Singular solutions

Hitherto we have shown that adiabatic models do not support nonsingular steady reconnection. One may also consider singular solutions.

Jerry Brackbill has studied symmetric 2D reconnection using an incompressible adiabatic ten-moment model. He uses *geocentric coordinates*, so he refers to the inflow axis as the z axis and the out-of-plane axis as the y axis. By neglecting partial derivatives of the pressure term with respect to x in the momentum evolution equations the evolution equations reduce to an ODE along the inflow axis. Specifically he neglects his $\partial_x \mathbb{P}_{xz}$ (which is dominated by his $\partial_z \mathbb{P}_{zz}$) and his $\partial_x \mathbb{P}_{xy}$ (which is dominated by his $\partial_z \mathbb{P}_{zy}$) for both species. Based on this simplification he has implemented a steady-state solver [9] which shows excellent agreement with kinetic simulations when the isotropization rate is appropriately tuned. The implication of this dissertation, however, is that a steady state solution does not actually exist for the equations he solves. He solves the temperature evolution equation without making any approximating assumption, and his assumption of incompressible flow implies that the continuity equation is also exactly satisfied. His model therefore satisfies the hypotheses of Corollary 3.3 and cannot support a solution that is smooth, nonsingular, and steady at the origin. In particular, his pressure tensors are not isotropic at the origin (see Fig. 1 in [9]) and therefore the entropy evolution equation cannot be (consistently) in steady state.

It would be of interest to attempt to drive his model to a singular steady state. In lieu of a full analysis, in section B.2 I assume a smooth prescribed velocity field (and magnetic field, which turns out to be irrelevant) and solve the temperature evolution equation along the inflow axis for the linearize problem in the vicinity of the origin. It would also be of interest to determine a reasonable heat flux that would allow his model to give a converged steady regular solution.

We now turn to dynamic simulations of the GEM magnetic reconnection challenge problem using a 10-moment adiabatic model; this problem seems to develop singularities shortly after peak reconnection evidently due to the absence of a heat flux to regularize the solutions. The analysis of this section was motivated by difficulties encountered when simulating the GEM problem as well as a consideration of modeling requirements for steady reconnection.

Chapter 4

GEM challenge problem

4.1 GEM magnetic reconnection challenge problem

As mentioned in the introduction, simulations of the **Geospace Environmental Modeling magnetic reconnection challenge problem** (*GEM problem*) with a variety of plasma models (resistive MHD, Hall MHD, and particle models) identified the Hall effect as critical to resolving fast magnetic reconnection [6]. It has been solved with a variety of plasma models and thus serves as a benchmark for comparison of plasma models. In particular, we study the ability of the ten-moment adiabatic model to match kinetic simulations of low-collisionality fast magnetic reconnection.

Since the Hall effect was identified as critical to magnetic reconnection, it was natural to study whether fast reconnection can occur in pair plasma, for which the Hall term of Ohm's law is zero. Bessho and Bhattacharjee have simulated a pair plasma version of the GEM problem using a particle code [3, 4, 5] and have obtained fast rates of magnetic reconnection. Chacón et al. [12] subsequently demonstrated that steady fast reconnection is possible in a viscous two-fluid model of magnetized pair plasma. In their simulations the reconnecting electric field is supported by the divergence of the pressure tensors.

In studying the modeling requirements for magnetic reconnection we seek the simplest problems that distinguish models. Reconnection in pair plasma is a singular and simple case which brings out modeling requirements for fast reconnection with exceptional clarity. In particular, *symmetric pair plasma* problems are 2D antiparallel reconnection problems where there is symmetry under exchange of species coupled with reflection in the out-of-plane axis; for this case the number of equations that must be solved is halved. The pair plasma version of the GEM problem studied by Bessho and Bhattacharjee is a symmetric pair plasma in the case of equal plasma temperatures.

This dissertation reports simulations of the GEM problem with an adiabatic ten-moment two-fluid-Maxwell plasma model for which the only collisional term retained is isotropization of the pressure tensor. I report simulations of the original GEM problem and of symmetric pair plasma and compare with kinetic simulations.

4.1.1 Specification of the GEM problem

We recall the definition of the GEM magnetic reconnection challenge problem [6]. The problem is symmetric under 180 degree rotation around the origin and in the case of zero guide field is also symmetric under reflection across both the horizontal and vertical axes.

Nondimensionalization.

The original GEM study [6] nondimensionalizes by the ion inertial length $\delta_i := \sqrt{\frac{m_i}{\mu_0 n_0 e^2}}$ and by the ion cyclotron frequency $\Omega_i := \frac{eB_0}{m_i}$. (This nondimensionalization is worked out in section A.2.) It then

states that in these units the velocities are normalized to the Alfvén speed v_A . In actuality $v_A = \delta_i \Omega_i \sqrt{\frac{m_i}{m_i + m_e}}$ (see (A.2)), a discrepancy which becomes significant in the pair plasma case $m_i = m_e$. In keeping with [3, 4], when plotting we use δ_i and Ω_i computed from m_i to nondimensionalize time and space values, but use v_A to nondimensionalize when displaying the electric field (as indicated in the plots). In the subsequent account we assume this nondimensionalization.

Domain.

(We designate the vertical axis y and the out-of-plane axis z , opposite to the convention employed in [6, 3, 4].) The computational domain is the rectangular domain $[-L_x/2, L_x/2] \times [-L_y/2, L_y/2]$. We set $L_x = r_s 8\pi$ and $L_y = r_s 4\pi$, where r_s is a rescaling factor. In the original GEM problem $r_s = 1$ and this scaling is used in this document except for some pair plasma simulations where results labeled “*rescaled problem*” use $r_s = 0.5$. We also refer to this as the “*half-scale*” problem.

Boundary conditions.

The domain is periodic along the x -axis. The boundaries parallel to the x -axis are thermally insulating conducting wall boundaries. A conducting wall boundary is a solid wall boundary (with slip boundary conditions in the case of ideal plasma) for the fluid variables, and any electric field at the boundary must be perpendicular to the boundary (see section 2.5 in [17]). Assuming the ideal MHD Ohm’s law $\mathbf{E} = \mathbf{B} \times \mathbf{u}$, which essentially says that the electric field and the magnetic field are always perpendicular, this implies that at the conducting boundary the magnetic field must be parallel to the boundary.

So at the conducting wall boundaries the five-moment two-fluid Maxwell variables satisfy

$$\begin{aligned} \partial_y u_{x,s} &= 0, & \partial_y B_x &= 0, & E_x &= 0, & \partial_y \rho_s &= 0, \\ u_{y,s} &= 0, & B_y &= 0, & \partial_y E_y &= 0, & \partial_y p_s &= 0 = \partial_y \tilde{p} \\ \partial_y u_{z,s} &= 0, & \partial_y B_z &= 0, & E_z &= 0, & \partial_y e_s &= 0 = \partial_y \tilde{\mathcal{E}}. \end{aligned}$$

These boundary conditions imply that gas particles are reflected off the conducting wall. Thus, for ten-moment gas-dynamic variables we use the boundary conditions

$$\begin{aligned} \partial_y (\mathbb{E}_s)_{xx} &= 0, \\ \partial_y (\mathbb{E}_s)_{xz} &= 0, & \text{and} & & (\mathbb{E}_s)_{xy} &= 0, \\ \partial_y (\mathbb{E}_s)_{yy} &= 0, & & & (\mathbb{E}_s)_{yz} &= 0, \\ \partial_y (\mathbb{E}_s)_{zz} &= 0, \end{aligned}$$

Initial conditions.

The initial conditions are a perturbed Harris sheet equilibrium. The unperturbed (Harris sheet) equilibrium is given by

$$\begin{aligned} \mathbf{B}_H(y) &= B_0 \tanh(y/\lambda) \mathbf{e}_x, & p(y) &= \frac{B_0^2}{2n_0} n(y), \\ n(y) &= n_0 (0.2 + \operatorname{sech}^2(y/\lambda)), & p_i(y) &= \frac{T_i}{T_i + T_e} p(y), \\ \mathbf{E} &= 0, & p_e(y) &= \frac{T_e}{T_i + T_e} p(y). \end{aligned}$$

On top of this the magnetic field is perturbed by

$$\mathbf{B}_P = \nabla \times (\psi \mathbf{e}_z) = \nabla \psi \times \mathbf{e}_z, \quad \text{where} \quad \psi(x, y) = \psi_0 \cos(2\pi x/L_x) \cos(\pi y/L_y). \quad (4.1)$$

In the GEM problem the initial condition constants are

$$T_i/T_e = 5, \quad \lambda = 0.5, \quad B_0 = 1, \quad n_0 = 1, \quad \psi_0 = B_0/10.$$

For pair plasma we reset the initial temperature ratio to 1 to get symmetry between the species. We set ψ_0 to $r_s^2 B_0/10$, so that in the vicinity of the X-point our initial conditions agree (up to first-order Taylor expansion) with the initial conditions of the GEM problem.

Model parameters.

The GEM problem specifies that the ion-to-electron mass ratio is $m_i/m_e = 25$. (The initial temperature ratio is defined to be the square root of the mass ratio.) We used this mass ratio for hydrogen plasma and of course $m_i/m_e = 1$ for pair plasma.

Auxiliary model parameters.

The GEM problem does not specify the speed of light. It seems to have been formulated with Galilean-invariant models in mind. Published simulations with models that have a light speed typically set the light speed to 20. This seems to be a sufficiently close approximation to infinity so that results are insensitive to the light speed. The fastest wave speeds in the electrons are less than half of this. In the ten-moment model the maximum wave speed in the electron gas is initially about 4 and increases to about 7.

In the pair plasma version of the problem we set the mass of each species to r_s (rather than the GEM values of 1 for ions and 1/25 for electrons). We set the speed of light to 10 (rather than 20 as in [3]); this seems close enough to infinity, since the maximum gas wave speed is about 3.

Implied initial quantities

Using the initial conditions we calculate the precise initial current. For convenience define

$$\begin{aligned} \omega_x &:= 2\pi/L_x, & \text{and} & & \theta_x &:= x\omega_x, \\ \omega_y &:= \pi/L_y, & & & \theta_y &:= y\omega_y. \end{aligned}$$

So equation (4.1) says

$$\psi = \psi_0 \cos \theta_x \cos \theta_y, \quad (4.2)$$

$$\text{so } \nabla \psi = \begin{bmatrix} -\omega_x \psi_0 \sin \theta_x \cos \theta_y \\ -\omega_y \psi_0 \cos \theta_x \sin \theta_y \\ 0 \end{bmatrix} \quad \text{and} \quad \nabla^2 \psi = -(\omega_x^2 + \omega_y^2) \psi.$$

and therefore

$$\begin{aligned} \mathbf{B}_P &= \nabla \psi \times \mathbf{e}_z = \begin{bmatrix} -\omega_y \psi_0 \cos \theta_x \sin \theta_y \\ \omega_x \psi_0 \sin \theta_x \cos \theta_y \\ 0 \end{bmatrix} \quad \text{and} \\ \mu_0 \mathbf{J}_P &= \nabla \times \mathbf{B}_P = -\nabla^2 \psi \mathbf{e}_z = (\omega_x^2 + \omega_y^2) \psi \mathbf{e}_z. \end{aligned} \quad (4.3)$$

Analogously, define

$$\begin{aligned}\phi_H &:= B_0 \lambda \ln \cosh(y/\lambda), \\ \text{so } \nabla \phi_H &= B_0 \tanh(y/\lambda) \mathbf{e}_x \quad \text{and} \quad \nabla^2 \phi_H = (B_0/\lambda) \operatorname{sech}^2(y/\lambda).\end{aligned}$$

Then

$$\begin{aligned}\mathbf{B}_H &= \nabla \times (\phi_H \mathbf{e}_z) = \nabla \phi_H \times \mathbf{e}_z = B_0 \tanh(y/\lambda) \mathbf{e}_y \quad \text{and} \\ \mu_0 \mathbf{J}_H &= \nabla \times \mathbf{B}_H = -\nabla^2 \phi_H \mathbf{e}_z = -(B_0/\lambda) \operatorname{sech}^2(y/\lambda) \mathbf{e}_z.\end{aligned}$$

Then

$$\mathbf{J} = \mathbf{J}_H + \mathbf{J}_P = \mu_0^{-1} \left(-\frac{B_0}{\lambda} \operatorname{sech}^2(y/\lambda) + (\omega_x^2 + \omega_y^2) \psi(x, y) \right) \mathbf{e}_z.$$

4.1.2 Discussion of the initial perturbation

The GEM problem begins with a Harris sheet equilibrium and perturbs it by adding \mathbf{B}_P from equation (4.2) to the magnetic field, leaving unchanged the density, the net gas-dynamic momentum (zero), and the net gas-dynamic pressure (i.e. energy). The current of course changes, since for MHD it is given by the curl of the magnetic field, and therefore, for full consistency of the two-fluid equations with MHD, one may consider the drift velocities

$$\mathbf{w}_s = \frac{\check{\mu}}{m_s n q_s} \mathbf{J}$$

to be correspondingly perturbed (although this probably does not matter much) in the pressure evolution equation and (in the case of the two-fluid Maxwell equations) in the species momentum equations.

The effect of the perturbation of the magnetic field is to take the momentum equation and Faraday's law out of equilibrium. This gets the fluid and the magnetic field lines moving.

To see the effect of the perturbation, we invoke the decomposition of the current and magnetic field into Harris sheet and perturbation components: $\mathbf{B} = \mathbf{B}_H + \mathbf{B}_P$ and $\mathbf{J} = \mathbf{J}_H + \mathbf{J}_P$. Substituting into momentum evolution equation (2.88) gives

$$\partial_t(\rho \mathbf{u}) + \underbrace{\nabla \cdot (\rho \mathbf{u} \mathbf{u} + \mathbb{P} + \mathbb{P}^d)}_{\text{these balance}} = \underbrace{\mathbf{J}_H \times \mathbf{B}_H + \mathbf{J}_H \times \mathbf{B}_P + \mathbf{J}_P \times \mathbf{B}_H}_{\text{these push out}} + \underbrace{\mathbf{J}_P \times \mathbf{B}_P}_{\text{small}}.$$

The term labeled “pushes out” generates a force away from the origin both on the x -axis and on the y -axis. It is not obvious whether this will initially result in forward or reverse reconnection. In some of my simulations there is an initial reverse reconnection and in others there is not. In either case, forward reconnection eventually takes off.

Initial conditions for the two-fluid model

How should the initial electric field be specified for the GEM problem? The GEM problem does not explicitly specify the initial electric field because it is formulated with MHD in mind. In the two-fluid model one needs to specify initial values of the electric field. Simply setting the electric field to zero results in massive oscillations that could destabilize the results. A guiding principle is

to specify quantities so that the Harris sheet is an equilibrium. The Harris sheet is designed so that net momentum evolution is satisfied. To ensure that the momentum evolution equations of both species are satisfied we also need Ohm's law to be satisfied. We can simply compute the electric field using the appropriate version of Ohm's law (3.1),

$$\begin{aligned}
\mathbf{E} = & \boldsymbol{\eta} \cdot \mathbf{J} && \text{(resistive term)} \\
& + \mathbf{B} \times \mathbf{u} && \text{(ideal term)} \\
& + \frac{d\tilde{m}}{\rho} \mathbf{J} \times \mathbf{B} && \text{(Hall term)} \\
& + \frac{\tilde{\mu}}{en} \left[\nabla \cdot \left(\frac{\mathbb{P}_i}{\tilde{m}_i} - \frac{\mathbb{P}_e}{\tilde{m}_e} \right) \right] && \text{(pressure term)} \\
& + \frac{\tilde{\mu}}{en} \left[\partial_t \mathbf{J} + \nabla \cdot \left(\mathbf{u} \mathbf{J} + \mathbf{J} \mathbf{u} - \frac{d\tilde{m}}{\rho} \mathbf{J} \mathbf{J} \right) \right] && \text{(inertial term)}.
\end{aligned} \tag{4.4}$$

The ideal term, Hall term, and inertial term are all initially zero; to see that the inertial term is indeed zero, the flux component of the inertial term is zero, because $\nabla \cdot \mathbf{J} = 0$, $\nabla \cdot \mathbf{u} = 0$, and $\mathbf{J} \cdot \nabla = 0$ (because \mathbf{J} is initially out-of-plane); we assume for the moment and will verify that $\partial_t \mathbf{J} = 0$. Assuming the absence of resistivity, the electric field must balance the pressure term. For the ten-moment two-fluid model the pressure should be calculated by solving the equation in the next section, and the initial electric field could be calculated to balance the pressure term. For the five-moment two-fluid model the pressure term essentially reduces to a linear combination of scalar pressure gradients. Using the initial pressure values of the GEM problem, the pressure term is

$$\nabla \left(\frac{p_i}{\tilde{m}_i} - \frac{p_e}{\tilde{m}_e} \right) = \frac{\tilde{m}_i T_e - \tilde{m}_e T_i}{T_i + T_e} \frac{B_0^2}{\rho} \text{sech}^2(y/\lambda) \tanh(y/\lambda) \mathbf{e}_y,$$

which we can take as $\mathbf{E}|_{t=0}$. In this case $\mathbf{E}|_{t=0}$ is of the form $g(y)\mathbf{e}_y$, so at time 0 $\partial_t \mathbf{B} = -\nabla \times \mathbf{E} = 0$, so $\partial_t \mathbf{J}|_{t=0} = 0$, as assumed.

Initial conditions for the ten-moment model

In the ten-moment model what are the appropriate initial values of the pressure tensor components? In the simulations reported here the pressure tensor is assumed initially isotropic. This results in strong oscillations between the pressure and inertial terms which decay over a time interval determined by the isotropization period.

A better way to set the initial conditions would have been to set \mathbb{P}° so that the Harris sheet is a near-equilibrium in the adiabatic case. Recall the adiabatic pressure tensor evolution equation (see (2.14)),

$$n_s d_t \mathbb{T}_s + \text{Sym}2(\mathbb{P}_s \cdot \nabla \mathbf{u}_s) = (q_s/m_s) \text{Sym}2(\mathbb{P}^\circ_s \times \mathbf{B}) - \mathbb{P}^\circ_s / \tau_s.$$

For a Harris sheet $d_t = 0$. Using the decomposition $\mathbb{P} = p \mathbb{1} + \mathbb{P}^\circ$, we need

$$p_s \text{Sym}2(\nabla \mathbf{u}_s) + \text{Sym}2(\mathbb{P}^\circ_s \cdot \nabla \mathbf{u}_s) = (q_s/m_s) \text{Sym}2(\mathbb{P}^\circ_s \times \mathbf{B}) - \mathbb{P}^\circ_s / \tau_s. \tag{4.5}$$

This is six equations in five unknowns. Taking the deviatoric part will give us five equations in five unknowns, which we can solve for \mathbb{P}° . The original equation would be satisfied if its trace is satisfied. Half the trace is steady state scalar pressure evolution (see (2.13)),

$$p_s \nabla \cdot \mathbf{u}_s + \mathbb{P}^\circ_s : (\nabla \mathbf{u}_s)^\circ = 0. \tag{4.6}$$

The initial conditions imply that $\nabla \cdot \mathbf{u} = 0$, but we do not expect the entropy production term $\mathbb{P}^\circ : (\nabla \mathbf{u})^\circ$ to be exactly zero, since the initial velocity is (see equation (2.85))

$$\mathbf{u}_s = \mathbf{w}_s = \frac{\check{\mu}}{m_s} \frac{\mathbf{J}}{nq_s}.$$

So we satisfy ourselves with enforcing the deviatoric part of equation (4.5), which is equivalent to the equation

$$\text{Sym2}(\mathbb{P}_s^\circ \cdot (\nabla \mathbf{u}_s - q_s/m_s \mathbf{1} \times \mathbf{B} + \mathbf{1} / \tau_s))^\circ = -p_s \text{Sym2}(\nabla \mathbf{u}_s)^\circ.$$

This is a matrix equation of the form

$$\text{Sym2}(\underline{\underline{X}}^\circ \cdot \underline{\underline{B}})^\circ = \underline{\underline{C}}^\circ.$$

It is five equations in five independent unknowns.

In the ten-moment case, attempting to satisfy pressure evolution also comes at the price of sacrificing that the net momentum evolution equation (2.88)

$$\partial_t(\rho \mathbf{u}) + \nabla \cdot (\rho \mathbf{u} \mathbf{u} + \mathbb{P}^d + \mathbb{P}) = en(\mathbf{J} \times \mathbf{B}), \quad (4.7)$$

is satisfied; this is consistent with the fact that the Harris sheet equilibrium exactly satisfies the net momentum equation in the five-moment two-fluid model only if viscosity is neglected.

I remark that if one assumes isotropic pressure then the Harris sheet equilibrium really does satisfy the net momentum equation exactly even if the diffusion pressure $\mathbb{P}^d = \tilde{m}_e \tilde{m}_i \mathbf{J} \mathbf{J} / \rho$ (see equation (2.89)) is included, because for the Harris sheet $\nabla \cdot \mathbb{P}^d = \tilde{m}_e \tilde{m}_i \mathbf{J} \cdot \nabla(\mathbf{J} / \rho) = 0$, using that $\mathbf{J} = \mu_0^{-1} \nabla \times \mathbf{B}$ is directly out of plane.

4.2 System of equations used to solve the GEM problem

To simulate the GEM challenge problem we used the adiabatic ten-moment two-fluid Maxwell model with pressure isotropization in each species. When the pressure isotropization period is zero the ten-moment model agrees with the adiabatic inviscid five-moment model, as we have verified numerically.

The hyperbolic two-fluid Maxwell equations have been simulated by Shumlak, Loverich, and Hakim. The hyperbolic five-moment two-fluid Maxwell system was simulated using the Finite Volume wave propagation method (described in [37]) in Hakim's thesis [18] and specifically for the GEM problem in [20]; the same system was used to solve the GEM problem using the discontinuous Galerkin method in [40]. Hakim solved the GEM problem using a hyperbolic two-fluid Maxwell system using ten moments for the ions and five moments for the electrons in [19]; at the conclusion of this paper Hakim proposes incorporation of collisions through relaxation to a Maxwellian and closure via use of a Chapman-Enskog type expansion about the Gaussian distribution, as has been carried out in this work. I have not been able to find studies of reconnection with an isotropizing ten-moment two-fluid model, although Hesse and Winske in [24] simulate collisionless ion tearing using particles for the ions and a ten-moment isotropizing fluid for the electrons. Miura and Groth [46] analyze dispersion in an adiabatic ten-moment two-fluid model with BGK collision source terms.

To simulate the GEM challenge problem we implemented adiabatic two-fluid-Maxwell models with five or ten moments for each species. These models solve Maxwell's equations and solve a

separate compressible gas dynamics system for each species. The general model uses ten-moment gas dynamics for each species and isotropizes the pressure tensor at a tunable rate. We did not include terms that represent collisional exchange between the species (that is, resistive drag force or thermal equilibration). We used a conservative shock-capturing method and therefore represented the system of equations in conservation form.

To solve Maxwell's equations we solved the system

$$\partial_t \begin{bmatrix} \mathbf{B} \\ \mathbf{E} \end{bmatrix} + \begin{bmatrix} \nabla \times \mathbf{E} + \chi \nabla \psi \\ -c^2 \nabla \times \mathbf{B} \end{bmatrix} = \begin{bmatrix} 0 \\ -\mathbf{J}/\epsilon_0 \end{bmatrix}, \quad (4.8)$$

where $\mathbf{J} = e(n_i \mathbf{u}_i - n_e \mathbf{u}_e)$ is the current. The correction potential ψ is initially zero. These equations imply a wave equation that propagates the divergence constraint error $\nabla \cdot \mathbf{B}$ at the speed $c\chi$. We chose $\chi = 1.05$.

The divergence constraint on the electric field is $\nabla \cdot \mathbf{E} = \sigma/\epsilon_0$, where $\sigma = e(n_i - n_e)$. The initial conditions of the GEM problem satisfy the divergence constraint, and physical solutions of Maxwell's equations maintain the divergence constraint, but we do not attempt to enforce this constraint numerically. In our simulations the divergence constraint on the electric field remains approximately satisfied in the sense that the error remains centered on zero and its growth tapers. Attempts to apply correction potentials to the electric field were counterproductive, increasing the magnitude of the error. In contrast, when we did not properly apply correction potentials to the magnetic field, the error on the magnetic field drifted from being centered at zero until the solution became grossly unphysical.

The adiabatic pressure-isotropizing ten-moment gas-dynamic system in conservation form, which we solved, is

$$\begin{aligned} \partial_t \rho_s + \nabla \cdot (\rho_s \mathbf{u}_s) &= 0, \\ \partial_t (\rho_s \mathbf{u}_s) + \nabla \cdot (\rho_s \mathbf{u}_s \mathbf{u}_s + \mathbb{P}_s) &= q_s/m_s \rho_s (\mathbf{E} + \mathbf{u}_s \times \mathbf{B}), \\ \partial_t \mathbb{E}_s + 3 \nabla \cdot \text{Sym}(\mathbf{u}_s \mathbb{E}_s) - 2 \nabla \cdot (\rho_s \mathbf{u}_s \mathbf{u}_s \mathbf{u}_s) &= q_s/m_s 2 \text{Sym}(\rho_s \mathbf{u}_s \mathbf{E} + \mathbb{E}_s \times \mathbf{B}) + \mathbb{R}_s, \end{aligned} \quad (4.9)$$

where the isotropization tensor is given by the closure

$$\mathbb{R}_s = \tau_s^{-1} (\mathbf{1} \text{tr } \mathbb{P}_s/3 - \mathbb{P}_s).$$

For the isotropization period τ_s we generally used

$$\tau_s = \tau_0 \frac{\sqrt{m_s \det \mathbb{T}_s}}{n_s},$$

where τ_0 is a tunable parameter. For pair plasma simulations, however, we simply chose τ_s to be a uniform constant.

In the limit $\tau_s \rightarrow 0$ the ten-moment system simplifies to the adiabatic inviscid five-moment model:

$$\begin{aligned} \partial_t \rho_s + \nabla \cdot (\rho_s \mathbf{u}_s) &= 0, \\ \partial_t (\rho_s \mathbf{u}_s) + \nabla \cdot (\rho_s \mathbf{u}_s \mathbf{u}_s) + \nabla p_s &= q_s/m_s \rho_s (\mathbf{E} + \mathbf{u}_s \times \mathbf{B}), \\ \partial_t \mathcal{E}_s + \nabla \cdot (\mathbf{u}_s (\mathcal{E}_s + p_s)) &= \mathbf{J}_s \cdot \mathbf{E}. \end{aligned} \quad (4.10)$$

Chapter 5

GEM pair plasma simulations

This chapter reports simulations of GEM problem described in the previous chapter for the case of pair plasma. We assumed zero guide field and equal temperature for both species. For equal temperature, symmetry between the two species halves the number of equations needed. For zero guide field the GEM problem is symmetric across both the horizontal and vertical axes. We enforced all these symmetries.

All simulations were computed on a 128 by 64 mesh unless otherwise indicated. To verify convergence we coarsened the grid by a factor of two in each direction.

As a proxy for Ohm's law we plotted the accumulation integrals of the terms of (3.3) (the positron momentum equation solved for the electric field):

$$\begin{aligned}
 \text{electric term:} & - \int_0^t \mathbf{E}_z, \\
 \text{pressure term:} & - \int_0^t \frac{(\nabla \cdot \mathbb{P}_i)_z}{en_i}, \\
 \text{inertial term:} & - \int_0^t \frac{m_i}{e} \partial_t (u_i)_z - \frac{m_i}{e} ((u_i)_z|_t - (u_i)_z|_{t=0}), \\
 \text{residual term:} & - \int_0^t \text{residual},
 \end{aligned}$$

where residual represents numerical resistance and is what must be added to the pressure term and inertial term to yield the reconnection electric field. We have plotted the loss of magnetic flux across the y -axis and have verified that it is indistinguishable from the electric term.

5.1 Rescaled pair-plasma GEM problem

To avoid the formation of magnetic islands, we modified (Bessho and Bhattacharjee's version of) the GEM problem, shrinking the dimensions of the domain and the particle mass to half their original values. The effect of these changes is to rescale the nondimensional parameters of the GEM problem, increasing the width of the current sheet from 1 to $\sqrt{2}$ times the ion inertial radius and decreasing the domain size from 8π by 4π to $8\pi/\sqrt{2}$ by $4\pi/\sqrt{2}$. We set the speed of light to be 10 times the Alfvén speed v_A .

We simulated this rescaled GEM problem for isotropization rates ranging from 0 to instantaneous. For intermediate isotropization rates increasing the rate of isotropization decreases the rate of reconnection, which seems to agree qualitatively with [25], but for extreme rates of isotropization we observed the opposite trend. (See figure 11).

For all simulations the peak rate of reconnection occurred when about 30% of the original flux through the y -axis had reconnected. The time until 30% reconnection showed trends similar to

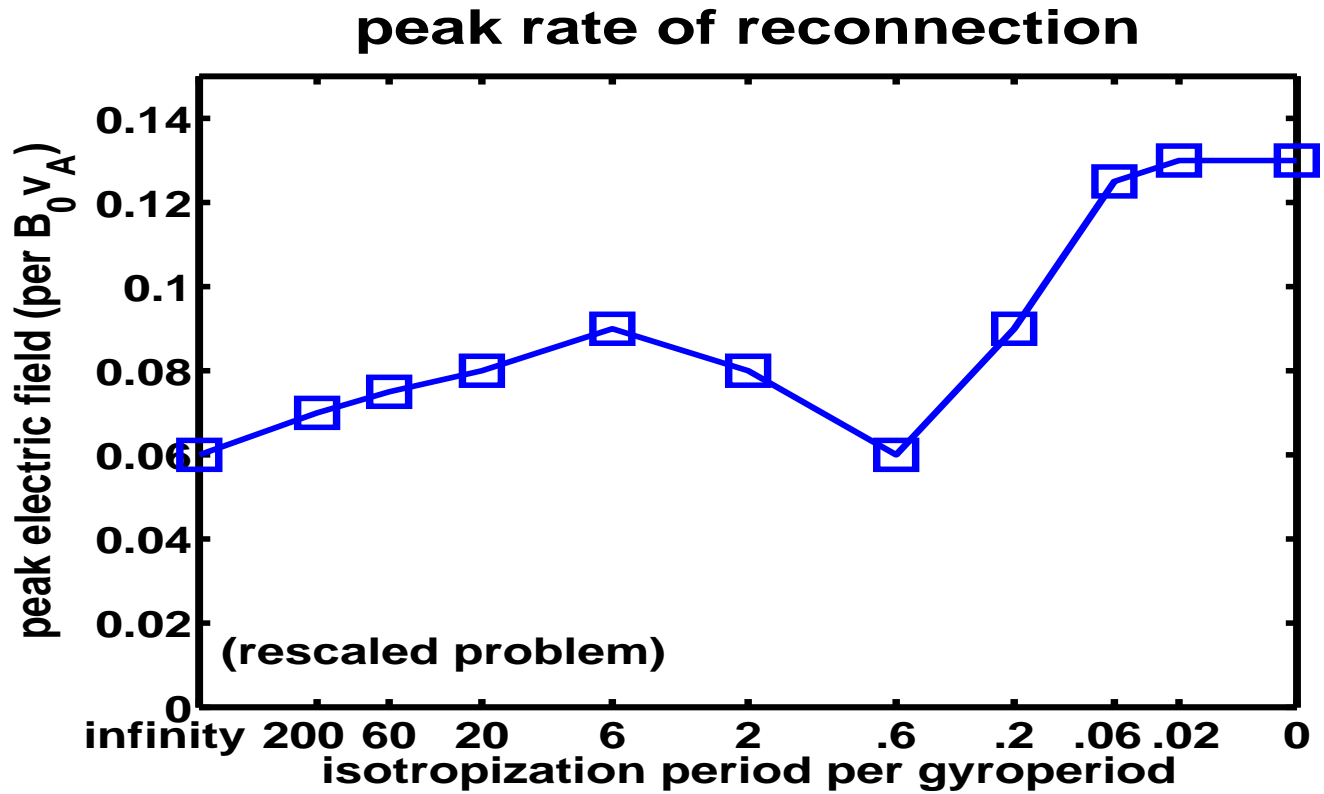


Figure 11: Peak rate of reconnection versus isotropization period in the half-scale symmetric pair plasma GEM problem.

Observe that for intermediate isotropization rates increasing the rate of isotropization decreases the rate of reconnection, as reported in [25], but for extreme rates of isotropization we observe the opposite trend.

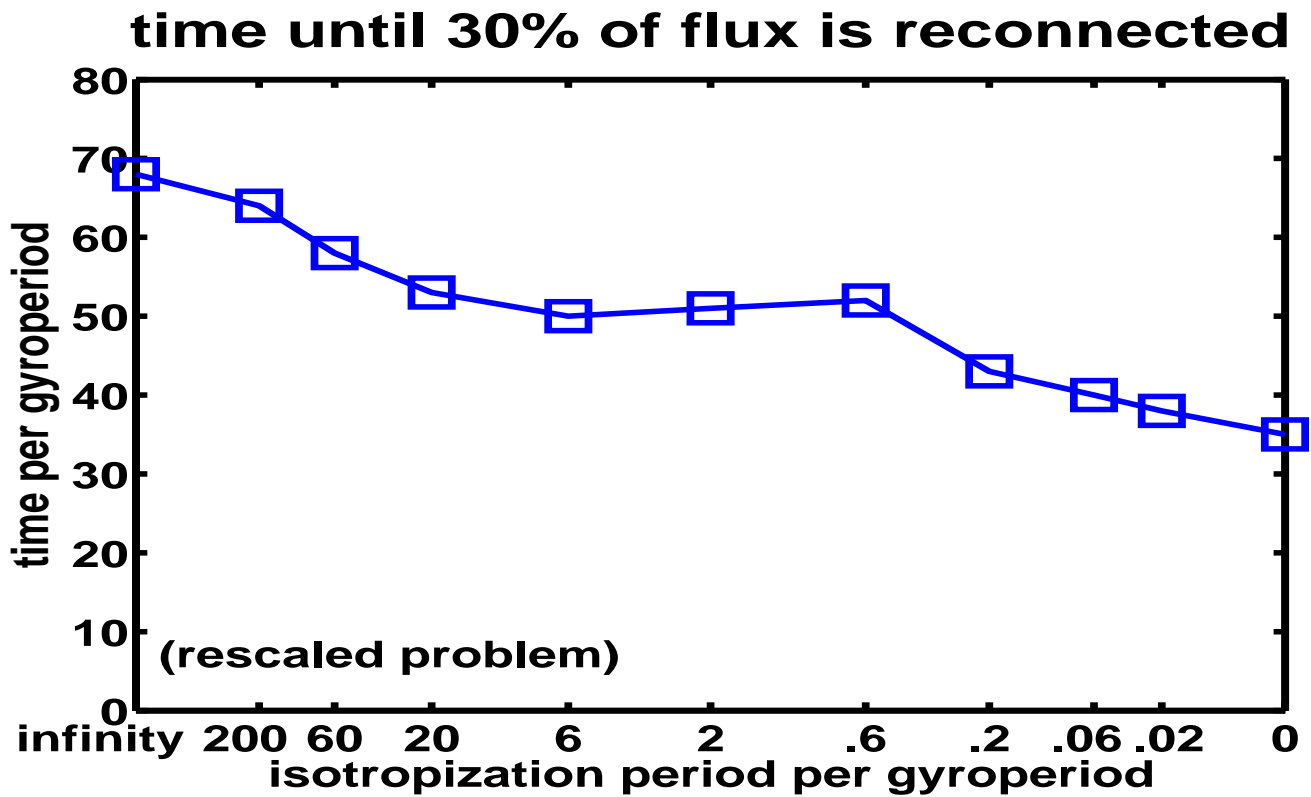


Figure 12: Time until 30% of flux is reconnected in the half-scale symmetric pair plasma GEM problem.

For all simulations the peak rate of reconnection occurred when about 30% of the original flux through the y-axis had reconnected.

the trends in the peak isotropization rate (see figure 12). In general we can say that the rate of reconnection is not very sensitive to the rate of isotropization, which seems to agree qualitatively with [35]. We display the accumulation integral of the terms of (3.3) for some of these isotropization periods (∞ , 6, 0.2, and 0) in figures (13, 14, 15, and 16).

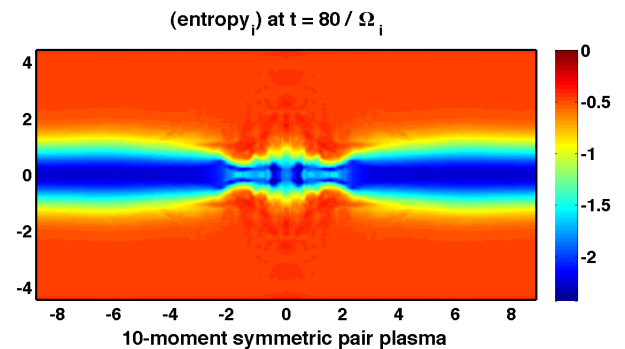
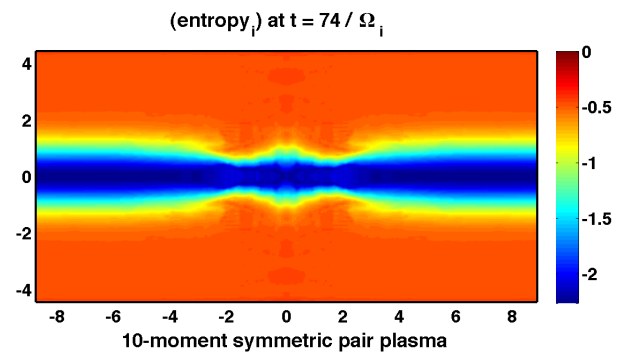
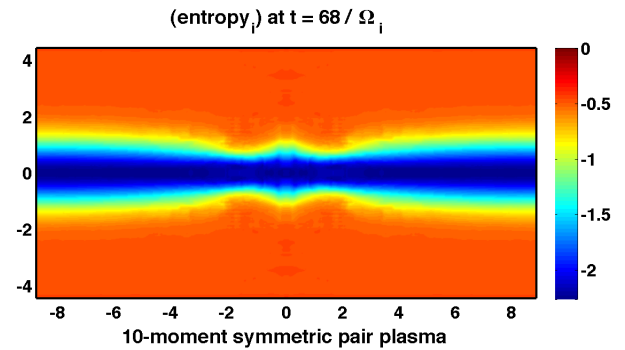
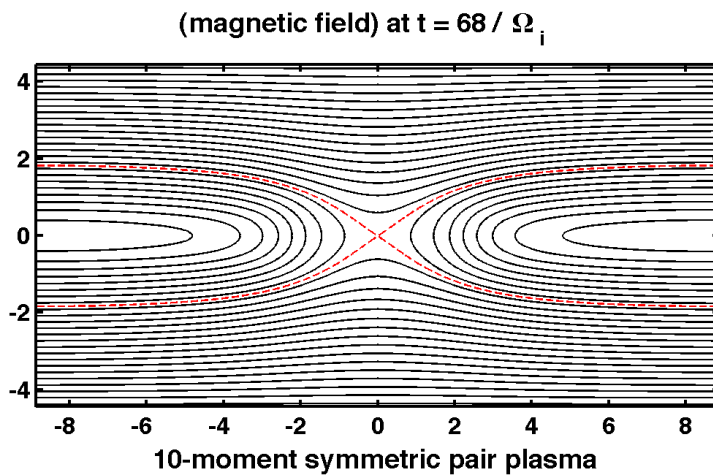
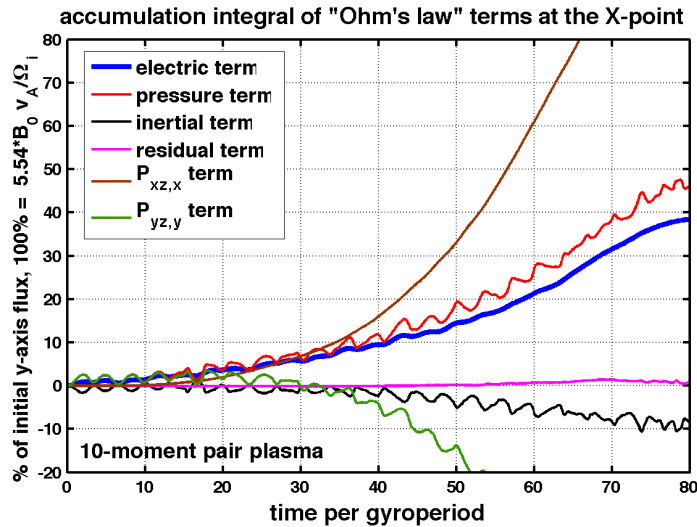


Figure 13: Reconnection for no isotropization (hyperbolic 10-moment model) in the half-scale symmetric pair plasma GEM problem.

Notice the undamped oscillatory exchange between the pressure and inertial terms. Notice also the U-shaped magnetic field line pattern near the X-point; as we increase the isotropization rate in the following figures the magnetic field becomes more V-shaped or even Y-shaped, evidently due to decreasing viscosity.

This model is hyperbolic and requires high resolution for convergence.

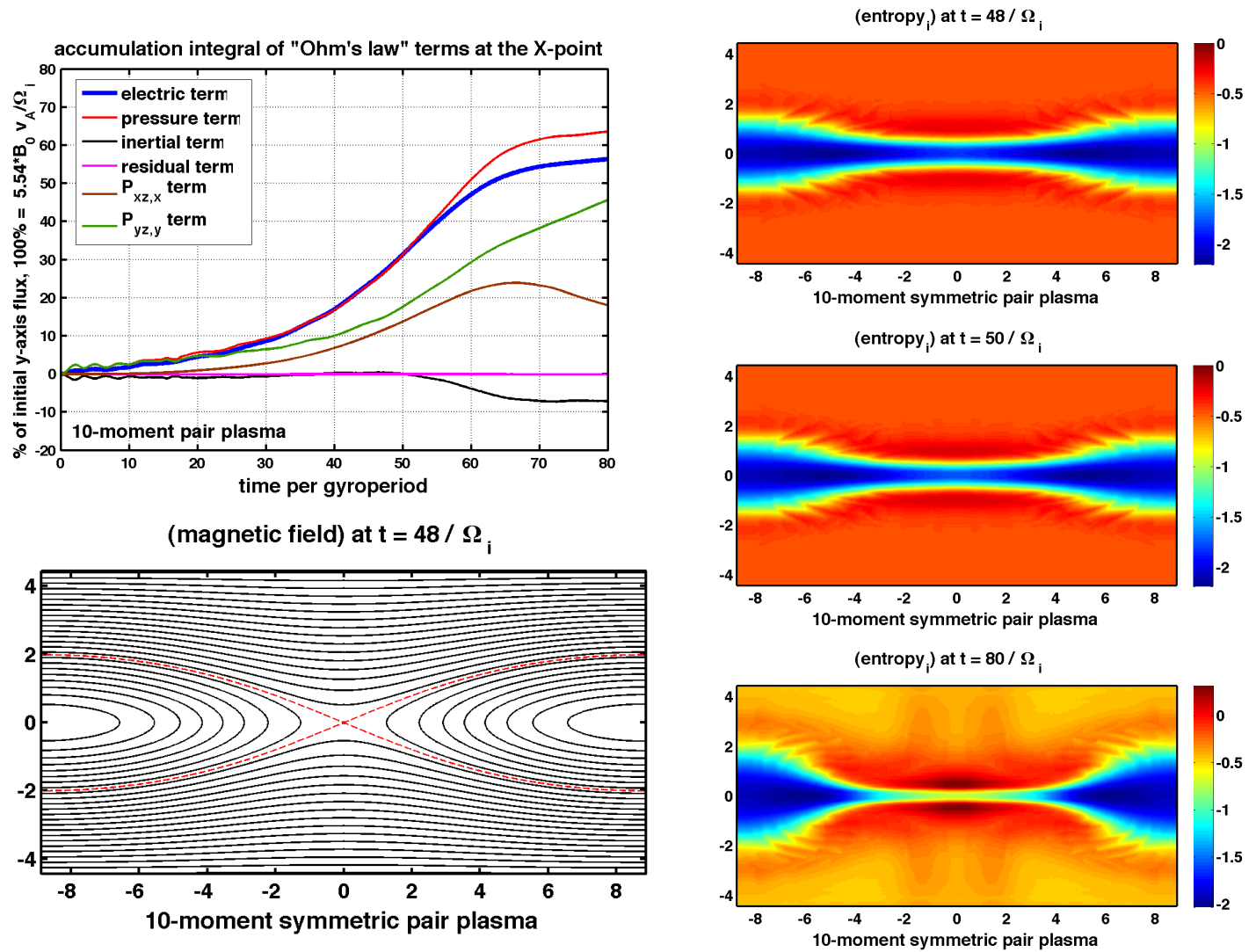


Figure 14: Reconnected flux for moderate isotropization in the half-scale symmetric pair plasma GEM problem.

Isotropization of the pressure tensor dampens the oscillatory exchange between the pressure and inertial terms. The pressure term supports reconnection, in agreement with steady-state theory and PIC simulations. The maximum Knudsen number is roughly 6 over the course of this simulation. The five-moment closure for the pressure tensor is completely incorrect and is an order of magnitude too large.

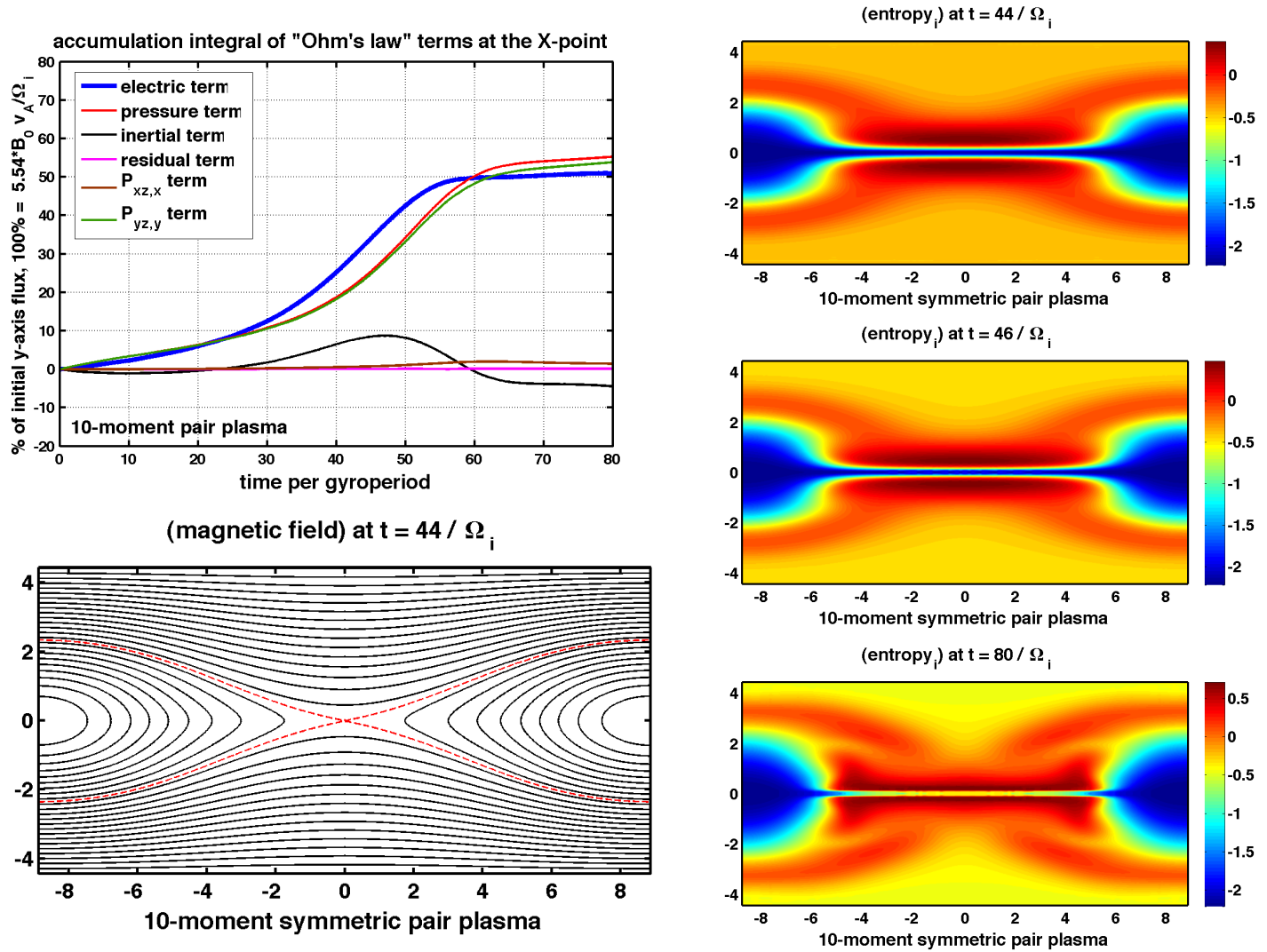


Figure 15: Reconnected flux for fast isotropization in the half-scale symmetric pair plasma GEM problem.

When the rate of isotropization is fast the inertial term initially provides some support for reconnection, although the pressure term ultimately provides the support. Entropy production occurs in the low-entropy sheet along the outflow axis due to pressure isotropization. Viscosity prevents turbulence from developing, and the solution remains regular over the whole course of the simulation. The maximum Knudsen number is roughly .25 over the course of this simulation. The pressure tensor generally shows good agreement with the five-moment closure.

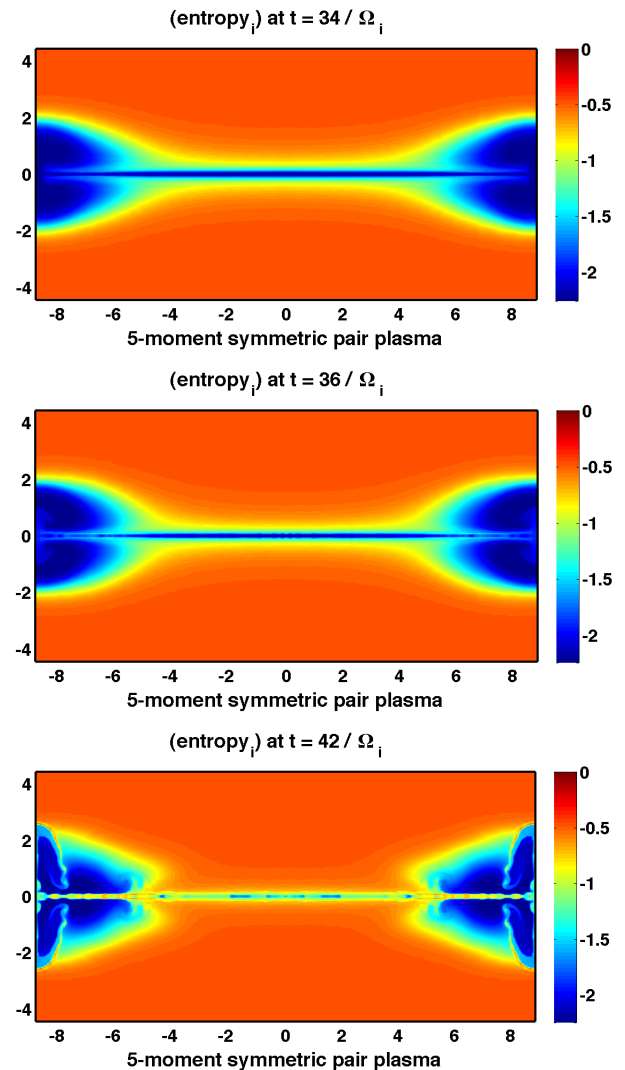
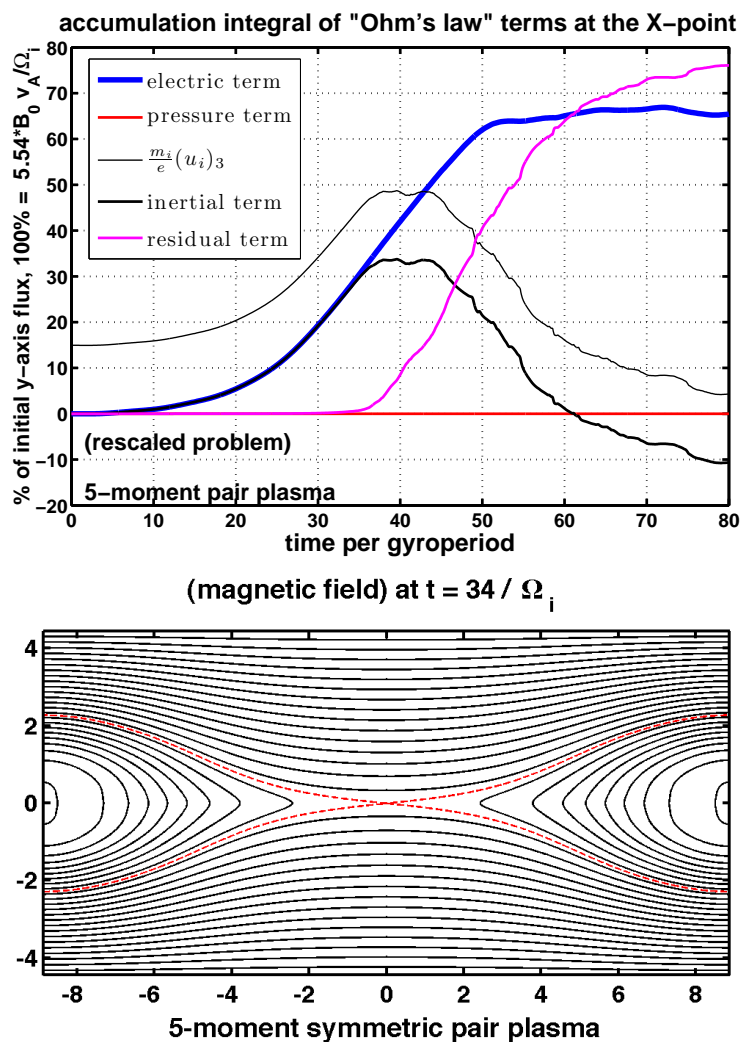


Figure 16: Reconnected flux for the five-moment model (instantaneous isotropization) in the half-scale symmetric pair plasma GEM problem.

In the five-moment model the inertial term initially tracks with reconnected flux until there is a narrow sheet of low entropy along the outflow axis, but beginning at a time of about 36 numerical residual kicks in. At almost exactly the the same time turbulence begins to form at the walls and the sheet of low entropy at the center begins to form beads. Sharp outflow jets generate strong turbulence at late times.

In this simulation we used a five-moment model computed on a 256 by 128 mesh. For coarser meshes we verified that the instantaneously relaxed ten-moment model agrees with the five-moment model.

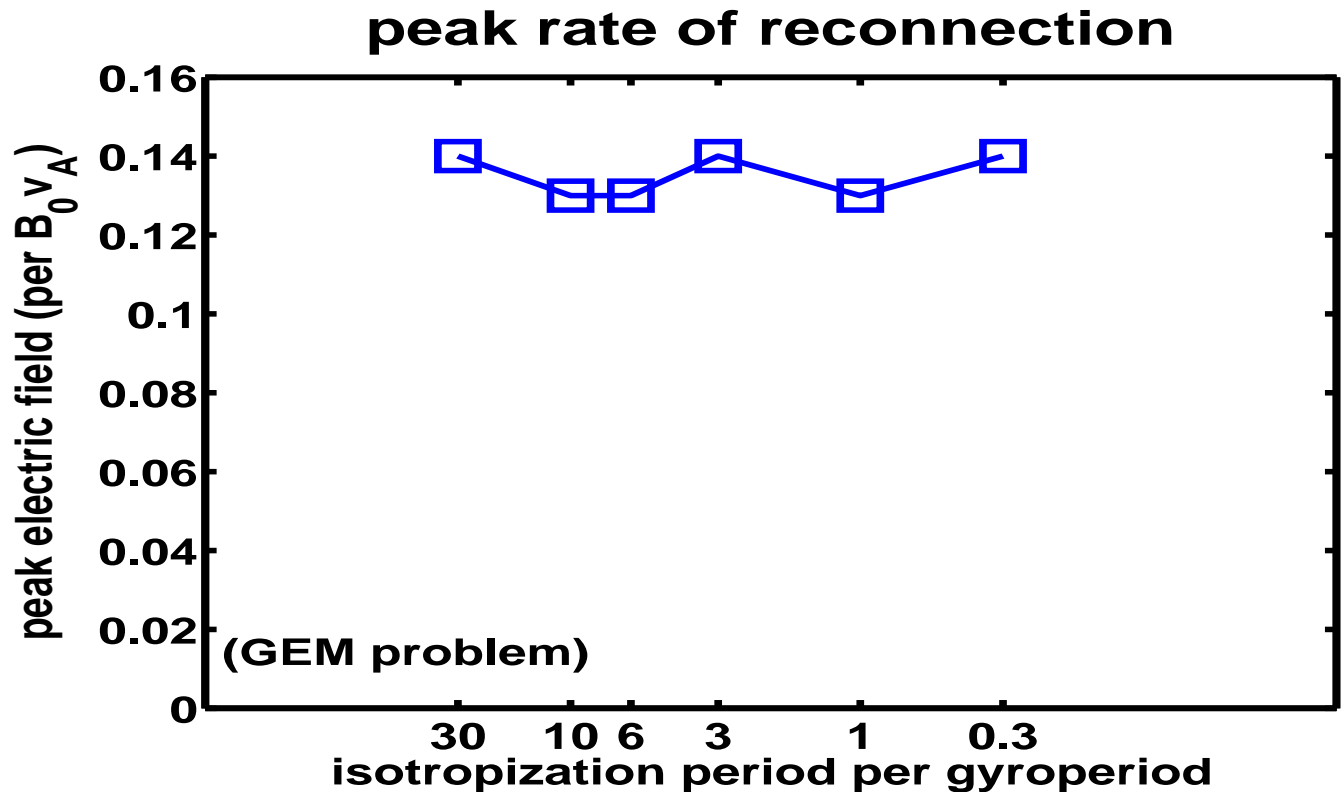


Figure 17: Peak rate of reconnection versus isotropization period in the full-scale symmetric pair plasma GEM problem.

5.2 Full-scaled pair plasma GEM problem

To compare with Bessho and Bhattacharjee [3, 4], we also used their GEM-like (full) scaling ($r_s = 1$). We allowed the isotropization period to vary over a smaller range (between .3 and 30), since for extreme isotropization periods central magnetic islands formed. Over this range our reconnection rate varied between .13 and .14, and our time to peak (i.e. 30%) reconnection increased from 32 for a slow isotropization period of 30 to 37 for a fast isotropization period of .3.

Our nondimensionalized peak rate of reconnection was about 60% of Bessho and Bhattacharjee’s peak rate of about .23, and our time to peak reconnection was roughly twice their time of about 18 (angular) gyroperiods (as seen in the red curve displayed in Figure 2 in either of [3, 4]). See figures 17 and 18.

To compare with their results we plot Ohm’s law terms on the inflow axis in figure 21 and plot calculated anomalous resistivity in 22. Our plots indicate a value of anomalous resistivity roughly half that reported in [4].

We display profiles and plots at the peak reconnection time of 34 gyroperiods. The shape of our profiles is similar to those of [4], though our rates are generally smaller.

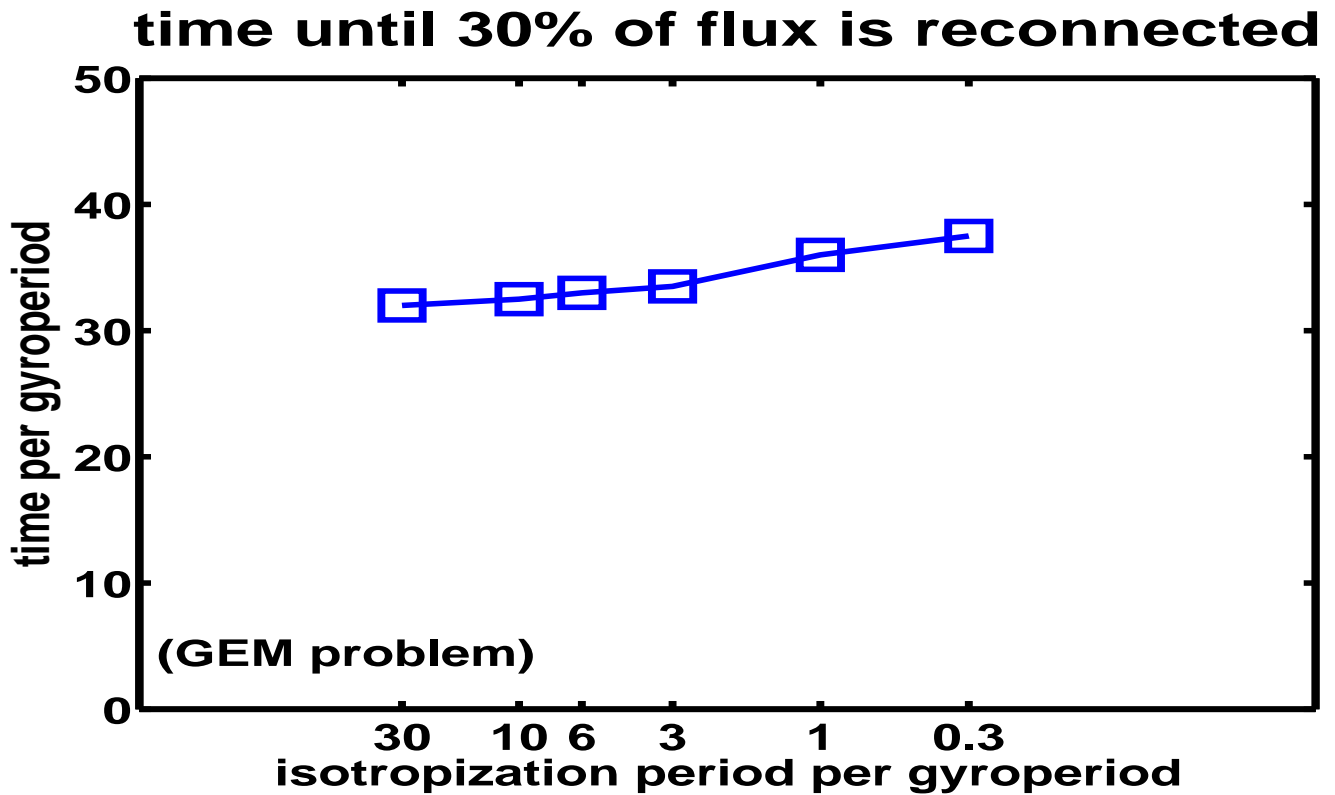


Figure 18: Time until 30% of flux is reconnected in the full-scale symmetric pair plasma GEM problem.

For all simulations the peak rate of reconnection occurred when about 30% of the original flux through the y-axis had reconnected.

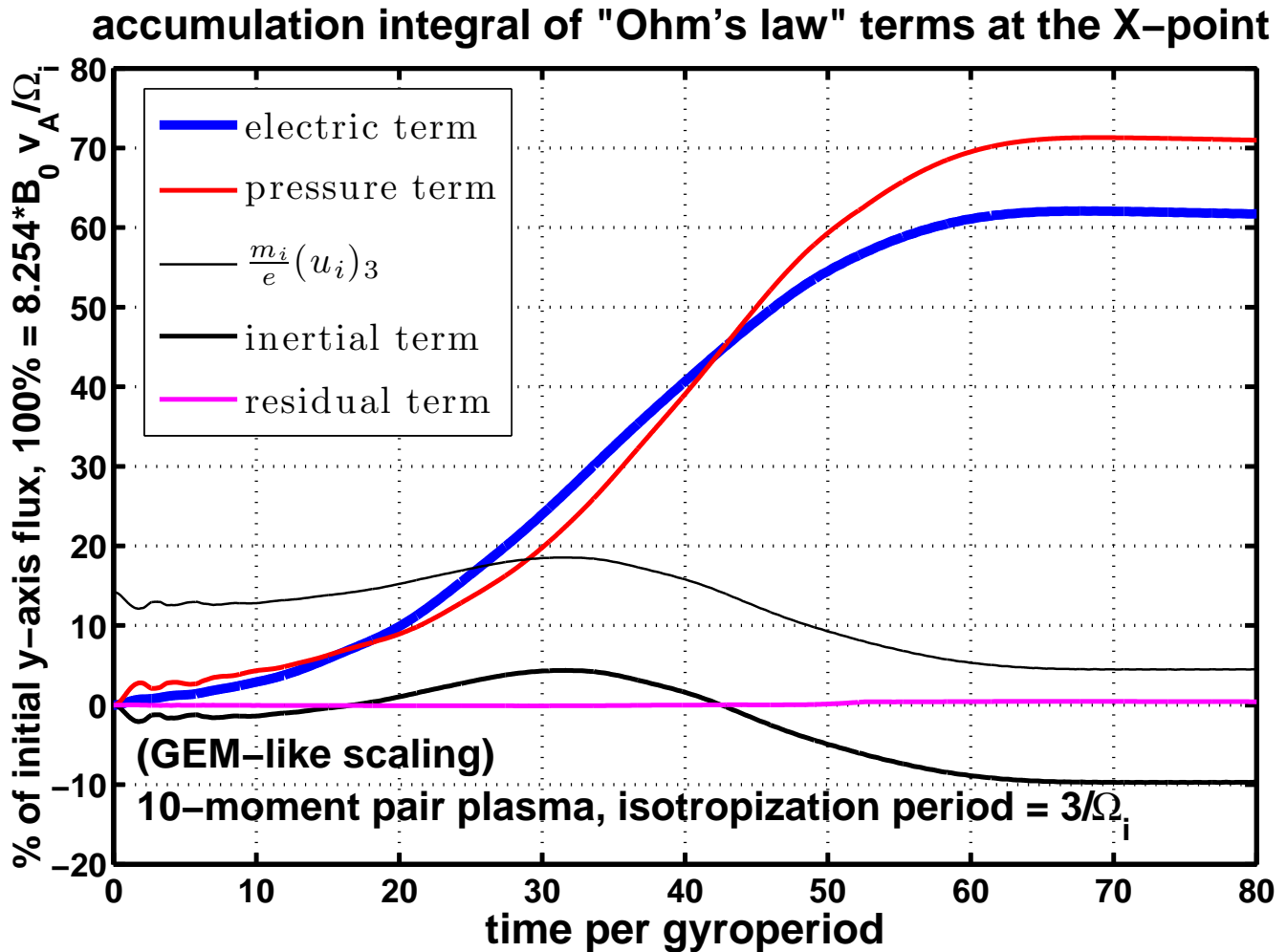


Figure 19: Reconnected flux for moderate isotropization in the full-scale symmetric pair plasma GEM problem.

The pressure term is the dominant contribution, in agreement with PIC simulations. The time to 30% reconnection is about 34 (angular) gyroperiods.

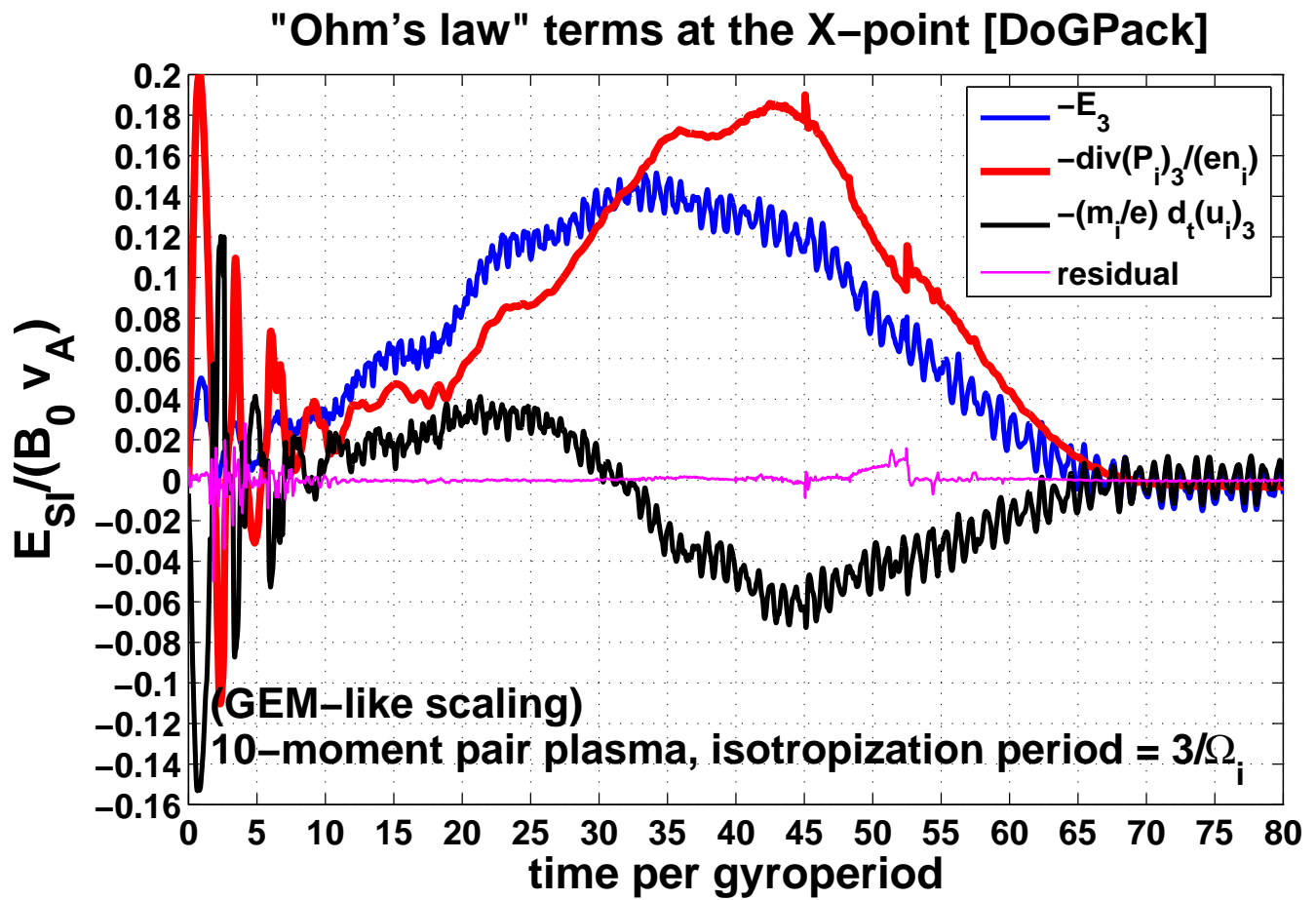


Figure 20: Reconnection rate for moderate isotropization in the full-scale symmetric pair plasma GEM problem.

The blue curve in this figure is the rate of reconnection and corresponds to the red curve in Figure 2 of [4]. Our peak reconnection rate is about .14.

y-axis profile at time $34 / \Omega_i$

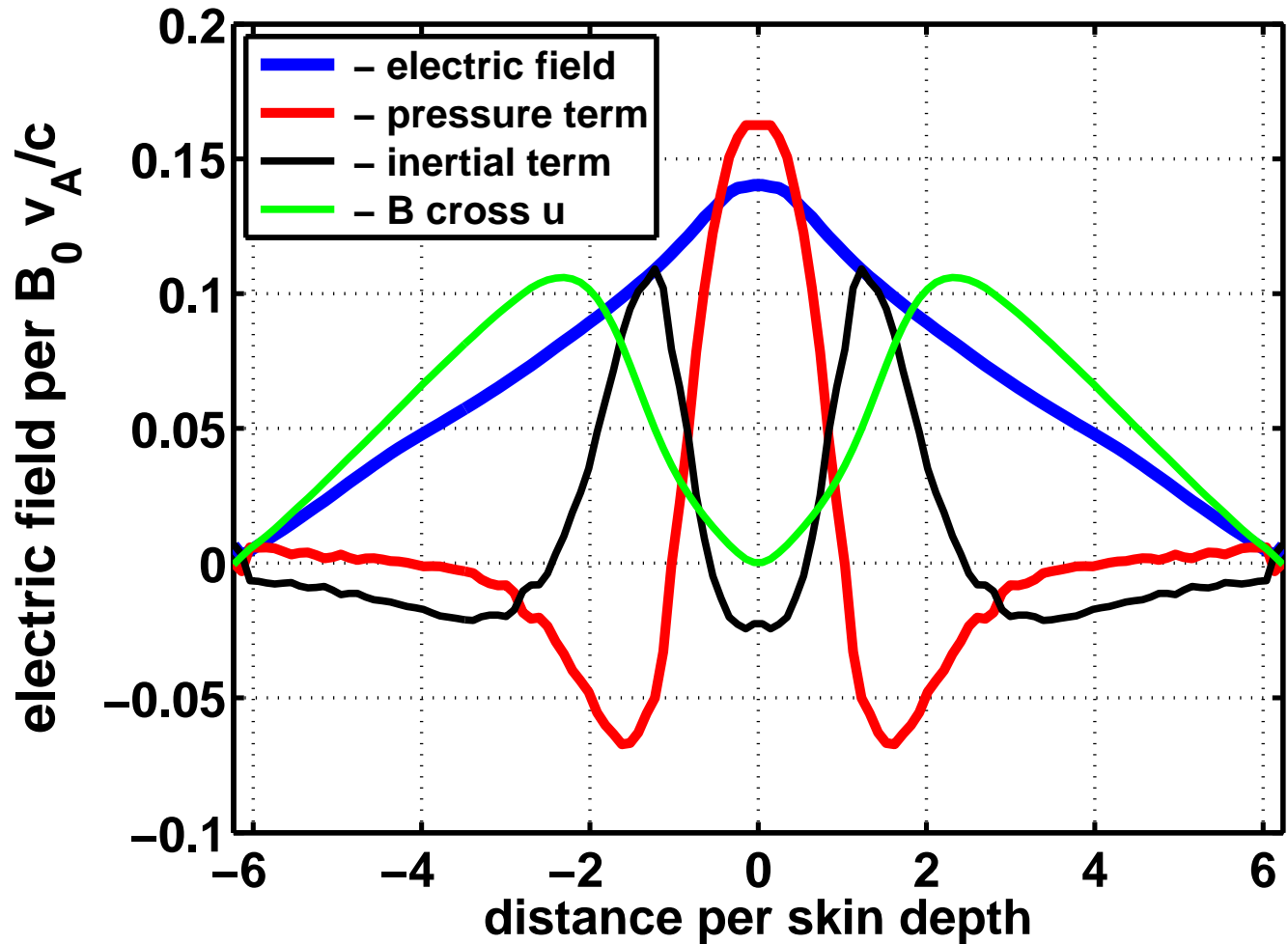


Figure 21: Profile of “Ohm’s law” terms at the peak reconnection time of 34 (angular) gyroperiods in the full-scale symmetric pair plasma GEM problem. Compare this figure with FIG. 5 in [4].

y-axis profile at time $34 / \Omega_i$

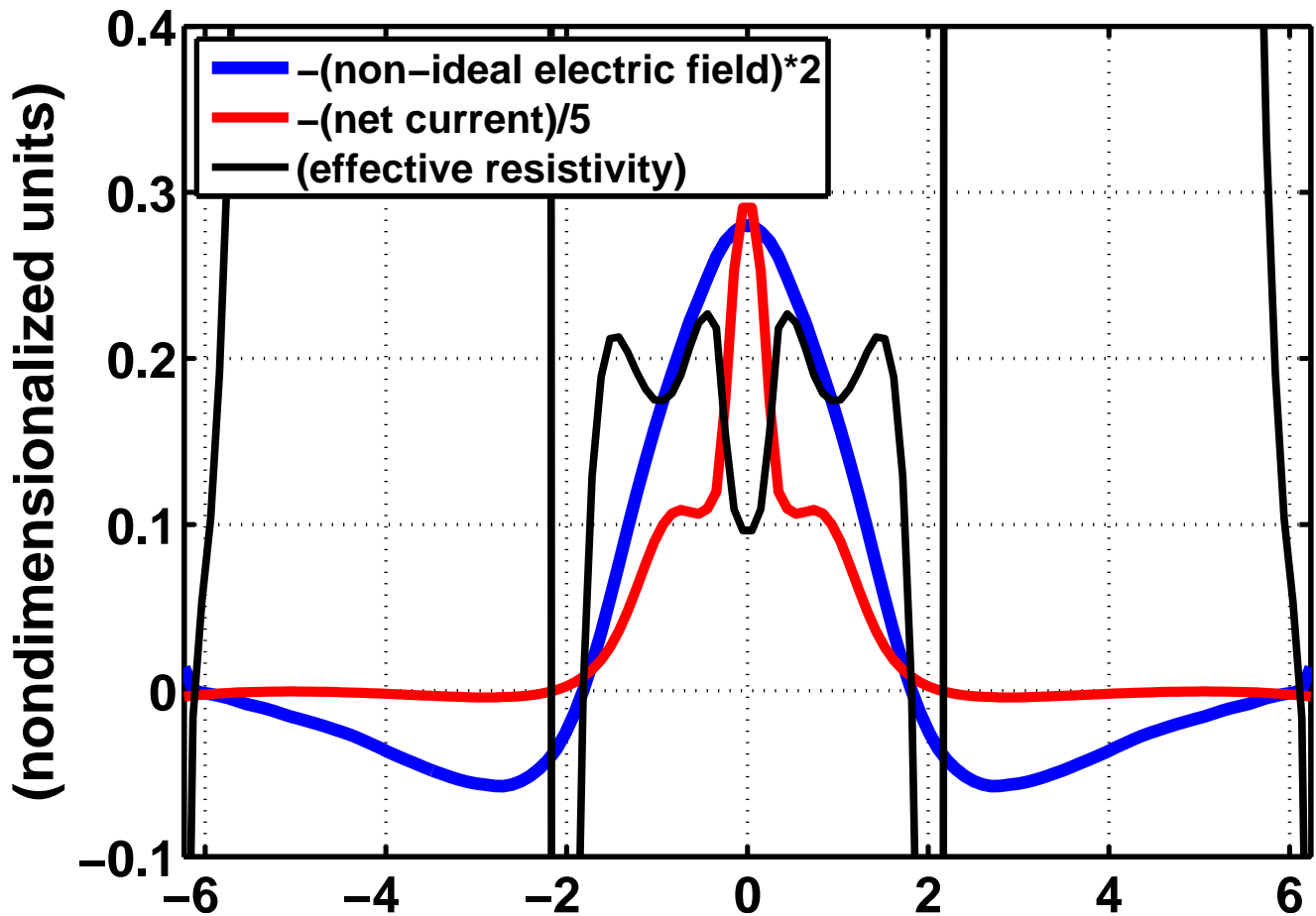
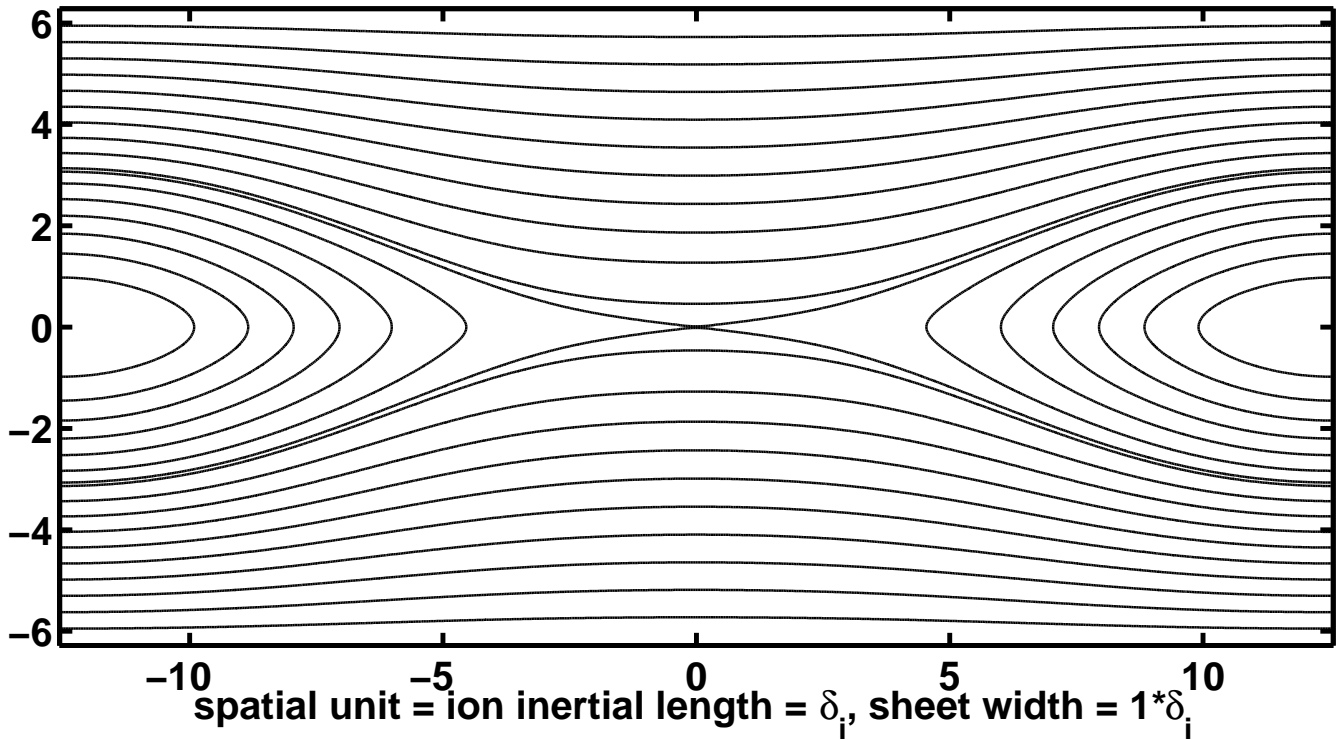


Figure 22: Anomalous resistivity along the y-axis at the peak reconnection time of 34 (angular) gyroperiods in the full-scale symmetric pair plasma GEM problem.

At the peak reconnection rate our effective anomalous resistivity at the X-point was about 0.1 (in units of $\frac{B_0}{en_0}$), in contrast to the value of roughly 0.19 reported in [4] (compare this figure with FIG. 5 in [4]).

B at $t = 34/\Omega_i$ (128x64 grid, isotropization period = $3/\Omega_i$)



-(net current) at $t = 34 / \Omega_i$

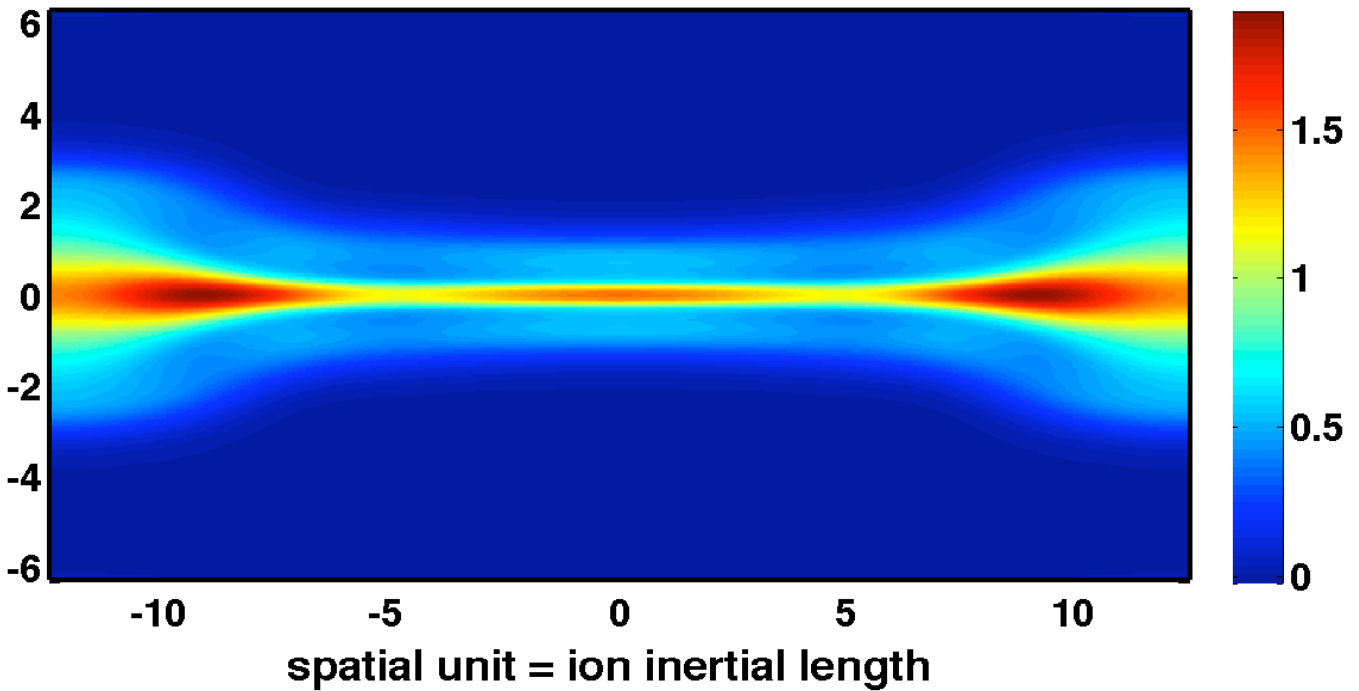


Figure 23: Magnetic field lines and current at the time of peak reconnection rate.

5.3 Conclusion

Our simulations of the GEM problem indicate that for antiparallel reconnection in pair plasma the ten-moment two-fluid model with isotropization admits a rate of reconnection a bit more than half the rate seen in particle simulations.

This raises the question of how to modify the fluid model we used so that we can get better agreement. An obvious way to get agreement is to use an anomalous resistivity. In the context of a collisionless simulation it would seem more physical to impose an anomalous viscosity. Our rate of reconnection was insensitive to the rate of isotropization. This might suggest use of a different (nonzero) nonzero heat flux, but heat flux should not affect the rate of reconnection much until significant temperature gradients have had time to develop.

In contrast to these results for pair plasmas, we find in the next chapter that for the original GEM problem a two-fluid ten-moment model with relaxation toward isotropy gives reconnection rates that agree well with kinetic simulations [32]. Perhaps the improved agreement can be attributed to the presence of the Hall effect as the primary driver of fast reconnection in hydrogen plasmas.

Chapter 6

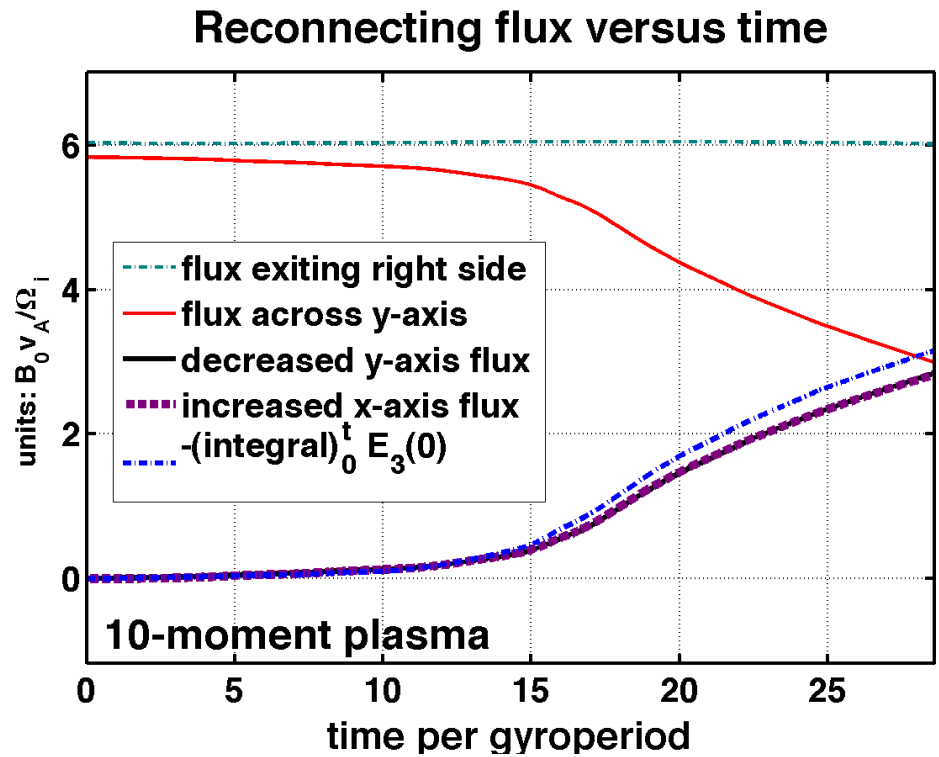
GEM hydrogen plasma simulations

This chapter reports simulations of GEM magnetic reconnection challenge problem described in chapter 4 (for the case of hydrogen plasma with $\frac{m_i}{m_e} = 25$). The main results of this chapter were also reported in [32].

We again used the adiabatic 10-moment two-fluid-Maxwell model with pressure tensor isotropization to simulate the problem, as well as the hyperbolic (adiabatic inviscid) 5-moment two-fluid Maxwell model. We compared our results with published Vlasov and PIC simulations at the time of peak reconnection. The magnetic field generally showed good agreement (see figure 25). We obtained good agreement for the time until one unit of flux was reconnected for both the 5-moment model and the 10-moment isotropizing model (see figure). For the 10-moment isotropizing model we obtained qualitatively good agreement for plots of pressure tensor components at the time of peak reconnection, as shown in figures 26 and 27.

As noted in table 1, it is standard to compare results at the time when one unit of flux has been reconnected, *including the .2 units of reconnected flux due to the initial perturbation*. I unfortunately have made my plots at the point in time when one unit of flux has been reconnected *not including the .2 units of reconnected flux due to the the GEM problem*, which puts my plots about one unit of time later than the time I should be looking at to compare against the simulations of others.

The ten-moment model attained 16% flux reconnected at about $t = 18/\Omega_i$:



The five-moment model attained 16% flux reconnected at about $t = 13.5/\Omega_i$:

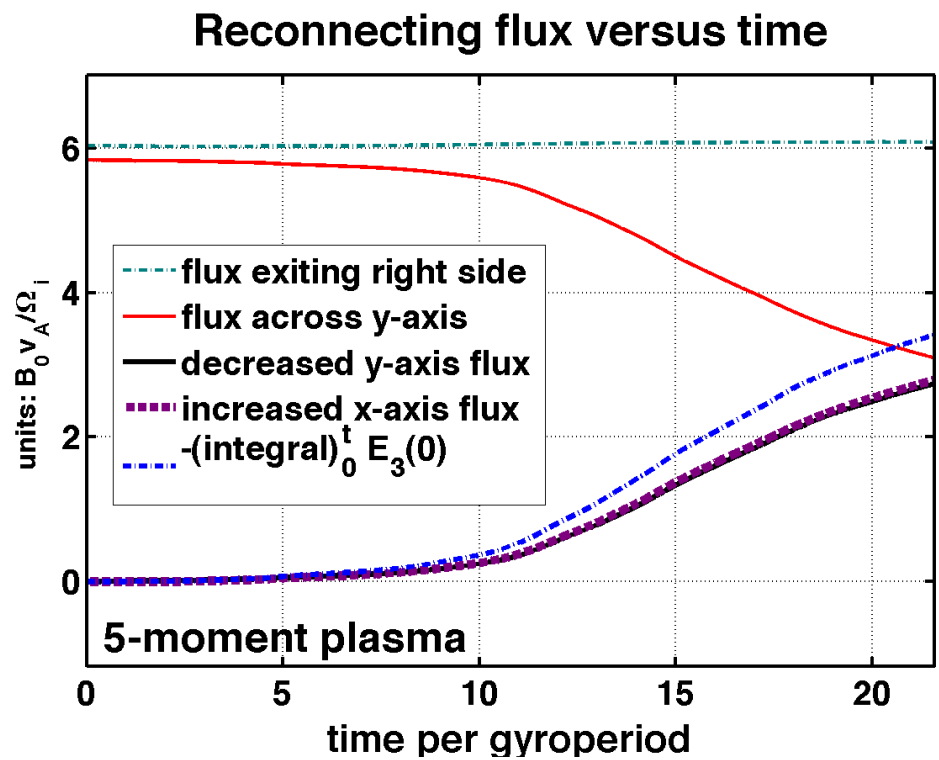


Figure 24: GEM simulations: reconnecting flux for 10- and 5-moment models. Each simulation crashed at the end time in its plot of reconnecting flux versus time.

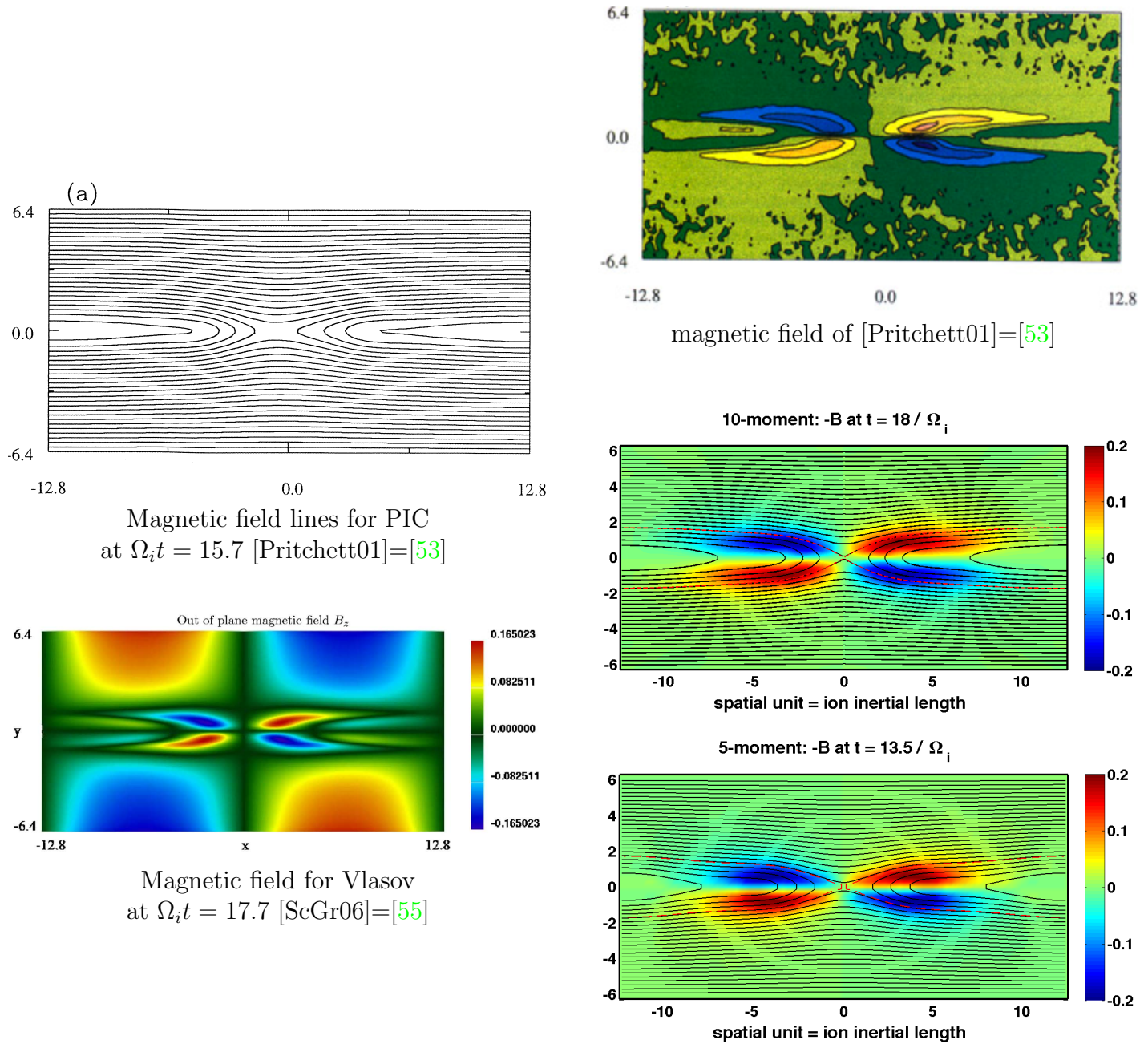


Figure 25: Magnetic field at 16% reconnected

| model | source | time when 16% flux reconnected |
|-------------|--------------------|--------------------------------|
| Vlasov | [55]=[ScGr06] | $t = 17.7/\Omega_i$: |
| PIC | [53]=[Pritchett01] | $t = 15.7/\Omega_i$: |
| 10-moment | [32]=[JoRo10] | $t = [16.2, 17.2]/\Omega_i$: |
| 5-moment | [32]=[JoRo10] | $t = [12.0, 12.9]/\Omega_i$: |
| 5-moment | [40]=[LoHaSh11] | $t = [15, 16]/\Omega_i$: |
| 10-5-moment | [19]=[Hakim08] | $t = 17.6/\Omega_i$: |

Table 1: Comparison of time required to reconnect one unit of flux for kinetic and two-fluid simulations of the GEM problem.

The 10-5-moment simulation modeled ions as a 10-moment gas and electrons as a 5-moment gas [19] and used hyperbolic (truncation) closures for both species. The 5-moment simulations of [32] and of [40] were hyperbolic in both species.

The rough range given for [40] reflects that this paper reports a number of simulations in its figures 16 and 17.

The ranges given for [32] (the results reported here) reflect that *there is an inconsistency in the time when I have chosen to report my results, both here and in [32]*. (I am unfortunately out of time to redo the plots and calculations before the deadline to deposit this work.) For the GEM problem it is standard to compare results at the point in time when one unit of flux has been reconnected, *including the initial perturbation*. I neglected to include the initial perturbation, and therefore my times were really the time until 1.2 units of flux were reconnected in the sense understood by the GEM standard. Therefore I have listed both times: the time until 1.0 total units of flux have been reconnected followed by the time until 1.2 units have been reconnected.

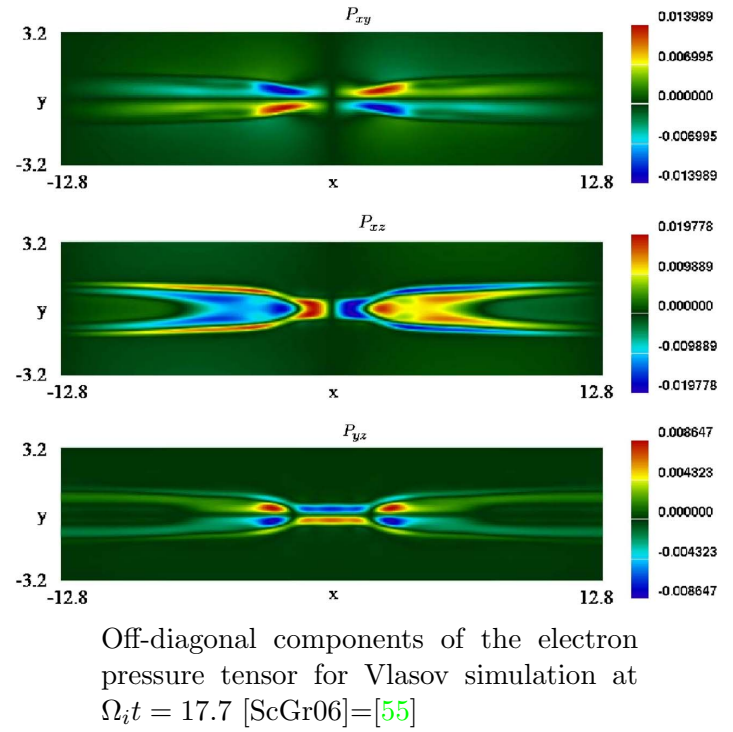
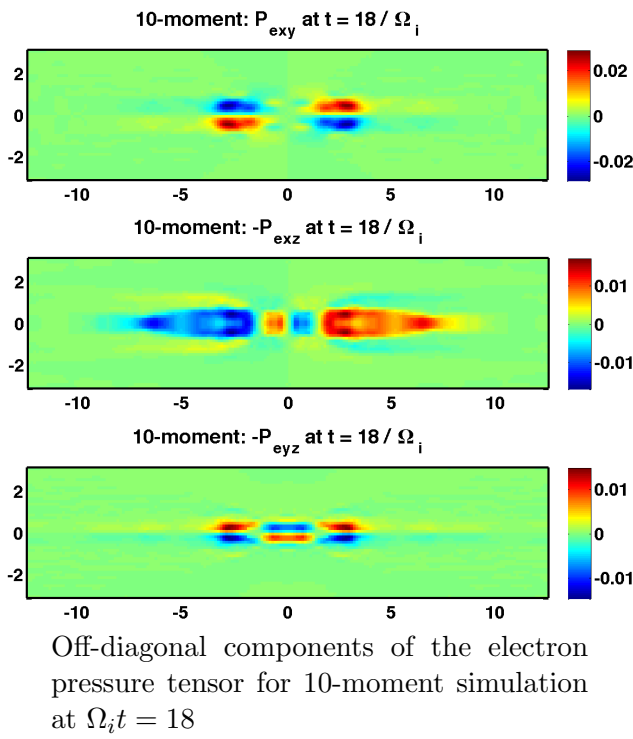


Figure 26: Off-diagonal components of electron pressure tensor

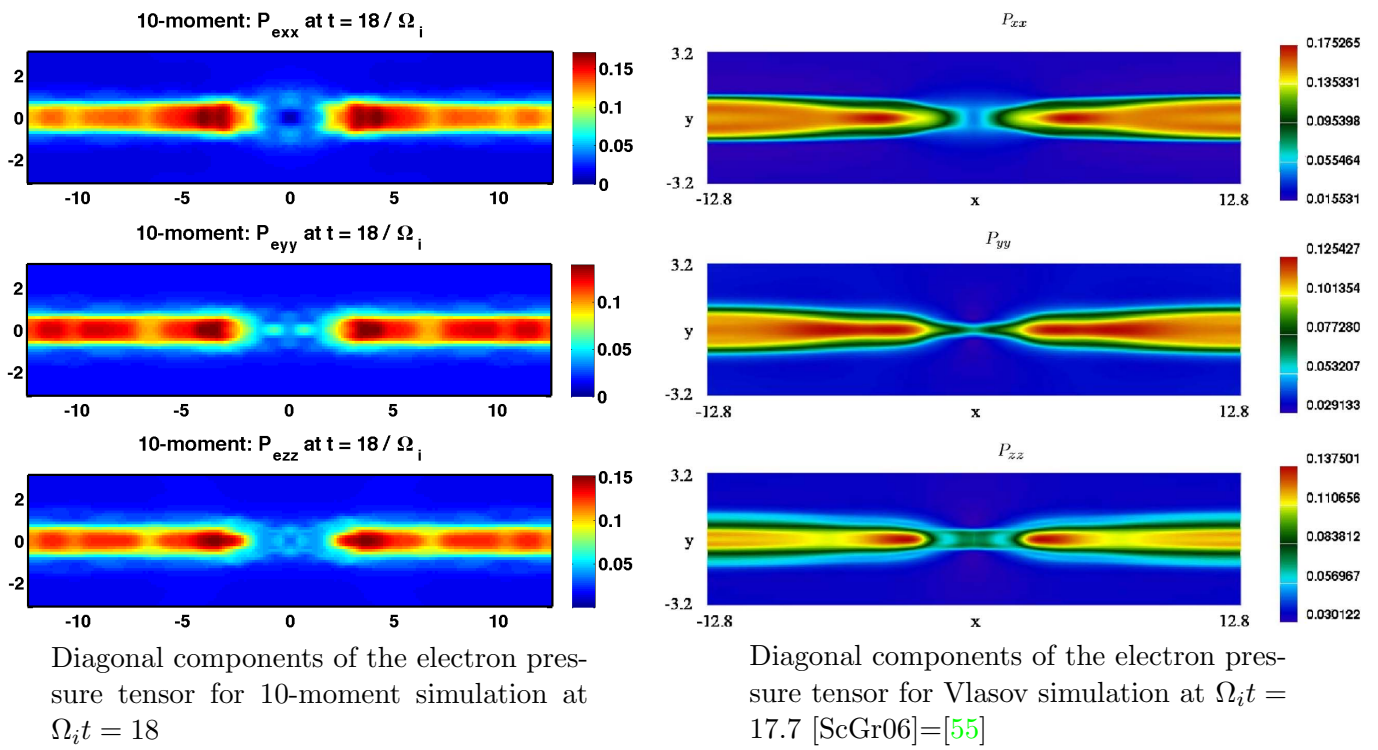


Figure 27: Diagonal components of electron pressure tensor

For a coarse mesh we can extend the time duration of the simulation to get a solution that appears quite regular. But for a refined mesh, after peak reconnection our simulations would eventually crash due to negative pressures or even densities, typically near the X-point. This happened chiefly in the zero guide field case. By implementing positivity limiters we were able to prevent the simulation from crashing, but the solution exhibits secondary instabilities past the point where positivity limiting becomes necessary.

These difficulties prompted a consideration of steady-state reconnection. The GEM problem is a 2D rotationally symmetric problem, and as shown in section 3.4, nonsingular 2D steady reconnection is not possible in an adiabatic model for a rotationally symmetric problem.

The implications are that steadily driven reconnection of an adiabatic model cannot go to steady state and will therefore either develop a singularity or will exhibit intermittent reconnection. (On a sufficiently small scale we expect a singularity, whereas for a larger scale, especially if symmetry is not enforced, we expect intermittent reconnection.)

It is reasonable to assume that near the time when the rate of reconnection peaks the evolution of the solution near the X-point may be approximated by steadily driven reconnection. If so, then since we are in the case of antiparallel reconnection, along the y axis near the origin we expect the solution to approach a singular steady state of the form

$$\mathbb{T}_{xx} = Cy^\lambda,$$

as seen in (3.16) and (B.3).

In practice, we typically observe an anisotropy that increasingly looks like a singularity at the X-point (see figures 28 and 29). The near-singularity then splits into a pair of near-singular points moving outward along the x axis (see figures 30 and 31). If we enforce positivity to prevent the simulation from crashing, then the origin becomes an O-point and reconnection ceases. If we do not enforce symmetry, then when this secondary island forms symmetry is broken and the island is ejected to one side or the other. I remark that in the adiabatic model very strong temperature gradients develop, especially if a fine mesh is used. For a coarse mesh the approximate singularities fail to become sharp enough to disrupt reconnection e.g. by causing second islands to form.

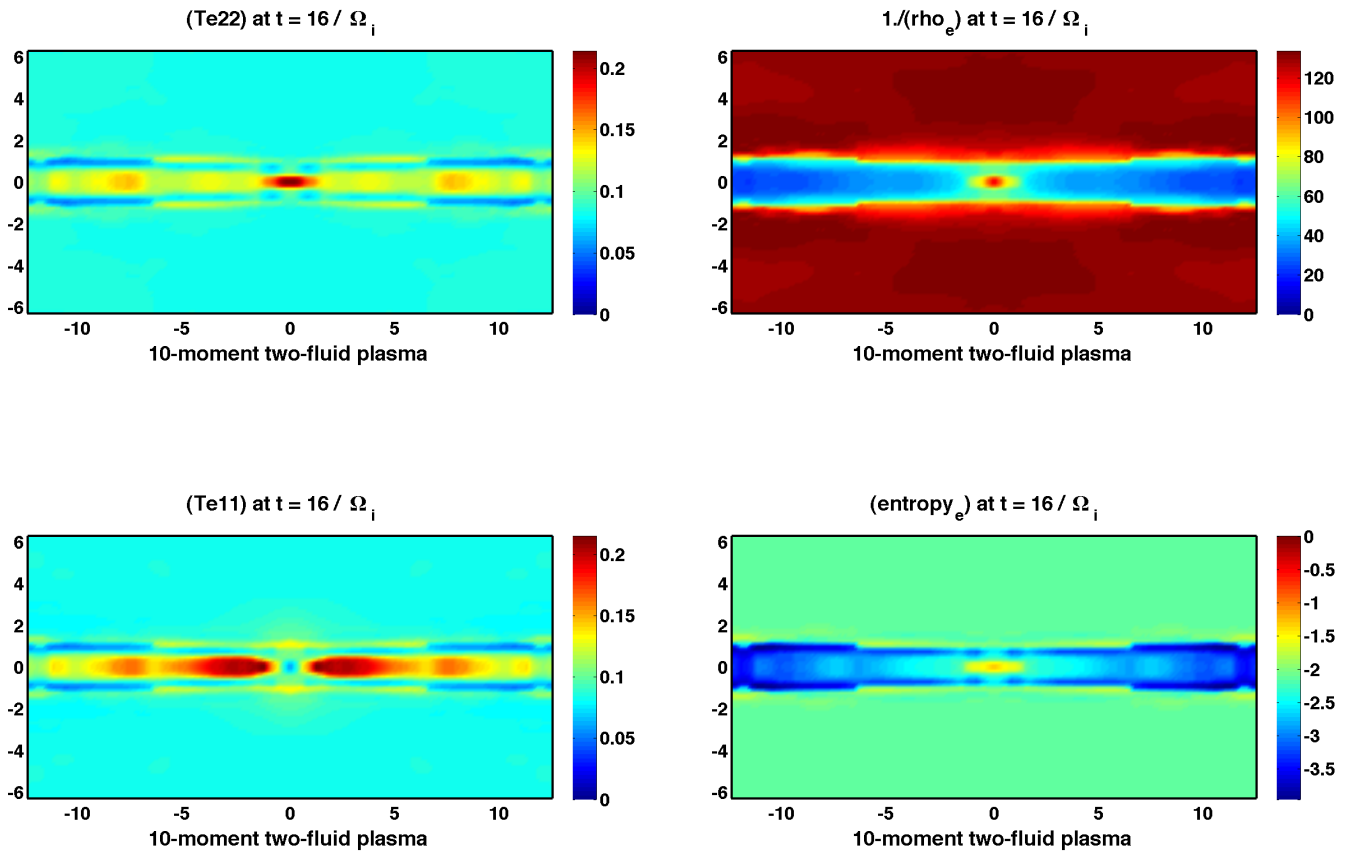


Figure 28: Electron gas at $t = 16$ (nascent singularity)

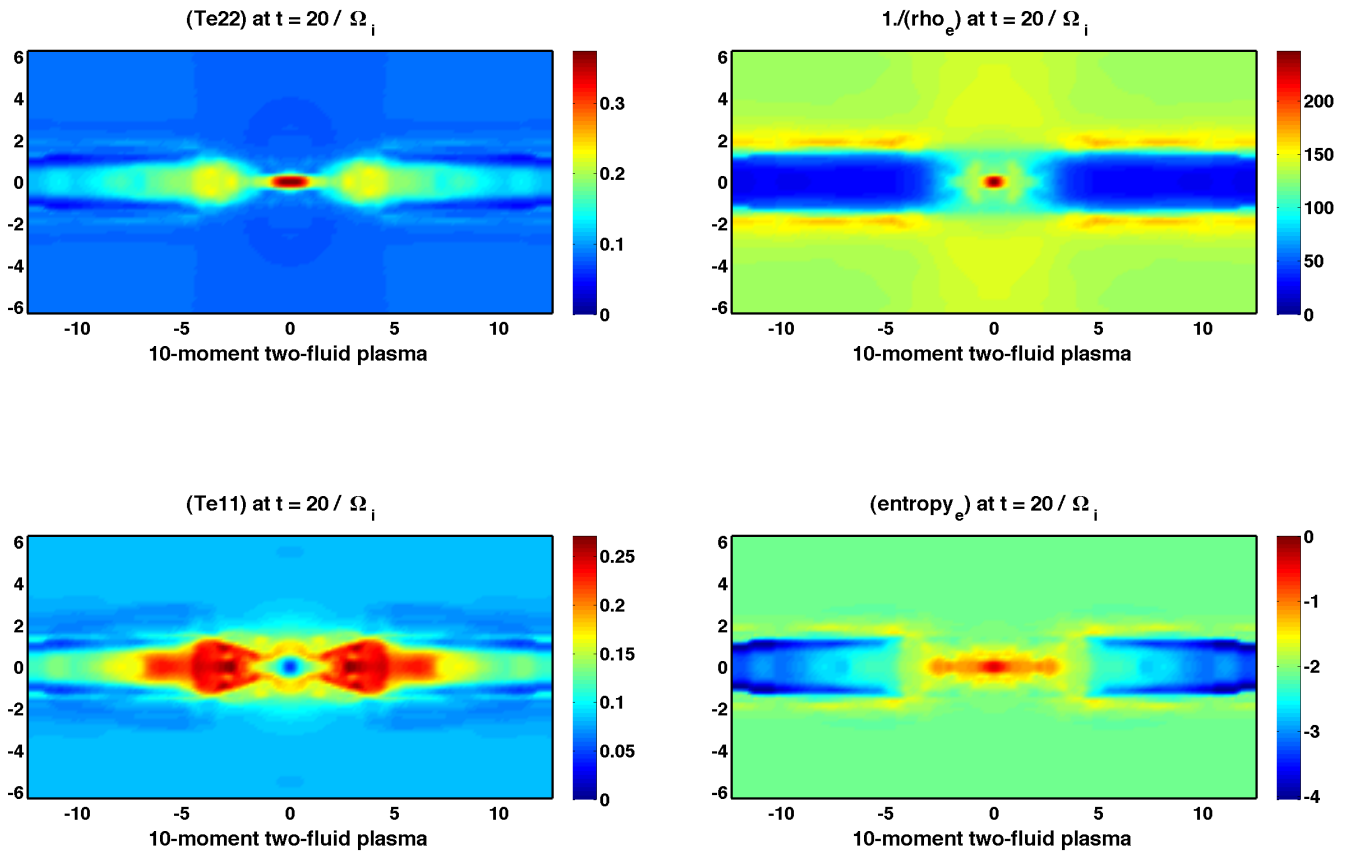


Figure 29: Electron gas at $t = 20$ (developing singularity)

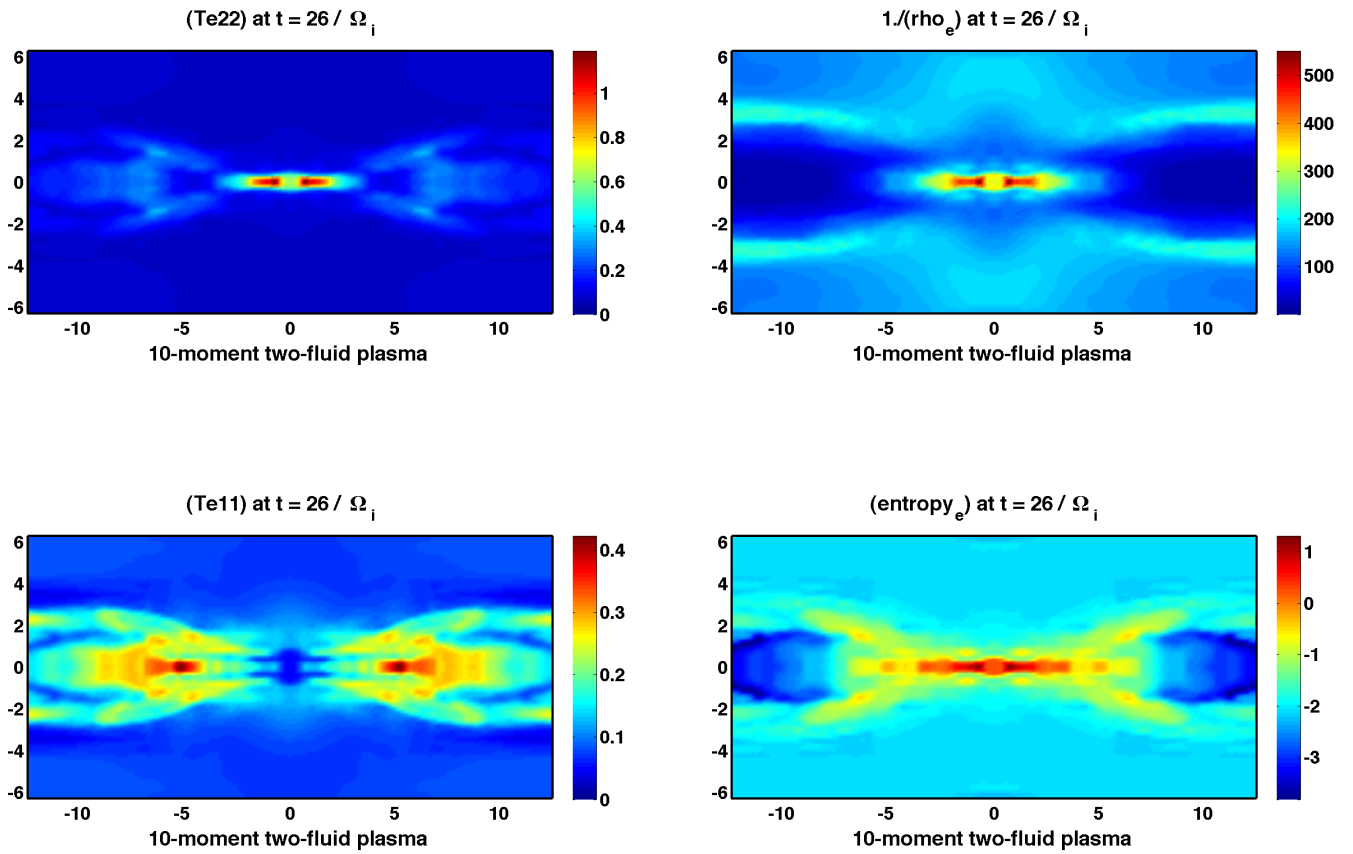


Figure 30: Electron gas at $t = 26$ (splitting singularity)

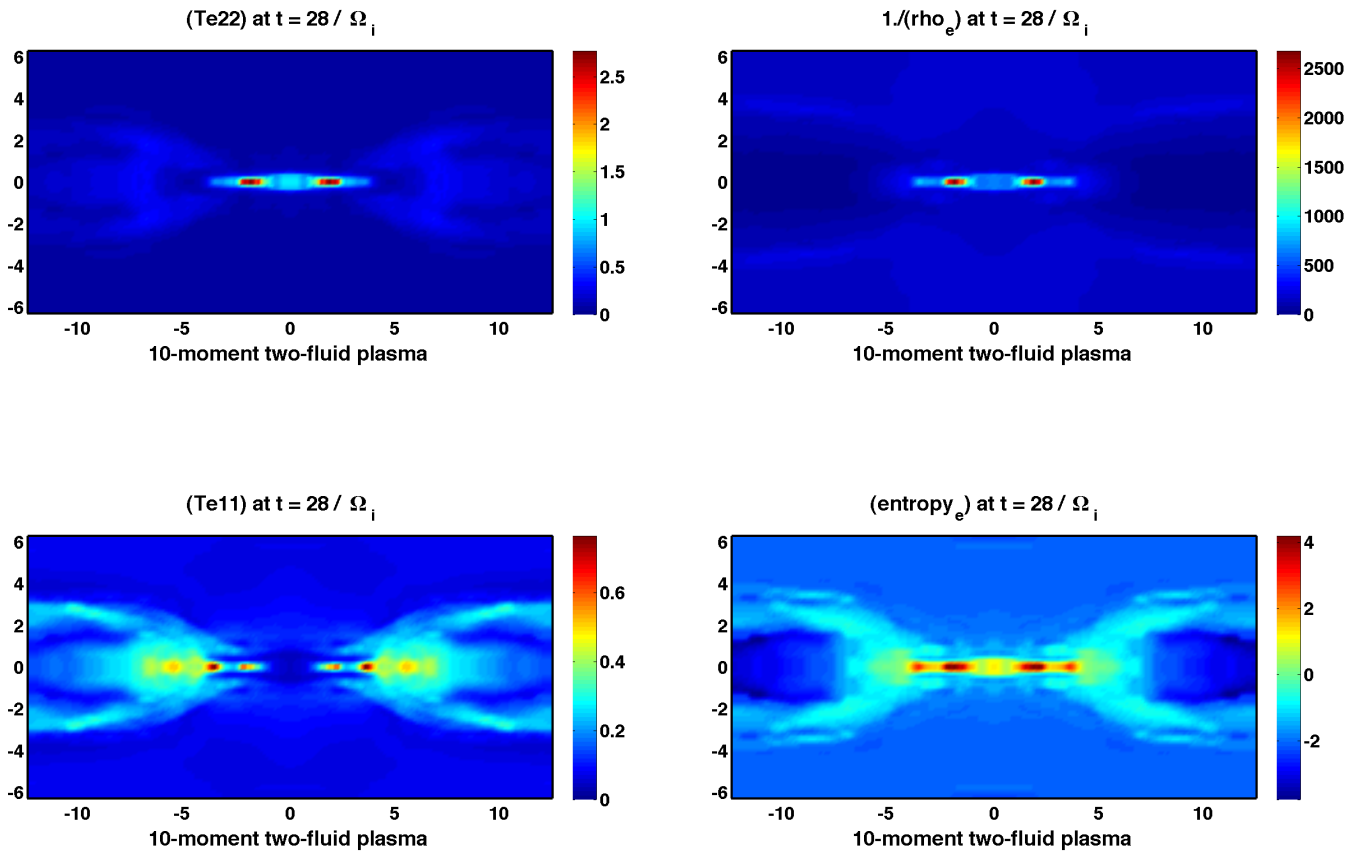


Figure 31: Electron gas at $t = 28$ (split singularity, just before crashing)

Chapter 7

Numerical method

This chapter describes the numerical method used in this dissertation to solve the two-fluid-Maxwell system. Recall that for the two-fluid-Maxwell system we use the coupled systems (4.8) for Maxwell's equations, (4.9) for each ten-moment fluid, and (4.10) for each five-moment fluid. Since we neglect all diffusive terms, the composite system we solve fits the hyperbolic conservation form

$$\partial_t \underline{u} + \nabla \cdot \underline{\mathbf{f}} = \underline{s}, \quad (7.1)$$

where $\underline{u}(t, \mathbf{x})$ is the state, $\underline{\mathbf{f}}(\underline{u})$ is the flux function, and $\underline{s}(\underline{u})$ is an undifferentiated source term. In two spatial dimensions we can write

$$\partial_t \underline{u} + \partial_x \underline{f} + \partial_y \underline{g} = \underline{s}, \quad (7.2)$$

where $\underline{f} := \mathbf{e}_x \cdot \underline{\mathbf{f}}$ and $\underline{g} := \mathbf{e}_y \cdot \underline{\mathbf{f}}$. We solve this system using the explicit discontinuous Galerkin (DG) method.

7.1 Discontinuous Galerkin method

The discontinuous Galerkin (DG) method was developed into a modern tool for computing solutions to hyperbolic PDEs in a series of papers by Cockburn and Shu (see [13] and references therein).

We define a Cartesian mesh S_h made up of N mesh cells. Solutions are represented by members of the *broken* finite element space

$$V^h = \{v^h \in L^\infty(S) : v^h|_{\mathcal{T}} \in P^k, \forall \mathcal{T} \in S_h\},$$

where h is the grid spacing, \mathcal{T} is a mesh cell, and P^k is the set of polynomials of degree at most k . Each cell can be mapped to the canonical mesh cell, $[-1, 1] \times [-1, 1]$, via a simple affine transformation. On the canonical mesh cell we define the following normalized Legendre polynomials up to degree two:

$$\{\phi^{(\ell)}\}_{\ell=1}^6 = \left\{ 1, \quad \sqrt{3}\xi, \quad \sqrt{3}\eta, \quad 3\xi\eta, \quad \frac{\sqrt{5}}{2}(3\xi^2 - 1), \quad \frac{\sqrt{5}}{2}(3\eta^2 - 1) \right\}. \quad (7.3)$$

These basis functions are orthonormal with respect to a cell-average inner product:

$$\frac{1}{4} \int_{-1}^1 \int_{-1}^1 \phi^{(m)}(\xi, \eta) \phi^{(n)}(\xi, \eta) d\xi d\eta = \delta_{mn}. \quad (7.4)$$

We seek approximate solutions of (7.2) which are a linear combination of basis functions,

$$q^h(\xi, \eta, t)|_{\tau_{ij}} := \sum_{k=1}^6 U_{ij}^{(k)}(t) \phi^{(k)}(\xi, \eta). \quad (7.5)$$

Multiplying (7.2) by a basis function and integrating by parts yields the following semi-discrete evolution equations for the Legendre coefficients, $U_{ij}^{(\ell)}$:

$$\frac{d}{dt} U_{ij}^{(\ell)} = N_{ij}^{(\ell)} - \frac{\mathcal{F}_{ij}^{(\ell)}}{\Delta x} - \frac{\mathcal{G}_{ij}^{(\ell)}}{\Delta y} + S_{ij}^{(\ell)}, \quad (7.6)$$

where Δx and Δy are the dimensions of the mesh cell and where

$$N_{ij}^{(\ell)} = \frac{1}{4} \int_{-1}^1 \int_{-1}^1 [\phi_{,x}^{(\ell)} f(q^h) + \phi_{,y}^{(\ell)} g(q^h)] d\xi d\eta, \quad (7.7)$$

$$\mathcal{F}_{ij}^{(\ell)} = \left[\frac{1}{2} \int_{-1}^1 \phi^{(\ell)} f(q^h) d\eta \right]_{\xi=-1}^{\xi=1}, \quad (7.8)$$

$$\mathcal{G}_{ij}^{(\ell)} = \left[\frac{1}{2} \int_{-1}^1 \phi^{(\ell)} g(q^h) d\xi \right]_{\eta=-1}^{\eta=1}, \quad (7.9)$$

$$S_{ij}^{(\ell)} = \frac{1}{4} \int_{-1}^1 \int_{-1}^1 \phi^{(\ell)} \psi(q^h) d\xi d\eta. \quad (7.10)$$

We approximate these averaging integrals with Gaussian quadrature rules. We use a Riemann solver to determine the flux values used in the edge integrals. In particular, we approximate the integrals in (7.10) via the standard 2D 9-point rule, the integrals in (7.7) via the standard 2D 4-point rule, and the integrals in (7.8)–(7.9) with the standard 1D 3-point rule and local Lax-Friedrichs Riemann solvers.

We handle time-stepping via a third-order TVD Runge-Kutta method [16]. After each time stage we apply a minmod limiter to the coefficients of the quadratic basis functions and, if limiting occurred, to the coefficients of the mixed and linear terms (a modification of the method in [33]). This method was implemented in the C++ code DOGPACK, which was developed by James Rossmannith and collaborators at UW-Madison.

7.2 Source term

For the two-fluid-Maxwell system, the source term \underline{s} in equation (7.1) is extremely stiff. Fortunately it is also linear. To handle the source term we use Strang splitting and alternately solve the flux equation (the *hyperbolic part*)

$$\partial_t \underline{u} + \nabla \cdot \underline{\mathbf{f}} = 0 \quad (7.11)$$

and the *source ODE*

$$\partial_t \underline{u} = \underline{s}. \quad (7.12)$$

This is a linear ODE with constant coefficients (with the caveat below) and can be solved exactly. The source ODE can be further decomposed into a sum of three commuting operators, for which splitting incurs no error:

$$\partial_t \underline{u} = \underline{s}_{\text{electro-momentum}} + \underline{s}_{\text{(pressure tensor rotation)}} + \underline{s}_{\text{(pressure isotropization)}}. \quad (7.13)$$

The electro-momentum and pressure tensor rotation terms have imaginary eigenvalues. The pressure isotropization term has a negative real eigenvalue equal in magnitude to the isotropization rate.

As a caveat, the isotropization ODE has constant coefficients if the isotropization rate remains constant as isotropization proceeds, which holds if the isotropization period is defined in terms of $\text{tr } \mathbb{T}_s$ but not if it is defined in terms of $\det \mathbb{T}_s$ (see section 2.7.2).

Splitting off the source ODE and solving it exactly (or via the trapezoid rule) ensures that the source ODE does not cause violation of positivity, energy conservation, or numerical stability. This technique of splitting off the two-fluid source term and solving it exactly was used for the five-moment two-fluid Maxwell system in [34].

7.3 Flux term

The chief challenges in solving the flux term are to ensure numerical stability and to guarantee that positivity of the solution is maintained.

To ensure numerical stability we take a time step which respects a CFL stability condition

$$\frac{\Delta t |\lambda|_{\max,e} dA_e}{|K|} \leq \frac{1}{2m-1},$$

for all edges e of the rectangle, where m is the order of the method (which in these simulations was $m = 3$); $|\lambda|_{\max,e}$ is the maximum wave speed perpendicular to the edge, dA_e is the “area” (length) of the edge, and $|K|$ is the “volume” (area) of the rectangle.

7.4 Variation limiters

To ensure numerical stability we apply limiters to the solution after each time step which limit oscillations. Effective limiting requires that we transform into the characteristic variables defined by the eigenstructure of the flux Jacobian of each separable subsystem. These eigenstructures are calculated in section C.2.

Note that for a PDE of the form (7.1),

$$\partial_t \underline{u} + \nabla \cdot \underline{\mathbf{f}} = \underline{s}, \tag{7.14}$$

a flux Jacobian such as $\mathbf{e}_x \cdot \partial \underline{\mathbf{f}} / \partial \underline{u}$ is independent of the source term \underline{s} and therefore application of limiters to equation (C.8) is identical to application of limiters to the conservation law

$$\partial_t \underline{u} + \nabla \cdot \underline{\mathbf{f}} = 0; \tag{7.15}$$

we call this conservation law the **hyperbolic part** of the system (C.8). For the hyperbolic part the system is decoupled into three noninteracting subsystems: gas dynamics for the ions, gas dynamics for the electrons, and Maxwell’s equations. To limit the solution we transform each subsystem into the characteristic variables defined by the eigenstructure of its flux Jacobian. We compute the eigenstructure for MHD (which generalizes a five-moment gas), a ten-moment gas, and Maxwell’s equations in appendix C.

7.4.1 Limiting of a 1D scalar problem

In accordance with the recipe of Krivodonova [33], the coefficients c_i^ℓ of the order- ℓ Legendre polynomial basis function in mesh cell i are limited only if limiters are triggered for all higher-order polynomials; in this case we define the limited coefficient

$$\bar{c}_i^\ell = \text{minmod}(c_i^\ell, D^{+\ell}, D^{-\ell}),$$

where

$$\text{minmod}(a, b, c) := \begin{cases} \text{sgn}(a) \min(|a|, |b|, |c|) & \text{if } \text{sgn}(a) = \text{sgn}(b) = \text{sgn}(c), \\ 0 & \text{otherwise} \end{cases}$$

and where $D^{+\ell}$ is a tunable constant times the forward difference $c_{i+1}^{\ell-1} - c_i^{\ell-1}$ and $D^{-\ell}$ is the same constant times the backward difference $c_i^{\ell-1} - c_{i-1}^{\ell-1}$; we say that limiting has been triggered for order ℓ if $\bar{c}_i^\ell \neq c_i^\ell$. The tunable constant determines the aggressiveness of the limiters and is bounded by the constant that defines a first-order-accurate finite-difference estimate of c_i^ℓ .

7.4.2 Limiting of a 1D system

To perform limiting on a 1D problem, we try to reduce it to the scalar case. A 1D hyperbolic problem is of the form

$$\partial_t \underline{u} + \partial_x \underline{f}(\underline{u}) = 0.$$

Applying the chain rule, we have

$$\partial_t \underline{u} + \underline{f}_{\underline{u}} \cdot \underline{u}_x = 0,$$

where $\underline{f}_{\underline{u}} := \partial \underline{f} / \partial \underline{u}$ is the flux Jacobian. If \underline{u} is smooth and oscillations are small, then the quasilinear ODE (7.4.2) is approximated by the linear ODE

$$\partial_t \underline{u} + \underline{\underline{A}} \cdot \underline{u}_x = 0,$$

where in a given cell we take $\underline{\underline{A}}$ to be $\underline{f}_{\underline{u}}$ evaluated at the cell average. By assumption this system is hyperbolic and therefore we can write the diagonalization

$$\underline{\underline{A}} = \underline{\underline{R}} \cdot \Lambda \cdot \underline{\underline{R}}^{-1},$$

where Λ is diagonal and real. The columns of $\underline{\underline{R}}$ are right eigenvectors and the rows of $\underline{\underline{L}}^T := \underline{\underline{R}}^{-1}$ are left eigenvectors. Multiplying equation (7.4.2) by $\underline{\underline{L}}^T$ gives

$$\partial_t \underline{v} + \Lambda \cdot \underline{v}_x = 0,$$

where the variables $\underline{v} := \underline{\underline{L}}^T \cdot \underline{u}$ are called **characteristic variables**; for smooth solution on a fine mesh this effectively decouples the PDE into scalar advection equations in the characteristic variables. We can apply 1D limiting in these variables and then transform back.

In detail, suppose the solution representation

$$\underline{U} = \sum_{\ell} \underline{U}^{\ell} \phi^{(\ell)}.$$

To get characteristic variables multiply by $\underline{\underline{L}}^T$:

$$\underline{V} = \underline{\underline{L}}^T \cdot \underline{U} = \sum_{\ell} (\underline{\underline{L}}^T \cdot \underline{U}^{\ell}) \phi^{(\ell)}.$$

We apply 1D limiters to the components $\underline{\underline{L}}^T \cdot \underline{U}^{\ell}$.

7.4.3 2D limiting for a Cartesian mesh

For a 2D Cartesian mesh we limit polynomial basis functions $\phi^{(\ell)}$ that depend only on x in each row of cells aligned with the x axis as if the problem were homogeneous perpendicular to the x axis. We do analogously for y .

For a third-order method one must also limit the coefficients of the mixed polynomial basis element xy . To limit these coefficients, we first limit in the x direction to obtain x -limited coefficients, then limit in the y direction to obtain y -limited coefficients, and then define the limited xy coefficient to be the minmod of the x -limited coefficient and the y -limited coefficient.

7.5 Positivity limiting

To guarantee positivity we use positivity limiters. Positivity limiters modify solutions which violate positivity by damping deviations from the cell average to ensure that positivity of the cell average is maintained from one time step to the next. We have applied the method of Zhang and Shu, generalized to 10-moment gas dynamics [63]. To ensure that the source term does not cause positivity violations we use time splitting and solve the source term equation exactly.

Chapter 8

Conclusions and future work

8.1 New results

This dissertation contains the following new results:

1. *Simulations of the **GEM magnetic reconnection challenge problem** with an adiabatic two-fluid model with pressure tensor evolution and isotropization.*
 - (a) Simulations of a **pair plasma** version of the GEM problem which dial the isotropization rate from zero to infinity.
 - The rate of reconnection is insensitive to the rate of isotropization and is roughly 60% of the rate of reconnection in published particle simulations.
 - For isotropic pressure the ramp-up of out-of-plane velocity at the origin with reconnecting flux is unphysical and ultimately not sustainable. For feasible convergence a small but sufficiently large viscosity must be present.
 - (b) Simulations of the GEM problem with an isotropizing pressure tensor.
 - At the time of peak reconnection rate the electron pressure tensor agrees well with published kinetic simulations and is strongly agyrotropic. The isotropization rate which yields this agreement is well below the rate for which the five- and ten-moment models agree, as would be expected in a regime that allows strong pressure anisotropy. Due to the strong pressure anisotropy at the X-point one would not expect to get this level of agreement with a viscous five-moment model, although I have not confirmed this with five-moment viscous simulations.
 - For late times and fine mesh resolution singularities develop in the adiabatic five- and ten-moment models, crashing the simulation code unless positivity limiting is enforced. This prompts the need for a ten-moment heat flux closure.
2. *A proof that **steady reconnection must be singular** for models which neglect intraspecies collisional terms when applied to problems that are invariant under 180-degree rotation about and translation along a symmetry axis.*
 - ***The Vlasov model does not admit nonsingular rotationally symmetric steady reconnection.*** The implication is that a nonzero collision operator for the kinetic equation must be specified to define a standard of truth for which converged solutions can be obtained. ***To obtained converged solutions it is not enough to say that collisions (whether particle-particle or wave-particle interactions) are present in a simulation; a nonzero collision operator must be specified (and known).*** To get converged solutions *you must know what equations you are solving and they must have a solution.*
 - This does not imply that it is necessary to have an explicit heat flux. Specifically, viscous incompressible models typically do not evolve an energy equation and can admit steady fast reconnection.

- In general we can say that use of truncation closure (for deviatoric stress or heat flux or the collision operator) results in a singularity.

3. A closure for tensor heat flux in the presence of a magnetic field.

- The closure is based on a Chapman-Enskog expansion about a Gaussian distribution of particle velocities and assumes a Gaussian-BGK collision model.
- The trace of this closure gives a closure for vector heat flux which Woods has shown agrees well with the more sophisticated closures of Braginskii and of Chapman and Cowling [62]. These more sophisticated closures assume Coulomb collision operators and define closure coefficients in terms of rational functions with higher order polynomials in the ratio $\tilde{\omega}$ of gyrofrequency to thermal relaxation rate.
- A closure for the heat flux tensor could be derived which is more accurate for Coulomb collisions. It is doubtful, however, that there is much benefit to be gained. In collisional regimes one might as well use the five-moment model. In general, extended moment modeling does not aim for high accuracy but for reasonable accuracy for the weakest possible collisionality. In the context of fast magnetic reconnection, the diffusion region is at most weakly collisional. Outside the diffusion region the pressure tensor (and thus the heat flux) does not make a significant contribution to the electric field in Ohm's law. Of course one can always cook up perfect agreement with kinetic simulations by using spatially and temporally dependent problem-specific anomalous closures, but the prospects for a generic closure with substantially improved agreement would seem not to be promising.

8.2 Questions raised

These results of this work raise the following questions for further investigation:

- *Is steady reconnection singular for truncation closure in non-symmetric 2D reconnection configurations?*

Symmetry under 180-degree rotation about the X-point is physically unlikely and unstable. The argument of section 3.4 turns on this symmetry and in particular that the stagnation point coincides with the X-point. In asymmetric reconnection these two points do not coincide [48, 47]. In simulations of reconnection, 180-degree rotational symmetry about the X-point is unstable to spontaneous symmetry-breaking.

- *Is steady reconnection singular for truncation closures for 3D reconnection? Is it possible to make a more general argument for the need for entropy production and diffusive entropy flux?*
- *What insight can be gained from a ten-moment two-fluid linear tearing analysis for weakly collisional plasma?*

How does the reconnection electric field and resistive, “viscous,” and inertial components depend on the viscosity and resistivity? Simple isotropization of the pressure tensor implies gyroviscosity already “built-in”, potentially facilitating and simplifying the linear tearing analysis developed in [45] and generalized in [28].

- *For the kinetic equation what collision operator should one specify as a standard of truth for magnetic reconnection problems?*

In current practice models used to simulation reconnection often rely on numerical diffusion and fail to admit converged reconnection. At a practical level people generally get away with it. The physical collision operator is generally unknown, and so for the purposes of validation against experiment and observed phenomena it is plausible that one might as well rely on numerical diffusivity. One can hope to get reliable results only for statistics which are insensitive to the choice of collision operator. If a statistic of interest does not change significantly as the mesh is refined then this is evidence that the statistic is insensitive to the choice of collision operator and the simulations are reasonably regarded as having physical validity.

The trouble with relying on numerical diffusivity, however, is that verification of solutions against equations is impossible because it is unknown what equations one is actually solving. It becomes impossible to quantify error.

These issues are particularly pertinent when attempting to adjudicate among models when simulations that use them disagree. The natural recourse is to refer to a modeling hierarchy and to prefer model A over model B if simulations using B differ from simulations using A and if B is a simplification of A. This heuristic can be used as a practical standard to adjudicate among any two models if all models are derived from a common ancestor, taken to be the *standard of truth*. Without a standard of truth it can become difficult or impossible to adjudicate among competing models.

The practical standard of truth in the plasma community has been PIC simulations. The natural question to ask becomes, “*What equation does a given PIC simulation solve?*” To answer this question one must consider convergence in the limit as the mesh is refined. Unless a nonzero collision operator is explicitly incorporated into the solution, one is presumably solving the Vlasov equation. The point here is that in simulating a problem one should be able to state the equations that one is solving and confirm that they actually have a solution. It is a critical result of this work that *the Vlasov equation does not admit nonsingular steady reconnection for 2D problems rotationally symmetric about the X-point*; a mechanism for entropy production is necessary. For such problems, unless an explicit nonzero collision operator is incorporated into a PIC simulation, it evidently fails to satisfy these two criteria.

For such problems, the standard of truth evidently requires specification of a nonzero collision operator, and there does not seem to be an obvious single standard of truth.

How sensitive are solutions to the choice of collision operator? What happens as one takes the collision operator to zero? The fact that steady-state solutions are singular in the absence of collisions indicates that, at least by some measure, the steady-state solution is *structurally unstable* in the limit as the collision operator goes to zero. (We say that a problem is **structurally unstable** when it depends discontinuously on the model parameters.)

Can we define a universal standard of truth using a statistical approach? In particular, can we show that for steadily driven reconnection a statistical steady state exists when the collision operator is zero? Can we study statistical steady state solutions to the Vlasov equation by defining a *stochastic collision operator* and taking it to zero? Can we define a set of statistics of interest and show that these statistics are structurally stable? If so, perhaps we can justify the use of PIC simulations for these problems without an explicit collision operator.

- *Can we formulate a fluid analog to the kinetic equation with Gaussian-BGK collision operators which allows us to study magnetic reconnection with vanishing collisionality?*

This work shows that for converged simulation of steady reconnection it is necessary to have nonzero heat flux and nonzero deviatoric pressure. Diffusive closures do not provide a way of exploring the zero-collisionality limit. The kinetic equation with a Gaussian-BGK collision operator makes it possible to study magnetic reconnection in the zero-collisionality limit, but only with great computational expense. What we seek in an extended moment fluid model is not detailed agreement but *analogous behavior* in comparison to the kinetic equation as the collision operator is taken to zero. ***We need a fluid model which evolves a heat flux tensor as well as a pressure tensor.*** With such a fluid model we can dial from infinity to zero the rate at which the heat flux tensor and deviatoric pressure tensor are relaxed to zero and gain insight into the zero-collisionality limit. A fluid model with heat flux evolution is, I propound, the Holy Grail of fluid modeling of collisionless magnetic reconnection.

Appendix A

Modeling

A.1 Maxwellian and Gaussian distributions

In this section entropy decreases, in accordance with the convention of mathematicians; that is, the definition of entropy is minus the definition of entropy elsewhere in this dissertation.

The Maxwellian and Gaussian distributions are the two working examples of Galilean-invariant *entropy-minimizing* closures for the equations of gas dynamics. The Maxwellian distribution is the assumed distribution of hyperbolic five-moment gas-dynamics (the compressible Euler equations). The Gaussian distribution is the assumed distribution of hyperbolic ten-moment gas-dynamics. A Maxwellian distribution is a normal distribution that is isotropic in the reference frame of the fluid. A Gaussian distribution is a distribution that in the reference frame of the fluid is a product of normal distributions with possibly different distribution widths in three principle orthogonal directions.

An entropy-minimizing closure (for a given set of moments) requires that particle distributions minimize entropy over all distributions which share the same given moments. Only variation in velocity is considered, not variation in space. This is consonant with the fact that collision operators ignore variation of particle density in space and only consider variation in velocity space. Thus in this document we ignore variation in space.

Definitions of conserved moments. Let $f(t, \mathbf{v})$ be the distribution of particle mass over velocity space.

$$\begin{aligned} \rho &:= \int_{\mathbf{v}} f && \text{is mass (density),} \\ \mathbf{M} &:= \int_{\mathbf{v}} f \mathbf{v} && \text{is momentum (density),} \\ \mathcal{E} &:= \int_{\mathbf{v}} f \mathbf{v}^2 / 2 && \text{is energy (density),} \\ \mathbb{E} &:= \int_{\mathbf{v}} f \mathbf{v} \mathbf{v} && \text{is energy tensor (density),} \end{aligned}$$

Definitions of statistical averages. Let $\chi(\mathbf{v})$ be a “generic” moment. Denote and define its statistical average by

$$\langle \chi \rangle := \frac{\int_{\mathbf{v}} f \chi}{\rho}.$$

Primitive variables are naturally defined in terms of statistical averages:

$$\begin{aligned} \mathbf{u} &:= \langle \mathbf{v} \rangle && \text{is bulk velocity,} \\ \mathbf{c} &:= \mathbf{v} - \mathbf{u} && \text{is thermal velocity,} \\ \Theta &:= \langle \mathbf{c} \mathbf{c} \rangle && \text{is the } \mathbf{pseudo\text{-}temperature tensor}, \text{ and} \\ \theta &:= \langle c^2 / 3 \rangle && \text{is } \mathbf{pseudo\text{-}temperature}. \end{aligned}$$

Relationships among primitive and conserved variables are

$$\begin{aligned}\rho\mathbf{u} &= \mathbf{M}, \\ \mathcal{E} &= (\rho\mathbf{u}^2 + 3\rho\theta)/2, \\ \mathbb{E} &= \rho\mathbf{u}\mathbf{u} + \rho\Theta, \\ \theta &= \text{tr } \Theta/3, \\ \mathcal{E} &= \text{tr } \mathbb{E}/3.\end{aligned}$$

Recall that entropy S is defined by

$$S := \int_{\mathbf{v}} \eta, \quad \text{where} \quad \eta := \beta f \ln f + \alpha f,$$

where $\beta > 0$ may be chosen arbitrarily for a single-species gas and where α is a constant that can be freely chosen; we will choose $\alpha = 3(\ln(2\pi) + 1)/2$ to make the formula for the gas-dynamic entropy simple. Note that

$$\eta' = \beta \ln f + (\beta + \alpha).$$

So to minimize the entropy of a single species we may conveniently choose $\eta = f \ln f - f$, for which $\eta' = \ln f$.

A.1.1 Maxwellian case

In the Maxwellian case we minimize S subject to the constraints that

$$\int_{\mathbf{v}} f = \rho, \quad \int_{\mathbf{v}} \mathbf{v}f = \mathbf{M}, \quad \int_{\mathbf{v}} \mathbf{v}^2 f = 2\mathcal{E}.$$

We use the technique of Lagrange multipliers. Define

$$g := \int_{\mathbf{v}} \eta + \lambda \left(\rho - \int_{\mathbf{v}} f \right) + \mu \cdot \left(\mathbf{M} - \int_{\mathbf{v}} \mathbf{v}f \right) + \nu \left(2\mathcal{E} - \int_{\mathbf{v}} \mathbf{v}^2 f \right).$$

Assume f minimizes entropy. Consider a perturbation $\tilde{f} = f + \epsilon f_1$. Then

$$\begin{aligned}0 = d_\epsilon g|_{\epsilon=0} &= \int_{\mathbf{v}} \eta' f_1 - \lambda \int_{\mathbf{v}} f_1 - \mu \cdot \int_{\mathbf{v}} \mathbf{v}f_1 - \nu \int_{\mathbf{v}} \mathbf{v}^2 f_1 \\ &= \int_{\mathbf{v}} f_1 \left(\ln f - \tilde{\lambda} - \mu \cdot \mathbf{v} - \nu \mathbf{v}^2 \right),\end{aligned}$$

where $\tilde{\lambda} := \lambda - \alpha - 1$. Since the integral must be zero for arbitrary perturbation f_1 the multiplier of f_1 in the integrand must be zero. Thus, f must be an exponential of an ‘‘isotropic’’ quadratic polynomial in \mathbf{v} :

$$f = \exp \left(\tilde{\lambda} + \mu \cdot \mathbf{v} + \nu \mathbf{v}^2 \right). \tag{A.1}$$

We impose the finiteness requirement that $\int_{\mathbf{v}} f < \infty$; that is, $\nu < 0$.

It remains to compute the moments of such a polynomial so that we can match them up with the constrained moments. We will show that

$$\boxed{f = f_\theta := \frac{\rho}{(2\pi\theta)^{3/2}} \exp\left(\frac{-|\mathbf{v} - \mathbf{u}|^2}{2\theta}\right)}. \quad (\text{A.2})$$

It is evident by completing the square that any exponential of a quadratic polynomial in \mathbf{v} of the form (A.1) can be put in this form. The issue is whether we indeed have that $\rho = \int_{\mathbf{v}} f$, $\rho\mathbf{u} := \int_{\mathbf{v}} \mathbf{v}f$, and $\rho\theta := \int_{\mathbf{v}} f|\mathbf{c}|^2/2$. So it remains to confirm these moments by computation.

Shifting into the reference frame of the fluid,

$$f_\theta = \frac{\rho}{(2\pi\theta)^{3/2}} \exp\left(\frac{-\mathbf{c}^2}{2\theta}\right).$$

It will be enough to show that:

$$\int_{\mathbf{c}} f_\theta = \rho, \quad \int_{\mathbf{c}} \mathbf{c}f_\theta = 0, \quad \int_{\mathbf{c}} \mathbf{c}^2 f_\theta = 3\rho\theta.$$

Recall how to integrate a Gaussian normal distribution:

$$\int_{-\infty}^{\infty} e^{-x^2/2} dx \int_{-\infty}^{\infty} e^{-y^2/2} dy = \int_0^{2\pi} \int_0^{\infty} e^{-r^2/2} r dr d\theta = 2\pi \left[e^{-r^2/2} \right]_{\infty}^0 = 2\pi,$$

so

$$\int_{-\infty}^{\infty} e^{-x^2/2} dx = \sqrt{2\pi},$$

so

$$\boxed{\int_{-\infty}^{\infty} \exp\left(\frac{-x^2}{2T}\right) dx = \sqrt{2\pi T}}.$$

The first moment is zero by even-odd symmetry:

$$\boxed{\int_{-\infty}^{\infty} x \exp\left(\frac{-x^2}{2T}\right) dx = 0}.$$

For the temperature we will need second moments. Integrating by parts,

$$\int_{-\infty}^{\infty} x^2 \exp\left(\frac{-x^2}{2}\right) dx = \int_{-\infty}^{\infty} x \left(x \exp\left(\frac{-x^2}{2}\right) \right) dx = \int_{-\infty}^{\infty} \exp\left(\frac{-x^2}{2}\right) dx = \sqrt{2\pi}. \quad (\text{A.3})$$

So

$$\boxed{\int_{-\infty}^{\infty} x^2 \exp\left(\frac{-x^2}{2T}\right) dx = T\sqrt{2\pi T}}.$$

For density we verify that

$$\int_{\mathbf{c}} \exp\left(\frac{-\mathbf{c}^2}{2\theta}\right) d^3\mathbf{c} = (2\pi\theta)^{3/2}.$$

For momentum we compute that

$$\int_{\mathbf{c}} c_1 \exp\left(\frac{-\mathbf{c}^2}{2\theta}\right) d^3\mathbf{c} = 0$$

by even/odd symmetry. For temperature we compute that

$$\int_{\mathbf{c}} c^2 \exp\left(\frac{-c^2}{2\theta}\right) = \int_{c_1} c_1^2 \exp\left(\frac{-c_1^2}{2\theta}\right) \int_{c_2} c_2^2 \exp\left(\frac{-c_2^2}{2\theta}\right) \int_{c_3} c_3^2 \exp\left(\frac{-c_3^2}{2\theta}\right) = 3\theta\sqrt{2\pi\theta}.$$

Maxwellian distributions have the property that the heat flux $\mathbf{q} := \int_{\mathbf{c}} \mathbf{c} c^2 f$ is zero. Indeed,

$$\mathbf{q} = \int_{\mathbf{c}} \mathbf{c} c^2 \exp\left(\frac{-c^2}{2\theta}\right) = 0,$$

because the integrand is odd.

A.1.2 Gaussian case

In the Gaussian case we minimize S subject to the constraints that

$$\int_{\mathbf{v}} f = \rho, \quad \int_{\mathbf{v}} \mathbf{v} f = \mathbf{M}, \quad \int_{\mathbf{v}} \mathbf{v} \mathbf{v} f = \mathbb{E}.$$

We use the technique of Lagrange multipliers. Define

$$g := \int_{\mathbf{v}} \eta + \lambda \left(\rho - \int_{\mathbf{v}} f \right) + \mu \cdot \left(\mathbf{M} - \int_{\mathbf{v}} \mathbf{v} f \right) + \nu \left(\mathbb{E} - \int_{\mathbf{v}} \mathbf{v} \mathbf{v} f \right).$$

Assume f minimizes entropy. Consider a perturbation $\tilde{f} = f + \epsilon f_1$. Then

$$\begin{aligned} 0 = d_{\epsilon} g|_{\epsilon=0} &= \int_{\mathbf{v}} \eta' f_1 - \lambda \int_{\mathbf{v}} f_1 - \mu \cdot \int_{\mathbf{v}} \mathbf{v} f_1 - \nu : \int_{\mathbf{v}} \mathbf{v} \mathbf{v} f_1 \\ &= \int_{\mathbf{v}} f_1 \left(\ln f - \tilde{\lambda} - \mu \cdot \mathbf{v} - \nu : \mathbf{v} \mathbf{v} \right). \end{aligned}$$

Since the integral must be zero for arbitrary perturbation f_1 the multiplier of f_1 in the integrand must be zero. Thus, f must be an exponential of a quadratic polynomial in \mathbf{v} :

$$f = \exp(\lambda + \mu \cdot \mathbf{v} + \nu : \mathbf{v} \mathbf{v}). \quad (\text{A.4})$$

We may require that ν is symmetric. We impose the finiteness requirement that $\int_{\mathbf{v}} f < \infty$; that is, $\nu < 0$, i.e., ν is negative definite.

We will show that

$$f = f_{\Theta} := \frac{\rho}{\sqrt{\det(2\pi\Theta)}} \exp\left(-(\mathbf{v} - \mathbf{u}) \cdot \Theta^{-1} \cdot (\mathbf{v} - \mathbf{u})/2\right).$$

That is (shifting into the reference frame of the fluid),

$$\boxed{f_{\Theta} = \frac{\rho}{\sqrt{\det(2\pi\Theta)}} \exp\left(-\mathbf{c} \cdot \Theta^{-1} \cdot \mathbf{c}/2\right)}, \quad (\text{A.5})$$

where recall that $\mathbf{c} := \mathbf{v} - \mathbf{u}$.

By substituting the expansion $(\mathbf{v} - \mathbf{u}) \cdot \Theta^{-1} \cdot (\mathbf{v} - \mathbf{u}) = \Theta^{-1} : \mathbf{v}\mathbf{v} - 2\mathbf{u} \cdot \Theta^{-1} \cdot \mathbf{v} + \mathbf{u} \cdot \Theta^{-1} \cdot \mathbf{u}$ and matching up with the terms in (A.4), it is evident that we can complete the square to put any entropy-minimizing closure in this form.

The issue is whether we indeed have that $\rho = \int_{\mathbf{v}} f_{\Theta}$, $\rho\mathbf{u} := \int_{\mathbf{v}} \mathbf{v}f_{\Theta}$, and $\rho\Theta := \int_{\mathbf{v}} f_{\Theta}\mathbf{c}\mathbf{c}$.

It will be enough to show that

$$\int_{\mathbf{c}} f_{\Theta} = \rho, \quad \int_{\mathbf{c}} \mathbf{c}f_{\Theta} = 0, \quad \int_{\mathbf{c}} \mathbf{c}\mathbf{c}f_{\Theta} = \rho\Theta.$$

Since Θ is positive definite we may choose orthogonal coordinates in which it is diagonal. So without loss of generality $\Theta = \text{diag}(\theta_1, \theta_2, \theta_3)$.

For the momentum we compute that

$$\int_{\mathbf{c}} \mathbf{c} \exp(-\mathbf{c} \cdot \Theta^{-1} \cdot \mathbf{c}/2) = 0$$

because the integrand is odd. For the density we compute that

$$\begin{aligned} & \int_{\mathbf{c}} \exp(-\mathbf{c} \cdot \Theta^{-1} \cdot \mathbf{c}/2) \\ &= \int_{c_1} \exp\left(\frac{-c_1^2}{2\theta_1}\right) \int_{c_2} \exp\left(\frac{-c_2^2}{2\theta_2}\right) \int_{c_3} \exp\left(\frac{-c_3^2}{2\theta_3}\right) \\ &= \sqrt{2\pi\theta_1} \sqrt{2\pi\theta_2} \sqrt{2\pi\theta_3} \\ &= \sqrt{\det(2\pi\Theta)}. \end{aligned}$$

For the temperature we compute that

$$\begin{aligned} & \int_{\mathbf{c}} c_1^2 \exp(-\mathbf{c} \cdot \Theta^{-1} \cdot \mathbf{c}/2) \\ &= \int_{c_1} c_1^2 \exp\left(\frac{-c_1^2}{2\theta_1}\right) \int_{c_2} \exp\left(\frac{-c_2^2}{2\theta_2}\right) \int_{c_3} \exp\left(\frac{-c_3^2}{2\theta_3}\right) \\ &= \theta_1 \sqrt{2\pi\theta_1} \sqrt{2\pi\theta_2} \sqrt{2\pi\theta_3} \\ &= \theta_1 \sqrt{\det(2\pi\Theta)} \end{aligned}$$

and that

$$\begin{aligned} & \int_{\mathbf{c}} c_1 c_2 \exp(-\mathbf{c} \cdot \Theta^{-1} \cdot \mathbf{c}/2) \\ &= \int_{c_1} c_1 \exp\left(\frac{-c_1^2}{2\theta_1}\right) \int_{c_2} c_2 \exp\left(\frac{-c_2^2}{2\theta_2}\right) \int_{c_3} \exp\left(\frac{-c_3^2}{2\theta_3}\right) \\ &= 0. \end{aligned}$$

Third-order moments

Gaussian distributions have the property that the heat flux tensor $\mathbf{q} := \int_{\mathbf{c}} \mathbf{c}\mathbf{c}\mathbf{c}f_{\Theta}$ is zero (because for any component at least one of the three independent integrals has an odd integrand).

Fourth-order moments

Fourth-order moments are needed in computing heat flux closure with a Chapman-Enskog expansion.

This requires computing the fourth moment of a normal distribution. Integrating by parts,

$$\int_{-\infty}^{\infty} x^4 \exp\left(\frac{-x^2}{2}\right) dx = \int_{-\infty}^{\infty} x^3 \left(x \exp\left(\frac{-x^2}{2}\right)\right) dx = \int_{-\infty}^{\infty} 3x^2 \exp\left(\frac{-x^2}{2}\right) dx = 3\sqrt{2\pi}$$

by (A.3). Thus,

$$\int_{-\infty}^{\infty} x^4 \exp\left(\frac{-x^2}{2T}\right) dx = 3T^2\sqrt{2\pi T}.$$

Representative nonvanishing fourth moments of the Gaussian distribution are

$$\begin{aligned} & \int_{\mathbf{c}} c_1^4 \exp(-\mathbf{c} \cdot \Theta^{-1} \cdot \mathbf{c}/2) \\ &= \int_{c_1} c_1^4 \exp\left(\frac{-c_1^2}{2\theta_1}\right) \int_{c_2} \exp\left(\frac{-c_2^2}{2\theta_2}\right) \int_{c_3} \exp\left(\frac{-c_3^2}{2\theta_3}\right) \\ &= 3\theta_1^2 \sqrt{2\pi\theta_1} \sqrt{2\pi\theta_2} \sqrt{2\pi\theta_3} \\ &= 3\theta_1^2 \sqrt{\det(2\pi\Theta)} \end{aligned}$$

and

$$\begin{aligned} & \int_{\mathbf{c}} c_1^2 c_2^2 \exp(-\mathbf{c} \cdot \Theta^{-1} \cdot \mathbf{c}/2) \\ &= \int_{c_1} c_1^2 \exp\left(\frac{-c_1^2}{2\theta_1}\right) \int_{c_2} c_2^2 \exp\left(\frac{-c_2^2}{2\theta_2}\right) \int_{c_3} \exp\left(\frac{-c_3^2}{2\theta_3}\right) \\ &= \theta_1 \sqrt{2\pi\theta_1} \theta_2 \sqrt{2\pi\theta_2} \sqrt{2\pi\theta_3} \\ &= \theta_1 \theta_2 \sqrt{\det(2\pi\Theta)}. \end{aligned}$$

So we have shown that if Θ is diagonalized along the principal axes then (for a Gaussian distribution) $\langle \mathbf{c}_1 \mathbf{c}_1 \mathbf{c}_1 \mathbf{c}_1 \rangle = 3\Theta_{11}^2$ and $\langle \mathbf{c}_1 \mathbf{c}_1 \mathbf{c}_2 \mathbf{c}_2 \rangle = \Theta_{11}\Theta_{22}$. These two representative moments imply that

$$\langle \mathbf{c} \mathbf{c} \mathbf{c} \mathbf{c} \rangle = \text{Sym}3(\Theta\Theta)$$

for a Gaussian distribution. That is,

$$\boxed{\int_{\mathbf{c}} \mathbf{c} \mathbf{c} \mathbf{c} \mathbf{c} f_{\Theta} = \text{Sym}3(\mathbb{P}\mathbb{P})/\rho}. \quad (\text{A.6})$$

A.1.3 Expressions for entropy

Now that we have found the distribution that minimizes entropy, what is the entropy?

Recall the Gaussian distribution,

$$\mathcal{G} = \frac{\rho}{\sqrt{\det(2\pi\Theta)}} \exp\left(\frac{-\mathbf{c} \cdot \Theta^{-1} \cdot \mathbf{c}}{2}\right).$$

By definition the entropy of the Gaussian distribution is

$$S = \int_{\mathbf{c}} \mathcal{G} \ln \mathcal{G} + \alpha \mathcal{G}.$$

By definition,

$$\int_{\mathbf{c}} \mathcal{G} = \rho.$$

Observe that

$$\ln \mathcal{G} = \ln \left(\frac{\rho}{\sqrt{\det(2\pi\Theta)}} \right) + \frac{-\mathbf{c} \cdot \Theta^{-1} \cdot \mathbf{c}}{2}.$$

To compute $\int_{\mathbf{c}} \mathcal{G} \ln \mathcal{G}$ the main result we need is:

$$\int_{\mathbf{c}} (\mathbf{c} \cdot \Theta^{-1} \cdot \mathbf{c}) \mathcal{G} = 3\rho.$$

To verify this claim, choose coordinates in which Θ is diagonal. By definition of θ_i ,

$$\int_{\mathbf{c}} (c_i)^2 \mathcal{G} = \theta_i \rho, \quad \text{i.e.,} \quad \int_{\mathbf{c}} (c_i \theta_i^{-1} c_i) \mathcal{G} = \rho.$$

Summing over all three dimensions yields the claim.

We now compute the entropy:

$$\begin{aligned} S &= \int_{\mathbf{c}} \mathcal{G} \ln \mathcal{G} + \alpha \mathcal{G} \\ &= \rho \ln \left(\frac{\rho}{\sqrt{\det(2\pi\Theta)}} \right) - \frac{3}{2} \rho + \alpha \rho. \\ &= -\rho \ln \left(\frac{\sqrt{\det(\Theta)}}{\rho} \right) + \rho \left(\alpha - \frac{3}{2} - \frac{3}{2} \ln(2\pi) \right). \end{aligned}$$

That is,

$$\boxed{S = -\rho \ln \left(\frac{\sqrt{\det(\Theta)}}{\rho} \right)}$$

if we choose $\alpha = 3(1 + \ln(2\pi))/2$.

The five-moment formula is a special case:

$$\boxed{S = -\rho \ln \left(\frac{\theta^{3/2}}{\rho} \right)}.$$

A.1.4 Number density

Hitherto f has represented mass density. Let \tilde{f} denote particle number density. Then $\tilde{f} = f/m$, where m is particle mass. We define $n := \int_{\mathbf{v}} \tilde{f} = \rho/m$ to be the number density. So the expression (A.2) for the 5-moment distribution becomes

$$\tilde{\mathcal{G}} = \frac{n}{(2\pi\theta)^{3/2}} \exp\left(\frac{-|\mathbf{v} - \mathbf{u}|^2}{2\theta}\right)$$

and the expression A.5 for the 10-moment distribution becomes

$$\tilde{\mathcal{G}} = \frac{n}{\sqrt{\det(2\pi\Theta)}} \exp\left(\frac{-\mathbf{c} \cdot \Theta^{-1} \cdot \mathbf{c}}{2}\right). \quad (\text{A.7})$$

The true temperature $T = m\langle \mathbf{c}^2 \rangle/3$ is related to the scalar pressure $p = \rho\langle \mathbf{c}^2 \rangle/3$ and to the pseudo-temperature $\theta := \langle \mathbf{c}^2 \rangle/3$ by the relations

$$nT = p = \rho\theta, \quad \text{i.e.,} \quad \theta = T/m.$$

The true temperature tensor $\mathbb{T} := m\langle \mathbf{c}\mathbf{c} \rangle$ is related to the pressure tensor $\mathbb{P} = \rho\langle \mathbf{c}\mathbf{c} \rangle$ and to the pseudo temperature tensor $\Theta := \langle \mathbf{c}\mathbf{c} \rangle$ by the relations

$$n\mathbb{T} = \mathbb{P} = \rho\Theta, \quad \text{i.e.,} \quad \Theta = \mathbb{T}/m.$$

Note that

$$\langle \chi \rangle = \frac{\int_{\mathbf{v}} f\chi}{\rho} = \frac{\int_{\mathbf{v}} \tilde{f}\chi}{n}.$$

A.1.5 Consistent entropy for interacting species

For a gas with multiple species we should define the entropy of each species consistently so that the total entropy obeys an entropy inequality when species interact. For such a consistent entropy we define the true entropy of each species in terms of the number density rather than the mass density:

$$\tilde{S} := \int_{\mathbf{v}} \tilde{\eta}, \quad \text{where} \quad \tilde{\eta} := \tilde{f} \ln \tilde{f} + \tilde{\alpha} \tilde{f}.$$

In the remainder of this section the casual reader may regard factors involving α or $\tilde{\alpha}$ (cyan text) as an arbitrary irrelevant constant. Since $\tilde{f} = m^{-1}f$,

$$\begin{aligned} \tilde{\eta} &= \tilde{f} \ln(m^{-1}f) + \tilde{\alpha} \tilde{f} \\ &= m^{-1}\eta + (\ln m^{-1} + \tilde{\alpha} - \alpha)\tilde{f}. \end{aligned}$$

So

$$\begin{aligned} \tilde{S} &= \int_{\mathbf{v}} \tilde{\eta} = \int_{\mathbf{v}} m^{-1}\eta + (\ln m^{-1} + \tilde{\alpha} - \alpha)\tilde{f} \\ &= m^{-1}S + (\ln m^{-1} + \tilde{\alpha} - \alpha)n. \end{aligned}$$

Recall that for $f = \mathcal{G}$,

$$S = -\rho \ln \left(\frac{\sqrt{\det(\Theta)}}{\rho} \right) + \rho \left(\alpha - \frac{3}{2} - \frac{3}{2} \ln(2\pi) \right).$$

So for $\tilde{f} = \tilde{\mathcal{G}}$,

$$\begin{aligned} \tilde{S} &= -n \ln \left(\frac{\sqrt{\det(\Theta)}}{\rho} \right) + n \left(\alpha - \frac{3}{2} - \frac{3}{2} \ln(2\pi) \right) \\ &\quad + n(\ln m^{-1} + \tilde{\alpha} - \alpha) \\ &= -n \ln \left(\frac{\sqrt{\det(\mathbb{T})}}{n} \right) \\ &\quad + n \left(\tilde{\alpha} + \frac{3}{2} \ln m - \frac{3}{2} - \frac{3}{2} \ln(2\pi) \right). \end{aligned}$$

In summary, the **ten-moment gas-dynamic entropy**, defined to be the entropy that the distribution would have if it were relaxed to minimum entropy subject to the constraint that all moments of order two or lower are conserved, may be consistently defined to be

$$\boxed{S_{\mathcal{G}} = -n \ln \left(\frac{\sqrt{\det(\mathbb{T})}}{n} \right)}, \quad (\text{A.8})$$

where we have chosen $\tilde{\alpha} = \frac{3}{2} (1 + \ln(2\pi/m))$.

The **five-moment gas-dynamic entropy**, defined to be the entropy that the distribution would have if it were relaxed to minimum entropy subject to the constraint that all conserved moments are conserved, is a special case and may be consistently defined to be

$$\boxed{S_{\mathcal{M}} = -n \ln \left(\frac{T^{3/2}}{n} \right)}. \quad (\text{A.9})$$

A.2 Collisionless Nondimensionalization

Physical constants that define an ion-electron plasma are:

1. e , the magnitude of the charge of an electron,
2. m_i, m_e , the ion and electron mass, and
3. c , the speed of light.

Three fundamental parameters that characterize the state of a plasma are:

1. n_0 , a typical particle density,
2. T_0 , a typical temperature (often per species), and
3. B_0 , a typical magnetic field strength.

In quasineutral equilibrium we can take $n_0 = n_i = n_e$ and $T_0 = T_i = T_e$. The thermal pressure is $p_0 := n_0 T_0$ and the magnetic pressure is $p_B := \frac{B_0^2}{2\mu_0}$.

Subsidiary space, time, and velocity scale parameters derived from the fundamental parameters are

$$\begin{aligned}
\text{gyrofrequencies: } \omega_{g,s} &:= \frac{eB_0}{m_s}, \\
\text{plasma frequencies: } \omega_{p,s}^2 &:= \frac{n_0 e^2}{\epsilon_0 m_s}, \\
\text{Alfvén speeds: } v_{A,s}^2 &:= \frac{B_0^2}{\mu_0 m_s n_0} = \frac{2p_B}{\rho_s}, \\
\text{thermal velocities: } v_{t,s}^2 &:= \frac{T_s}{m_s} = \frac{p_s}{\rho_s}, \quad \tilde{v}_{t,s}^2 := 2v_{t,s}^2, \\
\text{gyroradii: } r_{g,s} &:= \frac{v_{t,s}}{\omega_{g,s}} = \frac{m_s v_{t,s}}{eB_0}, \quad \tilde{r}_{g,s} := \frac{\tilde{v}_{t,s}}{\omega_{g,s}}, \\
\text{Debye length: } \lambda_D^2 &:= \left(\frac{v_{t,s}}{\omega_{p,s}} \right)^2 = \frac{\epsilon_0 T_0}{n_0 e^2}, \\
\text{inertial lengths: } \delta_s^2 &:= \left(\frac{c}{\omega_{p,s}} \right)^2 = \left(\frac{v_{A,s}}{\omega_{g,s}} \right)^2 = \frac{m_s}{\mu_0 n_s e^2};
\end{aligned}$$

the inertial length is also called the **skin depth**. Nondimensional parameters for the bulk fluid of a two-species quasi-neutral fluid are

$$\begin{aligned}
\text{plasma frequency: } \omega_p^2 &:= \omega_{pe}^2 + \omega_{pi}^2, \\
\text{Alfvén speed: } v_A^2 &:= \frac{B_0^2}{\mu_0 \rho} = \frac{2p_B}{\rho}, \\
\text{thermal velocity: } v_t^2 &:= \mathbf{v}_{t,i}^2 + \mathbf{v}_{t,e}^2 = \frac{T}{\tilde{\mu}}, \quad \tilde{v}_t^2 := 2v_t^2, \\
\text{inertial length: } \delta^2 &:= \delta_i^2 + \delta_e^2.
\end{aligned}$$

Note that *[(most?)]* often in the literature the thermal velocity is defined as $\tilde{v}_{t,s}$ rather than $v_{t,s}$. We say that two parameters are *equivalent* if one is a constant multiple of the other. For example, the thermal velocities are equivalent to one another and to the sound speed $\sqrt{\frac{\gamma p_0}{\rho_0}}$. Important nondimensional ratios are the **plasma beta** $\beta := \frac{p_0}{p_B}$ and the ratio of the speed of light to the Alfvén speed. Other nondimensional ratios can be defined in terms of these ratios:

$$\begin{aligned}
\text{plasma } \beta : \quad \beta &:= \frac{p_0}{p_B} = \left(\frac{\tilde{v}_{t,s}}{v_{A,s}} \right)^2 = \left(\frac{\tilde{r}_{g,s}}{\delta_s} \right)^2, \\
\text{[unnamed?]} : \quad \frac{c}{v_{A,s}} &= \frac{r_{g,s}}{\lambda_D} = \frac{\omega_{p,s}}{\omega_{g,s}}.
\end{aligned}$$

The subsidiary parameters (except for the temperature-related parameters $v_{t,s}$ and λ_D) emerge from a generic nondimensionalization of the particle (or Vlasov or 2-fluid) equations.

Choose values for:

| | | |
|-----------|------------------|--|
| t_0 | (time scale) | (e.g. ion gyroperiod $1/\omega_{g,i}$), |
| x_0 | (space scale) | (e.g. ion skin depth δ_i), |
| m_0 | (mass scale) | (e.g. ion mass m_i), |
| $e = q_0$ | (charge scale) | (e.g. ion charge e), |
| B_0 | (magnetic field) | (e.g. $\omega_{g,i}m_i/e$), and |
| n_0 | (number density) | (e.g. something $\gg 1/x_0^3$). |

This implies typical values for:

$$\begin{aligned}
v_0 &= x_0/t_0 && \text{(velocity),} \\
E_0 &= B_0v_0 && \text{(electric field),} \\
\sigma_0 &= en_0 && \text{(charge density),} \\
J_0 &= en_0v_0 && \text{(current density), and} \\
S_0 &= n_0 && \text{(no. particles per unit number density).}
\end{aligned}$$

Making the substitutions

$$\begin{aligned}
t &= \tilde{t}t_0, & \mathbf{E} &= \tilde{\mathbf{E}}B_0v_0, \\
\mathbf{x} &= \tilde{\mathbf{x}}x_0, & \sigma &= \tilde{\sigma}en_0, \\
q &= \tilde{q}e, & \mathbf{J} &= \tilde{\mathbf{J}}en_0v_0, \\
m &= \tilde{m}m_0, & S_p(\mathbf{x}_p) &= \tilde{S}_p(\tilde{\mathbf{x}}_p)n_0, \\
n &= \tilde{n}n_0, & c &= \tilde{c}v_0, \\
\mathbf{B} &= \tilde{\mathbf{B}}B_0, & \mathbf{v} &= \tilde{\mathbf{v}}v_0
\end{aligned}$$

in the fundamental equations

$$\begin{aligned}
\partial_t \mathbf{B} &= -\nabla_{\mathbf{x}} \times \mathbf{E}, & \nabla_{\mathbf{x}} \cdot \mathbf{B} &= 0, \\
\partial_t \mathbf{E} &= c^2 \nabla_{\mathbf{x}} \times \mathbf{B} - \mathbf{J}/\epsilon_0, & \nabla_{\mathbf{x}} \cdot \mathbf{E} &= \sigma/\epsilon_0, \\
\mathbf{J} &= \sum_p S_p(\mathbf{x}_p)q_p \mathbf{v}_p, & \sigma &= \sum_p S_p(\mathbf{x}_p)q_p,
\end{aligned}$$

and

$$d_t(\gamma \mathbf{v}_p) = \frac{q_p}{m_p} \left(\mathbf{E}(\mathbf{x}_p) + \mathbf{v}_p \times \mathbf{B}(\mathbf{x}_p) \right), \quad d_t \mathbf{x}_p = \mathbf{v}_p$$

gives the almost identical-appearing nondimensionalized system

$$\begin{aligned}
\partial_{\tilde{t}} \tilde{\mathbf{B}} &= -\nabla_{\tilde{\mathbf{x}}} \times \tilde{\mathbf{E}}, & \nabla_{\tilde{\mathbf{x}}} \cdot \tilde{\mathbf{B}} &= 0, \\
\partial_{\tilde{t}} \tilde{\mathbf{E}} &= \tilde{c}^2 \nabla_{\tilde{\mathbf{x}}} \times \tilde{\mathbf{B}} - \tilde{\mathbf{J}}/\tilde{\epsilon}, & \nabla_{\tilde{\mathbf{x}}} \cdot \tilde{\mathbf{E}} &= \tilde{\sigma}/\tilde{\epsilon}, \\
\tilde{\mathbf{J}} &= \sum_p \tilde{S}_p(\tilde{\mathbf{x}}_p) \tilde{q}_p \tilde{\mathbf{v}}_p, & \tilde{\sigma} &= \sum_p \tilde{S}_p(\tilde{\mathbf{x}}_p) \tilde{q}_p,
\end{aligned}$$

and

$$d_{\tilde{t}}(\gamma \tilde{\mathbf{v}}_p) = (t_0 \omega_g) \frac{\tilde{q}_p}{\tilde{m}_p} \left(\tilde{\mathbf{E}}(\tilde{\mathbf{x}}_p) + \tilde{\mathbf{v}}_p \times \tilde{\mathbf{B}}(\tilde{\mathbf{x}}_p) \right), \quad d_{\tilde{t}} \tilde{\mathbf{x}}_p = \tilde{\mathbf{v}}_p;$$

here $(t_0\omega_g) = t_0 \frac{q_0 B_0}{m_0}$ is the gyrofrequency nondimensionalized by a choice of t_0 (which can be chosen to be the gyroperiod in order to set this factor to unity) and

$$\frac{1}{\epsilon} = \frac{x_0 n_0 e}{v_0 B_0 \epsilon_0} = t_0 \frac{e B_0}{m_0} \frac{\mu_0 m_0 n_0}{B_0^2} c^2 = (t_0 \omega_g) \left(\frac{c}{v_A} \right)^2.$$

Note that we can also write $(t_0 \omega_g) = \frac{x_0}{r_g}$.

It is desirable to make the nondimensionalized system look exactly like the original system; in this way we can take any formula derived from the original system and interpret it as a nondimensional formula. If the gyrofrequency is not chosen to be the gyroperiod one can still accomplish this by absorbing the factor $(t_0 \omega_g)$ into the electromagnetic field and the definition of ϵ^{-1} .

A.3 Knudsen Number

A.4 Prandtl Number

The *Prandtl number* Pr of a gas (unmagnetized) is the rate of momentum diffusion divided by the rate of temperature diffusion for small perturbations from a global equilibrium. To obtain an expression for the Prandtl number we need evolution equations for the momentum and temperature.

Since perturbations from equilibrium are small, we can make simplifying approximating assumptions. In particular, the pressure is assumed constant and for the momentum equation the flow is assumed approximately incompressible. Near a Maxwellian linearized entropy-respecting closures are justified.

A.4.1 Rate of momentum diffusion

To calculate the rate of momentum diffusion we use the Stokes closure, derived in section 2.5.1, for the momentum evolution equation (2.8), which we here write in the form

$$\rho d_t \mathbf{u} + \nabla p = \nabla \cdot \boldsymbol{\sigma}^\circ; \tag{A.10}$$

here $\boldsymbol{\sigma} = -\mathbb{P}$ is the stress tensor and $\boldsymbol{\sigma}^\circ = -\mathbb{P}^\circ = -(\mathbb{P} - p \mathbb{1})$ is its deviatoric part, also called the viscous stress tensor. The Stokes closure (2.29) says that

$$\boldsymbol{\sigma}^\circ = 2\mu \mathbf{e}^\circ,$$

where μ is the viscosity coefficient and $\mathbf{e} = \text{Sym}(\nabla \mathbf{u})$ is the strain rate tensor and $\mathbf{e}^\circ = \text{Sym}(\nabla \mathbf{u} - \nabla \cdot \mathbf{u} \mathbb{1} / 3)$ is its deviatoric part. Assuming constant pressure ($\nabla p = 0$) and incompressible flow ($\nabla \cdot \mathbf{u} = 0$), the momentum equation simplifies to

$$d_t \mathbf{u} = \nu \nabla^2 \mathbf{u}, \tag{A.11}$$

where $\nu := \frac{\mu}{\rho}$, the **kinematic viscosity**, is the rate of momentum diffusion.

A.4.2 Rate of temperature diffusion

To calculate the rate of temperature diffusion we derive a temperature evolution equation. Rather than begin with the temperature evolution equation (2.17), which assumes that molecules have no internal energy modes, only translational modes, we begin with scalar energy balance (2.11) in the form

$$\rho d_t(e_{\text{int}} + |\mathbf{u}|^2/2) + \nabla \cdot (\mathbf{u}p) + \nabla \cdot \mathbf{q} = \nabla \cdot (\mathbf{u} \cdot \boldsymbol{\sigma}^\circ), \quad (\text{A.12})$$

where e_{int} is the internal (nontranslational) energy per mass. Dotting \mathbf{u} with the momentum evolution equation (A.10) gives the kinetic energy evolution equation

$$\rho d_t|\mathbf{u}|^2/2 + \mathbf{u} \cdot \nabla p + \nabla \cdot \mathbf{q} = \boldsymbol{\sigma}^\circ : \nabla \mathbf{u};$$

subtracting this from energy evolution (A.13) gives thermal energy evolution

$$\rho d_t e_{\text{int}} + p \nabla \cdot \mathbf{u} + \nabla \cdot \mathbf{q} = \boldsymbol{\sigma}^\circ : \nabla \mathbf{u}. \quad (\text{A.13})$$

Assume the classical thermodynamic relations for an ideal gas,

$$p = \rho RT, \quad \text{and} \quad e_{\text{int}} = c_v T,$$

where R is the gas constant (equal to $1/m$ for a gas with a single species of particle with particle mass m) and c_v is the heat capacity at constant volume. Assume the linear heat flux closure $\mathbf{q} = -k \nabla T$, in accordance with equation (2.24). Assume that k is constant. (In fact k is a function of temperature, which is approximately constant.) Neglect viscous heat production $\boldsymbol{\sigma}^\circ : \nabla \mathbf{u}$. Assume that the pressure p is constant. (So we do *not* assume that $\nabla \cdot \mathbf{u} = 0$.) Then $p = \rho RT$ says that ρT is constant, so $p \nabla \cdot \mathbf{u} = -\rho d_t \ln \rho = \rho d_t \ln T = \rho R d_t T$, so thermal energy evolution (A.13) reduces to

$$\rho c_v d_t T + \rho R d_t T = k \nabla^2 T,$$

that is,

$$d_t T = \kappa \nabla^2 T, \quad (\text{A.14})$$

where $\kappa := \frac{k}{\rho c_p}$, the thermal conductivity, is the rate of temperature diffusion and $c_p := c_v + R$ is the heat capacity at constant pressure.

A.4.3 Formula for the Prandtl number

Putting the results of equations (A.11) and (A.14) together, the *Prandtl number* is

$$\boxed{\text{Pr} = \frac{\nu}{\kappa} = \frac{c_p \mu}{k} = \frac{\gamma}{\gamma - 1} \frac{R \mu}{k}},$$

where $\gamma := c_p/c_v$ is the **adiabatic index**; that is,

$$\text{Pr} = \frac{\gamma}{\gamma - 1} \frac{\mu}{mk}$$

for an ideal gas. For a monatomic gas, $\gamma - 1 = R/c_v = 2/3$, $\gamma = 5/3$, and

$$\text{Pr} = \frac{5}{2} \frac{\mu}{mk}, \quad (\text{A.15})$$

which is the formula assumed in this dissertation.

A.5 Explicit closures

In this section we work out explicit five-moment closures for the heat flux and viscosity and an explicit ten-moment closure for the heat flux tensor beginning with the implicit closures obtained in section 2.6.

A.5.1 Splice tensor operators

To solve these equations, it will be convenient to define **splice tensor operations** which operate on tensors with an even number of indices. To define these operators, for a given tensor we partition the indices into the initial half and the final half and pair corresponding indices in the initial and final half, like this:

$$A_{i_1 i_2 \dots i_m | j_1 j_2 \dots j_m};$$

as here, for clarity we sometimes insert the symbol $|$ to separate the initial and final half of the indices of a tensor. Splice operators do exactly the same thing to the initial indices and final indices and can be thought of as operating on pairs of indices. An identity in terms of splice operators becomes an identity in terms of standard tensor operators if you replace splice operators with their corresponding standard tensor operators and delete the initial half (or the final half) of the indices of each tensor. For a given ordinary tensor operator (e.g. \otimes) we denote its splice operator equivalent with a superior tilde symbol (e.g. $\tilde{\otimes}$). Examples of splice products for simple cases are

$$(A\tilde{\otimes}B)_{ijkl} = A_{ik}B_{jl} \quad \text{and} \quad (K\tilde{\otimes}L)_{ij_1j_2kl_1l_2} = K_{ik}L_{j_1j_2l_1l_2}.$$

So in general the splice tensor product $\tilde{\otimes}$ is defined by

$$(K\tilde{\otimes}L)_{i_1 \dots i_m j_1 \dots j_n | k_1 \dots k_m l_1 \dots l_n} = K_{i_1 \dots i_m | k_1 \dots k_m} L_{j_1 \dots j_n | l_1 \dots l_n}.$$

Recall that we define the symmetric tensor product by $A \vee B := \text{Sym}(A \otimes B)$, where Sym averages over all permutations of its argument tensor. Similarly, we define a **splice symmetric tensor product** $\tilde{\vee}$ by

$$A\tilde{\vee}B = \widetilde{\text{Sym}}(A\tilde{\otimes}B),$$

where $\widetilde{\text{Sym}}$ averages over all permutations which permute the initial half of the indices and the final half of the indices in exactly the same manner.

In this section all tensors will be of even order and will be built from splice symmetric products of second-order tensors exactly as one can build standard symmetric tensors from symmetric products of vectors. Elsewhere in this dissertation the default product of tensors is the simple tensor product \otimes , but **in this section we will take the default tensor product to be the splice symmetric product** $\tilde{\vee}$, and when we wish to denote the splice symmetric product explicitly we will write it simply as \emptyset rather than $\tilde{\vee}$. Let A , B , and C be second-order tensors.

Examples of splice symmetric products are $2AB = A\tilde{\otimes}B + B\tilde{\otimes}A$ and

$$3!ABC = A\tilde{\otimes}B\tilde{\otimes}C + A\tilde{\otimes}C\tilde{\otimes}B + B\tilde{\otimes}A\tilde{\otimes}C + B\tilde{\otimes}C\tilde{\otimes}A + C\tilde{\otimes}A\tilde{\otimes}B + C\tilde{\otimes}B\tilde{\otimes}A.$$

A.5.2 Gyrotropic tensors

For ease on the eyes, in this section we use $\boldsymbol{\delta} := \mathbf{1}$ for the identity matrix. (Its components are given by the Kronecker delta.) We will build gyrotropic basis tensors by splice symmetric products of the following fundamental gyrotropic tensors:

$$\begin{aligned}\wedge &:= \boldsymbol{\delta}_\wedge := \mathbf{b} \times \boldsymbol{\delta} = \boldsymbol{\delta} \times \mathbf{b}, \\ \parallel &:= \boldsymbol{\delta}_\parallel := \mathbf{b}\mathbf{b}, \\ \perp &:= \boldsymbol{\delta}_\perp := \boldsymbol{\delta} - \boldsymbol{\delta}_\parallel.\end{aligned}$$

I remark that this does not generate a basis that spans all gyrotropic tensors — for that we would need to take ordinary tensor products and splice products — but we will see that it does generate exactly the basis needed to solve our implicit closures for the unknown.

Under the operation of matrix multiplication the fundamental gyrotropic tensors plus the zero tensor plus $\boldsymbol{\delta}$ are a commutative subring with unity with the following multiplication table:

| | | | | |
|-------------|----------|----------|-------------|--|
| \cdot | \wedge | \perp | \parallel | |
| \wedge | $-\perp$ | \wedge | 0 | |
| \perp | \wedge | \perp | 0 | |
| \parallel | 0 | 0 | \parallel | |

(A.16)

In particular, we will use the following mappings:

| | | | |
|-------------|------------------|-------------------------------|--|
| M | $\wedge \cdot M$ | $\boldsymbol{\delta} \cdot M$ | |
| \wedge | $-\perp$ | \wedge | |
| \perp | \wedge | \perp | |
| \parallel | 0 | \parallel | |

(A.17)

A.5.3 Gyrotropic linear operators on symmetric matrices

Splice symmetric products allow us to express gyrotropic linear operators on symmetric matrices.

Recall that matrices are a group under the multiplication \cdot . Fourth-order tensors are a group under the multiplication \vdots and sixth-order tensors are a group under the multiplication \vdots .

Just as $\boldsymbol{\delta}$ is the identity matrix, the tensor $\boldsymbol{\delta}\boldsymbol{\delta} = \boldsymbol{\delta} \tilde{\otimes} \boldsymbol{\delta}$ acts as the identity tensor on second-order tensors and $\boldsymbol{\delta}\boldsymbol{\delta}\boldsymbol{\delta} = \boldsymbol{\delta} \tilde{\otimes} \boldsymbol{\delta} \tilde{\otimes} \boldsymbol{\delta}$ acts as the identity tensor on third-order tensors:

$$\boldsymbol{\delta}\boldsymbol{\delta} : \underline{\underline{A}} = \underline{\underline{A}}, \quad \text{and} \quad \boldsymbol{\delta}\boldsymbol{\delta}\boldsymbol{\delta} : \underline{\underline{\underline{A}}} = \underline{\underline{\underline{A}}},$$

Recall that any linear transformation on vectors (first-order tensors) has a matrix (second-order tensor) $\underline{\underline{M}}$ which represents it by $\underline{V} \mapsto \underline{\underline{M}} \cdot \underline{V}$ and a unique inverse matrix $\underline{\underline{M}}^{-1}$ satisfying $\underline{\underline{M}}^{-1} \cdot \underline{\underline{M}} = \boldsymbol{\delta} = \underline{\underline{M}} \cdot \underline{\underline{M}}^{-1}$. Likewise, any linear transformation on second-order tensors has a “second-order matrix” (fourth-order tensor) $M_{[2]}$ which represents it by $V_{[2]} \mapsto M_{[2]} \vdots V_{[2]}$ and a unique inverse $M_{[2]}^{-1}$ satisfying $M_{[2]}^{-1} \vdots M_{[2]} = \boldsymbol{\delta}\boldsymbol{\delta} = M_{[2]} \vdots M_{[2]}^{-1}$, and any linear transformation on third-order tensors has a “third-order matrix” (sixth-order tensor) $M_{[3]}$ which represents it by $V_{[3]} \mapsto M_{[3]} \vdots V_{[3]}$, and a unique inverse $M_{[3]}^{-1}$ satisfying $M_{[3]}^{-1} \vdots M_{[3]} = \boldsymbol{\delta}\boldsymbol{\delta}\boldsymbol{\delta} = M_{[3]} \vdots M_{[3]}^{-1}$.

A.5.4 Implicit closures in splice product form

The implicit closures obtained in section 2.6 assuming a Gaussian-BGK collision operator and using a Chapman-Enskog expansion were equation (2.71)

$$\mathbf{q} + \tilde{\varpi} \mathbf{b} \times \mathbf{q} = -k \nabla T \quad (\text{A.18})$$

for the heat flux, equation (2.65)

$$\mathbb{P}^\circ + \text{Sym}2(\varpi \mathbf{b} \times \mathbb{P}^\circ) = -\mu 2 \mathbf{e}^\circ \quad (\text{A.19})$$

for the deviatoric stress, and equation (2.69)

$$\mathbf{q} + \text{Sym}3(\tilde{\varpi} \mathbf{b} \times \mathbf{q}) = -\frac{2}{5} k \text{Sym}3(\boldsymbol{\pi} \cdot \nabla \mathbb{T}) \quad (\text{A.20})$$

for the heat flux tensor.

Since we will solve each of these equations individually, we will neglect the distinction between $\tilde{\varpi}$ and ϖ that arises when $\text{Pr} \neq 1$ and will simply write ϖ for both.

Using that $\text{Sym}2(\mathbf{b} \times \mathbb{P}^\circ) = \text{Sym}2(\boldsymbol{\wedge} \cdot \mathbb{P}^\circ) = \text{Sym}2(\boldsymbol{\wedge} \cdot \mathbb{P}^\circ \cdot \boldsymbol{\delta}) = \text{Sym}2(\boldsymbol{\wedge} \tilde{\otimes} \boldsymbol{\delta} : \mathbb{P}^\circ) = 2 \boldsymbol{\wedge} \boldsymbol{\delta} : \mathbb{P}^\circ$ and that $\text{Sym}3(\mathbf{b} \times \mathbf{q}) = \text{Sym}3(\boldsymbol{\wedge} \cdot \mathbf{q}) = \text{Sym}3(\boldsymbol{\wedge} \boldsymbol{\delta} \boldsymbol{\delta} : \mathbf{q}) = 3 \boldsymbol{\wedge} \boldsymbol{\delta} \boldsymbol{\delta} : \mathbf{q}$, we can rewrite the implicit closure equations in the form

$$(\boldsymbol{\delta} + \varpi \boldsymbol{\wedge}) \cdot \mathbf{q} = -k \nabla T, \quad (\text{A.21})$$

$$(\boldsymbol{\delta} \boldsymbol{\delta} + \varpi 2 \boldsymbol{\wedge} \boldsymbol{\delta}) : \mathbb{P}^\circ = -\mu 2 \mathbf{e}^\circ, \quad (\text{A.22})$$

$$(\boldsymbol{\delta} \boldsymbol{\delta} \boldsymbol{\delta} + \varpi 3 \boldsymbol{\wedge} \boldsymbol{\delta} \boldsymbol{\delta}) : \mathbf{q} = -\frac{2}{5} k \text{Sym}3(\boldsymbol{\pi} \cdot \nabla \mathbb{T}). \quad (\text{A.23})$$

To solve these equations we need to invert the matrices in parentheses.

A.5.5 Heat flux

We need to solve equation (A.21) for \mathbf{q} . Let M_1 denote the inverse of the matrix $A_1 := \boldsymbol{\delta} + \varpi \boldsymbol{\wedge}$. It must be gyrotropic. The tensors \parallel , \perp , and $\boldsymbol{\wedge}$ comprise a basis for the space of gyrotropic tensors. So we can expand M_1 as

$$M_1 = m_n \parallel + m_0 \perp + m_1 \boldsymbol{\wedge}.$$

Substituting this into the required relation $A_1 \cdot M_1 = \boldsymbol{\delta}$ yields

$$m_n \parallel + m_0 \perp + m_1 \boldsymbol{\wedge} + \varpi (m_0 \boldsymbol{\wedge} - m_1 \perp) = \parallel + \perp,$$

where we have used that $\boldsymbol{\delta} = \parallel + \perp$ and that $\boldsymbol{\wedge} \cdot \perp = \boldsymbol{\wedge}$ and $\boldsymbol{\wedge} \cdot \boldsymbol{\wedge} = -\perp$. Matching coefficients reveals that $m_n = 1$ and gives a linear system

$$\begin{array}{l} \perp : \\ \boldsymbol{\wedge} : \end{array} \left(\begin{bmatrix} 1 & 0 \\ 0 & 1 \end{bmatrix} + \varpi \begin{bmatrix} 0 & -1 \\ 1 & 0 \end{bmatrix} \right) \begin{bmatrix} m_0 \\ m_1 \end{bmatrix} = \begin{bmatrix} 1 \\ 0 \end{bmatrix} \implies \begin{bmatrix} m_0 \\ m_1 \end{bmatrix} = \frac{1}{1 + \varpi^2} \begin{bmatrix} 1 \\ -\varpi \end{bmatrix}. \quad (\text{A.24})$$

That is,

$$M_1 = \tilde{\mathbf{k}} := \parallel + \frac{1}{1 + \varpi^2} (\perp - \varpi \boldsymbol{\wedge}). \quad (\text{A.25})$$

Observe that when $\varpi = 0$ then M_1 is the identity matrix, and in the limit of large magnetic field,

$$M_1 \approx // - \varpi^{-1} \wedge,$$

which effectively shuts down heat flux perpendicular to the magnetic field. So the heat flux closure is

$$\mathbf{q} = -k \left(// + \frac{1}{1 + \varpi^2} (\perp - \varpi \wedge) \right) \cdot \nabla T, \quad (\text{A.26})$$

that is,

$$\mathbf{q} = -k \left(\mathbf{b}\mathbf{b} + \frac{1}{1 + \varpi^2} \left((\mathbb{1} - \mathbf{b}\mathbf{b}) - \varpi \mathbf{b} \times \mathbb{1} \right) \right) \cdot \nabla T. \quad (\text{A.27})$$

This is the closure given by Woods in equations (5.107)–(5.109) in [62]. He identifies this result as that of Chapman and Cowling’s kinetic theory. His figure 5.6 plots m_0/m_n versus ϖ and shows that it agrees well those of Braginskii’s closure given on pages 249–51 of [10].

A.5.6 Deviatoric pressure tensor

Let $M_{[2]}$ denote the inverse of the matrix $A_{[2]} := \boldsymbol{\delta}\boldsymbol{\delta} + \varpi 2\wedge\boldsymbol{\delta}$. We will seek $M_{[2]}$ as a linear combination of basis tensors $\{M_i\}$, $M_{[2]} = \sum_i m_i M_i$, where $\text{span}\{M_i\}$ is closed under the map $M \mapsto A_{[2]} : M$, that is, which is closed under the map $L : M \mapsto 2\wedge\boldsymbol{\delta} : M$. We need that $(\boldsymbol{\delta}\boldsymbol{\delta} + \varpi L) : M_{[2]} = \boldsymbol{\delta}\boldsymbol{\delta}$, so it is evident that $\boldsymbol{\delta}\boldsymbol{\delta}$ should be in $\text{span}\{M_i\}$, so we simply compute what repeated applications of L can generate starting with $\boldsymbol{\delta}\boldsymbol{\delta}$. First, observe that L satisfies

$$2\wedge\boldsymbol{\delta} : XY = \wedge \cdot XY + \wedge \cdot YX.$$

Using that $\wedge \cdot \wedge = -\perp$ and $\wedge \cdot \perp = \wedge$, we generate a basis. Under the mapping $M \mapsto 2\wedge\boldsymbol{\delta} : M$, the calculations

$$\begin{aligned} M^0 : M_0^0 &:= \boldsymbol{\delta}\boldsymbol{\delta} \mapsto 2\wedge\boldsymbol{\delta} \\ M^1 : M_0^1 &:= \perp\boldsymbol{\delta} \mapsto \wedge\perp + \wedge\boldsymbol{\delta} \\ M^1 : M_1^1 &:= \wedge\boldsymbol{\delta} \mapsto \wedge\wedge - \perp\boldsymbol{\delta} \end{aligned}$$

and

$$\begin{aligned} M^2 : M_0^2 &:= \perp\perp \mapsto 2\wedge\perp \\ M^2 : M_1^2 &:= \wedge\perp \mapsto \wedge\wedge - \perp\perp \\ M^2 : M_2^2 &:= \wedge\wedge \mapsto -2\wedge\perp \end{aligned}$$

exhibit such a basis. The span of the M^2 subsystem is closed under the map $M \mapsto A_{[2]} : M$, but the span of the M^1 subsystem is not. This is easily remedied. Subtract the map of $\perp\perp$ from the map of $\perp\boldsymbol{\delta}$ and subtract the map of $\wedge\boldsymbol{\delta}$ from the map of $\wedge\perp$ to get the closed system

$$\begin{aligned} M^1 : M_0^1 &:= \perp// \mapsto \wedge// \\ M^1 : M_1^1 &:= \wedge// \mapsto -\perp// \end{aligned}$$

Similarly, beginning with the map of $\boldsymbol{\delta}\boldsymbol{\delta}$ we first subtract the map of $\perp\boldsymbol{\delta}$ to get a map of $\boldsymbol{\delta}//$ and then subtract the maps of $\perp//$ to get the map

$$M^0 : M_0^0 := // \mapsto 0.$$

The basis elements M_j^i generate the same space as the basis elements $M_j^{i'}$ and comprise a decoupled set of cycles.

On the M^1 subsystem L is an invertible map, but on M^2 we can separate out a one-dimensional null-space. Basis vectors for a decoupled system are

$$\begin{aligned} L^2 : 2\sigma_d &:= \perp\perp - \wedge\wedge \mapsto 4\wedge\perp \\ M_1^2 &:= \wedge\perp \mapsto \wedge\wedge - \perp\perp = -2\sigma_d \\ N^2 : 2\sigma_s &:= \perp\perp + \wedge\wedge \mapsto 0 \end{aligned}$$

We now decompose $\delta\delta$ into a sum of the decoupled basis vectors: $\delta\delta = (\parallel + \perp)(\parallel + \perp) = \parallel\parallel + \perp\perp + 2\perp\parallel = \left(\parallel\parallel + \frac{\perp\perp + \parallel\parallel}{2}\right) + \frac{\perp\perp - \parallel\parallel}{2} + 2\perp\parallel$, that is,

$$\delta\delta = \sigma_k + 2\perp\parallel + \sigma_d,$$

where $\sigma_k := \left(\parallel\parallel + \frac{\perp\perp + \parallel\parallel}{2}\right)$; note that there is one element from the null space and one element from each invertible subsystem. The matrix M is a linear combination of the basis we have defined:

$$M = s_k\sigma_k + 2(m_0^1\perp\parallel + m_1^1\wedge\parallel) + (s_d\sigma_d + m_1^2\wedge\perp),$$

where we use parentheses for components that correspond to decoupled subsystems. To find the five unknown viscosity coefficients we substitute this into the required identity $(\delta\delta + \varpi\wedge\delta) : M = \delta\delta$, that is,

$$\begin{aligned} s_k\sigma_k + 2(m_0^1\perp\parallel + m_1^1\wedge\parallel) + (s_d\sigma_d + m_1^2\wedge\perp) \\ + \varpi [2(m_0^1\wedge\parallel - m_1^1\perp\parallel) + (2s_d\wedge\perp - 2m_1^2\sigma_d)] \\ = \sigma_k + 2\perp\parallel + \sigma_d. \end{aligned}$$

Matching up coefficients gives $s_k = 1$ and two linear systems,

$$\begin{aligned} \perp\parallel : \left(\begin{bmatrix} 1 & 0 \\ 0 & 1 \end{bmatrix} + \varpi \begin{bmatrix} 0 & -1 \\ 1 & 0 \end{bmatrix} \right) \begin{bmatrix} m_0^1 \\ m_1^1 \end{bmatrix} = \begin{bmatrix} 1 \\ 0 \end{bmatrix} \implies \begin{bmatrix} m_0^1 \\ m_1^1 \end{bmatrix} = \frac{1}{1 + \varpi^2} \begin{bmatrix} 1 \\ -\varpi \end{bmatrix} \end{aligned} \quad (\text{A.28})$$

and

$$\begin{aligned} \sigma_d : \left(\begin{bmatrix} 1 & 0 \\ 0 & 1 \end{bmatrix} + \varpi \begin{bmatrix} 0 & -2 \\ 2 & 0 \end{bmatrix} \right) \begin{bmatrix} s_d \\ m_1^2 \end{bmatrix} = \begin{bmatrix} 1 \\ 0 \end{bmatrix} \implies \begin{bmatrix} s_d \\ m_1^2 \end{bmatrix} = \frac{1}{1 + 4\varpi^2} \begin{bmatrix} 1 \\ -2\varpi \end{bmatrix}. \end{aligned} \quad (\text{A.29})$$

Putting it all together,

$$M = \sigma_k + \frac{2}{1 + \varpi^2}(\perp\parallel - \varpi\wedge\parallel) + \frac{1}{1 + 4\varpi^2}(\sigma_d - 2\varpi\wedge\perp).$$

Recalling the definitions $\sigma_k = \parallel\parallel + \frac{\perp\perp + \wedge\wedge}{2}$ and $\sigma_d = \frac{\perp\perp - \wedge\wedge}{2}$,

$$M = \tilde{\boldsymbol{\mu}} := \left(\parallel\parallel + \frac{\perp\perp + \wedge\wedge}{2} \right) + \frac{2}{1 + \varpi^2}(\perp\parallel - \varpi\wedge\parallel) + \frac{1}{1 + 4\varpi^2} \left(\frac{\perp\perp - \wedge\wedge}{2} - 2\varpi\wedge\perp \right). \quad (\text{A.30})$$

As a check, observe that when ϖ is zero M is the identity $\delta\delta$. In the limit of strong magnetic field,

$$M \cong \left(\parallel\parallel + \frac{\perp\perp + \wedge\wedge}{2} \right) - 2\varpi^{-1}\wedge\delta + \mathcal{O}(\varpi^{-2}).$$

Using the general properties that

$$XY : 2\mathbf{e}^\circ = \text{Sym}2(X \cdot \mathbf{e}^\circ \cdot Y^T) \quad \text{and} \quad \wedge^T = -\wedge,$$

the closure for the deviatoric stress, $\mathbb{P}^\circ = -\mu 2M : \mathbf{e}^\circ$, is thus

$$\begin{aligned} \mathbb{P}^\circ = -\mu \text{Sym}2 \left(\right. & \delta_{\parallel} \cdot \mathbf{e}^\circ \cdot \delta_{\parallel} + \frac{\delta_{\perp} \cdot \mathbf{e}^\circ \cdot \delta_{\perp} - \delta_{\wedge} \cdot \mathbf{e}^\circ \cdot \delta_{\wedge}}{2} \\ & + \frac{2}{1 + \varpi^2} (\delta_{\perp} \cdot \mathbf{e}^\circ \cdot \delta_{\parallel} + \varpi \delta_{\parallel} \cdot \mathbf{e}^\circ \cdot \delta_{\wedge}) \\ & \left. + \frac{1}{1 + 4\varpi^2} \left(\frac{\delta_{\perp} \cdot \mathbf{e}^\circ \cdot \delta_{\perp} + \delta_{\wedge} \cdot \mathbf{e}^\circ \cdot \delta_{\wedge}}{2} + 2\varpi \delta_{\parallel} \cdot \mathbf{e}^\circ \cdot \delta_{\wedge} \right) \right) \end{aligned} \quad (\text{A.31})$$

where we have reverted to the notation $\wedge = \delta_{\wedge} = \mathbf{b} \times \delta$, $\perp = \delta_{\perp} = \mathbf{1} - \mathbf{b}\mathbf{b}$, and $\parallel = \delta_{\parallel} = \mathbf{b}\mathbf{b}$. The result agrees with equations (5.125)–(5.128) in [62] if one corrects the typo in his equation (5.127) by replacing his definition $\mathbf{W}_2 := (\mathbf{1}_{\parallel} \diamond \mathbf{1}_{\parallel} + \mathbf{1}_{\wedge} \diamond \mathbf{1}_{\wedge})/2$ (which would result in an M (his \mathbf{W}) which fails to be the identity operator for $\varpi = 0$) with the correct definition $\mathbf{W}_2 := (\mathbf{1}_{\perp} \diamond \mathbf{1}_{\perp} + \mathbf{1}_{\wedge} \diamond \mathbf{1}_{\wedge})/2$.

A.5.7 Heat flux tensor

Let $M_{[3]}$ denote the inverse of the matrix $A_{[3]} := \delta\delta\delta + \varpi 3\wedge\delta\delta$. We will seek $M_{[3]}$ as a linear combination of basis tensors $\{M_i\}$, $M_{[3]} = \sum_i m_i M_i$, where $\text{span}\{M_i\}$ is closed under the map $M \mapsto A_{[3]} : M$, that is, which is closed under the map $L : M \mapsto 3\wedge\delta\delta : M$. We need that $(\delta\delta\delta + \varpi L) : M_{[3]} = \delta\delta\delta$, so it is evident that $\delta\delta\delta$ should be in $\text{span}\{M_i\}$, so we simply compute what repeated applications of L can generate starting with $\delta\delta\delta$. First, observe that L satisfies

$$3\wedge\delta\delta : XYZ = \wedge \cdot XYZ + \wedge \cdot YXZ + \wedge \cdot ZXY.$$

Using that $\wedge \cdot \wedge = -\perp$ and $\wedge \cdot \perp = \wedge$, we generate a basis. Under the mapping $M \mapsto 3\wedge\delta\delta : M$, the calculations

$$\begin{aligned} M^0 : M_0^0 &:= \delta\delta\delta \mapsto 3\wedge\delta\delta \\ M^1 : M_0^1 &:= \perp\delta\delta \mapsto 2\wedge\perp\delta + \wedge\delta\delta \\ &M_1^1 := \wedge\delta\delta \mapsto 2\wedge\wedge\delta - \perp\delta\delta \\ M^2 : M_0^2 &:= \perp\perp\delta \mapsto \wedge\perp\perp + 2\wedge\perp\delta \\ &M_1^2 := \wedge\perp\delta \mapsto \wedge\wedge\perp + \wedge\wedge\delta - \perp\perp\delta \\ &M_2^2 := \wedge\wedge\delta \mapsto \wedge\wedge\wedge - 2\wedge\perp\delta \end{aligned}$$

and

$$\begin{aligned} M^3 : M_0^3 &:= \perp\perp\perp \mapsto 3\wedge\perp\perp \\ &M_1^3 := \wedge\perp\perp \mapsto 2\wedge\wedge\perp - \perp\perp\perp \\ &M_2^3 := \wedge\wedge\perp \mapsto \wedge\wedge\wedge - 2\wedge\perp\perp \\ &M_3^3 := \wedge\wedge\wedge \mapsto -3\wedge\wedge\perp \end{aligned} \quad (\text{A.32})$$

exhibit such a basis. The span of the M^3 subsystem is closed under the map $M \mapsto A_{[3]} : M$, but the span of the other M^k systems is not. This is easily remedied. For each mapping in an M^k subsystem subtract the corresponding mapping in the M^{k+1} system and repeat until all δ 's have

been turned into \llcorner 's. This gives a new set of basis elements which satisfy a simpler, decoupled set of mappings and which still span the same set:

$$\begin{aligned}
M^0 : M_0^0 &:= \llcorner\llcorner\llcorner \mapsto 0 \\
M^1 : M_0^1 &:= \perp\llcorner\llcorner \mapsto \wedge\llcorner\llcorner \\
&M_1^1 := \wedge\llcorner\llcorner \mapsto -\perp\llcorner\llcorner \\
M^2 : M_0^2 &:= \perp\perp\llcorner \mapsto 2\wedge\perp\llcorner \\
&M_1^2 := \wedge\perp\llcorner \mapsto \wedge\wedge\llcorner - \perp\perp\llcorner \\
&M_2^2 := \wedge\wedge\llcorner \mapsto -2\wedge\perp\llcorner
\end{aligned}$$

Ignoring the final \llcorner in all these maps, this is identical to the decoupled system with the same variable names M_j^k that we obtained in section A.5.6 when closing the deviatoric pressure. We therefore separate out the null space for this system in the same way, and we replace the system M^2 with

$$\begin{aligned}
L^2 : 2\sigma_d\llcorner &:= (\perp\perp - \wedge\wedge)\llcorner \mapsto 4\wedge\perp\llcorner \\
&M_1^2 := \wedge\perp\llcorner \mapsto (\wedge\wedge - \perp\perp)\llcorner = -2\sigma_d\llcorner \\
N^2 : 2\sigma_s\llcorner &:= (\perp\perp + \wedge\wedge)\llcorner \mapsto 0
\end{aligned}$$

Again, the null space for the subsystems M^k where k is odd is trivial.

We now decompose $\delta\delta\delta = \delta^3$ into a sum of decoupled basis vectors:

$$\begin{aligned}
\delta^3 &= (\perp + \llcorner)^3 \\
&= \perp\perp\perp + 3\perp\llcorner\llcorner + 3\perp\perp\llcorner + \llcorner\llcorner\llcorner \\
&= \perp\perp\perp + 3\perp\llcorner\llcorner + 3\sigma_d\llcorner + (3\sigma_s\llcorner + \llcorner\llcorner\llcorner).
\end{aligned}$$

The matrix M is a linear combination of the basis that we have defined:

$$\begin{aligned}
M &= m_n(3\sigma_s\llcorner + \llcorner\llcorner\llcorner) + 2(m_0^1\perp\llcorner\llcorner + m_1^1\wedge\llcorner\llcorner) + (s_d\sigma_d\llcorner + m_1^2\wedge\perp\llcorner) \\
&\quad + (m_0^3\perp\perp\perp + m_1^3\wedge\perp\perp + m_2^3\wedge\wedge\perp + m_3^3\wedge\wedge\wedge),
\end{aligned} \tag{A.33}$$

where we use parentheses for components that correspond to decoupled subsystems. To find the nine heat flux coefficients we substitute this into the required identity $(\delta\delta\delta + \varpi\wedge\delta\delta) : M = \delta\delta\delta$, that is,

$$\begin{aligned}
&m_n(3\sigma_s\llcorner + \llcorner\llcorner\llcorner) \\
&+ 2(m_0^1\perp\llcorner\llcorner + m_1^1\wedge\llcorner\llcorner) + \varpi 2(m_0^1\wedge\llcorner\llcorner - m_1^1\perp\llcorner\llcorner) \\
&+ (s_d\sigma_d\llcorner + m_1^2\wedge\perp\llcorner) + \varpi(2s_d\wedge\perp\llcorner - 2m_1^2\sigma_d\llcorner) \\
&+ (m_0^3\perp\perp\perp + m_1^3\wedge\perp\perp + m_2^3\wedge\wedge\perp + m_3^3\wedge\wedge\wedge) \\
&\quad + \varpi(-3m_0^3\wedge\perp\perp + m_1^3(2\wedge\wedge\perp - \perp\perp\perp) + m_2^3(\wedge\wedge\wedge - 2\wedge\perp\perp) - 3m_3^3\wedge\wedge\perp) \\
&= (3\sigma_s\llcorner + \llcorner\llcorner\llcorner) + 3\perp\llcorner\llcorner + 3\sigma_d\llcorner + \perp\perp\perp.
\end{aligned}$$

Matching up coefficients gives the expected equation $m_n = 1$, two linear systems almost identical to those in section A.5.6, and one new system corresponding to the M^3 system (A.32). For the first two systems, we have one nearly identical to system (A.28),

$$\begin{aligned}
\perp\llcorner\llcorner : &\left(\begin{bmatrix} 1 & 0 \\ 0 & 1 \end{bmatrix} + \varpi \begin{bmatrix} 0 & -1 \\ 1 & 0 \end{bmatrix} \right) \begin{bmatrix} m_0^1 \\ m_1^1 \end{bmatrix} = \begin{bmatrix} 3/2 \\ 0 \end{bmatrix} \implies \begin{bmatrix} m_0^1 \\ m_1^1 \end{bmatrix} = \frac{3/2}{1 + \varpi^2} \begin{bmatrix} 1 \\ -\varpi \end{bmatrix},
\end{aligned}$$

the only real modification being the replacement $2 \rightarrow 3/2$ due to the appearance of $3\perp//$ in place of $2\perp//$ on the right hand side, and one system nearly identical to system (A.29),

$$\begin{aligned} \sigma_d// : \left(\begin{bmatrix} 1 & 0 \\ 0 & 1 \end{bmatrix} + \varpi \begin{bmatrix} 0 & -2 \\ 2 & 0 \end{bmatrix} \right) \begin{bmatrix} s_d \\ m_1^2 \end{bmatrix} = \begin{bmatrix} 3 \\ 0 \end{bmatrix} \implies \begin{bmatrix} s_d \\ m_1^2 \end{bmatrix} = \frac{3}{1+4\varpi^2} \begin{bmatrix} 1 \\ -2\varpi \end{bmatrix}, \\ \wedge\perp// : \end{aligned}$$

the only real modification being the replacement $1 \rightarrow 3$ due to the appearance of $3\sigma_d//$ in place of σ_d on the right hand side. For the new system corresponding to the M^3 system (A.32), we have

$$\begin{aligned} \perp\perp\perp : \left(\begin{bmatrix} 1 & 0 & 0 & 0 \\ 0 & 1 & 0 & 0 \\ 0 & 0 & 1 & 0 \\ 0 & 0 & 0 & 1 \end{bmatrix} + \varpi \begin{bmatrix} 0 & -1 & 0 & 0 \\ 3 & 0 & -2 & 0 \\ 0 & 2 & 0 & -3 \\ 0 & 0 & 1 & 0 \end{bmatrix} \right) \begin{bmatrix} m_0^3 \\ m_1^3 \\ m_2^3 \\ m_3^3 \end{bmatrix} = \begin{bmatrix} 1 \\ 0 \\ 0 \\ 0 \end{bmatrix}. \\ \wedge\perp\perp : \\ \wedge\wedge\perp : \\ \wedge\wedge\wedge : \end{aligned}$$

That is, we need to solve the linear system

$$\begin{bmatrix} 1 & -\varpi & 0 & 0 \\ 3\varpi & 1 & -2\varpi & 0 \\ 0 & 2\varpi & 1 & -3\varpi \\ 0 & 0 & \varpi & 1 \end{bmatrix} \begin{bmatrix} m_0^3 \\ m_1^3 \\ m_2^3 \\ m_3^3 \end{bmatrix} = \begin{bmatrix} 1 \\ 0 \\ 0 \\ 0 \end{bmatrix}.$$

We solve by row reduction and back substitution. Subtracting 3ϖ times row 1 from row 2 gives

$$\begin{bmatrix} 1 & -\varpi & 0 & 0 \\ 0 & 1+3\varpi^2 & -2\varpi & 0 \\ 0 & 2\varpi & 1 & -3\varpi \\ 0 & 0 & \varpi & 1 \end{bmatrix} \begin{bmatrix} m_0^3 \\ m_1^3 \\ m_2^3 \\ m_3^3 \end{bmatrix} = \begin{bmatrix} 1 \\ -3\varpi \\ 0 \\ 0 \end{bmatrix}.$$

Subtracting 2ϖ times row 2 from $1+3\varpi^2$ times row 3 gives

$$\begin{bmatrix} 1 & -\varpi & 0 & 0 \\ 0 & 1+3\varpi^2 & -2\varpi & 0 \\ 0 & 0 & 1+7\varpi^2 & -3\varpi(1+3\varpi^2) \\ 0 & 0 & \varpi & 1 \end{bmatrix} \begin{bmatrix} m_0^3 \\ m_1^3 \\ m_2^3 \\ m_3^3 \end{bmatrix} = \begin{bmatrix} 1 \\ -3\varpi \\ 6\varpi^2 \\ 0 \end{bmatrix}.$$

Subtracting ϖ times row 3 from $1+7\varpi^2$ times row 4 gives

$$\begin{bmatrix} 1 & -\varpi & 0 & 0 \\ 0 & 1+3\varpi^2 & -2\varpi & 0 \\ 0 & 0 & 1+7\varpi^2 & -3\varpi(1+3\varpi^2) \\ 0 & 0 & 0 & 1+10\varpi^2+9\varpi^4 \end{bmatrix} \begin{bmatrix} m_0^3 \\ m_1^3 \\ m_2^3 \\ m_3^3 \end{bmatrix} = \begin{bmatrix} 1 \\ -3\varpi \\ 6\varpi^2 \\ -6\varpi^3 \end{bmatrix}.$$

Back substituting yields

$$\begin{aligned} k_3 := m_3^3 &= \frac{-6\varpi^3}{1+10\varpi^2+9\varpi^4} = -(2/3)\varpi^{-1} + \mathcal{O}(\varpi^{-3}), \\ k_2 := m_2^3 &= \frac{6\varpi^2+3\varpi(1+3\varpi^2)m_3^3}{1+7\varpi^2} = \mathcal{O}(\varpi^{-2}), \\ k_1 := m_1^3 &= \frac{-3\varpi+2\varpi m_2^3}{1+3\varpi^2} = -\varpi^{-1} + \mathcal{O}(\varpi^{-3}), \\ k_0 := m_0^3 &= 1 + \varpi m_1^3 = \mathcal{O}(\varpi^{-2}). \end{aligned} \tag{A.34}$$

In summary, the heat flux is given by

$$\mathbf{q} = -\frac{2}{5}\mathbf{K} \colon \text{Sym}3(\boldsymbol{\pi} \cdot \nabla \mathbb{T}), \quad (\text{A.35})$$

where the heat conductivity tensor is given by $\mathbf{K} = k\widetilde{\mathbf{K}}$, where $\widetilde{\mathbf{K}} := M$ is the shape of the heat conductivity tensor. The heat conductivity is thus a sixth order gyrotropic tensor and is given by equation (A.33),

$$\begin{aligned} \widetilde{\mathbf{K}} = & (3\sigma_s \parallel + \parallel \parallel \parallel) + \frac{3}{1+\varpi^2} (\perp \parallel \parallel - \varpi \wedge \parallel \parallel) + \frac{3}{1+4\varpi^2} (\sigma_d \parallel - 2\varpi \wedge \perp \parallel) \\ & + (k_0 \perp \perp \perp + k_1 \wedge \perp \perp + k_2 \wedge \wedge \perp + k_3 \wedge \wedge \wedge), \end{aligned} \quad (\text{A.36})$$

that is, recalling that $\sigma_s := \frac{\perp \perp + \wedge \wedge}{2}$ and $\sigma_d := \frac{\perp \perp - \wedge \wedge}{2}$, and using powers to denote splice symmetric product powers,

$$\begin{aligned} \widetilde{\mathbf{K}} = & (\parallel^3 + \frac{3}{2}\parallel(\perp^2 + \wedge^2)) \\ & + \frac{3}{1+\varpi^2} (\perp \parallel^2 - \varpi \wedge \parallel^2) + \frac{3}{1+4\varpi^2} \left(\frac{\perp^2 - \wedge^2}{2} \parallel - 2\varpi \wedge \perp \parallel \right) \\ & + (k_0 \perp^3 + k_1 \wedge \perp^2 + k_2 \wedge^2 \perp + k_3 \wedge^3), \end{aligned} \quad (\text{A.37})$$

where the coefficients k_i are given in (A.34). Note that when ϖ is zero $\widetilde{\mathbf{K}}$ is the identity $\boldsymbol{\delta}\boldsymbol{\delta}\boldsymbol{\delta}$. In the limit of strong magnetic field,

$$\widetilde{\mathbf{K}} = (\parallel^3 + \frac{3}{2}\parallel(\perp^2 + \wedge^2)) - \varpi^{-1} \left(3\wedge \parallel^2 + 6\wedge \perp \parallel + \wedge \perp^2 + \frac{2}{3}\wedge^3 \right) + \mathcal{O}(\varpi^{-2}).$$

For computational efficiency, one can make use of the identity

$$XYZ \colon S = \text{Sym}((X \widetilde{\otimes} Y \widetilde{\otimes} Z) \colon S),$$

which holds for any symmetric tensor S . So we can write the heat flux closure as

$$\mathbf{q} = -\frac{2}{5}k \text{Sym} \left(\widetilde{\mathbf{K}}' \colon \text{Sym}3(\boldsymbol{\pi} \cdot \nabla \mathbb{T}) \right), \quad (\text{A.38})$$

where the formula for $\widetilde{\mathbf{K}}'$ is the same as for $\widetilde{\mathbf{K}}$ except that because we symmetrize at the end we can now take the default product of tensors to be simple splice products (in order to avoid averaging over $3! = 6$ splice products for each triple product).

Appendix B

Reconnection

B.1 Inflow ODE for the ten-moment equations.

Jerry Brackbill has studied two-dimensional antiparallel reconnection using the 10-moment two-fluid equations, assuming symmetry across the inflow axis. With mild approximating assumptions for steady state he reduces the adiabatic ($\mathbf{q} = 0$) equations on the y -axis to an ODE [9].

Recall that symmetry in the x -axis says that all tensor components are even or odd in x based on whether x appears as a subscript an even or odd number of times. (For a pseudo-tensor such as the magnetic field \mathbf{B} components are even iff the number of x subscripts is odd; for a proper tensor components are even iff the number of x subscripts is even.)

- Even: $\mathbf{u}_z, \mathbf{u}_y, \mathbb{P}_{xx}, \mathbb{P}_{yy}, \mathbb{P}_{zz}, \mathbb{P}_{yz}, \mathbf{B}_x, \mathbf{E}_y, \mathbf{E}_z,$
- Odd: $\mathbf{u}_x, \mathbb{P}_{xy}, \mathbb{P}_{xz}, \mathbf{B}_z, \mathbf{B}_y, \mathbf{E}_x,$

Odd functions (including x -derivatives of even functions but not x -derivatives of odd functions) vanish on the $x = 0$ axis.

All quantities are independent of z , so $\partial_z = 0$. So on the $x = 0$ axis the convective derivative is simply $d_t := \partial_t + \mathbf{u}_y \partial_y$. By using convective derivative we avoid x -derivatives. Therefore we work with the temperature evolution equation (2.14)

$$nd_t \mathbb{T} + \text{Sym}2(\mathbb{P} \cdot \nabla \mathbf{u}) + \nabla \cdot \mathbf{q} = (q/m) \text{Sym}2(\mathbb{P} \times \mathbf{B}) + \mathbb{R},$$

where we assume a default species index.

B.1.1 Component evolution

For arbitrary indices a and b we have

$$\begin{aligned} 2 \text{Sym}(\mathbb{P} \cdot \nabla \mathbf{u})_{ab} &= \mathbb{P}_{ax} \partial_x \mathbf{u}_b + \mathbb{P}_{bx} \partial_x \mathbf{u}_a \\ &\quad + \mathbb{P}_{ay} \partial_y \mathbf{u}_b + \mathbb{P}_{by} \partial_y \mathbf{u}_a. \end{aligned}$$

In particular, on the $x = 0$ axis we have

$$\begin{aligned} 2 \text{Sym}(\mathbb{P} \cdot \nabla \mathbf{u})_{yz} &= \mathbb{P}_{yz} \partial_y \mathbf{u}_y + \mathbb{P}_{yy} \partial_y \mathbf{u}_z, \\ 2 \text{Sym}(\mathbb{P} \cdot \nabla \mathbf{u})_{xx} &= 2 \mathbb{P}_{xx} \partial_x \mathbf{u}_x, \\ 2 \text{Sym}(\mathbb{P} \cdot \nabla \mathbf{u})_{yy} &= 2 \mathbb{P}_{yy} \partial_y \mathbf{u}_y, \\ 2 \text{Sym}(\mathbb{P} \cdot \nabla \mathbf{u})_{zz} &= 2 \mathbb{P}_{yz} \partial_y \mathbf{u}_z. \end{aligned}$$

On the x axis $\mathbf{B}_z = 0 = \mathbf{B}_y$. So for arbitrary indices, on the x axis we have

$$2 \text{Sym}(\mathbb{P} \times \mathbf{B})_{ab} = \mathbf{B}_x (\mathbb{P}_{aj} \epsilon_{xbj} + \mathbb{P}_{bj} \epsilon_{xaj}).$$

In particular,

$$\begin{aligned} 2 \text{Sym}(\mathbb{P} \times \mathbf{B})_{yz} &= \mathbf{B}_x (-\mathbb{P}_{zz} + \mathbb{P}_{yy}), \\ 2 \text{Sym}(\mathbb{P} \times \mathbf{B})_{xx} &= 0, \\ 2 \text{Sym}(\mathbb{P} \times \mathbf{B})_{yy} &= -2\mathbf{B}_x \mathbb{P}_{yz}, \\ 2 \text{Sym}(\mathbb{P} \times \mathbf{B})_{zz} &= 2\mathbf{B}_x \mathbb{P}_{yz}. \end{aligned}$$

Along the y axis the isotropization components are

$$\begin{aligned} \mathbb{R}_{yz} &= -\mathbb{P}_{yz}/\tau, \\ \mathbb{R}_{xx} &= (p - \mathbb{P}_{xx})/\tau, \\ \mathbb{R}_{yy} &= (p - \mathbb{P}_{yy})/\tau, \\ \mathbb{R}_{zz} &= (p - \mathbb{P}_{zz})/\tau. \end{aligned}$$

The foregoing component identities continue to hold if we replace the pressure tensor with the temperature tensor. Ignoring heat flux, and assuming $\partial_z = 0$, the components of the temperature tensor evolution equation on the inflow axis are thus

$$\begin{aligned} d_t \mathbb{T}_{yz} + \mathbb{T}_{yz} \partial_y \mathbf{u}_y + \mathbb{T}_{yy} \partial_y \mathbf{u}_z &= \frac{q}{m} \mathbf{B}_x (-\mathbb{T}_{zz} + \mathbb{T}_{yy}) - \mathbb{T}_{yz}/\tau, \\ d_t \mathbb{T}_{xx} + 2\mathbb{T}_{xx} \partial_x \mathbf{u}_x &= (T - \mathbb{T}_{xx})/\tau, \\ d_t \mathbb{T}_{yy} + 2\mathbb{T}_{yy} \partial_y \mathbf{u}_y &= -2\frac{q}{m} \mathbf{B}_x \mathbb{T}_{yz} + (T - \mathbb{T}_{yy})/\tau, \\ d_t \mathbb{T}_{zz} + 2\mathbb{T}_{yz} \partial_y \mathbf{u}_z &= 2\frac{q}{m} \mathbf{B}_x \mathbb{T}_{yz} + (T - \mathbb{T}_{zz})/\tau. \end{aligned} \tag{B.1}$$

Along the inflow axis, by symmetry $d_t = \partial_t + \mathbf{u}_y \partial_y$. In steady state this becomes $d_t = \mathbf{u}_y \partial_y$.

B.2 Adiabatic ten-moment stagnation point flow.

B.2.1 Abstract framework for linearization about the X-point

What can smooth, steady reconnection look like near the X-point? Linearize about the X-point. Then spatial derivatives of \mathbf{B} and \mathbf{u} become constants, so equation (B.1) is a linear ODE in y of the form

$$y\mathbf{U}' = A \cdot \mathbf{U} + yB \cdot \mathbf{U},$$

where A and B are matrices of constant coefficients (and where B involves magnetic field components), prime denotes differentiation with respect to y , and $\mathbf{U}(y)$ is a vector containing the four non-vanishing components of \mathbb{T} .

Near the X-point the magnetic field vanishes and we get

$$y\mathbf{U}' \approx A \cdot \mathbf{U} \tag{B.2}$$

We will see that we can take $\mathbf{U} = (\mathbb{T}_{xx}, \mathbb{T}_{zz}, \mathbb{T}_{yy})^T$. To solve such an ODE you can use the eigenstructure of A . Suppose that it has a full eigenvector decomposition. Then $A = R \cdot \Lambda \cdot R^{-1}$, so we have

$$y(R^{-1} \cdot \mathbf{U})' = \Lambda \cdot (R^{-1} \cdot \mathbf{U}).$$

Let $\mathbf{W} := R^{-1} \cdot \mathbf{U}$. Then this system decouples into scalar equations of the form

$$yW' = \lambda W.$$

Separating and integrating gives

$$W = Cy^\lambda. \tag{B.3}$$

So existence of a smooth, strictly positive steady-state \mathbb{T} requires that $\lambda = 0$ is an eigenvalue (else any steady solution must be zero or singular at the origin) for an eigenvector with positive components. I remark that existence of a positive definite solution (whether singular or not) requires existence of an eigenvector representing a positive-definite solution.

To confirm physically that the neglect of the magnetic field in (B.2) is justifiable, note that the magnetic field simply rotates the temperature tensor at a rate proportional to the strength of the magnetic field. Since \mathbf{u}_y and \mathbf{B}_x are both proportional to distance from $y = 0$, $\frac{d\theta}{dy} = \frac{d\theta}{dt} \frac{dt}{dy} = \frac{y\partial_y \mathbf{B}_x}{y\partial_y \mathbf{u}_y} = \frac{\partial_y \mathbf{B}_x}{\partial_y \mathbf{u}_y}$, so the angle of rotation is proportional to the distance moved along the y axis and rotation can be neglected as y approaches 0.

B.2.2 Stagnation point flow for an adiabatic isotropizing ten-moment gas

We now use the framework outlined in section B.2.1 to argue that smooth steady-state stagnation point flow is singular in an anisotropic ten-moment model without heat flux.

Ignoring both magnetic field as well heat flux, the terms involving \mathbf{B}_x drop out of (B.1). At the X-point the vorticity $\partial_y \mathbf{u}_z$ is zero, so in the linear analysis these terms also drop out. At the X-point steady flow must be incompressible, $\nabla \cdot \mathbf{u} = -d_t \ln \rho = 0$, so $\partial_x \mathbf{u}_x = -\partial_y \mathbf{u}_y$. In the linearization we replace $\partial_y \mathbf{u}_y$ with its value at the X-point. Define $\mathbf{u}_{y,y} := \partial_y \mathbf{u}_y|_{y=0}$. So near the X-point the components of the temperature tensor evolve according to

$$\begin{aligned} d_t \mathbb{T}_{yz} + \mathbb{T}_{yz} \mathbf{u}_{y,y} &= -\mathbb{T}_{yz} / \tau, \\ d_t \mathbb{T}_{xx} - 2\mathbb{T}_{xx} \mathbf{u}_{y,y} &= (T - \mathbb{T}_{xx}) / \tau, \\ d_t \mathbb{T}_{yy} + 2\mathbb{T}_{yy} \mathbf{u}_{y,y} &= (T - \mathbb{T}_{yy}) / \tau, \\ d_t \mathbb{T}_{zz} &= (T - \mathbb{T}_{zz}) / \tau, \end{aligned} \tag{B.4}$$

where recall that $T = (\mathbb{T}_{xx} + \mathbb{T}_{zz} + \mathbb{T}_{yy})/3$. Steady-state-flow implies that $d_t = \mathbf{u} \cdot \nabla = \mathbf{u}_y \partial_y$. So, in the linearization, $d_t = y \mathbf{u}_{y,y} \partial_y$. Note that \mathbb{T}_{yz} decouples from the other components and is zero if initially zero. Dividing by $\mathbf{u}_{y,y}$ and expressing (B.4) in matrix form,

$$y\partial_y \underbrace{\begin{bmatrix} \mathbb{T}_{xx} \\ \mathbb{T}_{yy} \\ \mathbb{T}_{zz} \end{bmatrix}}_{\mathbf{U}} = \frac{1}{3\bar{\tau}} \underbrace{\begin{bmatrix} -2 + 6\bar{\tau} & 1 & 1 \\ 1 & -2 - 6\bar{\tau} & 1 \\ 1 & 1 & -2 \end{bmatrix}}_{\text{Call } \tilde{A}} \begin{bmatrix} \mathbb{T}_{xx} \\ \mathbb{T}_{yy} \\ \mathbb{T}_{zz} \end{bmatrix},$$

where $\bar{\tau} := \tau \mathbf{u}_{y,y}$. (So $\bar{\tau} < 0$ if there is inflow along y and $\bar{\tau} > 0$ if there is outflow along y .) We have now matched up with the framework of (B.2). Note that the matrix \tilde{A} is symmetric, so it must have real eigenvalues and a full set of orthogonal eigenvectors.

Summary of eigenvalue/eigenvector results.

In the inflow case ($\bar{\tau} < 0$) there is one negative eigenvalue $\lambda^{(1)}$ and all components of its eigenvector can be positive. The solution for this component blows up as y goes to zero. The other two eigenvalues are positive (representing decay as y goes to zero) and have eigenvector components of mixed sign which cannot be combined to give all-positive components. Using these three eigenvectors you can match any positive data at a boundary $y = \pm Y$ and positivity then holds between $\pm Y$ and 0. This solution represents a heating singularity as inflow approaches the X-point.

In the outflow case ($\bar{\tau} > 0$) there is one positive eigenvalue $\lambda^{(1)}$ and all components of its eigenvector can be positive. The solution for this component blows up as y goes to ∞ . The other two eigenvalues are negative (representing decay as y goes to ∞ and have eigenvector components of mixed sign which cannot be combined to give all-positive components. Thus a steady outflow solution which is positive at $y = Y_{\min}$ will be positive for all y between Y_{\min} and ∞ .

If the y axis is an inflow axis then the x axis is an outflow axis. From the previous two paragraphs we conclude that a steady-state solution must be not only singular but discontinuous at the X-point (even in the topology of the real line which includes a point at infinity). In practice absence of heat flux will be violated in the immediate vicinity of the X-point.

Except when crossing the singular point $\bar{\tau}^{-1} = 0$ all eigenvalues (and all eigenvector components, using consistent scaling) change monotonically with $\bar{\tau}$ and do not change in sign.

When there is outflow (rather than inflow) in the y axis, the y and x components effectively swap places and eigenvalues are negated ($\lambda^{(1)} > \lambda^{(2)} > \lambda^{(3)}$) See table 2.)

| | | | | | |
|---------------------------|-----------|--------|----------|--------|-----------|
| $\bar{\tau}^{-1} :$ | $-\infty$ | \leq | 0 | \leq | ∞ |
| $\lambda^{(1)} :$ | ∞ | \geq | 2 | \geq | 0 |
| $\mathbb{T}_{xx}^{(1)} :$ | .7887 | \leq | 1 | \geq | .5774 |
| $\mathbb{T}_{yy}^{(1)} :$ | -.2113 | \leq | 0 · 1 | \leq | .5774 |
| $\mathbb{T}_{zz}^{(1)} :$ | -.5774 | \leq | 0 · 2 | \leq | .5774 |
| $\lambda^{(2)} :$ | ∞ | \geq | 0 | \geq | $-\infty$ |
| $\mathbb{T}_{xx}^{(2)} :$ | .2113 | \geq | 0 · (-1) | \geq | -.7887 |
| $\mathbb{T}_{yy}^{(2)} :$ | -.7887 | \leq | 0 · 1 | \leq | .2113 |
| $\mathbb{T}_{zz}^{(2)} :$ | .5774 | \leq | 1 | \geq | .5774 |
| $\lambda^{(3)} :$ | 0 | \geq | -2 | \geq | $-\infty$ |
| $\mathbb{T}_{xx}^{(3)} :$ | .5774 | \geq | 0 · (-1) | \geq | -.2113 |
| $\mathbb{T}_{yy}^{(3)} :$ | .5774 | \leq | 1 | \geq | .7887 |
| $\mathbb{T}_{zz}^{(3)} :$ | .5774 | \geq | 0 · (-2) | \geq | -.5774 |

Table 2: Eigenstructure for solutions to adiabatic ten-moment linearized stagnation point flow. In this table multiplication of 0 by a constant is used to indicate asymptotic relative scaling of eigenvector components near $\bar{\tau}^{-1} \cong 0$; .5774 is an approximation for $\sqrt{3}^{-1}$, .2113 is an approximation for $\frac{1-\sqrt{3}^{-1}}{2}$, and .7887 is an approximation for $\frac{1+\sqrt{3}^{-1}}{2}$. Except when crossing the singular point $\bar{\tau}^{-1} = 0$, eigenvalues and eigenvector components change monotonically with $\bar{\tau}$ and do not change in sign.

In the case of no isotropization, $\bar{\tau}^{-1} = 0$, the ODE simplifies to

$$y\partial_y \begin{bmatrix} \mathbb{T}_{xx} \\ \mathbb{T}_{yy} \\ \mathbb{T}_{zz} \end{bmatrix} = \begin{bmatrix} 2 & 0 & 0 \\ 0 & -2 & 0 \\ 0 & 0 & 0 \end{bmatrix} \begin{bmatrix} \mathbb{T}_{xx} \\ \mathbb{T}_{yy} \\ \mathbb{T}_{zz} \end{bmatrix}$$

and the solution is simply

$$\begin{aligned} \mathbb{T}_{xx}(y) &= \mathbb{T}_{xx}|_{y=1}y^2, \\ \mathbb{T}_{yy}(y) &= \mathbb{T}_{yy}|_{y=1}y^{-2}, \\ \mathbb{T}_{zz}(y) &= \mathbb{T}_{zz}|_{y=1}, \end{aligned}$$

which is singular at the origin, contradicting the smoothness assumption.

Calculation of eigenvalues and eigenvectors.

This section incompletely works out the results tabulated in section [B.2.2](#).

If $\tilde{\lambda}$ is an eigenvalue of \tilde{A} then $\lambda := \tilde{\lambda}/(3\bar{\tau})$ is an eigenvalue of $A := \tilde{A}/(3\bar{\tau})$. To find the eigenstructure of the coefficient matrix \tilde{A} , we solve $(\tilde{A} - \mathbf{1}\tilde{\lambda}) \cdot \mathbf{U} = \mathbf{0}$. We represent this system with the matrix

$$\begin{bmatrix} -2 + 6\bar{\tau} - \tilde{\lambda} & 1 & 1 \\ 1 & -2 - 6\bar{\tau} - \tilde{\lambda} & 1 \\ 1 & 1 & -2 - \tilde{\lambda} \end{bmatrix}.$$

To facilitate finding the eigenvectors, subtract the third row from the first and the second and get

$$\begin{bmatrix} 6\bar{\tau} - (\tilde{\lambda} + 3) & 0 & \tilde{\lambda} + 3 \\ 0 & -6\bar{\tau} - (\tilde{\lambda} + 3) & \tilde{\lambda} + 3 \\ 1 & 1 & -2 - \tilde{\lambda} \end{bmatrix}.$$

For convenience define

$$\begin{aligned} h &:= 6\bar{\tau} = 6\tau\mathbf{u}_{y,y}, \\ \mu &:= \tilde{\lambda} + 3 = 3\bar{\tau}\lambda + 3 = \tau\mathbf{u}_{y,y}\lambda + 3. \end{aligned}$$

Then we have

$$\begin{bmatrix} h - \mu & 0 & \mu \\ 0 & -(h + \mu) & \mu \\ 1 & 1 & 1 - \mu \end{bmatrix}.$$

Since the null space must be nonzero the rows are linearly dependent. So we can ignore the last row. The first and second rows reveal that an eigenvector must be proportional to something of the form

$$\begin{bmatrix} \mu(\mu + h) \\ \mu(\mu - h) \\ (\mu - h)(\mu + h) \end{bmatrix}.$$

The last row then reveals the characteristic equation that μ must satisfy to be a (shifted) eigenvalue:

$$\begin{aligned} \mu(\mu + h) + (1 - \mu)(\mu^2 - h^2) + \mu(\mu - h) &= 0, \text{ i.e.,} \\ -\mu^3 + 3\mu^2 + h^2\mu - h^2 &= 0. \end{aligned}$$

For nonzero h , $\mu = 3$ is not a root, so $\tilde{\lambda} = \mu - 3$ cannot be zero, so there is no steady-state finite smooth solution with nonzero temperature at the origin.

In case $h = \infty$ this becomes

$$\mu = 1, \text{ i.e., } \tilde{\lambda} = -2.$$

In the limit $h \rightarrow 0$ of instantaneous isotropization this becomes

$$\mu^2(3 - \mu) = 0, \text{ i.e., } (\tilde{\lambda} + 3)^2\tilde{\lambda} = 0,$$

and the eigenvectors collapse to a single eigenvector with equal components representing isotropic temperature, agreeing with the fact that isotropic pressure can support stagnation point flow.

Appendix C

Numerics

C.1 Source ODE

C.1.1 Basic Equations

If we neglect spatial derivatives, then the two-fluid-Maxwell equations reduce to an ODE. The purpose of this appendix section is to solve this **source term ODE**; we assume throughout that spatial derivatives are zero.

If we neglect collisional terms then this ODE is linear with imaginary eigenvalues and can be solved exactly. If we incorporate entropy-respecting collisional closures then the ODE is linear if we make the approximating assumption that the closure coefficients are frozen. In fact, closure coefficients are functions of temperature, and collisions increase the temperature, so the frozen-coefficient assumption incurs time-splitting error. The collisional terms come from symmetric matrices and have negative real eigenvalues.

Maxwell's equations (2.1) assert that the magnetic field is constant and that the displacement current balances the net electrical current:

$$\begin{aligned}\partial_t \mathbf{B} &= 0, \\ \partial_t \mathbf{E} &= -\mathbf{J}/\varepsilon_0 = e(n_e \mathbf{u}_e - n_i \mathbf{u}_i).\end{aligned}$$

The density evolution equations (2.6) and (2.7) assert that the densities (whether mass density or particle density or charge density) remain constant:

$$\partial_t \rho_s = 0, \quad \text{i.e.,} \quad \partial_t n_s = 0, \quad \text{i.e.,} \quad \partial_t \sigma_s = 0.$$

The momentum equation (2.8) for species s is

$$\partial_t(\rho_s \mathbf{u}_s) = \frac{q_s}{m_s} \rho_s (\mathbf{E} + \mathbf{u}_s \times \mathbf{B}) + R_s.$$

We will neglect the collisional drag force R_s . Since densities are constant, we can divide by density.

We thus get the electro-momentum system

$$\begin{aligned}\partial_t \mathbf{E} &= e(n_e \mathbf{u}_e - n_i \mathbf{u}_i), \\ \partial_t \mathbf{u}_i &= \frac{e}{m_i} (\mathbf{E} + \mathbf{u}_i \times \mathbf{B}), \\ \partial_t \mathbf{u}_e &= \frac{-e}{m_e} (\mathbf{E} + \mathbf{u}_e \times \mathbf{B}).\end{aligned}\tag{C.1}$$

Evolution of energy is implied by evolution of momentum (which implies evolution of kinetic energy) and evolution of pressure (which is equivalent to evolution of thermal energy). Note that pressure evolution is temperature evolution times the constant density.

The five-moment pressure evolution equation (2.13)

$$(3/2)\partial_t p_s = Q_s$$

says that pressure is constant in the absence of interspecies collisional heating due to resistive drag and thermal equilibration. If the drag force is non-negligible, and assuming that the resistive drag coefficient is a function of temperature, the electro-momentum system coupled to pressure evolution comprises a minimally closed system. Neglecting collisional terms, pressure evolution simply asserts that pressure is constant.

The pressure tensor evolution equation (2.12) of a ten-moment gas,

$$\partial_t \mathbb{P}_s = (q_s/m_s) \text{Sym}2(\mathbb{P}_s \times \mathbf{B}) + \mathbb{R}_s + \mathbb{Q}_s^f + \mathbb{Q}_s^t, \quad (\text{C.2})$$

depends on the solution to the electro-momentum system if the frictional heating term \mathbb{Q}_s^f is retained, but is otherwise independent. We will neglect \mathbb{Q}_s^f and the thermal equilibration \mathbb{Q}_s^t and will assume the entropy-respecting isotropization closure (2.32),

$$\mathbb{R}_s = -\tau_s^{-1} \mathbb{P}_s^\circ, \quad (\text{C.3})$$

which exponentially dampens the deviatoric pressure $\mathbb{P}_s^\circ := \mathbb{P}_s - p_s \mathbb{1}$. This equation is linear if τ_s is defined in terms of T_s (rather than in terms of $\det \mathbb{T}_s$).

C.1.2 The electro-momentum system

Written in matrix form, the non-resistive electro-momentum system (C.1) reads

$$\partial_t \begin{bmatrix} \mathbf{E} \\ \mathbf{u}_i \\ \mathbf{u}_e \end{bmatrix} = \begin{bmatrix} 0 & -\frac{en_i}{\varepsilon_0} & \frac{en_e}{\varepsilon_0} \\ \frac{e}{m_i} & -\frac{e\mathbf{B}}{m_i} \times \mathbb{1} & 0 \\ -\frac{e}{m_e} & 0 & \frac{e\mathbf{B}}{m_e} \times \mathbb{1} \end{bmatrix} \begin{bmatrix} \mathbf{E} \\ \mathbf{u}_i \\ \mathbf{u}_e \end{bmatrix}.$$

We can make this ODE antisymmetric by rescaling. For a generic rescaling, suppose

$$\begin{aligned} \mathbf{E} &= \tilde{\mathbf{E}} \mathbf{E}_0, \\ \mathbf{u}_i &= \tilde{\mathbf{u}}_i \mathbf{u}_{i0}, \\ \mathbf{u}_e &= \tilde{\mathbf{u}}_e \mathbf{u}_{e0}. \end{aligned}$$

Making this substitution gives the system

$$\partial_t \begin{bmatrix} \tilde{\mathbf{E}} \\ \tilde{\mathbf{u}}_i \\ \tilde{\mathbf{u}}_e \end{bmatrix} = \begin{bmatrix} 0 & -\frac{en_i}{\varepsilon_0} \frac{\mathbf{u}_{i0}}{\mathbf{E}_0} & \frac{en_e}{\varepsilon_0} \frac{\mathbf{u}_{e0}}{\mathbf{E}_0} \\ \frac{e}{m_i} \frac{\mathbf{E}_0}{\mathbf{u}_{i0}} & -\frac{e\mathbf{B}}{m_i} \times \mathbb{1} & 0 \\ -\frac{e}{m_e} \frac{\mathbf{E}_0}{\mathbf{u}_{e0}} & 0 & \frac{e\mathbf{B}}{m_e} \times \mathbb{1} \end{bmatrix} \begin{bmatrix} \tilde{\mathbf{E}} \\ \tilde{\mathbf{u}}_i \\ \tilde{\mathbf{u}}_e \end{bmatrix}.$$

If we require this system to be antisymmetric then

$$\frac{\mathbf{E}_0}{\mathbf{u}_{i0}} = \sqrt{\frac{\rho_i}{\varepsilon_0}} \quad \text{and} \quad \frac{\mathbf{E}_0}{\mathbf{u}_{e0}} = \sqrt{\frac{\rho_e}{\varepsilon_0}},$$

(where recall that $\rho_i = m_i n_i$ and $\rho_e = m_e n_e$) and the system becomes

$$\partial_t \begin{bmatrix} \tilde{\mathbf{E}} \\ \tilde{\mathbf{u}}_i \\ \tilde{\mathbf{u}}_e \end{bmatrix} = \begin{bmatrix} 0 & -\Omega_i \mathbb{1} & \Omega_e \mathbb{1} \\ \Omega_i \mathbb{1} & -\mathbf{B}_i \times \mathbb{1} & 0 \\ -\Omega_e \mathbb{1} & 0 & -\mathbf{B}_e \times \mathbb{1} \end{bmatrix} \begin{bmatrix} \tilde{\mathbf{E}} \\ \tilde{\mathbf{u}}_i \\ \tilde{\mathbf{u}}_e \end{bmatrix},$$

where each entry in the block matrix represents a 3×3 matrix and where

$$\Omega_i = e\sqrt{\frac{n_i}{\varepsilon_0 m_i}} \quad \text{and} \quad \Omega_e = e\sqrt{\frac{n_e}{\varepsilon_0 m_e}}$$

denote the ion and electron plasma frequencies and

$$\mathbf{B}_i = \frac{e\mathbf{B}}{m_i} \quad \text{and} \quad \mathbf{B}_e = \frac{-e\mathbf{B}}{m_e}$$

are the magnetic field rescaled for ions and electrons. Their magnitudes are the ion gyrofrequency $\omega_i := |\mathbf{B}_i|$ and the electron gyrofrequency $\omega_e := |\mathbf{B}_e|$.

Solution of perpendicular system

To solve the system we decompose into parallel and perpendicular components. Without loss of generality assume that \mathbf{B} is in the direction of the third axis. Then our system decouples into a parallel system

$$\partial_t \begin{bmatrix} \tilde{\mathbf{E}}_3 \\ \tilde{\mathbf{u}}_{i3} \\ \tilde{\mathbf{u}}_{e3} \end{bmatrix} = \begin{bmatrix} 0 & -\Omega_i & \Omega_e \\ \Omega_i & 0 & 0 \\ -\Omega_e & 0 & 0 \end{bmatrix} \begin{bmatrix} \tilde{\mathbf{E}}_3 \\ \tilde{\mathbf{u}}_{i3} \\ \tilde{\mathbf{u}}_{e3} \end{bmatrix},$$

and a perpendicular system

$$\partial_t \begin{bmatrix} \tilde{\mathbf{E}}_1 \\ \tilde{\mathbf{E}}_2 \\ \tilde{\mathbf{u}}_{i1} \\ \tilde{\mathbf{u}}_{i2} \\ \tilde{\mathbf{u}}_{e1} \\ \tilde{\mathbf{u}}_{e2} \end{bmatrix}' = \begin{bmatrix} 0 & 0 & -\Omega_i & 0 & \Omega_e & 0 \\ 0 & 0 & 0 & -\Omega_i & 0 & \Omega_e \\ \Omega_i & 0 & 0 & \omega_i & 0 & 0 \\ 0 & \Omega_i & -\omega_i & 0 & 0 & 0 \\ -\Omega_e & 0 & 0 & 0 & 0 & -\omega_e \\ 0 & -\Omega_e & 0 & 0 & \omega_e & 0 \end{bmatrix} \begin{bmatrix} \tilde{\mathbf{E}}_1 \\ \tilde{\mathbf{E}}_2 \\ \tilde{\mathbf{u}}_{i1} \\ \tilde{\mathbf{u}}_{i2} \\ \tilde{\mathbf{u}}_{e1} \\ \tilde{\mathbf{u}}_{e2} \end{bmatrix}.$$

This is an antisymmetric matrix and therefore has imaginary eigenvalues and orthogonal eigenvectors. If we view the first and second components of each vector as real and imaginary parts, then this becomes a 3×3 complex linear differential equation with a skew hermitian coefficient matrix:

$$\partial_t \begin{bmatrix} \tilde{\mathbf{E}}_{\perp} \\ \tilde{\mathbf{u}}_{i\perp} \\ \tilde{\mathbf{u}}_{e\perp} \end{bmatrix} = \begin{bmatrix} 0 & -\Omega_i & \Omega_e \\ \Omega_i & -i\omega_i & 0 \\ -\Omega_e & 0 & i\omega_e \end{bmatrix} \begin{bmatrix} \tilde{\mathbf{E}}_{\perp} \\ \tilde{\mathbf{u}}_{i\perp} \\ \tilde{\mathbf{u}}_{e\perp} \end{bmatrix}, \quad (\text{C.4})$$

where we have used the natural isomorphism between $SO(2, \mathbb{R})$ and complex numbers

$$a + ib \longleftrightarrow \begin{bmatrix} a & -b \\ b & a \end{bmatrix}.$$

Observe that the parallel system is the special case of this system when the magnetic field is zero.

To generalize, suppose we want to solve the constant-coefficient linear ODE

$$\underline{x}' = \underline{A} \cdot \underline{x}.$$

Seeking a solution $\underline{x}(t) = \underline{v} \exp(\lambda t)$ (where $\underline{v} \neq \underline{0}$) leads to the eigenvector problem

$$\underline{v}\lambda = \underline{A} \cdot \underline{v}, \quad \text{i.e.,} \quad (\underline{A} - \mathbb{1}\lambda) \cdot \underline{v} = 0.$$

We recall the theory of skew-Hermitian and Hermitian matrices. Since \underline{A} is skew-Hermitian (i.e. $\underline{A}^* = -\underline{A}$, where $*$ denotes the conjugate of the transpose), $\underline{B} := i\underline{A}$ is Hermitian (i.e. $\underline{B}^* = \underline{B}$).

The eigenvalues of a Hermitian matrix are real. Indeed, assuming without loss of generality that $\underline{v}^*\underline{v} = 1$,

$$\begin{aligned} \lambda &= \underline{v}^*\underline{v}\lambda = \underline{v}^*\underline{B}\underline{v} = \underline{v}^*\underline{B}^*\underline{v} = (\underline{v}^*\underline{B}\underline{v})^* = (\underline{v}^*\underline{v}\lambda)^* \\ &= \underline{v}^*\underline{v}\lambda^* = \lambda^*, \end{aligned}$$

and eigenvectors for different eigenvalues are orthogonal:

$$\begin{aligned} \underline{v}_2^*\underline{v}_1\lambda_1 &= \underline{v}_2^*\underline{B}\underline{v}_1 = \underline{v}_2^*\underline{B}^*\underline{v}_1 = (\underline{v}_1^*\underline{B}\underline{v}_2)^* = (\underline{v}_1^*\underline{v}_2\lambda_2)^* \\ &= \underline{v}_2^*\underline{v}_1\lambda_2, \end{aligned}$$

which says that either $\underline{v}_2^*\underline{v}_1 = 0$ or $\lambda_1 = \lambda_2$.

Note that if (\underline{v}, ω) is an eigenvector-eigenvalue pair for \underline{B} then $(\underline{v}, i\omega)$ is an eigenvector-eigenvalue pair for \underline{A} .

To find the eigenstructure we solve

$$0 = (\underline{A} - i\omega) \cdot \underline{v} = \begin{bmatrix} -i\omega & -\Omega_i & \Omega_e \\ \Omega_i & -i(\omega_i + \omega) & 0 \\ -\Omega_e & 0 & i(\omega_e - \omega) \end{bmatrix} \cdot \underline{v}. \quad (\text{C.5})$$

If this has a nontrivial solution then the first row is a linear combination of the second two and we can ignore it. The second two equations then show that an eigenvector must be a multiple of the form

$$\underline{v} = \begin{bmatrix} i\beta_e\beta_i \\ \Omega_i\beta_e \\ \Omega_e\beta_i \end{bmatrix}, \quad \text{where} \quad \beta_i = \omega_i + \omega \quad \text{and} \quad \beta_e = \omega_e - \omega,$$

as is confirmed (for the last two rows) by computing $(\underline{A} - i\omega) \cdot \underline{v}$; the relation implied by the first row reveals the characteristic equation. Alternatively, the calculation

$$\underline{A} \cdot \underline{v} = \begin{bmatrix} 0 & -\Omega_i & \Omega_e \\ \Omega_i & -i\omega_i & 0 \\ -\Omega_e & 0 & i\omega_e \end{bmatrix} \cdot \begin{bmatrix} i\beta_e\beta_i \\ \Omega_i\beta_e \\ \Omega_e\beta_i \end{bmatrix} = \begin{bmatrix} -\Omega_i^2\beta_e + \Omega_e^2\beta_i \\ i\beta_i(\Omega_i\beta_e) - i\omega_i(\Omega_i\beta_e) \\ -i(\Omega_e\beta_i)\beta_e + i\omega_e(\Omega_e\beta_i) \end{bmatrix} = \underline{v}i\omega = \begin{bmatrix} i\beta_e\beta_i \\ \Omega_i\beta_e \\ \Omega_e\beta_i \end{bmatrix} i\omega$$

shows that ω must satisfy

$$\begin{aligned} \beta_e\beta_i\omega &= \Omega_i^2\beta_e - \Omega_e^2\beta_i, \\ \omega &= \beta_i - \omega_i, \\ \omega &= -\beta_e + \omega_e. \end{aligned}$$

The last two equations confirm that

$$\begin{aligned}\beta_i &= \omega_i + \omega, \\ \beta_e &= \omega_e - \omega,\end{aligned}$$

and substituting these two relationships into the first equation gives the characteristic equation that an eigenvalue must satisfy:

$$(\omega_e - \omega)(\omega_i + \omega)\omega = \Omega_i^2(\omega_e - \omega) - \Omega_e^2(\omega_i + \omega).$$

Expanding in ω and collecting like terms gives

$$0 = \omega^3 + (\omega_i - \omega_e)\omega^2 - (\omega_i\omega_e + \Omega_i^2 + \Omega_e^2)\omega + (\Omega_i^2\omega_e - \Omega_e^2\omega_i), \quad (\text{C.6})$$

which can be solved using the formula for the roots of a cubic with three real roots.

Note that the eigenvector $\underline{v} = \begin{bmatrix} i\beta_e\beta_i \\ \Omega_i\beta_e \\ \Omega_e\beta_i \end{bmatrix}$ is never zero; indeed, Ω_i and Ω_e are strictly positive, and $\beta_i = \omega_i + \omega$ and $\beta_e = \omega_e - \omega$ cannot both be zero since otherwise $\omega_i = -\omega$ and $\omega_e = \omega$, contradicting that ω_i and ω_e are both strictly positive.

By the theory of Hermitian matrices a full set of orthogonal eigenvectors must exist. Since each eigenvector has a one-dimensional eigenspace, there must be three distinct eigenvalues ω .

Decompose \underline{v} into real and imaginary parts:

$$\underline{v} = \underline{a} + i\underline{b} = \begin{bmatrix} 0 \\ \Omega_i\beta_e \\ \Omega_e\beta_i \end{bmatrix} + i \begin{bmatrix} \beta_e\beta_i \\ 0 \\ 0 \end{bmatrix}.$$

Observe that the real and imaginary parts are orthogonal. Note that

$$-i\underline{v} = \underline{b} - i\underline{a} = \begin{bmatrix} \beta_e\beta_i \\ 0 \\ 0 \end{bmatrix} - i \begin{bmatrix} 0 \\ \Omega_i\beta_e \\ \Omega_e\beta_i \end{bmatrix}$$

is also an eigenvector with eigenvalue $i\omega$ and that these two eigenvectors are orthogonal: $\underline{v}^*(-i\underline{v}) = 2\underline{a} \cdot \underline{b} = 0$. The eigenvector-eigenvalue pair $(\underline{v}, i\omega)$ corresponds to the solution

$$\begin{aligned}\underline{v} \exp(i\omega t) &= (\underline{a} + i\underline{b})(\cos \omega t + i \sin \omega t) \\ &= (\underline{a} \cos \omega t - \underline{b} \sin \omega t) + i(\underline{b} \cos \omega t + \underline{a} \sin \omega t) \\ &= \begin{bmatrix} -\beta_e\beta_i \sin \omega t \\ \Omega_i\beta_e \cos \omega t \\ \Omega_e\beta_i \cos \omega t \end{bmatrix} + i \begin{bmatrix} \beta_e\beta_i \cos \omega t \\ \Omega_i\beta_e \sin \omega t \\ \Omega_e\beta_i \sin \omega t \end{bmatrix},\end{aligned}$$

and the eigenvector-eigenvalue pair $(-i\underline{v}, i\omega)$ corresponds to the solution

$$\begin{aligned}-i\underline{v} \exp(i\omega t) &= (\underline{b} - i\underline{a})(\cos \omega t + i \sin \omega t) \\ &= (\underline{b} \cos \omega t + \underline{a} \sin \omega t) + i(\underline{b} \cos \omega t - \underline{a} \sin \omega t) \\ &= \begin{bmatrix} \beta_e\beta_i \cos \omega t \\ \Omega_i\beta_e \sin \omega t \\ \Omega_e\beta_i \sin \omega t \end{bmatrix} + i \begin{bmatrix} \beta_e\beta_i \sin \omega t \\ -\Omega_i\beta_e \cos \omega t \\ -\Omega_e\beta_i \cos \omega t \end{bmatrix}.\end{aligned}$$

Observe that in each of these solutions the ion and electron currents are in phase and the electric field is 90 degrees out of phase relative to them.

These two solutions are independent when interpreted (in $SO(2, \mathbb{R})$) as real solutions:

$$\begin{bmatrix} \tilde{\mathbf{E}}_1 \\ \tilde{\mathbf{E}}_2 \\ \tilde{\mathbf{u}}_{i1} \\ \tilde{\mathbf{u}}_{i2} \\ \tilde{\mathbf{u}}_{e1} \\ \tilde{\mathbf{u}}_{e2} \end{bmatrix} = \begin{bmatrix} -\beta_e \beta_i \sin \omega t \\ \beta_e \beta_i \cos \omega t \\ \Omega_i \beta_e \cos \omega t \\ \Omega_i \beta_e \sin \omega t \\ \Omega_e \beta_i \cos \omega t \\ \Omega_e \beta_i \sin \omega t \end{bmatrix} \quad \text{and} \quad \begin{bmatrix} \tilde{\mathbf{E}}_1 \\ \tilde{\mathbf{E}}_2 \\ \tilde{\mathbf{u}}_{i1} \\ \tilde{\mathbf{u}}_{i2} \\ \tilde{\mathbf{u}}_{e1} \\ \tilde{\mathbf{u}}_{e2} \end{bmatrix} = \begin{bmatrix} \beta_e \beta_i \cos \omega t \\ \beta_e \beta_i \sin \omega t \\ \Omega_i \beta_e \sin \omega t \\ -\Omega_i \beta_e \cos \omega t \\ \Omega_e \beta_i \sin \omega t \\ -\Omega_e \beta_i \cos \omega t \end{bmatrix}.$$

Evaluated at time 0 these solutions are

$$\begin{bmatrix} \tilde{\mathbf{E}}_1 \\ \tilde{\mathbf{E}}_2 \\ \tilde{\mathbf{u}}_{i1} \\ \tilde{\mathbf{u}}_{i2} \\ \tilde{\mathbf{u}}_{e1} \\ \tilde{\mathbf{u}}_{e2} \end{bmatrix} = \begin{bmatrix} 0 \\ \beta_e \beta_i \\ \Omega_i \beta_e \\ 0 \\ \Omega_e \beta_i \\ 0 \end{bmatrix} \quad \text{and} \quad \begin{bmatrix} \tilde{\mathbf{E}}_1 \\ \tilde{\mathbf{E}}_2 \\ \tilde{\mathbf{u}}_{i1} \\ \tilde{\mathbf{u}}_{i2} \\ \tilde{\mathbf{u}}_{e1} \\ \tilde{\mathbf{u}}_{e2} \end{bmatrix} = \begin{bmatrix} \beta_e \beta_i \\ 0 \\ 0 \\ -\Omega_i \beta_e \\ 0 \\ -\Omega_e \beta_i \end{bmatrix}.$$

Note that orthogonality of complex solutions is equivalent to orthogonality of real solutions. So we have found three distinct imaginary eigenvalues and 6 orthogonal eigenvectors for the original 6×6 antisymmetric matrix.

Parallel system

The parallel system

$$\partial_t \begin{bmatrix} \tilde{\mathbf{E}}_3 \\ \tilde{\mathbf{u}}_{i3} \\ \tilde{\mathbf{u}}_{e3} \end{bmatrix} = \begin{bmatrix} 0 & -\Omega_i & \Omega_e \\ \Omega_i & 0 & 0 \\ -\Omega_e & 0 & 0 \end{bmatrix} \begin{bmatrix} \tilde{\mathbf{E}}_3 \\ \tilde{\mathbf{u}}_{i3} \\ \tilde{\mathbf{u}}_{e3} \end{bmatrix}$$

is the special, singular case of the perpendicular system (C.4) when the magnetic field is zero.

In this case the system (C.5) becomes

$$0 = (\underline{\mathbf{A}} - i\omega) \cdot \underline{\mathbf{v}} = \begin{bmatrix} -i\omega & -\Omega_i & \Omega_e \\ \Omega_i & -i\omega & 0 \\ -\Omega_e & 0 & -i\omega \end{bmatrix} \cdot \underline{\mathbf{v}}.$$

So eigenvalue/eigenvector pairs are

$$\omega = 0, \quad \underline{\mathbf{v}} = \begin{bmatrix} 0 \\ \Omega_e \\ \Omega_i \end{bmatrix} \quad \text{and} \quad \omega = \pm \Omega_p, \quad \underline{\mathbf{v}} = \begin{bmatrix} i\omega \\ \Omega_i \\ -\Omega_e \end{bmatrix},$$

where $\Omega_p := \sqrt{\Omega_i^2 + \Omega_e^2}$ is the plasma frequency.

To get real solutions we look at the real and imaginary parts of one of the complex-conjugate pair of solutions. Choose $\omega = \Omega_p$. Write

$$\underline{\mathbf{a}} + i\underline{\mathbf{b}} = \begin{bmatrix} 0 \\ \Omega_i \\ -\Omega_e \end{bmatrix} + i \begin{bmatrix} \Omega_p \\ 0 \\ 0 \end{bmatrix}.$$

Analogous to (C.1.2), the real and imaginary parts are real solutions:

$$\begin{aligned} \underline{v} \exp(i\Omega_p t) &= (\underline{a} + i\underline{b})(\cos \Omega_p t + i \sin \Omega_p t) \\ &= (\underline{a} \cos \Omega_p t - \underline{b} \sin \Omega_p t) + i(\underline{b} \cos \Omega_p t + \underline{a} \sin \Omega_p t) \\ &= \begin{bmatrix} -\Omega_p \sin \Omega_p t \\ \Omega_i \cos \Omega_p t \\ -\Omega_e \cos \Omega_p t \end{bmatrix} + i \begin{bmatrix} \Omega_p \cos \Omega_p t \\ \Omega_i \sin \Omega_p t \\ -\Omega_e \sin \Omega_p t \end{bmatrix}. \end{aligned}$$

So three orthogonal eigensolutions are

$$\begin{bmatrix} 0 \\ \Omega_e \\ \Omega_i \end{bmatrix}, \quad \begin{bmatrix} -\Omega_p \sin \Omega_p t \\ \Omega_i \cos \Omega_p t \\ -\Omega_e \cos \Omega_p t \end{bmatrix}, \quad \begin{bmatrix} \Omega_p \cos \Omega_p t \\ \Omega_i \sin \Omega_p t \\ -\Omega_e \sin \Omega_p t \end{bmatrix}.$$

Evaluated at time 0 these solutions are

$$\begin{bmatrix} 0 \\ \Omega_e \\ \Omega_i \end{bmatrix}, \quad \begin{bmatrix} 0 \\ \Omega_i \\ -\Omega_e \end{bmatrix}, \quad \begin{bmatrix} \Omega_p \\ 0 \\ 0 \end{bmatrix}.$$

Agreement with perpendicular system. If we take the limit as $|\mathbf{B}| \rightarrow 0$ in the perpendicular system we expect the solutions to decouple into solutions for $(\tilde{\mathbf{E}}_1, \tilde{\mathbf{u}}_{i1}, \tilde{\mathbf{u}}_{e1})^T$ and $(\tilde{\mathbf{E}}_2, \tilde{\mathbf{u}}_{i2}, \tilde{\mathbf{u}}_{e2})^T$ that agree with the solutions for the parallel system. As $|\mathbf{B}| \rightarrow 0$, $\omega_i \rightarrow 0$ and $\omega_e \rightarrow 0$ and so $\beta_i \rightarrow \omega$ and $\beta_e \rightarrow -\omega$. For the limiting eigenfrequency $\omega = \Omega_p$ the parallel solutions

$$\begin{bmatrix} \tilde{\mathbf{E}}_1 \\ \tilde{\mathbf{E}}_2 \\ \tilde{\mathbf{u}}_{i1} \\ \tilde{\mathbf{u}}_{i2} \\ \tilde{\mathbf{u}}_{e1} \\ \tilde{\mathbf{u}}_{e2} \end{bmatrix} = \begin{bmatrix} -\beta_e \beta_i \sin \omega t \\ \beta_e \beta_i \cos \omega t \\ \Omega_i \beta_e \cos \omega t \\ \Omega_i \beta_e \sin \omega t \\ \Omega_e \beta_i \cos \omega t \\ \Omega_e \beta_i \sin \omega t \end{bmatrix} \quad \text{and} \quad \begin{bmatrix} \tilde{\mathbf{E}}_1 \\ \tilde{\mathbf{E}}_2 \\ \tilde{\mathbf{u}}_{i1} \\ \tilde{\mathbf{u}}_{i2} \\ \tilde{\mathbf{u}}_{e1} \\ \tilde{\mathbf{u}}_{e2} \end{bmatrix} = \begin{bmatrix} \beta_e \beta_i \cos \omega t \\ \beta_e \beta_i \sin \omega t \\ \Omega_i \beta_e \sin \omega t \\ -\Omega_i \beta_e \cos \omega t \\ \Omega_e \beta_i \sin \omega t \\ -\Omega_e \beta_i \cos \omega t \end{bmatrix}$$

when divided by $\beta_e = -\Omega_p$ become

$$\begin{bmatrix} \tilde{\mathbf{E}}_1 \\ \tilde{\mathbf{E}}_2 \\ \tilde{\mathbf{u}}_{i1} \\ \tilde{\mathbf{u}}_{i2} \\ \tilde{\mathbf{u}}_{e1} \\ \tilde{\mathbf{u}}_{e2} \end{bmatrix} = \begin{bmatrix} -\Omega_p \sin \Omega_p t \\ \Omega_p \cos \Omega_p t \\ \Omega_i \cos \Omega_p t \\ \Omega_i \sin \Omega_p t \\ -\Omega_e \cos \Omega_p t \\ -\Omega_e \sin \Omega_p t \end{bmatrix} \quad \text{and} \quad \begin{bmatrix} \tilde{\mathbf{E}}_1 \\ \tilde{\mathbf{E}}_2 \\ \tilde{\mathbf{u}}_{i1} \\ \tilde{\mathbf{u}}_{i2} \\ \tilde{\mathbf{u}}_{e1} \\ \tilde{\mathbf{u}}_{e2} \end{bmatrix} = \begin{bmatrix} \Omega_p \cos \Omega_p t \\ \Omega_p \sin \Omega_p t \\ \Omega_i \sin \Omega_p t \\ -\Omega_i \cos \Omega_p t \\ -\Omega_e \sin \Omega_p t \\ \Omega_e \cos \Omega_p t \end{bmatrix},$$

and for the limiting eigenfrequency $\omega = -\Omega_p$ the parallel solutions when divided by $\beta_e = \Omega_p$ become

$$\begin{bmatrix} \tilde{\mathbf{E}}_1 \\ \tilde{\mathbf{E}}_2 \\ \tilde{\mathbf{u}}_{i1} \\ \tilde{\mathbf{u}}_{i2} \\ \tilde{\mathbf{u}}_{e1} \\ \tilde{\mathbf{u}}_{e2} \end{bmatrix} = \begin{bmatrix} -\Omega_p \sin \Omega_p t \\ -\Omega_p \cos \Omega_p t \\ \Omega_i \cos \Omega_p t \\ -\Omega_i \sin \Omega_p t \\ -\Omega_e \cos \Omega_p t \\ \Omega_e \sin \Omega_p t \end{bmatrix} \quad \text{and} \quad \begin{bmatrix} \tilde{\mathbf{E}}_1 \\ \tilde{\mathbf{E}}_2 \\ \tilde{\mathbf{u}}_{i1} \\ \tilde{\mathbf{u}}_{i2} \\ \tilde{\mathbf{u}}_{e1} \\ \tilde{\mathbf{u}}_{e2} \end{bmatrix} = \begin{bmatrix} -\Omega_p \cos \Omega_p t \\ \Omega_p \sin \Omega_p t \\ -\Omega_i \sin \Omega_p t \\ -\Omega_i \cos \Omega_p t \\ \Omega_e \sin \Omega_p t \\ \Omega_e \cos \Omega_p t \end{bmatrix}.$$

When projected onto axis 1 these solutions all agree with the second and third eigensolutions for the parallel component, and likewise for axis 2.

For the limiting eigenfrequency $\omega = 0$, $\beta_e := \omega_e + \omega$ and $\beta_i := \omega_i - \omega$ both go to zero (since ω_e and ω_i go to zero as \mathbf{B} goes to zero). We may infer that $\beta_e \beta_i$ goes very quickly to zero. When ω is small $\cos \omega t \approx 1$ and $\sin \omega t \approx 0$. So for small magnetic field we expect

$$\begin{bmatrix} \tilde{\mathbf{E}}_1 \\ \tilde{\mathbf{E}}_2 \\ \tilde{\mathbf{u}}_{i1} \\ \tilde{\mathbf{u}}_{i2} \\ \tilde{\mathbf{u}}_{e1} \\ \tilde{\mathbf{u}}_{e2} \end{bmatrix} = \begin{bmatrix} -\beta_e \beta_i \sin \omega t \\ \beta_e \beta_i \cos \omega t \\ \Omega_i \beta_e \cos \omega t \\ \Omega_i \beta_e \sin \omega t \\ \Omega_e \beta_i \cos \omega t \\ \Omega_e \beta_i \sin \omega t \end{bmatrix} \approx \begin{bmatrix} 0 \\ 0 \\ \Omega_i \beta_e \\ 0 \\ \Omega_e \beta_i \\ 0 \end{bmatrix},$$

which agrees with the direction of the expected limiting eigensolution

$$\begin{bmatrix} \tilde{\mathbf{E}}_1 \\ \tilde{\mathbf{u}}_{i1} \\ \tilde{\mathbf{u}}_{e1} \end{bmatrix} \approx \begin{bmatrix} 0 \\ \Omega_e \\ \Omega_i \end{bmatrix}$$

if $\frac{\beta_e}{\beta_i} \rightarrow \left(\frac{\Omega_e}{\Omega_i}\right)^2$ as $\mathbf{B} \rightarrow 0$. I do not see how to show this in general, but in the neutral case where $n_i = n_e$, $\Omega_i^2 \omega_e = \Omega_e^2 \omega_i$, so the constant term vanishes in the characteristic polynomial equation (C.6), $\omega = 0$ is always an eigenvalue, and $\beta_i = \omega_i$ and $\beta_e = \omega_e$, so $\frac{\beta_e}{\beta_i} = \left(\frac{\Omega_e}{\Omega_i}\right)^2$ as needed.

C.1.3 The pressure tensor system

Ignoring interspecies collisions, the pressure tensor evolution equation (C.2) with linear closure (C.3) is

$$\partial_t \mathbb{P}_s = (q_s/m_s) \text{Sym2}(\mathbb{P}_s \times \mathbf{B}) - \tau_s^{-1} \mathbb{P}_s^\circ,$$

Observe that temperature isotropization leaves temperature invariant. So if one uses the closure (2.75),

$$\tau = \tau_0 \sqrt{m} \frac{T^{3/2}}{n}, \tag{C.7}$$

then this is a linear ODE with constant coefficients. The $\mathbb{P} \times \mathbf{B}$ term rotates the pressure tensor around the magnetic field. The relaxation term relaxes the pressure toward isotropy. These two operations commute. So we can trivially solve this ODE exactly.

C.1.4 Rotation of the pressure tensor

The $\mathbb{P} \times \mathbf{B}$ term rotates the pressure tensor around the magnetic field vector. The rate of rotation is the species gyrofrequency, so the angle of rotation of the ion pressure tensor in time interval dt is $\omega_i dt$.

Let \mathbf{e}_i denote the i th standard basis vector. Let $\mathbf{e}'_i(t)$ denote the rotated version of \mathbf{e}_i . Let $\mathbb{P}(t)$ denote the rotated pressure tensor. The pressure tensor components are $\mathbb{P}_{mn}(t) = \mathbf{e}_m \cdot \mathbb{P} \cdot \mathbf{e}_n$. The pressure tensor components are invariant in a rotating (primed) coordinate frame:

$$\mathbb{P}(t) = \mathbb{P}_{ij}(0) \mathbf{e}'_i \mathbf{e}'_j.$$

Therefore, the components in the standard basis are:

$$\mathbb{P}_{mn}(t) = \mathbb{P}_{ij}(0)(\mathbf{e}'_i \cdot \mathbf{e}_m)(\mathbf{e}'_j \cdot \mathbf{e}_n).$$

Thus, to evolve the pressure tensor \mathbb{P}_s for species s over a time interval dt , we need to apply to the standard basis vectors a rotation with rotation vector $\vec{R} := \frac{q_s}{m_s} \mathbf{B} dt$, i.e. with direction $\mathbf{b} := \mathbf{B}/|\mathbf{B}|$ and angle $\theta := \omega_s dt$, where $\omega_s := |\mathbf{B}| \frac{q_s}{m_s}$ is the gyrofrequency of species s .

To rotate a vector \mathbf{u} by the vector $\vec{R} = \theta \mathbf{b}$, where $\theta = |\vec{R}|$, decompose it into parallel and perpendicular components and rotate the perpendicular component:

$$\begin{aligned} \mathbf{u}_{\parallel} &= \mathbf{u} \cdot \mathbf{b} \mathbf{b} \\ \mathbf{u}_{\perp} &= \mathbf{u} - \mathbf{u}_{\parallel} \\ \mathbf{u} &= \mathbf{u}_{\parallel} + \mathbf{u}_{\perp} \end{aligned}$$

The rotated vector is

$$\begin{aligned} \mathbf{u}' &= \mathbf{u}_{\parallel} + (\cos \theta) \mathbf{u}_{\perp} + (\sin \theta) \mathbf{u} \times \mathbf{b} \\ &= \mathbf{u}(\cos \theta) + (1 - \cos \theta) \mathbf{u}_{\parallel} + (\sin \theta) \mathbf{u} \times \mathbf{b} \end{aligned}$$

We can avoid renormalizing the rotation vector if we use the sine cardinal function.

$$\begin{aligned} \mathbf{u}' &= \mathbf{u}(\cos \theta) + 2 \left(\sin \frac{\theta}{2} \right)^2 \mathbf{u} \cdot \mathbf{b} \mathbf{b} \\ &\quad + 2 \left(\cos \frac{\theta}{2} \right) \left(\sin \frac{\theta}{2} \right) \mathbf{u} \times \mathbf{b} \\ &= \mathbf{u}(\cos \theta) + \frac{1}{2} \left(\text{sinc} \frac{\theta}{2} \right)^2 \mathbf{u} \cdot \vec{R} \vec{R} \\ &\quad + \left(\cos \frac{\theta}{2} \right) \left(\text{sinc} \frac{\theta}{2} \right) \mathbf{u} \times \vec{R} \end{aligned}$$

Recall that \mathbf{e}'_i is the rotated version of the elementary basis vector \mathbf{e}_i . To express the components of the rotation matrix $\underline{\underline{R}}_{ij} := \mathbf{e}_i \cdot \mathbf{e}'_j$, adopt the abbreviations $c := \cos \theta$ and $s := \sin \theta$. The rotated vector is

$$\begin{aligned} \mathbf{e}'_j &= c \mathbf{e}_j + (1 - c) \mathbf{e}_j \cdot \mathbf{b} \mathbf{b} + s \mathbb{I} \times \mathbf{b} \\ &= \mathbf{e}_j \cdot \underbrace{(c \mathbb{I} + (1 - c) \mathbf{b} \mathbf{b} + s \mathbb{I} \times \mathbf{b})}_{\underline{\underline{R}}^T} \end{aligned}$$

To determine the components of $\mathbb{I} \times \mathbf{b}$, match up the identity

$$\mathbf{u} \times \mathbf{b} = \mathbf{u} \cdot \mathbb{I} \times \mathbf{b} = (\mathbb{I} \times \mathbf{b})^T \cdot \mathbf{u}$$

with the coordinate expansion

$$\mathbf{u} \times \mathbf{b} = \begin{pmatrix} u_2 b_3 - u_3 b_2 \\ u_3 b_1 - u_1 b_3 \\ u_1 b_2 - u_2 b_1 \end{pmatrix} = \underbrace{\begin{pmatrix} 0 & b_3 & -b_2 \\ -b_3 & 0 & b_1 \\ b_2 & -b_1 & 0 \end{pmatrix}}_{(\mathbb{I} \times \mathbf{b})^T} \begin{pmatrix} u_1 \\ u_2 \\ u_3 \end{pmatrix}$$

So the rotation matrix \underline{R} is:

$$\begin{bmatrix} b_1 b_1 (1 - c) + c & b_1 b_2 (1 - c) + s b_3 & b_1 b_3 (1 - c) - s b_2 \\ b_2 b_1 (1 - c) - s b_3 & b_2 b_2 (1 - c) + c & b_2 b_3 (1 - c) + s b_1 \\ b_3 b_1 (1 - c) + s b_2 & b_3 b_2 (1 - c) - s b_1 & b_3 b_3 (1 - c) + c \end{bmatrix},$$

where we are free to make the replacements

$$\begin{aligned} (1 - c) b_i b_j &= (1/2) \operatorname{sinc}^2(\theta/2) R_i R_j, \\ s b_i &= \operatorname{sinc}(\theta/2) \cos(\theta/2) R_i. \end{aligned}$$

C.2 Eigenstructure of the flux Jacobian for a ten-moment gas

I have verified the ten-moment eigenstructure calculated in this section with extensive computational checks.

C.2.1 Ten-moment system in conservation form

To perform limiting in shock-capturing methods, we consider the hyperbolic ten-moment system in balance law form (7.1),

$$\partial_t \underline{u} + \nabla \cdot \underline{\mathbf{f}} = \underline{s}, \quad (\text{C.8})$$

and compute the eigenstructure of the flux Jacobian $\partial \underline{f} / \partial \underline{u}$, where $\underline{f} := \mathbf{e}_x \cdot \underline{\mathbf{f}}$. This requires that we express the flux $\underline{\mathbf{f}}$ in terms of conserved variables.

For a single species, the full 10-moment system in balance law form specifies the flux and sources of mass density ρ , momentum $\mathbf{M} = \rho \mathbf{u}$, and the energy tensor $\mathbb{E} = \rho \mathbf{u} \mathbf{u} + \mathbb{P}$,

$$\begin{aligned} \partial_t \rho + \nabla \cdot (\rho \mathbf{u}) &= 0, \\ \partial_t (\rho \mathbf{u}) + \nabla \cdot (\rho \mathbf{u} \mathbf{u} + \mathbb{P}) &= \frac{q}{m} \rho (\mathbf{E} + \mathbf{u} \times \mathbf{B}), \\ \partial_t (\rho \mathbf{u} \mathbf{u} + \mathbb{P}) + \nabla \cdot (\rho \mathbf{u} \mathbf{u} \mathbf{u} + \operatorname{Sym}3(\mathbf{u} \mathbb{P})) &= \frac{q}{m} \operatorname{Sym}2(\rho \mathbf{u} \mathbf{E} + (\mathbb{P} + \rho \mathbf{u} \mathbf{u}) \times \mathbf{B}). \end{aligned}$$

To write this entirely in terms of conserved variables, we note that $\mathbf{u} = \mathbf{M}/\rho$ and $\mathbb{P} = \mathbb{E} - \mathbf{M} \mathbf{M}/\rho$. So

$$\begin{aligned} \partial_t \rho + \nabla \cdot \mathbf{M} &= 0, \\ \partial_t \mathbf{M} + \nabla \cdot \mathbb{E} &= \frac{q}{m} (\rho \mathbf{E} + \mathbf{M} \times \mathbf{B}), \\ \partial_t \mathbb{E} + \nabla \cdot \left(\frac{\operatorname{Sym}3(\mathbf{M} \mathbb{E})}{\rho} - \frac{2 \mathbf{M} \mathbf{M} \mathbf{M}}{\rho^2} \right) &= \frac{q}{m} \operatorname{Sym}2(\mathbf{M} \mathbf{E} + \mathbb{E} \times \mathbf{B}). \end{aligned} \quad (\text{C.9})$$

C.2.2 Quasilinear system in primitive quantities

Shock-capturing limiters need the eigenstructure of the quasilinearized system. To calculate the eigenstructure, we put the system in quasilinear form. The eigenstructure is most easily calculated in primitive variables. In primitive variables and quasilinear form the full system is

$$\begin{aligned}\partial_t \rho + \mathbf{u} \cdot \nabla \rho + \rho \nabla \cdot \mathbf{u} &= 0 \\ \partial_t \mathbf{u} + \mathbf{u} \cdot \nabla \mathbf{u} + \frac{\nabla \cdot \mathbb{P}}{\rho} &= \frac{q}{m} (\mathbf{E} + \mathbf{u} \times \mathbf{B}) \\ \partial_t \mathbb{P} + \mathbf{u} \cdot \nabla \mathbb{P} + \mathbb{P} \nabla \cdot \mathbf{u} + \text{Sym}2(\mathbb{P} \cdot \nabla \mathbf{u}) &= \frac{q}{m} \text{Sym}2(\mathbb{P} \times \mathbf{B})\end{aligned}$$

C.2.3 Quasilinear 1-D system in primitive variables

As discussed in sections 7.4.2 and 7.4.3, to perform limiting on a 2D Cartesian mesh we need to be able to compute the eigenstructure of the flux Jacobian $\underline{f}_{\underline{u}}$ for the 1D problem of the form

$$\partial_t \underline{u} + \partial_x \underline{f}(\underline{u}) = \underline{s}$$

which obtains when the problem is homogeneous perpendicular to x .

For a problem homogeneous perpendicular to the x axis equation (C.8) simplifies to

$$\partial_t \underline{u} + \partial_x \underline{f} = \underline{s}, \tag{C.10}$$

where $\underline{f} := \mathbf{e}_x \cdot \mathbf{f}$.

Assuming homogeneity in all space dimensions except the first (x), the 1-D system in primitive variables becomes

$$\begin{aligned}\partial_t \rho + u_1 \partial_x \rho + \rho \partial_x u_1 &= 0, \\ \partial_t \mathbf{u} + u_1 \partial_x \mathbf{u} + \frac{\partial_x \mathbb{P}_1}{\rho} &= \frac{q}{m} (\mathbf{E} + \mathbf{u} \times \mathbf{B}), \\ \partial_t \mathbb{P} + u_1 \partial_x \mathbb{P}_1 + \mathbb{P} \partial_x u_1 + \text{Sym}2(\mathbb{P}_1 \partial_x \mathbf{u}) &= \frac{q}{m} \text{Sym}2(\mathbb{P} \times \mathbf{B}).\end{aligned}$$

We align derivatives to prepare to put this quasilinear system in matrix form.

$$\begin{aligned}0 &= \partial_t \rho + u_1 \partial_x \rho + \rho \partial_x u_1, \\ \frac{q}{m} (\mathbf{E} + \mathbf{u} \times \mathbf{B}) &= \partial_t \mathbf{u} + u_1 \partial_x \mathbf{u} + \frac{\partial_x \mathbb{P}_1}{\rho}, \\ \frac{q}{m} \text{Sym}2(\mathbb{P} \times \mathbf{B}) &= \partial_t \mathbb{P} + \mathbb{P} \partial_x u_1 + \text{Sym}2(\mathbb{P}_1 \partial_x \mathbf{u}) + u_1 \partial_x \mathbb{P}_1.\end{aligned}$$

In matrix form this reads

$$\begin{bmatrix} \rho \\ u_1 \\ u_2 \\ u_3 \\ \mathbb{P}_{11} \\ \mathbb{P}_{12} \\ \mathbb{P}_{13} \\ \mathbb{P}_{23} \\ \mathbb{P}_{22} \\ \mathbb{P}_{33} \end{bmatrix}_t + \begin{bmatrix} u_1 & \rho & 0 & 0 & 0 & 0 & 0 & 0 & 0 & 0 \\ 0 & u_1 & 0 & 0 & 1/\rho & 0 & 0 & 0 & 0 & 0 \\ 0 & 0 & u_1 & 0 & 0 & 1/\rho & 0 & 0 & 0 & 0 \\ 0 & 0 & 0 & u_1 & 0 & 0 & 1/\rho & 0 & 0 & 0 \\ 0 & 3\mathbb{P}_{11} & 0 & 0 & u_1 & 0 & 0 & 0 & 0 & 0 \\ 0 & 2\mathbb{P}_{12} & \mathbb{P}_{11} & 0 & 0 & u_1 & 0 & 0 & 0 & 0 \\ 0 & 2\mathbb{P}_{13} & 0 & \mathbb{P}_{11} & 0 & 0 & u_1 & 0 & 0 & 0 \\ 0 & \mathbb{P}_{23} & \mathbb{P}_{31} & \mathbb{P}_{21} & 0 & 0 & 0 & u_1 & 0 & 0 \\ 0 & \mathbb{P}_{22} & 2\mathbb{P}_{12} & 0 & 0 & 0 & 0 & 0 & u_1 & 0 \\ 0 & \mathbb{P}_{33} & 0 & 2\mathbb{P}_{13} & 0 & 0 & 0 & 0 & 0 & u_1 \end{bmatrix} \cdot \begin{bmatrix} \rho \\ u_1 \\ u_2 \\ u_3 \\ \mathbb{P}_{11} \\ \mathbb{P}_{12} \\ \mathbb{P}_{13} \\ \mathbb{P}_{23} \\ \mathbb{P}_{22} \\ \mathbb{P}_{33} \end{bmatrix}_x = \frac{q}{m} \begin{bmatrix} 0 \\ E_1 + (u_2 B_3 - u_3 B_2) \\ E_2 + (u_3 B_1 - u_1 B_3) \\ E_3 + (u_1 B_2 - u_2 B_1) \\ 2(\mathbb{P}_{12} B_3 - \mathbb{P}_{13} B_2) \\ \mathbb{P}_{13} B_1 - \mathbb{P}_{23} B_2 + (\mathbb{P}_{22} - \mathbb{P}_{11}) B_3 \\ \mathbb{P}_{32} B_3 - \mathbb{P}_{12} B_1 + (\mathbb{P}_{11} - \mathbb{P}_{33}) B_2 \\ \mathbb{P}_{21} B_2 - \mathbb{P}_{31} B_3 + (\mathbb{P}_{33} - \mathbb{P}_{22}) B_1 \\ 2(\mathbb{P}_{23} B_1 - \mathbb{P}_{21} B_3) \\ 2(\mathbb{P}_{31} B_2 - \mathbb{P}_{32} B_1) \end{bmatrix}.$$

C.2.4 Eigenstructure for primitive variables

If we neglect the source term, the eigenvalues of the matrix represent wave speeds, and the corresponding eigenvectors represent the corresponding waves. Let $u := u_1 + c$ denote wave speed (i.e., c is wave speed in the reference frame moving with the fluid, where $u_1 = 0$). To find the eigenstructure of the quasilinearized system we put the matrix

$$\begin{bmatrix} -c & \rho & 0 & 0 & 0 & 0 & 0 & 0 & 0 & 0 \\ 0 & -c & 0 & 0 & 1/\rho & 0 & 0 & 0 & 0 & 0 \\ 0 & 0 & -c & 0 & 0 & 1/\rho & 0 & 0 & 0 & 0 \\ 0 & 0 & 0 & -c & 0 & 0 & 1/\rho & 0 & 0 & 0 \\ 0 & 3\mathbb{P}_{11} & 0 & 0 & -c & 0 & 0 & 0 & 0 & 0 \\ 0 & 2\mathbb{P}_{12} & \mathbb{P}_{11} & 0 & 0 & -c & 0 & 0 & 0 & 0 \\ 0 & 2\mathbb{P}_{13} & 0 & \mathbb{P}_{11} & 0 & 0 & -c & 0 & 0 & 0 \\ 0 & \mathbb{P}_{23} & \mathbb{P}_{31} & \mathbb{P}_{21} & 0 & 0 & 0 & -c & 0 & 0 \\ 0 & \mathbb{P}_{22} & 2\mathbb{P}_{12} & 0 & 0 & 0 & 0 & 0 & -c & 0 \\ 0 & \mathbb{P}_{33} & 0 & 2\mathbb{P}_{13} & 0 & 0 & 0 & 0 & 0 & -c \end{bmatrix}$$

in upper triangular form.

Right primitive eigenstructure

For the right eigenvectors we combine rows to do so:

$$\begin{bmatrix} -c & \rho & 0 & 0 & 0 & 0 & 0 & 0 & 0 & 0 \\ 0 & -\rho c^2 & 0 & 0 & c & 0 & 0 & 0 & 0 & 0 \\ 0 & 0 & -\rho c^2 & 0 & 0 & c & 0 & 0 & 0 & 0 \\ 0 & 0 & 0 & -\rho c^2 & 0 & 0 & c & 0 & 0 & 0 \\ 0 & 3\mathbb{P}_{11} & 0 & 0 & -c & 0 & 0 & 0 & 0 & 0 \\ 0 & 2\mathbb{P}_{12} & \mathbb{P}_{11} & 0 & 0 & -c & 0 & 0 & 0 & 0 \\ 0 & 2\mathbb{P}_{13} & 0 & \mathbb{P}_{11} & 0 & 0 & -c & 0 & 0 & 0 \\ 0 & \mathbb{P}_{23} & \mathbb{P}_{31} & \mathbb{P}_{21} & 0 & 0 & 0 & -c & 0 & 0 \\ 0 & \mathbb{P}_{22} & 2\mathbb{P}_{12} & 0 & 0 & 0 & 0 & 0 & -c & 0 \\ 0 & \mathbb{P}_{33} & 0 & 2\mathbb{P}_{13} & 0 & 0 & 0 & 0 & 0 & -c \end{bmatrix} \cdot \begin{bmatrix} \rho \\ u_1 \\ u_2 \\ u_3 \\ \mathbb{P}_{11} \\ \mathbb{P}_{12} \\ \mathbb{P}_{13} \\ \mathbb{P}_{23} \\ \mathbb{P}_{22} \\ \mathbb{P}_{33} \end{bmatrix}' = 0.$$

So

$$\begin{bmatrix} -c & \rho & 0 & 0 & 0 & 0 & 0 & 0 & 0 & 0 \\ 0 & 3\mathbb{P}_{11} - \rho c^2 & 0 & 0 & 0 & 0 & 0 & 0 & 0 & 0 \\ 0 & 2\mathbb{P}_{12} & \mathbb{P}_{11} - \rho c^2 & 0 & 0 & 0 & 0 & 0 & 0 & 0 \\ 0 & 2\mathbb{P}_{13} & 0 & \mathbb{P}_{11} - \rho c^2 & 0 & 0 & 0 & 0 & 0 & 0 \\ 0 & 3\mathbb{P}_{11} & 0 & 0 & -c & 0 & 0 & 0 & 0 & 0 \\ 0 & 2\mathbb{P}_{12} & \mathbb{P}_{11} & 0 & 0 & -c & 0 & 0 & 0 & 0 \\ 0 & 2\mathbb{P}_{13} & 0 & \mathbb{P}_{11} & 0 & 0 & -c & 0 & 0 & 0 \\ 0 & \mathbb{P}_{23} & \mathbb{P}_{31} & \mathbb{P}_{21} & 0 & 0 & 0 & -c & 0 & 0 \\ 0 & \mathbb{P}_{22} & 2\mathbb{P}_{12} & 0 & 0 & 0 & 0 & 0 & -c & 0 \\ 0 & \mathbb{P}_{33} & 0 & 2\mathbb{P}_{13} & 0 & 0 & 0 & 0 & 0 & -c \end{bmatrix} \cdot \begin{bmatrix} \rho \\ u_1 \\ u_2 \\ u_3 \\ \mathbb{P}_{11} \\ \mathbb{P}_{12} \\ \mathbb{P}_{13} \\ \mathbb{P}_{23} \\ \mathbb{P}_{22} \\ \mathbb{P}_{33} \end{bmatrix}' = 0.$$

Denote the fast and slow speeds by

$$c_f := \sqrt{\frac{3\mathbb{P}_{11}}{\rho}}, \quad c_s := \sqrt{\frac{\mathbb{P}_{11}}{\rho}}.$$

In the most difficult case, where $c = \pm c_f$, we have that $3\mathbb{P}_{11} - \rho c_f^2 = 0$, so $\mathbb{P}_{11} - \rho c_f^2 = -2\mathbb{P}_{11}$.

So right eigenvectors are:

| $c:$ | $\pm\sqrt{\frac{3\mathbb{P}_{11}}{\rho}}$ | $\pm\sqrt{\frac{\mathbb{P}_{11}}{\rho}}$ | 0 | | | | |
|---|--|---|---|--|--|--|--|
| $\begin{bmatrix} \rho \\ u_1 \\ u_2 \\ u_3 \\ \mathbb{P}_{11} \\ \mathbb{P}_{12} \\ \mathbb{P}_{13} \\ \mathbb{P}_{23} \\ \mathbb{P}_{22} \\ \mathbb{P}_{33} \end{bmatrix}^T$ | $\begin{bmatrix} \rho\mathbb{P}_{11} \\ \pm c_f\mathbb{P}_{11} \\ \pm c_f\mathbb{P}_{12} \\ \pm c_f\mathbb{P}_{13} \\ 3\mathbb{P}_{11}\mathbb{P}_{11} \\ 3\mathbb{P}_{12}\mathbb{P}_{11} \\ 3\mathbb{P}_{13}\mathbb{P}_{11} \\ \mathbb{P}_{23}\mathbb{P}_{11} + 2\mathbb{P}_{13}\mathbb{P}_{12} \\ \mathbb{P}_{22}\mathbb{P}_{11} + 2\mathbb{P}_{12}\mathbb{P}_{12} \\ \mathbb{P}_{33}\mathbb{P}_{11} + 2\mathbb{P}_{13}\mathbb{P}_{13} \end{bmatrix}$ | $\begin{bmatrix} 0 \\ 0 \\ \pm c_s \\ 0 \\ 0 \\ \mathbb{P}_{11} \\ 0 \\ \mathbb{P}_{13} \\ 2\mathbb{P}_{12} \\ 0 \end{bmatrix}$ | $\begin{bmatrix} 0 \\ 0 \\ 0 \\ 0 \\ 0 \\ \mathbb{P}_{11} \\ \mathbb{P}_{12} \\ 0 \\ 0 \\ 2\mathbb{P}_{13} \end{bmatrix}$ | $\begin{bmatrix} 1 \\ 0 \\ 0 \\ 0 \\ 0 \\ 0 \\ 0 \\ 0 \\ 0 \\ 0 \end{bmatrix}$ | $\begin{bmatrix} 0 \\ 0 \\ 0 \\ 0 \\ 0 \\ 0 \\ 0 \\ 1 \\ 0 \\ 0 \end{bmatrix}$ | $\begin{bmatrix} 0 \\ 0 \\ 0 \\ 0 \\ 0 \\ 0 \\ 0 \\ 0 \\ 1 \\ 0 \end{bmatrix}$ | $\begin{bmatrix} 0 \\ 0 \\ 0 \\ 0 \\ 0 \\ 0 \\ 0 \\ 0 \\ 0 \\ 1 \end{bmatrix}$ |

Left primitive eigenstructure

To find the left eigenstructure, we combine columns to reduce to upper triangular form.

$$\begin{bmatrix} \rho \\ u_1 \\ u_2 \\ u_3 \\ \mathbb{P}_{11} \\ \mathbb{P}_{12} \\ \mathbb{P}_{13} \\ \mathbb{P}_{23} \\ \mathbb{P}_{22} \\ \mathbb{P}_{33} \end{bmatrix}^T \begin{bmatrix} -c & \rho & 0 & 0 & 0 & 0 & 0 & 0 & 0 & 0 \\ 0 & -c & 0 & 0 & 1/\rho & 0 & 0 & 0 & 0 & 0 \\ 0 & 0 & -c & 0 & 0 & 1/\rho & 0 & 0 & 0 & 0 \\ 0 & 0 & 0 & -c & 0 & 0 & 1/\rho & 0 & 0 & 0 \\ 0 & 3\mathbb{P}_{11} & 0 & 0 & -c & 0 & 0 & 0 & 0 & 0 \\ 0 & 2\mathbb{P}_{12} & \mathbb{P}_{11} & 0 & 0 & -c & 0 & 0 & 0 & 0 \\ 0 & 2\mathbb{P}_{13} & 0 & \mathbb{P}_{11} & 0 & 0 & -c & 0 & 0 & 0 \\ 0 & \mathbb{P}_{23} & \mathbb{P}_{31} & \mathbb{P}_{21} & 0 & 0 & 0 & -c & 0 & 0 \\ 0 & \mathbb{P}_{22} & 2\mathbb{P}_{12} & 0 & 0 & 0 & 0 & 0 & -c & 0 \\ 0 & \mathbb{P}_{33} & 0 & 2\mathbb{P}_{13} & 0 & 0 & 0 & 0 & 0 & -c \end{bmatrix} = 0.$$

In case $c \neq 0$ this reduces to

$$\begin{bmatrix} \rho \\ u_1 \\ u_2 \\ u_3 \\ \mathbb{P}_{11} \\ \mathbb{P}_{12} \\ \mathbb{P}_{13} \\ \mathbb{P}_{23} \\ \mathbb{P}_{22} \\ \mathbb{P}_{33} \end{bmatrix}^T \begin{bmatrix} -c & 0 & 0 & 0 & 0 & 0 & 0 & 0 & 0 & 0 & 0 \\ 0 & -c & 0 & 0 & 0 & 0 & 0 & 0 & 0 & 0 & 0 \\ 0 & 0 & -c & 0 & 0 & 0 & 0 & 0 & 0 & 0 & 0 \\ 0 & 0 & 0 & -c & 0 & 0 & 0 & 0 & 0 & 0 & 0 \\ 0 & 3\mathbb{P}_{11} & 0 & 0 & 3\mathbb{P}_{11} - \rho c^2 & 0 & 0 & 0 & 0 & 0 & 0 \\ 0 & 2\mathbb{P}_{12} & \mathbb{P}_{11} & 0 & 2\mathbb{P}_{12} & \mathbb{P}_{11} - \rho c^2 & 0 & 0 & 0 & 0 & 0 \\ 0 & 2\mathbb{P}_{13} & 0 & \mathbb{P}_{11} & 2\mathbb{P}_{13} & 0 & \mathbb{P}_{11} - \rho c^2 & 0 & 0 & 0 & 0 \\ 0 & \mathbb{P}_{23} & \mathbb{P}_{31} & \mathbb{P}_{21} & \mathbb{P}_{23} & \mathbb{P}_{31} & \mathbb{P}_{21} & -c & 0 & 0 & 0 \\ 0 & \mathbb{P}_{22} & 2\mathbb{P}_{12} & 0 & \mathbb{P}_{22} & 2\mathbb{P}_{12} & 0 & 0 & -c & 0 & 0 \\ 0 & \mathbb{P}_{33} & 0 & 2\mathbb{P}_{13} & \mathbb{P}_{33} & 0 & 2\mathbb{P}_{13} & 0 & 0 & -c & 0 \end{bmatrix} = 0.$$

Here the most difficult case is $c = \pm c_s$, when $\mathbb{P}_{11} = \rho c^2$, so $3\mathbb{P}_{11} - \rho c^2 = 2\mathbb{P}_{11}$. The left eigenvectors for nonzero speeds are thus:

| $c:$ | $\pm\sqrt{\frac{3\mathbb{P}_{11}}{\rho}}$ | $\pm\sqrt{\frac{\mathbb{P}_{11}}{\rho}}$ | |
|--|---|---|---|
| $\begin{bmatrix} \rho \\ u_1 \\ u_2 \\ u_3 \\ \mathbb{P}_{11} \\ \mathbb{P}_{12} \\ \mathbb{P}_{13} \\ \mathbb{P}_{23} \\ \mathbb{P}_{22} \\ \mathbb{P}_{33} \end{bmatrix}'$ | $\propto \begin{bmatrix} 0 \\ 3\mathbb{P}_{11} \\ 0 \\ 0 \\ \pm c_f \\ 0 \\ 0 \\ 0 \\ 0 \\ 0 \end{bmatrix}$ | $\begin{bmatrix} 0 \\ -\mathbb{P}_{12}\mathbb{P}_{11} \\ \mathbb{P}_{11}\mathbb{P}_{11} \\ 0 \\ \mp c_s\mathbb{P}_{12} \\ \pm c_s\mathbb{P}_{11} \\ 0 \\ 0 \\ 0 \\ 0 \end{bmatrix}$ | $\begin{bmatrix} 0 \\ -\mathbb{P}_{13}\mathbb{P}_{11} \\ 0 \\ \mathbb{P}_{11}\mathbb{P}_{11} \\ \mp c_s\mathbb{P}_{13} \\ 0 \\ \pm c_s\mathbb{P}_{11} \\ 0 \\ 0 \\ 0 \end{bmatrix}$ |

The left eigenvectors for $c = 0$, are readily obtained from the original system:

$$\begin{bmatrix} \rho \\ u_1 \\ u_2 \\ u_3 \\ \mathbb{P}_{11} \\ \mathbb{P}_{12} \\ \mathbb{P}_{13} \\ \mathbb{P}_{23} \\ \mathbb{P}_{22} \\ \mathbb{P}_{33} \end{bmatrix}' = \alpha_1 \begin{bmatrix} 3\mathbb{P}_{11} \\ 0 \\ 0 \\ 0 \\ -\rho \\ 0 \\ 0 \\ 0 \\ 0 \\ 0 \end{bmatrix} + \alpha_2 \begin{bmatrix} 0 \\ 0 \\ 0 \\ 0 \\ 4\mathbb{P}_{12}\mathbb{P}_{13} - \mathbb{P}_{23}\mathbb{P}_{11} \\ -3\mathbb{P}_{11}\mathbb{P}_{13} \\ -3\mathbb{P}_{11}\mathbb{P}_{12} \\ 3\mathbb{P}_{11}^2 \\ 0 \\ 0 \end{bmatrix} + \alpha_3 \begin{bmatrix} 0 \\ 0 \\ 0 \\ 0 \\ 4\mathbb{P}_{12}^2 - \mathbb{P}_{11}\mathbb{P}_{22} \\ -6\mathbb{P}_{12}\mathbb{P}_{11} \\ 0 \\ 0 \\ 3\mathbb{P}_{11}^2 \\ 0 \end{bmatrix} + \alpha_4 \begin{bmatrix} 0 \\ 0 \\ 0 \\ 0 \\ 4\mathbb{P}_{13}^2 - \mathbb{P}_{11}\mathbb{P}_{33} \\ 0 \\ -6\mathbb{P}_{13}\mathbb{P}_{11} \\ 0 \\ 0 \\ 3\mathbb{P}_{11}^2 \end{bmatrix}$$

C.2.5 Eigenstructure for “conserved” variables

Let

$$\underline{q} := (\rho, \mathbf{M}, \widetilde{\mathbb{E}})^T = (\rho, \rho\mathbf{u}, \widetilde{\rho\mathbf{u}\mathbf{u}} + \widetilde{\mathbb{P}})^T$$

denote conserved quantities, and let

$$\underline{p} := (\rho, \mathbf{u}, \widetilde{\mathbb{P}})^T = (\rho, \mathbf{M}/\rho, \widetilde{\mathbb{E}} - \widetilde{\mathbf{M}\mathbf{M}}/\rho)^T$$

denote primitive quantities, where for an arbitrary symmetric tensor \mathbb{P} we define the tuple $\widetilde{\mathbb{P}}$ to be the six distinct components listed in the following order:

$$\widetilde{\mathbb{P}} := [\mathbb{P}_{11}, \mathbb{P}_{12}, \mathbb{P}_{13}, \mathbb{P}_{23}, \mathbb{P}_{22}, \mathbb{P}_{33}]^T.$$

In the one-dimensional case, the balance law states

$$\underline{q}_t + f(\underline{q})_x = s(\underline{q}).$$

General theory of state variable conversion

In quasilinear form this reads

$$\underline{q}_t + f_{\underline{q}} \cdot \underline{q}_x = s.$$

Converting to primitive variables, $\underline{q}_{\underline{p}} \cdot \underline{p}_t + f_{\underline{q}} \cdot \underline{q}_{\underline{p}} \cdot \underline{p}_x = s$, i.e.,

$$\underline{p}_t + (\underline{p}_{\underline{q}} \cdot f_{\underline{q}} \cdot \underline{q}_{\underline{p}}) \cdot \underline{p}_x = s.$$

Let \underline{q}^L and \underline{q}^R denote conservative left and right eigenvectors with eigenvalue λ :

$$\underline{f}_{\underline{q}} \cdot \underline{q}^R = \lambda \underline{q}^R, \quad \underline{q}^L \cdot \underline{f}_{\underline{q}} = \lambda \underline{q}^L.$$

Then

$$\underline{p}^R := \underline{p}_{\underline{q}} \cdot \underline{q}^R, \quad \underline{p}^L := \underline{q}^L \cdot \underline{q}_{\underline{p}}$$

are the corresponding primitive left and right eigenvectors of the primitive-variable wave propagation matrix $\underline{p}_{\underline{q}} \cdot \underline{f}_{\underline{q}} \cdot \underline{q}_{\underline{p}}$. So we can calculate conservative eigenvectors from primitive eigenvectors using the relations

$$\underline{q}^R = \underline{q}_{\underline{p}} \cdot \underline{p}^R, \quad \underline{q}^L = \underline{p}^L \cdot \underline{p}_{\underline{q}}.$$

Observe that inner product is preserved under transformation of state variables:

$$\underline{p}^L \cdot \underline{p}^R = \underline{q}^L \cdot \underline{q}_{\underline{p}} \cdot \underline{p}_{\underline{q}} \cdot \underline{q}^R = \underline{q}^L \cdot \underline{q}^R$$

Derivative of state variable transformation

To convert our primitive eigenvectors to conservative eigenvectors, we need to calculate the derivative of the conserved variables with respect to the primitive variables. The conversion matrix for right eigenvectors is

$$\underline{q}_{\underline{p}} = \partial \begin{bmatrix} \rho \\ \rho \mathbf{u} \\ \widetilde{\rho \mathbf{u} \mathbf{u}} + \widetilde{\mathbb{P}} \end{bmatrix} / \partial \begin{bmatrix} \rho \\ \mathbf{u} \\ \widetilde{\mathbb{P}} \end{bmatrix} = \begin{bmatrix} 1 & \underline{0}^T & \underline{\underline{0}}^T \\ \mathbf{u} & \rho \mathbb{1} & \underline{\underline{0}} \widetilde{\underline{0}}^T \\ \widetilde{\mathbf{u} \mathbf{u}} & \rho (\widetilde{\mathbf{u} \mathbf{u}})_{\mathbf{u}} & \underline{\underline{1}} \end{bmatrix},$$

(where $\mathbb{1}$ is the identity tensor), i.e.,

$$\underline{q}_{\underline{p}} = \partial \begin{bmatrix} \rho \\ \rho u_1 \\ \rho u_2 \\ \rho u_3 \\ \rho u_1 u_1 + \mathbb{P}_{11} \\ \rho u_1 u_2 + \mathbb{P}_{12} \\ \rho u_1 u_3 + \mathbb{P}_{13} \\ \rho u_2 u_3 + \mathbb{P}_{23} \\ \rho u_2 u_2 + \mathbb{P}_{22} \\ \rho u_3 u_3 + \mathbb{P}_{33} \end{bmatrix} / \partial \begin{bmatrix} \rho \\ u_1 \\ u_2 \\ u_3 \\ \mathbb{P}_{11} \\ \mathbb{P}_{12} \\ \mathbb{P}_{13} \\ \mathbb{P}_{23} \\ \mathbb{P}_{22} \\ \mathbb{P}_{33} \end{bmatrix} = \begin{bmatrix} 1 & 0 & 0 & 0 & 0 & 0 & 0 & 0 & 0 & 0 & 0 \\ u_1 & \rho & 0 & 0 & 0 & 0 & 0 & 0 & 0 & 0 & 0 \\ u_2 & 0 & \rho & 0 & 0 & 0 & 0 & 0 & 0 & 0 & 0 \\ u_3 & 0 & 0 & \rho & 0 & 0 & 0 & 0 & 0 & 0 & 0 \\ u_1 u_1 & 2\rho u_1 & 0 & 0 & 1 & 0 & 0 & 0 & 0 & 0 & 0 \\ u_1 u_2 & \rho u_2 & \rho u_1 & 0 & 0 & 1 & 0 & 0 & 0 & 0 & 0 \\ u_1 u_3 & \rho u_3 & 0 & \rho u_1 & 0 & 0 & 1 & 0 & 0 & 0 & 0 \\ u_2 u_3 & 0 & \rho u_3 & \rho u_2 & 0 & 0 & 0 & 1 & 0 & 0 & 0 \\ u_2 u_2 & 0 & 2\rho u_2 & 0 & 0 & 0 & 0 & 0 & 1 & 0 & 0 \\ u_3 u_3 & 0 & 0 & 2\rho u_3 & 0 & 0 & 0 & 0 & 0 & 0 & 1 \end{bmatrix}$$

The conversion matrix for left eigenvectors is slightly different:

$$\underline{p}_{\underline{q}} = \partial \begin{bmatrix} \rho \\ \mathbf{M}/\rho \\ \widetilde{\mathbb{E}} - \widetilde{\mathbf{M} \mathbf{M}}/\rho \end{bmatrix} / \partial \begin{bmatrix} \rho \\ \mathbf{M} \\ \widetilde{\mathbb{E}} \end{bmatrix} = \begin{bmatrix} 1 & \underline{0}^T & \underline{\underline{0}}^T \\ -\mathbf{M}/\rho^2 & \mathbb{1}/\rho & \underline{\underline{0}} \widetilde{\underline{0}}^T \\ \widetilde{\mathbf{M} \mathbf{M}}/\rho^2 & -(\widetilde{\mathbf{M} \mathbf{M}})_{\mathbf{M}}/\rho & \underline{\underline{1}} \end{bmatrix} = \begin{bmatrix} 1 & \underline{0}^T & \underline{\underline{0}}^T \\ -\mathbf{u}/\rho & \mathbb{1} \rho & \underline{\underline{0}} \widetilde{\underline{0}}^T \\ \widetilde{\mathbf{u} \mathbf{u}} & -(\widetilde{\mathbf{u} \mathbf{u}})_{\mathbf{u}} & \underline{\underline{1}} \end{bmatrix},$$

The fast right eigenvectors are more involved. So we just give names to the primitive components and multiply:

$$Q^R = \begin{bmatrix} 1 & 0 & 0 & 0 & 0 & 0 & 0 & 0 & 0 & 0 \\ u_1 & \rho & 0 & 0 & 0 & 0 & 0 & 0 & 0 & 0 \\ u_2 & 0 & \rho & 0 & 0 & 0 & 0 & 0 & 0 & 0 \\ u_3 & 0 & 0 & \rho & 0 & 0 & 0 & 0 & 0 & 0 \\ u_1u_1 & 2\rho u_1 & 0 & 0 & 1 & 0 & 0 & 0 & 0 & 0 \\ u_1u_2 & \rho u_2 & \rho u_1 & 0 & 0 & 1 & 0 & 0 & 0 & 0 \\ u_1u_3 & \rho u_3 & 0 & \rho u_1 & 0 & 0 & 1 & 0 & 0 & 0 \\ u_2u_3 & 0 & \rho u_3 & \rho u_2 & 0 & 0 & 0 & 1 & 0 & 0 \\ u_2u_2 & 0 & 2\rho u_2 & 0 & 0 & 0 & 0 & 0 & 1 & 0 \\ u_3u_3 & 0 & 0 & 2\rho u_3 & 0 & 0 & 0 & 0 & 0 & 1 \end{bmatrix} \cdot \begin{bmatrix} \rho' := \rho \mathbb{P}_{11} \\ \pm(u'_1 := c_f \mathbb{P}_{11}) \\ \pm(u'_2 := c_f \mathbb{P}_{12}) \\ \pm(u'_3 := c_f \mathbb{P}_{13}) \\ \mathbb{P}'_{11} := 3\mathbb{P}_{11}\mathbb{P}_{11} \\ \mathbb{P}'_{12} := 3\mathbb{P}_{12}\mathbb{P}_{11} \\ \mathbb{P}'_{13} := 3\mathbb{P}_{13}\mathbb{P}_{11} \\ \mathbb{P}'_{23} := \mathbb{P}_{23}\mathbb{P}_{11} + 2\mathbb{P}_{13}\mathbb{P}_{12} \\ \mathbb{P}'_{22} := \mathbb{P}_{22}\mathbb{P}_{11} + 2\mathbb{P}_{12}\mathbb{P}_{12} \\ \mathbb{P}'_{33} := \mathbb{P}_{33}\mathbb{P}_{11} + 2\mathbb{P}_{13}\mathbb{P}_{13} \end{bmatrix}.$$

So

$$Q^R = \begin{bmatrix} 0 & & +\rho' \\ \rho'u_1 & & \pm u'_1 \rho \\ \rho'u_2 & & \pm u'_2 \rho \\ \rho'u_3 & & \pm u'_3 \rho \\ \rho'u_1u_1 & \pm u'_1(2\rho u_1) & +\mathbb{P}'_{11} \\ \rho'u_1u_2 & \pm u'_1\rho u_2 \pm u'_2\rho u_1 + \mathbb{P}'_{12} & \\ \rho'u_1u_3 & \pm u'_1\rho u_3 \pm u'_3\rho u_1 + \mathbb{P}'_{13} & \\ \rho'u_2u_3 & \pm u'_2\rho u_3 \pm u'_3\rho u_2 + \mathbb{P}'_{23} & \\ \rho'u_2u_2 & \pm u'_2(2\rho u_2) & +\mathbb{P}'_{22} \\ \rho'u_3u_3 & \pm u'_3(2\rho u_3) & +\mathbb{P}'_{33} \end{bmatrix} = \rho \begin{bmatrix} 0 \\ \mathbb{P}_{11}u_1 \\ \mathbb{P}_{11}u_2 \\ \mathbb{P}_{11}u_3 \\ \mathbb{P}_{11}u_1(u_1 \pm 2c_f) \\ \mathbb{P}_{11}u_2(u_1 \pm c_f) \pm c_f u_1 \mathbb{P}_{12} \\ \mathbb{P}_{11}u_3(u_1 \pm c_f) \pm c_f u_1 \mathbb{P}_{13} \\ \mathbb{P}_{11}u_2u_3 \pm c_f u_3 \mathbb{P}_{12} \pm c_f u_2 \mathbb{P}_{13} \\ \mathbb{P}_{11}u_2u_2 \pm c_f u_2 2\mathbb{P}_{12} \\ \mathbb{P}_{11}u_3u_3 \pm c_f u_3 2\mathbb{P}_{13} \end{bmatrix} + \begin{bmatrix} \rho \mathbb{P}_{11} \\ \pm c_f \mathbb{P}_{11} \rho \\ \pm c_f \mathbb{P}_{12} \rho \\ \pm c_f \mathbb{P}_{13} \rho \\ 3\mathbb{P}_{11}\mathbb{P}_{11} \\ 3\mathbb{P}_{12}\mathbb{P}_{11} \\ 3\mathbb{P}_{13}\mathbb{P}_{11} \\ \mathbb{P}_{23}\mathbb{P}_{11} + 2\mathbb{P}_{13}\mathbb{P}_{12} \\ \mathbb{P}_{22}\mathbb{P}_{11} + 2\mathbb{P}_{12}\mathbb{P}_{12} \\ \mathbb{P}_{33}\mathbb{P}_{11} + 2\mathbb{P}_{13}\mathbb{P}_{13} \end{bmatrix}.$$

Left eigenvectors for conserved variables

Similarly, let P^L denote a matrix of primitive left eigenvectors. We can compute conservative left eigenvectors from the primitive left eigenvectors by the relationship

$$Q^L = P^L \cdot \underline{p}_q,$$

where Q^L denotes a matrix of conservative left eigenvectors.

To avoid big expressions, we give a simple name to each nonzero matrix component before multiplying the matrices.

For the slow eigenvector pair for \mathbb{P}_{12} and \mathbb{P}_{13} define

$$\begin{aligned} u' &:= \mathbb{P}_{11}\mathbb{P}_{11} \\ \mathbb{P}' &:= c_s \mathbb{P}_{11}, \end{aligned}$$

and define

$$\begin{aligned} u'_{1b} &:= -\mathbb{P}_{12}\mathbb{P}_{11}, & u'_{1c} &:= -\mathbb{P}_{13}\mathbb{P}_{11}, \\ u'_{2b} &:= u', & u'_{3c} &:= u', \\ \mathbb{P}'_{11b} &:= -c_s \mathbb{P}_{12}, & \mathbb{P}'_{11c} &:= -c_s \mathbb{P}_{13}, \\ \mathbb{P}'_{12b} &:= \mathbb{P}', & \mathbb{P}'_{13c} &:= \mathbb{P}'. \end{aligned}$$

So in terms of these quantities the left eigenvectors are

$$Q^L = \begin{bmatrix} \begin{bmatrix} 0 \\ 3\mathbb{P}_{11} \\ 0 \\ 0 \\ \pm c_f \\ 0 \\ 0 \\ 0 \\ 0 \\ 0 \end{bmatrix} \begin{bmatrix} 0 \\ u'_{1b} \\ u' \\ 0 \\ \pm \mathbb{P}'_{11b} \\ \pm \mathbb{P}' \\ 0 \\ 0 \\ 0 \\ 0 \end{bmatrix} \begin{bmatrix} 0 \\ u'_{1c} \\ 0 \\ u' \\ \pm \mathbb{P}'_{11c} \\ \pm \mathbb{P}' \\ 0 \\ 0 \\ 0 \\ 0 \end{bmatrix} \end{bmatrix}^T \cdot \begin{bmatrix} 1 & 0 & 0 & 0 & 0 & 0 & 0 & 0 & 0 & 0 & 0 \\ -u_1/\rho & 1/\rho & 0 & 0 & 0 & 0 & 0 & 0 & 0 & 0 & 0 \\ -u_2/\rho & 0 & 1/\rho & 0 & 0 & 0 & 0 & 0 & 0 & 0 & 0 \\ -u_3/\rho & 0 & 0 & 1/\rho & 0 & 0 & 0 & 0 & 0 & 0 & 0 \\ u_1u_1 & -2u_1 & 0 & 0 & 1 & 0 & 0 & 0 & 0 & 0 & 0 \\ u_1u_2 & -u_2 & -u_1 & 0 & 0 & 1 & 0 & 0 & 0 & 0 & 0 \\ u_1u_3 & -u_3 & 0 & -u_1 & 0 & 0 & 1 & 0 & 0 & 0 & 0 \\ u_2u_3 & 0 & -u_3 & -u_2 & 0 & 0 & 0 & 1 & 0 & 0 & 0 \\ u_2u_2 & 0 & -2u_2 & 0 & 0 & 0 & 0 & 0 & 1 & 0 & 0 \\ u_3u_3 & 0 & 0 & -2u_3 & 0 & 0 & 0 & 0 & 0 & 0 & 1 \end{bmatrix}.$$

So

$$Q^L = \begin{bmatrix} \begin{bmatrix} -3\frac{\mathbb{P}_{11}}{\rho}u_1 \pm c_f u_1 u_1 \\ 3\frac{\mathbb{P}_{11}}{\rho} \mp 2c_f u_1 \\ 0 \\ 0 \\ \pm c_f \\ 0 \\ 0 \\ 0 \\ 0 \\ 0 \end{bmatrix} \begin{bmatrix} \frac{-u'_{1b}u_1 - u'u_2}{\rho} \pm u_1u_1\mathbb{P}'_{11b} \pm u_1u_2\mathbb{P}' \\ u'_{1b}/\rho \mp 2u_1\mathbb{P}'_{11b} \mp u_2\mathbb{P}' \\ u'/\rho \mp u_1\mathbb{P}' \\ 0 \\ \pm \mathbb{P}'_{11b} \\ \pm \mathbb{P}' \\ 0 \\ 0 \\ 0 \\ 0 \end{bmatrix} \begin{bmatrix} \frac{-u'_{1c}u_1 - u'u_3}{\rho} \pm u_1u_1\mathbb{P}'_{11c} \pm u_1u_3\mathbb{P}' \\ u'_{1c}/\rho \mp 2u_1\mathbb{P}'_{11c} \mp u_3\mathbb{P}' \\ 0 \\ u'/\rho \mp u_1\mathbb{P}' \\ \pm \mathbb{P}'_{11c} \\ 0 \\ \pm \mathbb{P}' \\ 0 \\ 0 \\ 0 \end{bmatrix} \end{bmatrix}^T$$

For the $c = 0$ eigenvectors define

$$\mathbb{P}'_{11e} = 4\mathbb{P}_{12}\mathbb{P}_{13} - \mathbb{P}_{32}\mathbb{P}_{11},$$

$$\mathbb{P}'_{12e} := -3\mathbb{P}_{11}\mathbb{P}_{13},$$

$$\mathbb{P}'_{13e} := -3\mathbb{P}_{11}\mathbb{P}_{12},$$

and define

$$\mathbb{P}'_{11f} := 4\mathbb{P}_{12}^2 - \mathbb{P}_{11}\mathbb{P}_{22},$$

$$\mathbb{P}'_{11g} := 4\mathbb{P}_{13}^2 - \mathbb{P}_{11}\mathbb{P}_{33},$$

$$\mathbb{P}'_{12f} := -6\mathbb{P}_{12}\mathbb{P}_{11},$$

$$\mathbb{P}'_{13g} := -6\mathbb{P}_{13}\mathbb{P}_{11}.$$

The left eigenvectors for $c = 0$ are given by

$$Q^L = \begin{bmatrix} \begin{bmatrix} 3\mathbb{P}_{11} \\ 0 \\ 0 \\ 0 \\ -\rho \\ 0 \\ 0 \\ 0 \\ 0 \\ 0 \end{bmatrix} \begin{bmatrix} 0 \\ 0 \\ 0 \\ 0 \\ \mathbb{P}'_{11e} \\ \mathbb{P}'_{12e} \\ \mathbb{P}'_{13e} \\ 3\mathbb{P}_{11}^2 \\ 0 \\ 0 \end{bmatrix} \begin{bmatrix} 0 \\ 0 \\ 0 \\ 0 \\ \mathbb{P}'_{11f} \\ \mathbb{P}'_{12f} \\ 0 \\ 3\mathbb{P}_{11}^2 \\ 0 \end{bmatrix} \begin{bmatrix} 0 \\ 0 \\ 0 \\ 0 \\ \mathbb{P}'_{11g} \\ 0 \\ \mathbb{P}'_{13g} \\ 0 \\ 3\mathbb{P}_{11}^2 \\ 3\mathbb{P}_{11}^2 \end{bmatrix} \end{bmatrix}^T \cdot \begin{bmatrix} 1 & 0 & 0 & 0 & 0 & 0 & 0 & 0 & 0 & 0 & 0 \\ -u_1/\rho & 1/\rho & 0 & 0 & 0 & 0 & 0 & 0 & 0 & 0 & 0 \\ -u_2/\rho & 0 & 1/\rho & 0 & 0 & 0 & 0 & 0 & 0 & 0 & 0 \\ -u_3/\rho & 0 & 0 & 1/\rho & 0 & 0 & 0 & 0 & 0 & 0 & 0 \\ u_1u_1 & -2u_1 & 0 & 0 & 1 & 0 & 0 & 0 & 0 & 0 & 0 \\ u_1u_2 & -u_2 & -u_1 & 0 & 0 & 1 & 0 & 0 & 0 & 0 & 0 \\ u_1u_3 & -u_3 & 0 & -u_1 & 0 & 0 & 1 & 0 & 0 & 0 & 0 \\ u_2u_3 & 0 & -u_3 & -u_2 & 0 & 0 & 0 & 1 & 0 & 0 & 0 \\ u_2u_2 & 0 & -2u_2 & 0 & 0 & 0 & 0 & 0 & 1 & 0 & 0 \\ u_3u_3 & 0 & 0 & -2u_3 & 0 & 0 & 0 & 0 & 0 & 0 & 1 \end{bmatrix}.$$

So the $c = 0$ left eigenvectors are

$$\underline{q}^L = \begin{bmatrix} 3\mathbb{P}_{11} - \rho u_1 u_1 \\ 2\rho u_1 \\ 0 \\ 0 \\ -\rho \\ 0 \\ 0 \\ 0 \\ 0 \\ 0 \\ 0 \end{bmatrix}, \begin{bmatrix} u_1 u_1 \mathbb{P}'_{11e} + u_1 u_2 \mathbb{P}'_{12e} + u_1 u_3 \mathbb{P}'_{13e} + 3u_2 u_3 \mathbb{P}_{11}^2 \\ -(2u_1 \mathbb{P}'_{11e} + u_2 \mathbb{P}'_{12e} + u_3 \mathbb{P}'_{13e}) \\ -(u_1 \mathbb{P}'_{12e} + 3u_3 \mathbb{P}_{11}^2) \\ -(u_1 \mathbb{P}'_{13e} + 3u_2 \mathbb{P}_{11}^2) \\ \mathbb{P}'_{11e} \\ \mathbb{P}'_{12e} \\ \mathbb{P}'_{13e} \\ 3\mathbb{P}_{11}^2 \\ 0 \\ 0 \end{bmatrix},$$

$$\begin{bmatrix} u_1 u_1 \mathbb{P}'_{11f} + u_1 u_2 \mathbb{P}'_{12f} + u_2 u_2 3\mathbb{P}_{11}^2 \\ -(2u_1 \mathbb{P}'_{11f} + u_2 \mathbb{P}'_{12f}) \\ -(u_1 \mathbb{P}'_{12f} + 6u_2 \mathbb{P}_{11}^2) \\ 0 \\ \mathbb{P}'_{11f} \\ \mathbb{P}'_{12f} \\ 0 \\ 0 \\ 3\mathbb{P}_{11}^2 \\ 0 \end{bmatrix}, \begin{bmatrix} u_1 u_1 \mathbb{P}'_{11g} + u_1 u_3 \mathbb{P}'_{13g} + u_3 u_3 3\mathbb{P}_{11}^2 \\ -(2u_1 \mathbb{P}'_{11g} + u_3 \mathbb{P}'_{13g}) \\ 0 \\ -(u_1 \mathbb{P}'_{13g} + 6u_3 \mathbb{P}_{11}^2) \\ \mathbb{P}'_{11g} \\ 0 \\ \mathbb{P}'_{13g} \\ 0 \\ 0 \\ 3\mathbb{P}_{11}^2 \end{bmatrix}.$$

Bibliography

- [1] P. ANDRIES, P. LE TALLEC, J.-P. PERLAT, AND B. PERTHAME, *The Gaussian-BGK model of Boltzmann equation with small prandtl number*, Tech. Rep. 3716, INRIA, 1999.
- [2] R. BALESCU, *Transport Processes in Plasmas*, vol. 1. Classical transport theory, North-Holland, 1988.
- [3] N. BESSHO AND A. BHATTACHARJEE, *Collisionless reconnection in an electron-positron plasma*, Phys. Rev. Letters, 95 (2005), p. 245001.
- [4] —, *Fast collisionless reconnection in electron-positron plasmas*, Physics of Plasmas, 14 (2007), p. 056503.
- [5] —, *Fast magnetic reconnection in low-density electron-positron plasmas*, Phys. Plasmas, 17 (2010).
- [6] J. BIRN, J. DRAKE, M. SHAY, B. ROGERS, R. DENTON, M. HESSE, M. KUZNETSOVA, Z. MA, A. BHATTACHARJEE, A. OTTO, AND P. PRITCHETT, *Geospace environmental modeling (GEM) magnetic reconnection challenge*, Journal of Geophysical Research – Space Physics, 106 (2001), pp. 3715–3719.
- [7] J. BIRN AND E. PRIEST, *Reconnection of Magnetic Fields: Magnetohydrodynamics and Collisionless Theory and Observations*, Cambridge University Press, 2007.
- [8] J. U. BRACKBILL. private communication, 2011.
- [9] J. U. BRACKBILL, *A comparison of fluid and kinetic models for steady magnetic reconnection*, Physics of Plasmas, 18 (2011), pp. 1–9.
- [10] S. I. BRAGINSKII, *Transport Processes in a Plasma*, Reviews of Plasma Physics, 1 (1965), pp. 205–311.
- [11] S. V. BULANOV, S. I. SYROVATSKY, AND J. SAKAI, *Stabilizing influence of plasma flow on dissipative tearing instability*, Sov. Phys. JETP Lett., 28 (1978), pp. 177–179.
- [12] L. CHACÓN, A. N. SIMAKOV, V. S. LUKIN, AND A. ZOCCO, *Fast reconnection in nonrelativistic 2D electron-positron plasmas*, Phys. Rev. Letters, 101 (2008), p. 025003.
- [13] B. COCKBURN AND C.-W. SHU, *The Runge-Kutta discontinuous Galerkin method for conservation laws V: Multidimensional systems*, J. Comp. Phys., 141 (1998), pp. 199–224.
- [14] J. W. DUNGEY, *Conditions for the occurrence of electrical discharges in astrophysical systems.*, Phil. Mag., 44 (1953), pp. 725–738.
- [15] H. P. FURTH, J. KILLEEN, AND M. N. ROSENBLUTH, *Finite-resistivity of a sheet pinch*, Phys. Fluids, 6 (1963), pp. 459–484.
- [16] S. GOTTLIEB AND C.-W. SHU, *Total variation diminishing Runge-Kutta schemes*, Math. Comp., 67 (1998), pp. 73–85.

- [17] D. J. GRIFFITHS, *Introduction to Electrodynamics*, Prentice Hall, 2nd ed., 1989.
- [18] A. HAKIM, *High Resolution Wave Propagation Schemes for Two-Fluid Plasma Simulations*, PhD thesis, University of Washington, 2006.
- [19] A. HAKIM, *Extended MHD modelling with the ten-moment equations*, Journal of Fusion Energy, 27 (2008), pp. 36–43.
- [20] A. HAKIM, J. LOVERICH, AND U. SHUMLAK, *A high-resolution wave propagation scheme for ideal two-fluid plasma equations*, J. Comp. Phys., 219 (2006), pp. 418–442.
- [21] R. D. HAZELTINE AND J. D. MEISS, *Plasma Confinement*, Addison-Wesley, 1992.
- [22] R. D. HAZELTINE AND F. L. WAELBROECK, *The Framework of Plasma Physics*, Westview Press, 2004.
- [23] M. HESSE, M. KUZNETSOVA, AND J. BIRN, *The role of electron heat flux in guide-field magnetic reconnection*, Physics of Plasmas, 11 (2004), pp. 5387–5397.
- [24] M. HESSE AND D. WINSKE, *Hybrid simulations of collisionless ion tearing*, Geophys. Res. Lett., 20 (1993), pp. 1207–1210.
- [25] ———, *Hybrid simulations of collisionless ion tearing*, Geophysical Research Letters, 20 (1993), pp. 1207–1210.
- [26] L. H. HOLWAY, *New statistical models for kinetic theory: Methods of construction*, The Physics of Fluids, 9 (1966), pp. 1658–1673.
- [27] G. HORNIG AND K. SCHINDLER, *Magnetic topology and the problem of its invariant definition*, Phys. Plasmas, 3 (1996), p. 781.
- [28] M. HOSSEINPOUR, N. BIAN, AND G. VEKSTEIN, *Two-fluid regimes of the resistive and collisionless tearing instability*, Phys. Plasmas, 16 (2009).
- [29] Y.-M. HUANG AND A. BHATTACHARJEE, *Scaling laws of resistive magnetohydrodynamic reconnection in the high-lundquist-number, plasmoid-unstable regime*, Phys. Plasmas, 17 (2010).
- [30] Y.-M. HUANG, A. BHATTACHARJEE, AND B. P. SULLIVAN, *Onset of fast reconnection in Hall magnetohydrodynamics mediated by the plasmoid instability*, Phys. Plasmas (submitted), (2010).
- [31] S. H. JEFFREYS, *On isotropic tensors*, Proc. Camb. Phil. Soc., 73 (1973), pp. 173–176.
- [32] E. A. JOHNSON AND J. A. ROSSMANITH, *Ten-moment two-fluid plasma model agrees well with PIC/Vlasov in GEM problem*. Submitted to the 13th International Conference on Hyperbolic Problems, 2010.
- [33] L. KRIVODONOVA, *Limiters for high-order discontinuous Galerkin methods*, J. Comp. Phys., 226 (2007), pp. 879–896.
- [34] H. KUMAR, *Finite volume methods for the two-fluid MHD equations*, Tech. Rep. 2010–29, Hyp 2010 Beijing and ETH Seminar for Applied Mathematics, September 2010.

- [35] M. M. KUZNETSOVA, M. HESSE, AND D. WINSKE, *Collisionless reconnection supported by nongyrotopropic pressure effects in hybrid and particle simulations*, Journal of Geophysical Research, 106 (2001), pp. 3799–3810.
- [36] J. M. LEE, *Introduction to Smooth Manifolds*, Springer-Verlag, 2003.
- [37] R. LEVEQUE, *Finite Volume Methods for Hyperbolic Problems*, Cambridge University Press, 2002.
- [38] C. D. LEVERMORE. private communication, 2011.
- [39] N. F. LOUREIRO, A. A. SCHEKOCHIHIN, AND S. C. COWLEY, *Instability of current sheets and formation of plasmoid chains*, Physics of Plasmas, 14 (2007).
- [40] J. LOVERICH, A. HAKIM, AND U. SHUMLAK, *A discontinuous Galerkin method for ideal two-fluid plasma equations*, Commun. Comput. Phys., 9 (2011), pp. 240–268.
- [41] J. LYMAN SPITZER, *Physics of Fully Ionized Gases*, Interscience Publishers, New York, second revised edition ed., 1962.
- [42] J. G. McDONALD, *Extended Fluid-Dynamic Modelling for Numerical Solution of Micro-Scale Flows*, PhD thesis, University of Toronto, 2011.
- [43] J. G. McDONALD AND C. P. T. GROTH, *Extended fluid-dynamic model for micron-scale flows based on Gaussian moment closure*, 46th AIAA Aerospace Sciences Meeting and Exhibit, (2008).
- [44] J. G. McDONALD AND C. P. T. GROTH, *Physically-realizable hyperbolic moment closures for predicting non-equilibrium gaseous flows*, in 17th Annual Conference of the CFD Society of Canada, CFD Society of Canada, May 2009.
- [45] V. V. MIRNOV, C. C. HEGNA, AND S. C. PRAGER, *Two-fluid tearing instability in force-free magnetic configuration*, Phys. Plasmas, 11 (2004), pp. 4468–4482.
- [46] K. MUIRA AND C. P. T. GROTH, *Development of two-fluid magnetohydrodynamics model for non-equilibrium anisotropic plasma flows*, Miami, Florida, June 2007, AIAA, 38th AIAA Plasmadynamics and Lasers Conference.
- [47] N. A. MURPHY, *Simulation and Analysis of Magnetic Reconnection in a Laboratory Plasma Astrophysics Experiment*, PhD thesis, UW–Madison, 2009.
- [48] N. A. MURPHY AND C. R. SOVINEC, *Global axisymmetric simulations of two-fluid reconnection in an experimentally relevant geometry*, Phys. Plasmas, 15 (2008).
- [49] E. N. PARKER, *Sweet’s mechanism for merging magnetic fields in conducting fluids*, J. Geophys. Res., 62 (1957), pp. 509–520.
- [50] —, *The solar flare phenomenon and theory of reconnection and annihilation of magnetic fields*, Astrophys. J. Suppl., 8 (1963), pp. 177–211.
- [51] H. E. PETSCHKEK, *Magnetic field annihilation*, in Physics of Solar Flares, W. N. Hess, ed., NASA SP-50, Washington, D.C., 1964, pp. 425–439.

- [52] E. R. PRIEST AND T. G. FORBES, *Magnetic Reconnection: MHD Theory and Applications*, Cambridge University Press, 2000.
- [53] P. L. PRITCHETT, *Geospace Environmental Modeling magnetic reconnection challenge: Simulations with a full particle code*, *Journal of Geophysical Research – Space Physics*, 106 (2001), pp. 3783–3798.
- [54] T. SATO AND T. HAYASHI, *Externally driven magnetic reconnection and a powerful magnetic energy converter*, *Phys. Fluids*, 22 (1979), pp. 1189–1202.
- [55] H. SCHMITZ AND R. GRAUER, *Darwin–Vlasov simulations of magnetised plasmas*, *J. Comp. Phys.*, 214 (2006), pp. 738–756.
- [56] M. A. SHAY, J. F. DRAKE, B. N. ROGERS, AND R. E. DENTON, *Alfvénic collisionless magnetic reconnection and the Hall term*, *J. Geophys. Res. – Space Physics*, 106 (2001), pp. 3759–3772.
- [57] P. A. STURROCK, *Plasma Physics: An Introduction to the Theory of Astrophysical, Geophysical and Laboratory Plasmas*, Cambridge University Press, 1994.
- [58] P. A. SWEET, *The neutral point theory of solar flares*, in *Electromagnetic Phenomena in Cosmical Physics*, B. Lehnert, ed., IAU Symp. 6, Cambridge University Press, 1958, pp. 123–134.
- [59] T. TERASAWA, *Hall current effect on tearing mode instability*, *Geophys. Res. Lett.*, 10 (1983), pp. 475–478.
- [60] M. TORRILHON, *Hyperbolic moment equations in kinetic gas theory based on multi-variate pearson-iv-distributions*, *Commun. Comput. Phys.*, 7 (2010), pp. 639–673.
- [61] V. M. VASYLIUNAS, *Theoretical models of magnetic field line merging, 1*, *Reviews of Geophysics and Space Physics*, 13 (1975), pp. 303–336.
- [62] L. C. WOODS, *Physics of Plasmas*, WILEY-VCH, 2004.
- [63] X. ZHANG AND C.-W. SHU, *On positivity preserving high order discontinuous Galerkin schemes for compressible Euler equations on rectangular meshes*, *Journal of Computational Physics*, (2010).
- [64] E. ZWEIBEL AND M. YAMADA, *Magnetic reconnection in astrophysical and laboratory plasmas*, *Annu. Rev. Astron. Astrophys.*, 47 (2009), pp. 291–332.

Vocabulary Glossary

Boltzmann equation conservation of particle density in phase space. [1](#), [19](#), [23](#)

collision operator the error when the particle density is substituted into the Vlasov equation. That is, it is assumed that particle density satisfies an evolution equation of the form

$$\partial_t f + \mathbf{v} \cdot \nabla_{\mathbf{x}} f + a \cdot \nabla_{\mathbf{v}} f = C,$$

where C is the collision operator. See section [1.1](#). [1](#)

five-moment model the [Maxwellian-moment model](#). [1](#)

Gaussian-moment model a model of a gas which evolves all quadratic velocity moments. In three dimensions of space the Gaussian-moment model evolves ten monomial moments and is therefore also referred to as the [ten-moment model](#). [1](#)

kinetic equation the [Boltzmann equation](#). [1](#), [23](#)

Maxwellian-moment model a model of a gas which evolves the subquadratic monomial moments (mass and momentum) and the energy (a quadratic moment). In three dimensions of space the Maxwellian-moment model evolves five monomial moments and is therefore also referred to as the [five-moment model](#). [1](#)

quasineutrality the assumption that the net charge density is approximately zero. [4](#), [51](#), [55](#)

ten-moment model the [Gaussian-moment model](#). [1](#)

Symbol Glossary

- 0 origin (used in the context of reconnection, usually the X-point). 57
- \vdots triple dot product of tensors, e.g. $A \vdots B = A_{ijk}B_{ijk}$. 31
- \cdot double dot product of tensors, defined by contracting two adjacent indices, e.g. $A : B = A_{ij}B_{ij}$. 27
- ∇ del operator. 18
- \diamond diamond product of tensors, defined by $(A \diamond B)_{ijkl} = A_{ik}B_{lj}$, i.e., $A \diamond B = A \tilde{\otimes} B^T$. 39
- $\nabla \cdot$ divergence operator. 18
- ∇^2 Laplacian operator, $\sum_i \partial_{x_i}^2$. 66
- $\langle \chi \rangle$ statistical average over velocity space of χ . 24
- \parallel as a subscript on a vector, denotes the component parallel to the magnetic field direction \mathbf{b} ; as a superscript denotes the component parallel to the out-of-plane direction $\mathbf{e}^\parallel = \mathbf{e}_z$. 60
- \perp as a subscript on a vector, denotes the component perpendicular to the magnetic field direction \mathbf{b} ; as a superscript denotes the component perpendicular to the out-of-plane direction. 60
- $\tilde{\otimes}$ splice product of tensors, defined in section A.5.1. 128
- $\tilde{\vee}$ splice symmetric product of tensors, defined in section A.5.1. 128
- \vee vee product; rescales the symmetric product $\underline{\vee}$ so that the vee product of symmetric tensors is the sum over all distinguishable permutations of the indices of their tensor product; see section 2.3.1. 25
- $\underline{\vee}$ symmetric product of tensors, defined in section 2.3.1. 25
- γ Lorentz factor (derivative of time with respect to proper time). 23
- $\bar{\delta}_t$ bulk derivative; $\bar{\delta}_t^s \alpha := \partial_t \alpha + \nabla \cdot (\mathbf{u}_s \alpha)$. 11, 12
- δ_s inertial length. 6, 124
- ϵ_0 permittivity of space. 23
- η resistivity. 52
- $\boldsymbol{\eta}$ resistivity tensor. 11–14
- Θ_s pseudo temperature tensor, \mathbb{T}_s/m_s . 27, 40, 115
- θ_s pseudo temperature, T_s/m_s . 27, 40, 115
- λ_D Debye length, $\sqrt{\frac{\epsilon_0 T_0}{n_0 e^2}}$. 4, 124
- μ the viscosity, $p\tau$. 33, 46, 126
- $\boldsymbol{\mu}$ the viscosity tensor. 33
- $\check{\mu}$ the reduced mass, $\frac{m_i m_e}{m_e + m_e}$. 52
- $\tilde{\boldsymbol{\mu}}$ the viscosity shape tensor, defined by $\boldsymbol{\mu} = \mu \tilde{\boldsymbol{\mu}}$. 33
- $\tilde{\check{\mu}} = \check{\mu}/e$. 52
- $\boldsymbol{\pi}$ pressure tensor shape, \mathbb{P}/p . 36
- $\boldsymbol{\pi}^\circ$ deviatoric part of $\boldsymbol{\pi}$, i.e. \mathbb{P}°/p . 32, 34, 36
- ϖ gyrofrequency per pressure isotropization rate, $\tau\omega_c$. 38
- $\tilde{\varpi}$ gyrofrequency per heat flux relaxation rate, $\tilde{\tau}\omega_c$. 45, 112
- ρ mass per volume. 20, 26
- σ charge per volume. 23
- τ relaxation/collision period for deviatoric pressure and for the BGK collision operator. 33, 34, 46
- $\tilde{\tau}$ relaxation period for heat flux and for the Gaussian-BGK collision operator; $\tilde{\tau} = \tau/\text{Pr}$. 40

- ω_p plasma frequency; $\omega_{ps}^2 = \frac{n_0 e^2}{\epsilon_0 m_s}$. 4, 124
- ω_c gyrofrequency (alias cyclotron frequency), $q|\mathbf{B}|/m$. 38
- B** magnetic field. 23
- b** magnetic field direction, $\mathbf{B}/|\mathbf{B}|$. 38
- C collision operator. See note at [collision operator](#). 19
- C^T total collision operator, e.g. $C^T_i = C_i + C_{ie}$. See note at [collision operator](#). 1
- c speed of light. 23
- \mathbf{c}_s velocity in the reference frame of the fluid velocity of species s (an independent variable or the thermal velocity of a particle). 20
- dm species mass difference, $m_i - m_e$. 52
- $d\tilde{m} = dm/e$. 52
- \mathbb{E} energy tensor. 26
- E** electric field. 23
- \mathcal{E}_s energy per volume of species s . 20, 26
- e charge on a proton. 52
- \mathbf{e} energy tensor per mass. 26
- e_s energy per mass of species s . 20, 26
- \mathbf{e} strain rate, $\text{Sym}(\nabla \mathbf{u})$. 32, 126
- \mathbf{e}_i elementary basis vector aligned with axis i . 18
- \mathbf{e}° deviatoric strain rate $\mathbf{e} - \mathbf{1} \nabla \cdot \mathbf{u}/3$. 32, 126
- f_s mass density of species s in phase space (\mathbf{x}, \mathbf{v}) . 19, 23
- J** current per volume. 23
- K** heat tensor conductivity tensor. 136
- k heat conductivity. 32, 46
- $\widetilde{\mathbf{K}}$ heat tensor conductivity tensor shape, defined by $\mathbf{K} = \mathbf{K} \widetilde{\mathbf{K}}$. 136
- M** momentum per volume. 20, 26
- m_s particle mass of species s . 23
- m_e electron mass. 52
- $\tilde{m}_e = m_e/e$. 52
- m_i ion mass. 52
- $\tilde{m}_i = m_i/e$. 52
- n particle number per volume (of either species in a neutral two-species plasma with equal charge on each species). 26, 52
- n_e electron number density. 52
- n_i ion number density. 52
- \mathbb{P} pressure tensor. 26
- p scalar pressure. 27
- p particle index. 23
- \mathbb{P}° deviatoric part of pressure tensor. 12, 14, 33, 37
- \mathbb{P}^d drift pressure tensor. 54
- Pr Prandtl number. 40, 45, 46, 126, 127
- \mathbb{Q}_s tensor heating due to collisions with other species; $\mathbb{Q}_s = \mathbb{Q}_s^f + \mathbb{Q}_s^t$. 26
- Q_s heat source due to collisions with other species; $Q_s = Q_s^f + Q_s^t$. 11–14, 26
- q particle charge. 23, 52
- \mathbf{q}_s heat flux tensor. 11–14, 26
- \mathbf{q} heat flux. 14, 26
- \mathbf{q}° deviatoric heat flux tensor, i.e. the traceless part, $\mathbf{q} - \text{Sym}3(\mathbf{1} \mathbf{q})/5$. 37, 42
- \mathbb{Q}_s^f tensor heating due to resistive drag. 11, 13
- Q_s^f heat source due to resistive drag. 12, 14
- \mathbb{Q}_s^t tensor heating due to thermal equilibration. 11, 13
- Q_s^t heat source due to thermal equilibration. 12, 14

- \mathbf{R}_s resistive drag force on species s due to collisions with other species. 11–14, 26
- \mathbb{R} set of all real numbers. 20
- \mathbb{R}_s relaxation (isotropization) tensor. 11, 13, 26
- $s_{\mathcal{M}}$ gas-dynamic entropy per volume. 29, 30
- Sym symmetric part of its tensor argument. 26
- Sym2 twice the symmetric part of a tensor with two indices. 26
- Sym3 thrice the symmetric part of a tensor with three indices. 37
- $\widetilde{\text{Sym}}$ splice symmetrization of a second-order tensor, defined in section A.5.1. 128
- \mathbb{T} temperature tensor. 27
- T temperature. 27
- \mathbb{T}° deviatoric part of temperature tensor. 27
- \mathbf{u}_s fluid velocity of species s . 20
- $\tilde{\mathbf{v}}$ proper velocity ($\gamma\mathbf{v}$). 23
- \mathbf{v} velocity (of a particle or as an independent variable). 19, 23
- v_A Alfvén speed. 124
- v_{ts} thermal velocity. 4, 124
- \mathbf{w}_s drift velocity of species s relative to the bulk fluid velocity \mathbf{u} . 52, 54
- \mathbf{x} position in space (e.g. of a particle or as an independent variable). 19, 23

Index

- n*th order moment, [19](#)
- z* axis, [57](#)
- “bulk derivative”, [25](#)
- “half-scale”, [73](#)
- “quasi” temperature, [27](#)
- “quasi” temperature tensor, [27](#)
- “rescaled problem”, [73](#)

- adiabatic index, [127](#)
- Alfvén speed, [124](#)
- Alfvén speeds, [124](#)
- antiparallel reconnection, [59](#)
- aspect ratio, [5](#)

- characteristic variables, [109](#)
- charge velocity, [53](#), [60](#)
- collision operator, [19](#)
- collisions, [1](#)
- conservation variables, [20](#)
- conserved moments, [19](#)
- convective derivative, [25](#)
- Coulomb collision operator, [23](#)

- Debye length, [124](#)
- density, [26](#)
- deviatoric heat flux tensor, [37](#), [42](#)
- deviatoric part, [27](#)
- deviatoric strain rate, [32](#)
- diamond product, [39](#)
- diffusion region, [5](#)
- diffusive entropy flux, [29](#), [30](#), [31](#)
- divergence-free, [2](#)
- drag force, [26](#)
- drift pressure, [54](#)
- drift velocity, [2](#)

- electrokinetic pressure tensor, [52](#)
- electron diffusion region, [7](#)
- Ellipsoidal-Statistical BGK, [40](#)
- energy tensor, [26](#)
- entropy density
 - statistical, [28](#)
- entropy flux, [28](#)
- entropy production, [28](#)

- even function of velocity, [29](#)
- extended MHD, [4](#)
- Extended-moment fluid models, [20](#)

- fast reconnection, [5](#)
- five-moment gas-dynamic entropy, [29](#), [123](#)
- five-moment model, [20](#)
- fluid models, [19](#), [19](#)
- flux-transporting flow, [60](#)
- flux-transporting velocity, [2](#)

- Galilean transformation, [18](#)
- Galilean-invariant, [18](#)
- Gaussian distribution, [29](#), [40](#)
- Gaussian-BGK, [21](#), [40](#)
- GEM magnetic reconnection challenge problem,
 - [21](#), [60](#)
- GEM problem, [7](#), [72](#)
- geocentric coordinates, [57](#), [71](#)
- Geospace Environmental Modeling magnetic reconnection challenge problem, [7](#)
- Geospace Environmental Modeling magnetic reconnection reconnection challenge problem, [72](#)
- guide field, [59](#)
- guiding magnetic field, [59](#)
- gyrofrequencies, [124](#)
- gyrofrequency, [38](#)
- gyroradii, [124](#)
- gyrotropic, [20](#)
- gyrotropic pressure, [62](#)
- gyrotropic tensor, [32](#)

- Hall-mediated reconnection, [6](#)
- heat conductivity, [32](#), [45](#)
- higher-moment models, [21](#)
- hydrogen plasmas, [1](#)
- hyperbolic five-moment model, [29](#)
- hyperbolic part, [107](#), [108](#)
- hyperbolic ten-moment model, [30](#)

- Ideal MHD, [2](#)
- inertial length, [124](#)
- inertial lengths, [124](#)

- ion diffusion region, [6](#)
- isotropic pressure, [62](#)
- kinematic viscosity, [126](#)
- Kinetic models, [19](#)
- Lorentz transformation, [18](#)
- Lorentz-invariant, [18](#)
- Lorentz-invariant hyperbolic higher-moment closure, [21](#)
- macro-scale, [23](#)
- magnetic field line, [2](#)
- magnetic flux, [2](#)
- magnetohydrodynamic (MHD) fluid, [2](#)
- magnetohydrodynamics (MHD), [51](#)
- Maxwellian, [28](#)
- Maxwellian distribution, [19](#), [39](#)
- Maxwellian moments, [19](#)
- microscale field, [23](#)
- moments, [19](#)
- momentum density, [26](#)
- O-point, [58](#)
- Ohm's law, [2](#), [4](#), [51](#), [51](#)
- one-fluid MHD models, [55](#)
- origin, [57](#)
- out-of-plane axis, [57](#)
- pair plasmas, [1](#)
- parallel pressure, [63](#)
- particle density functions, [19](#)
- particle models, [19](#)
- particle number density, [26](#)
- Particle-in-cell (PIC), [19](#)
- perpendicular pressure, [63](#)
- phase space, [19](#), [23](#)
- physically realizable, [64](#)
- Plasma, [1](#)
- plasma beta, [124](#)
- plasma frequencies, [124](#)
- plasma frequency, [124](#)
- plasmoids, [6](#)
- positivity conditions, [64](#)
- Prandtl number, [40](#), [126](#), [127](#)
- pressure tensor, [26](#)
- Primitive variables, [24](#)
- primitive variables, [20](#)
- proper tensor, [58](#)
- pseudo-temperature, [40](#), [115](#)
- pseudo-temperature tensor, [40](#), [115](#)
- pseudo-tensor, [58](#)
- rate of magnetic reconnection, [60](#)
- realizable, [22](#)
- reconnect, [3](#), [60](#)
- reflectional symmetry, [59](#)
- relativistic, [18](#)
- relativity principle, [18](#)
- relaxation period, [34](#), [40](#)
- relaxation rate, [34](#)
- resistive Hall MHD, [2](#)
- Resistive MHD, [2](#)
- rotationally symmetric, [57](#)
- satisfies positivity, [64](#)
- scalar pressure, [27](#)
- separatrices, [3](#), [58](#)
- skin depth, [124](#)
- slow reconnection, [5](#)
- source ODE, [107](#)
- source term ODE, [143](#)
- species, [18](#)
- species drift velocity, [52](#)
- splice symmetric tensor product, [128](#)
- splice tensor operations, [128](#)
- standard of truth, [113](#)
- stochastic collision operator, [113](#)
- strain rate, [32](#)
- structurally unstable, [113](#), [113](#)
- symmetric pair plasma, [55](#), [72](#)
- tearing mode instability, [6](#)
- temperature, [27](#)
- temperature tensor, [27](#)
- ten-moment gas-dynamic entropy, [30](#), [123](#)
- ten-moment model, [20](#)
- the plane, [57](#)
- thermal entropy production, [30](#), [31](#)
- thermal velocities, [124](#)
- thermal velocity, [20](#), [124](#)
- two-dimensional (2D), [57](#)
- two-fluid, [2](#)
- two-fluid MHD, [2](#), [55](#)
- two-species, [1](#)
- viscosity, [33](#)
- Vlasov equation, [19](#), [23](#)
- X-point, [58](#)